– An international journal for New Concepts in Global Tectonics –

NCGT JOURNAL

Volume 5, Number 1, March 2017. ISSN 2202-0039. Editor: Dong R. CHOI (research@ncgtjournal.com)
www.ncgtjournal.com

CONTENTS

For contact, correspondence, or inclusion of material in the NCGT Journal please use the following methods: *NEWCONCEPTSINGLOBAL TECTONICS.* 1. E-mail: research@ncgtjournal.org; admin@ncgtjournal.org, 2. Mail, air express, etc., 6 Mann Place, Higgins, ACT2615, Australia (files in MS Word format, and figures in jpg, bmp or tif format); 3. Telephone, +61-2-6254 4409.
 NCGT Journal is a refereed quarterly international online journal and appears in March, June, September and December. For Mac computer users, this journal in pdf format must be opened with Acrobat or Acrobat Reader. ***ISSN numbers***; ISSN 2202-0039. Global impact factor for 2015: 0.876.

FROM THE EDITOR

NCGT Journal has been commercialized

Effective with the March 31, 2017 edition of the New Concepts in Global Tectonics (NCGT) Journal, we will be operating as a commercial enterprise!

In cooperation with the International Earthquake and Volcano Prediction Center (IEVPC), where I am a co-founder and Director, the Journal will begin to charge a small subscription fee for each new edition and all back issues of the Journal. The IEVPC has been granted full rights to market the Journal and will do so from their web site and other means. The IEVPC web site is at www.ievpc.org. The new website of the Journal is now, www.ncgtjournal.com. The editor of the Journal can be contacted at research@ncgtjournal.com.

This is a big step forward for our group of global contributors and readers of the Journal and will have lasting, wide ranging benefits for us all. Here are some of them:

1. Sustained Income. Going commercial with the Journal will solve a fundamental financial problem - the routine lack of funding that our geological community has long had to face. With a regular cash flow from sales of the Journal and related products, we will finally be able to reach out to many more independent thinkers and those in need of a widely read, no cost, source for publication of their work and opinions.
2. Journal and IEVPC Permanency. With a minimal level of funding provided by Journal sales, the IEVPC and the Journal will be able to establish permanent offices and staff that will increase their capability to achieve their important missions. This also solves a basic problem of how to continue these worthy organizations after the founders have gone.
3. Increased Organizational Recognition and Credibility. Sadly, the real world still revolves around money. It is necessary for us to finally create a financial base from which we can achieve the international recognition that our organizations deserve.
4. Enhanced Platform for Contributors. With the commercialization of the Journal, we will have a much improved capability to promote those who contribute to the Journal. In this way, contributors of research papers and opinions to the Journal will be able to have their work reach an even greater audience far beyond our own scientific community members. The new Journal will have the “marketing muscle” to extend awareness of Journal’s individual researchers to the global media networks, and international leaders as well as to a much larger public audience.

For over twenty years now, you have been loyal contributors and readers of the New Concepts in Global Tectonics (NCGT) Journal. I am deeply indebted to you for your past support for making the Journal the success that it is today. With the assistance of the IEVPC we will now be able to do much more for you and our efforts to bring to light innovative ideas and research and promote the people who have made the Journal a great piece of scientific literature.

I look forward to this new phase of the Journal and encourage you to spread the word through your own list of contacts that this important next phase of the Journal has begun.

Dong Choi
Editor-in-Chief
research@ncgtjournal.com
www.ncgtjournal.com

LETTERS TO THE EDITOR

Geological events that occur close together in space and time may be linked causally: four examples from western North America

In my seventy years working over a large area that included the states of Washington, Oregon, California, Nevada, Idaho and Montana as well as Alberta and British Columbia in Canada, I had found plenty of evidence for cataclysm but little to demonstrate an overall pattern or sequence. This is a deviation, my attempt to collate events and knit their disparate parts into a sensibly feasible concept. I will start with a south-central feature, extinct Lake Lahonton, central to a large area that had long been referred to by geologists as "the Great Basin".

Its extent over most of Utah, northern Nevada, southern Idaho and southwestern Montana never was filled with water, although most people were satisfied with the explanation that it held the residual salt water of an extensive lake, known as Lake Lahonton. The following geological events would have contributed the huge volume of water needed for such a large lake as Lake Lahonton, and I propose the following event series.

It is my view that the lake was created by a series of Earth shifts that from today's perspective were nearly simultaneous. I can identify four such events.

1. One of the proposed four Earth shifts was likely an abrupt rise of the Wasatch Range at the Rocky Mountain front. That cut off the previous eastward out-flow from the Lahonton basin (into the Mississippi system).

2. A second Earth shift was upward growth of a high east-west trending ridge within the northern borders of the Lahonton basin. This ridge cut off southward flow of rivers into Lahonton from Idaho and western Montana. The diverted drainage from the north flowed westward, cutting the deep canyon of the Snake River, and then proceeding northwest, cutting a gorge to Columbia River level and expediting river flow to the Pacific Ocean.

3. The third Earth shift that I can recognize is the Calgary Flood, wherein water from the Gulf of Mexico swept up the Mississippi valley and flooded the Canadian Rocky Mountain front up to its present 11,000 foot elevation; and then receded, leaving a trail of stranded ice floes, some carrying boulders (one up to house size). This inundation could have over-filled Lake Lahonton.

4. The fourth Earth shift that I can recognize, profoundly affected the State of Washington and the mountains of western Montana. This event was the westward tilting and emptying of Lake Missoula. The high altitude lake cradled in north-south orientation was not far south of the US/CANADA border. Its existence was abruptly ended by abrupt tipping westward, its entire water volume racing down Clark Fork River and across central Washington State, stripping away soil and vegetation, and leaving a surface that has aptly been called a "scabland".

Now let us consider the broader picture. All four of the Earth shifts occurred in late Pleistocene time, perhaps within a few years. The volcanic arc, Mts. Baker to Shasta, is dated back to at least Eocene time. Thus, it seems reasonable to regard the four events that are very close together in space and time as causally linked.

Charles Warren Hunt
archeanc@gmail.com
17 January 2017

Dear Editor:

In December 2016, Earth & Space Science News (“EOS”) carried an online article by Michael Rempino entitled “A Meeting That Helped Foster the Acceptance of Global Tectonics” in honor of the 50th anniversary of the 1966 “History of the Earth’s Crust Symposium” held at the American Geophysical Union’s Fall Meeting in San Francisco. The theme of the article, well written and designed to be a brief historical summary, is that the meeting was a scientific pivot point as described in the following hyperlink. https://eos.org/features/meeting-gave-birth-idea-global-tectonics.

Unfortunately, the article failed to recognize the essential precursor tectonic work of the previous 30 years without which the Symposium could not have been convened in 1966.

The EOS article generated a few reader comments that point out the omission of important prior work. For the information of NCGT Journal readers, I include below my comment on the article, slightly expanded, edited and with a graphic from my very informal “Free Range Tectonics” presentation.

“Interesting, but incomplete. The real story starts 30 years earlier when Samuel Carey introduced his subduction, spreading ridge and mobile plate tectonic theory. This essential foundational work is well documented by Google’s Ngram Viewer when setting the date span to 1930-2010 and entering 'subduction" or alternatively "plate tectonics".

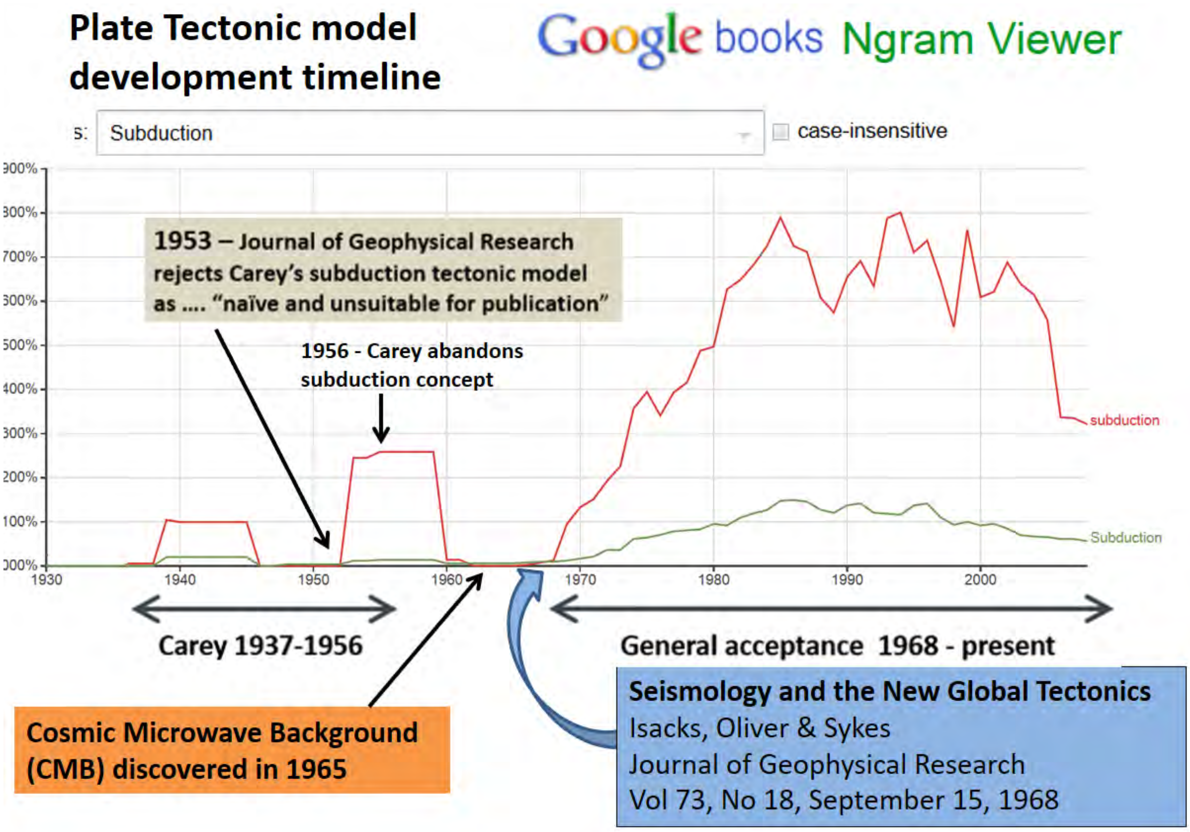

The first bump, running from 1937 to 1960 reflects Carey’s subduction model keywords entering Google's vast corpus of digitized literature, interrupted by a post-world war hiatus. Following the hiatus, Carey unsuccessfully tried to validate his then wild and crazy theory with incontrovertible lithologic and fossil evidence. This caused subduction model keywords to re-enter the scientific literature in the early 1950’s. Eventually, the evidence forced Carey to reject his model of 19 years to be replaced with an expansion tectonic model in the mid-1950’s. The subduction model keywords persisted in the literature until their frequency dropped and flatlined in 1959.

The second bump begins in September 1968 when the "New Global Tectonics" went mainstream and was renamed “Plate Tectonics” in 1969. It is interesting to read the literature and correspondence of the day to "hear" some of the Earth scientists mentioned in the article discussing, between 1964 and 1967, which of Carey's theories, ("subduction tectonics" or "expansion tectonics"), should be adopted to explain the growing body of oceanographic information. I suspect that the NASA funding frenzy of the 1960's doomed Carey's expansion option since it required the Earth's mass to increase, thereby directly contradicting the trending inflation theory of the universe which solidified its own trendy name in 1965 following the very convenient discovery of the long sought Cosmic Microwave Background."

Rick Boulay, Calgary
rickboulay@shaw.ca
February 8, 2017

Reference:
Rampino, M. R. (2016), A meeting that helped foster the acceptance of global tectonics, *Eos*, 97, https://doi.org/10.1029/2016EO063933. Published on 12 December 2016.

****

Geological origin of El Niño

Hello Editor,

Please find in the link below a text, leaving aside the plate tectonics references, presents an interesting theory about the geological origin of El Niño.

http://climatechangedispatch.com/further-proof-el-ninos-are-fueled-by-deep-sea-geological-heat-flow/

Oscar Javier Arevalo
oscarjarevalo@gmail.com

Editor's note: Because this paper (by James E. Kamis) has a wide ramification, some extracts are added below:

…The 2014-2017 El Niño "warm blob" was likely created, maintained, and partially recharged on two separate occasions by massive pulses of super-heated and chemically charged seawater from deep-sea geological features in the western North Pacific Ocean. This strongly supports the theory all El Niños are naturally occurring and geological in origin. Climate change / global warming had nothing to do with generating, rewarming, intensifying, or increasing the frequency of the 2014-2017 El Niño or any previous El Niño.

…El Niño intensity and date of initial ocean warming data was gathered from several reliable published data sources. This cross plot/comparison process yielded an excellent correlation, specifically that all historical and modern data confirm the onset of El Niño ocean warming occurs a few months after the beginning of very high magnitude earthquake swarms located in the greater Solomon Island area.

…The consistent failure of atmospherically based climate models has been plain to see for all scientists. The models have failed to properly predict the timing and intensity of El Niño warming, La Nina cooling, and of late El Niño partial rewarming. Why?

…Deep-ocean geological seafloor forces act to alter overlying ocean currents, temperatures, and chemistry (iron content, acidity, etc.) in a complex and constantly changing fashion. This changed/changing overlying ocean water then acts to change the overlying atmosphere (alters Trade Winds, rain patterns, storm tracks, etc.). Computer climate models that ignore these side effects of atmospheric and oceanic data are doomed to fail. In the vernacular, climate scientists are chasing their tails. Resulting climate models are constantly changing and always a dollar short and a day late. The latest sanctioned model utilizes Trade Wind data. The ongoing rewarming events of the 2014-2017 El Niño will prove to be a death blow to this latest forward-looking model.

…The atmospheric bias of consensus climate scientists is another very broad reason why obvious geological observations have been overlooked or just plain ignored by many, not all, but many climate scientists study El Niño generation. These well-intentioned folks were trained by "atmospheric" climate professors, have abundant atmospheric data at their disposal, and most importantly, very little deep-sea geological data at their disposal.

ARTICLES

The upper mantle structure of the Northern Eurasia from the seismic profiling with nuclear explosions

Nina I. Pavlenkova and Galina A. Pavlenkova
Institute of the Earth Physics RAN, Moscow, Russia.
ninapav@mail.ru

Abstract: The long-range seismic profiles with large chemical and with Peaceful Nuclear Explosions (PNEs) were carried out in Russia during the last decades of the XX century. The profiles cross several large tectonic structures: The East European Craton, the Urals, the young Timan-Pechora and West-Siberian plates and the Siberian Craton. They differ in age, in geological history and geophysical fields.

2-D crust and upper mantle velocity models up to depth of 700 km were constrained for all these profiles using a common method for the wave analysis and velocity modeling. As a result, 3-D velocity model of the upper mantle was compiled for this large area. The models show that the old and cold East-European and Siberian Cratons have higher velocities in the thick (about 300 km) lithosphere than the young Timan-Pechora and West Siberian platforms with higher heat flows. Mostly horizontal inhomogeneity is observed in the uppermost mantle: the velocities change from the average 8.0-8.1 km/s to 8.3-8.4 km/s in some blocks of the Urals and in the Siberian Craton. Along all the profiles the prominent velocity boundaries are observed in the lithosphere: N1 and N2 at a depth 70-130 km, L boundary [Lehman,1964] at a depth of 180-240 km and H boundary at 300-330 km. Analyses of the waves from the mantle transition zone indicate strong velocity discontinuities at 420, 510 and 660 km depths. All the boundaries are not simple discontinuities, they are heterogeneous (thin layering) zones which generate multiphase reflections.

It is difficult to determine the lithosphere-asthenosphere boundary in traditional form because the 'thermal' asthenosphere at depths of 250-300 km was not traced as a lower velocity zone. The rheological stratification follows, however, from the regular change of horizontal heterogeneity which determines three layers of different plasticity. The layers are divided by the seismic boundaries N1 and L. The block structure typical of the upper brittle part of the lithosphere disappears beneath the N1 boundary and the thin low velocity layer is observed above the boundary. These structural features propose that the depth of 100-120 km is a bottom of a brittle part of the lithosphere. Beneath the L boundary the Q factor decreases and the H boundary form makes the isostatic compensation of the lithosphere in homogeneities. That marks this boundary as a possible top of the asthenosphere.

The velocity-density modeling, performed along the PNE profiles revealed significant distinctions in the upper mantle composition in the Northern Eurasia. The Siberian Craton of the same age and of the same heat flow as the East-European Craton is characterized by the higher upper mantle velocities and by the lower densities. That proposes the depleted upper mantle beneath the Siberian Craton, which is characterized by negative gravity anomaly.

Keywords: *crust, upper mantle, Eurasia, seismic profiling, Peaceful Nuclear Explosions, asthenosphere, lithosphere, deep fluids*

(Submitted 18 January 2017. Accepted 30 January 2017)

1. Introduction

During the last decades of the XX century several long-range seismic profiles with large chemical and with Peaceful Nuclear Explosions (PNE) were carried out in Russia (**Fig. 1**). The studies were made by the GEON Center of the USSR Ministry of Geology (now Ministry of Natural Resources of Russia). It was large project of seismic profiling carried out in 1970-1980 in order to study comprehensively the structures of the upper mantle and the mantle transition zone to a depth of 700 km (Egorkin and Kun, 1978; Yegorkin and Pavenkova, 1981; Egorkin et al., 1987; Benz et. al., 1992; Pavlenkova, 1988)

The profiles cross several large geostructures of the Northern Eurasia: the East European-Craton (EEC), the Siberian Craton (SC), the Urals, the West-Siberian Plate (WSP) and Timan-Pechora Plate (T-P) (**Fig. 1**). The geosturtures differ in age, in geological history, in crustal structure and geophysical fields (Cermak, 1985; Pavlenkova, 1996b; Artemieva and Mooney, 2001).

The East-European Craton (EEC) is of the Archean-Proterozoic ages. Two large geostructures are distinguished in the northern part of the craton: the Baltic Shield and the Russian platform. Crustal thickness changes from 40 to 50 km and the average velocity in the consolidated crust is about 6.5 km/s. The strongly differentiated mosaic potential and magnetic fields characterize a complex structure of the consolidated crust. The heat flow distribution is rather smooth (40-50 mW/m^2).

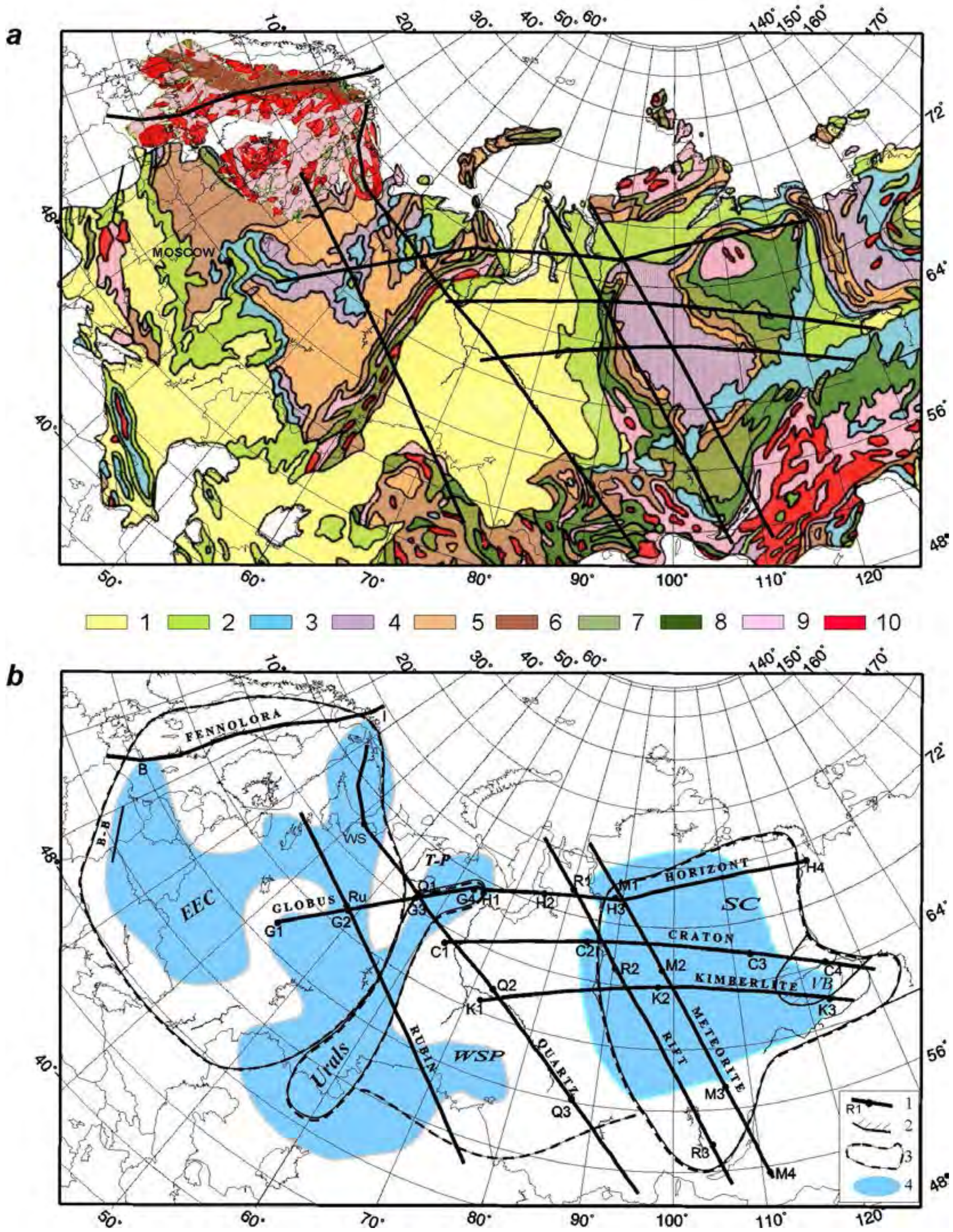

Fig. 1. **(a)** Geological map for the Northern Eurasia and location of the long-range seismic profiles. **(b)** Scheme of the seismic profiles. Legend: 1 – seismic profile, 2 – the Vilyui Basin, 3 – the tectonic unit boundary (EEC – the East-European Craton, SC – the Siberian Craton, WSP – the West-Siberian Plate, T-P – the Timan-Pechora Plate), 4 – area of the lower heat flow. The letters mark locations of the Peace Nuclear Explosions (PNE) and the large chemical explosions B and I along the profile Fennolora.

The Timan-Pechora Plate (T-P in **Fig. 1**), of the Caledonian age, has a fairly thick, particularly in the pre-Ural region, sedimentary cover. The crustal thickness almost the same as that of the craton (40 km), but the geophysical fields are much less disturbed and generally reflect the topography of the basement surface. The heat flow is elevated up to 60 mW/m^2.

The Urals is a Paleozoic orogenic belt with its own specific features of the crustal structure: the thickness of the crust is high (up to 55 km) and its upper part contains higher density rocks whose occurrence is delineated by significant magnetic and gravity anomalies all along the belt. The heat flow is lowered down to 40 mW/m^2.

The West-Siberian Plate (WSP in **Fig.1**), of the Caledonian–Hercynian age, is covered by Mesozoic sediments 3–15 km thick. The sedimentary cover is the thickest (more than 15 km) in the northern part of the plate. The magnetic and gravitational fields differ little from those of the EEC. In contrast, the heat flow differs strongly, attaining values of 60–70 mW/m^2.

The Siberian Craton (SC) is of Archean-Proterozoic age. Several large basins are distinguished in the craton area. They are of 8-10 km deep and filled with high density sediments and with plateau-basalts. Only the deep Vilyui Basin (VB in **Fig. 1b**) is filled with younger sediments. The crustal thickness is 40-45 km, the average velocity is 6.5-6.6 km/s in the cratonic areas. The magnetic and gravity fields are sharply differentiated due to the plateau-basalts. The heat-flow is much lower than in the East-European Craton: 30 mW/m^2.

The PNE profiles have detail observation system. Three-component analogue seismic stations equipped with short period seismometers (1-2 Hz) were deployed along the profiles to record all events (explosions and earthquakes) during a week. The distance between the stations was 10 km. Record sections from the nuclear explosions (**Fig. 2**) show the complex structure of the upper mantle wave fields with drastically varying apparent velocities and amplitudes of first arrivals and numerous later high-amplitude arrivals at the offsets 200-2000 km . The most records, however, show that observed waves may be approximated by several regular wave groups: Pn, P_{N1}, P_{N2}, P_L and P_N.

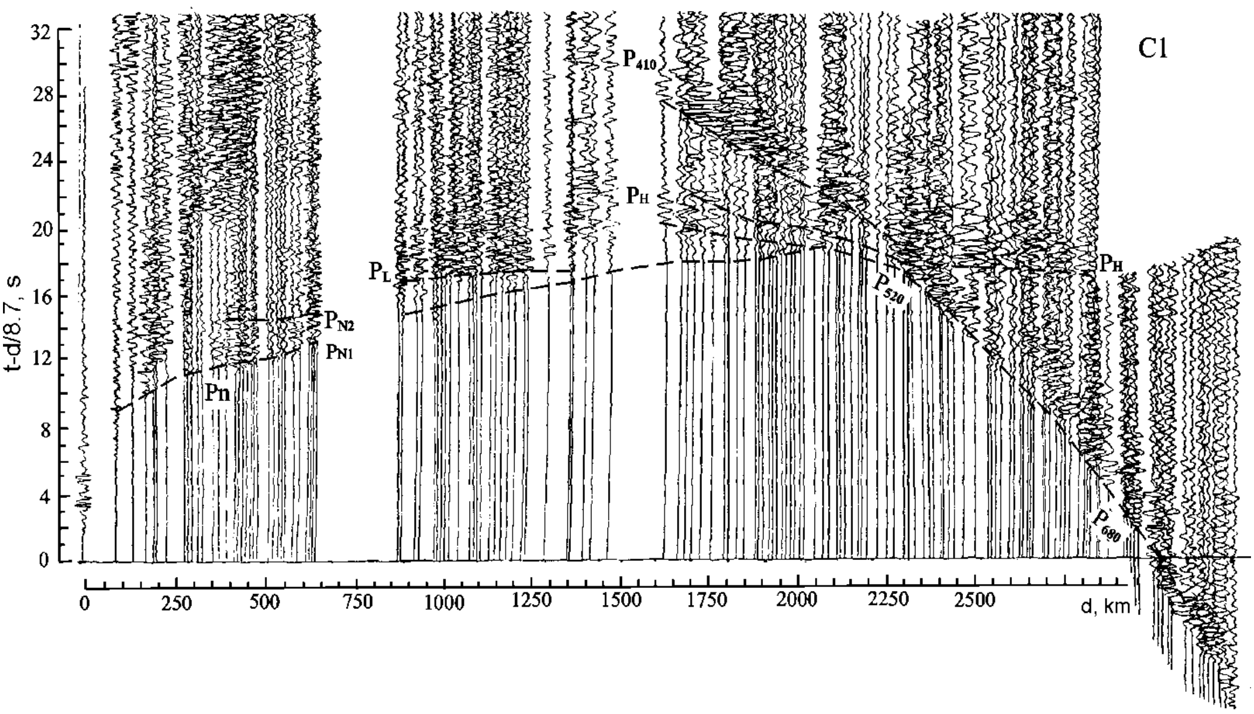

Fig. 2. Record-section for the PNE C1 along the Craton profile (the reduction velocity is 8.7 km/s). The regular mantle waves: Pn – refraction in the uppermost mantle; P_{N1}, P_{N2} , P_L and P_H are the reflections and refractions from the corresponding seismic boundaries N1, N2, L and H. The waves P_{410}, P_{520} and P_{680} are from the boundaries of the mantle transition zone at the depths of around 410, 520 and 680 km.

The first interpretation of these data was made by GEON Centre. At first the crustal models were constructed from the chemical explosion records. The PNE data were processed mainly during the last decades of the past century (Egorkin, 1999). During 1990s the PNE records were digitised and some of data became available for the proceeding of the international groups of researchers (the profiles Quartz, Rift and Craton). The profiles were interpreted and discussed in many publications: Quartz (Mechie et al., 1993; Ryberg et al., 1998; Morozov et al., 1999), Rift (Cipar et al., 1993; Priestly et al., 1994; Pavlenkova et al., 2002) and Craton (Nielsen and Thybo, 1999). The profiles Globus, Rubin and Horizont have been interpreted only in last years (Pavlenkova and Pavlenkova, 2006). General analysis of the data and their comparison with the other long range seismic profiles was made in (Fuchs, 1997).

Comparison of the models obtained by the mentioned authors shows no serious difference between them in regional plan. In all models significant changes in velocities are observed between the cratons and young platforms and in the mantle transition zone three boundaries are recognized approximately at the same average depth. The models differ, however, in some important details of the upper mantle structure. It is due to the ambiguous solutions of the inverse seismic problems, the different volumes of information used and to different methods for data analysis. For example, some researchers obtained only I-D mantle velocity models (Cipar et al., 1993; Priestly et al., 1994) or used only the first waves for seismic tomographic inversion (Nielsen and Thybo, 1999); the others, on the contrary, applied velocity filtering to pick as much the secondary waves as possible (Egorkin, 1999). The most researchers determined the mantle structure only from nuclear-explosion data, not involving chemical explosion records. All velocity cross-sections were constructed at different detail levels. Some authors show many boundaries and many inversion zones (Egorkin et al., 1987; Morozov et al., 1999), and other authors present very simple models (Nielsen and Thybo, 1999). Beside the models are presented in different forms and it is difficult to use them for the compilation of maps or 3-D velocity model.

During the last years an additional analysis of all long-range profiles data was made to refine the general structure of the upper mantle and to make all resulting models agree with each other at intersection points of profiles (Pavlenkova and Pavlenkova, 2014). The additional 2-D velocity modeling was made with spherical surfaces, thereby increasing the reliability of the models. The long-range profile Fennolora was also included in these studies. All obtained models were presented in the common form. They characterise structure of the crust, upper mantle and transition zone to the lower mantle. This article is a short summary of these results.

2. Velocity cross-sections along the profiles

Craton and Kimberlite profiles. The seismic cross-sections along the Craton and Kimberlite profiles (**Fig. 3**) reflect the major specific structure of the crust and upper mantle of the Siberian Craton and West-Siberian Plate.

The velocity models of the crust include four layers: sedimentary cover and three layers of consolidated part with velocities of 6.0-6.4 km/s (upper crust), 6.5-6.7 km/s (the middle crust), and 6.8-7.2 km/s (the lower crust). The thickness of sediments along most of the profile is small (0-3 km), but it increases to 10 km in the area of the Vilyui basin, where the sedimentary cover is characterized by velocities of 3.5-5.0 km/s. In the other parts of the craton, the velocities in sediments are often high, 4.5-5.0 km/s due to the plateau-basalts.

The structure of the crystalline crust also significantly varies mainly in the area of the Vilyui basin. The upper crust is 10 km thick in the platform area, whereas beneath the basin it becomes thinner. The thickness of the middle crust also varies along the profile: it is 20 km in the platform area and is 10 km beneath the basin. The lower crust is 15-17 km throughout the profile.

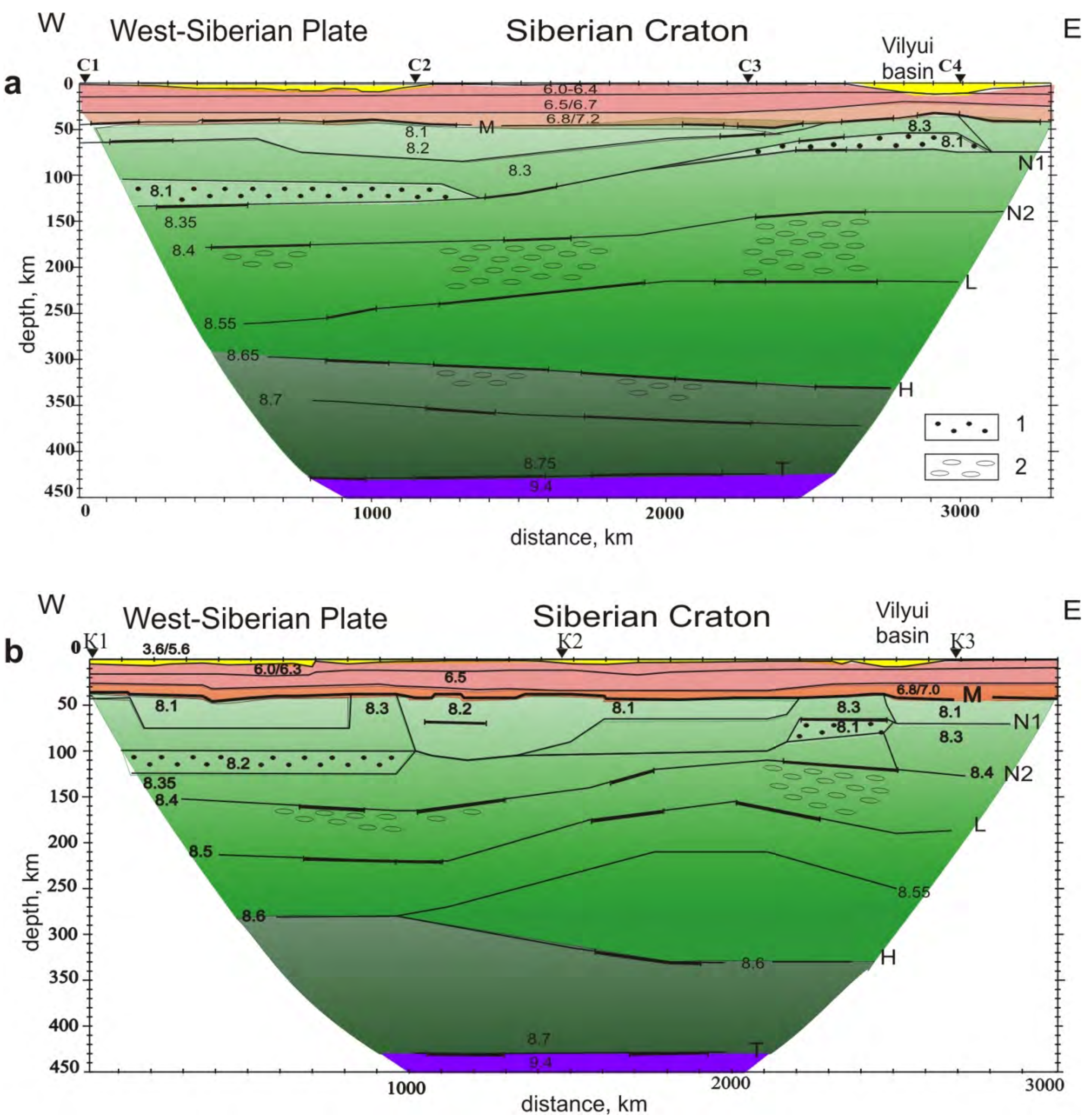

Fig. 3 Velocity cross-sections along the profiles Craton (**a**) and Kimberlite (**b**). The seismic boundaries N1, N2, L, H are the upper mantle basic boundaries with constant velocity (the velocities increase linearly between the boundaries). T boundary is the top of the upper/lower mantle transition zone. The reflectors are shown by the thick lines. 1- low velocity layer; 2 – zones of higher heterogeneity.

The average depth to the Moho varies along the profiles within 40-45 km decreasing to 36 km beneath the Vilyui basin. The velocities beneath the Moho are average 8.1-8.2 km/s, except the Craton profile interval 2500-3000 km where they increase to 8.3 km/s, and the Kimberlite profile intervals 800-1000 km and 2200-2500 km. These anomalous high-velocity block are located in the western part of the Vilyui basin, and its eastern margin coincides with the area of the sharpest subsidence of the basement.

The obtained upper mantle models show that the highest heterogeneity of the velocity section is specific for the upper 130 km of the mantle. The Pn wave velocities from the chemical and nuclear shots differ from 8.0 to 8.4 km/s. They reveal the block structure beneath the Moho.

In addition to a high-velocity block, low-velocity layers have been revealed at depths of 100-130 km in the western parts and at depths of 60-70 km in the eastern parts of the profiles.

The boundaries N1, N2 and L are of the similar structure. They rise from west to east. Along the Craton profile the depth to the boundary N1 changes from 130 km in the west to 70 km in the east of the profiles; the N2 depth is 150-180 km in the west and about 150 km in the east. The L boundary appears at a depth of 220- 260 km in the west and rises to a depth of 180- 220 km in the eastern part of the profiles. The boundary H slightly tends to subsidence from west to east in contrast to the rise of the upper boundaries.

The Kimberlite profile shows the similar crust and upper mantle structure. In both profiles the evident difference is observed between the Siberian and West-Siberian platforms. There are, however, some differences between the profiles. In average the mantle waves along the Kimberlite profile show the higher velocities than along the Craton profile. The Tunguss high velocity block is not distinguished on the Craton profile. On the contrary in this part of the profile the uppermost mantle velocities are lower than those in the other areas of the craton. The profiles differ in the L boundary structure which show larger uplift beneath the Siberian craton along the Kimberlite profile.

Rift and Meteorite profiles cross the Siberian Craton and the Baikal Rift Zone from north to south (**Fig. 1**). The Rift profile crosses also the West-Siberian Plate in the area of deep Pur-Gidan Basin, and the northern part of the Meteorite profile crosses the Taimir Orogen Belt.

The velocity models of the consolidated crust along the profiles are similar to the models of other profiles (**Fig. 4**): it contains three main layers with velocities 6.0-6.3, 6.5 and 6.8-7.0 km/s of approximately the same thicknesses. Only beneath the Low Angara Basin the thickness of the upper layer significantly increases. The most complicate crustal structure are observed in the Pur-Gedan Basin. The wave field is defined by low velocities in the sediments (3.5 km/s) and by extremely large basement depth of 15-20 km.

The upper mantle velocity models show strong horizontal heterogeneity, particularly in the upper 100 km of the upper mantle. Two blocks (500 km long) of anomalously high velocity (8.4 km/s) are represented along the Rift profile: one in the northern part (Tunguss block) and one in the southern part near the Baikal Rift (Pre-Baikal block). The high-velocity blocks are distinctly recognized along the Meteorite profile in the intervals 2100-2400 and 1000-1600 km.

The velocity inversion zone is distinguished at the depth of 70-100 km along the Rift profile. The velocities beneath the zone are 8.35-8.4 km/s. In the inversion zone they were supposed to be 8.1 km/s. Along the Meteorite profile two low-velocity layers were recognized at depths of 80-100 km and at depths of 130-150 km.

The topography of the mantle boundaries is much more intricate along these profiles as compared with the other profiles. In the Rift profile interval 1000-1300 km the N2 and L boundaries uplift. It suggests that in this area (depth 100-250 km) there is a fault zone with the reflector dipping to the north. The zone generates reflections with anomalous high apparent velocities and complex wave pattern. In the Meteorite profile N2 boundary is near horizontal, but the L boundary goes down. The H boundary is nearly horizontal along both profiles and some additional reflectors are revealed below and above this boundary.

Quartz Profile crosses the East-European Craton (EEC), Timan-Pechora Plate (T-P), the Northern Urals, the West-Siberian Plate (WSP) (**Fig. 1**). Forty-eight chemical explosions and four PNEs WS, Q1, Q2, and Q3 were fired on the profile. The most prominent horizontal heterogeneities in the crustal structure are seen in the transitional zones between the Russian platform, the Timan-Pechora Plate and the Urals (**Fig. 5**). The velocities at the basement are 6.2 km/s beneath the Russian platform and 5.9–6.0 km/s beneath the Timan-Pechora Plate, where the high velocity (6.8-7.0 km/s) layer of the lower crust is absent. The depth to Moho varies along the profile from 40-45 km beneath the East European Craton to 55 km beneath the Urals. A relatively thin crust is characteristic of the Timan-Pechora Plate.

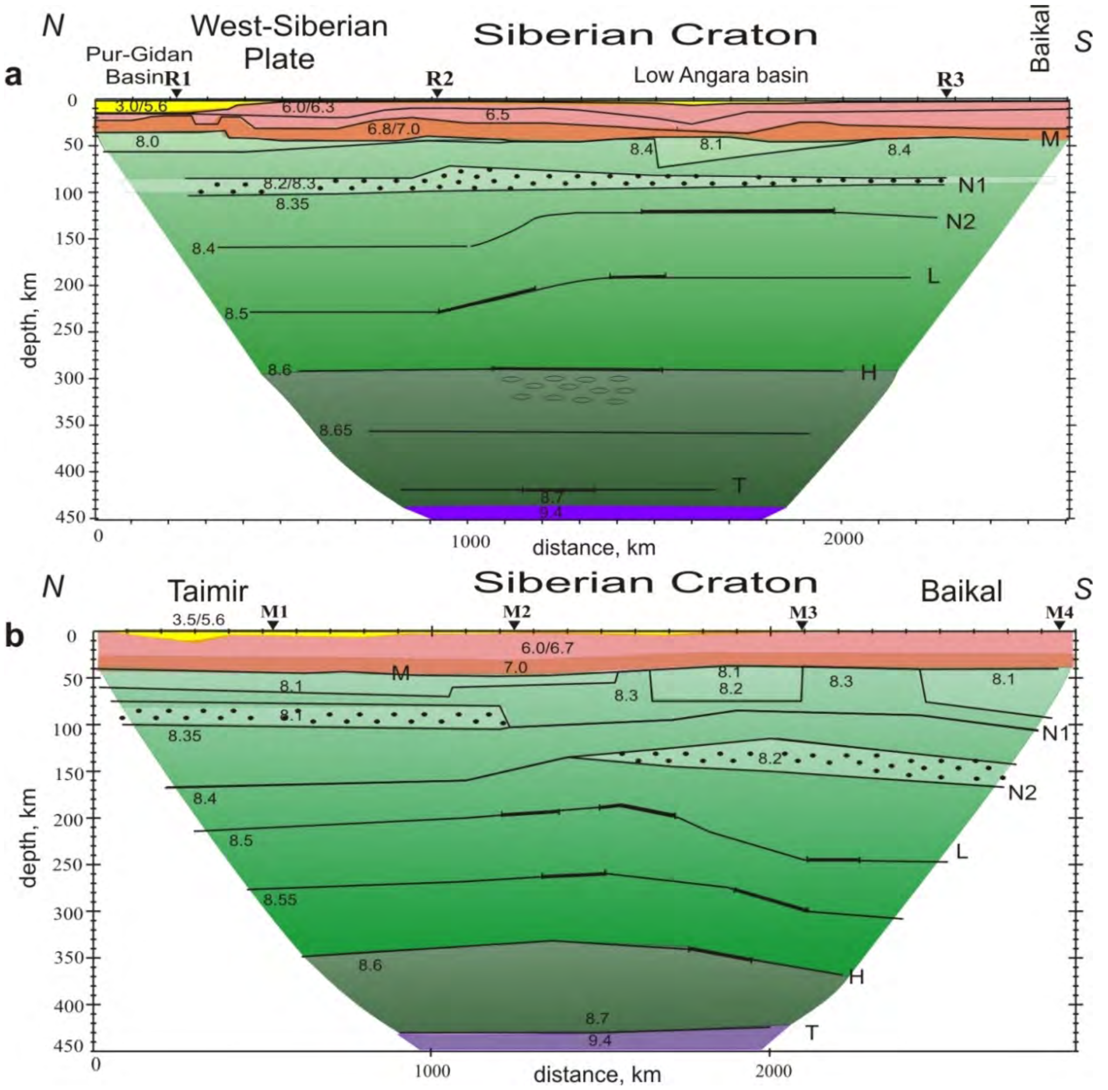

Fig. 4. Velocity cross-sections along the profiles Rift (**a**) and Meteorite (**b**). Legend is in Fig. 3.

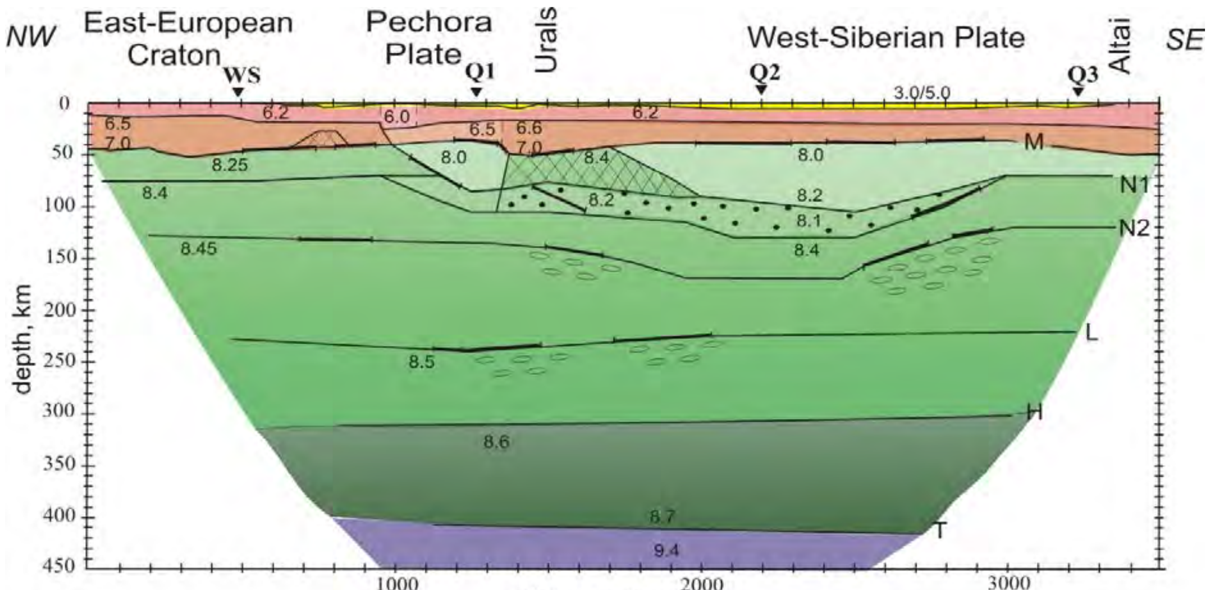

Fig. 5. Velocity cross-sections along the Quartz profile. Legend is in Fig. 3.

A high velocity body is recognizable in the middle crust beneath the Russian platform edge. This indicates that the crust at the EEC edge was significantly transformed by mantle intrusions, which is generally untypical of the northern margin of the platform. A characteristic feature of the crustal structures in the Russian platform – the Urals transition zone is the presence of evident fault zones separating the platform from the Timan Ridge and the Pechora Plate from the Urals. The type of the crust and the Moho structure changes across these zones. Likewise, the upper mantle velocities abruptly change here from 8.25 to 8.0 km/s. This change takes place at the inclined reflector dipping eastward from Moho to a depth of 80 km.

The structure of the Urals is asymmetric. Beneath its western slope, the Moho abruptly dips, forming a bench, while beneath the eastern slope it rises rather smoothly towards the West-Siberian Plate. The upper mantle is also very heterogeneous hear. A layer of anomalously high velocities (more than 8.4 km/s) underlying Moho is revealed beneath the Urals. Overall, the sharpest variations in the upper mantle structure are typical of the Timan–Urals region. Here, velocity variations are significant in both crust and mantle, the crustal thickness also varies, and the reflectors dipping eastward are resolved. Their dip angle evidently reflects the general tendency of tectonic movements in this region, with thrusts overriding the EEC margin.

The structure of the crust and uppermost mantle in the remaining part of the profile is less disturbed. The crustal thickness gradually increases from 40 km under the WSP to 50 km under the Altai, and abrupt changes in the crust type are not observed.

The main feature of the upper mantle structure along the Quartz profile is its significant heterogeneity in the upper 150 km correlating well with large tectonic structures. Higher velocities (over 8.2 km/s) in the upper mantle are characteristic of the East European Craton, the Urals, and the Altai, while smaller values (8.0–8.1 km/s) are observed beneath the Timan-Pechora Plate and West-Siberian plate. Higher velocities (8.4 km/s) are observed in the Urals immediately under Moho. Another characteristic feature of the uppermost mantle structure is the presence of a lower velocity zone at depths of 70–100 km mainly beneath the West Siberian plate). The mantle structure at depth 200-400 km is simple: the boundaries L and H are near horizontal.

Globus, Horizont and Rubin profiles cross the eastern part of the East-European platform, the Urals, the northern parts of the West-Siberian Plate and of the Siberian Craton (**Fig. 1**). On these profiles the records from 8 PNEs were obtained to the offsets 1200-1500 km and the upper mantle structure was studied only down to 150-250 km. The observation system is different in these profiles. The Rubin profile has a dense system of the chemical explosions but only one PNE Ru. The Clobus profile is 1500 km long and 4 PNEs were recorded with the intervals of 400 km between the shot-points. But no chemical explosion was made along the profile. Along the Horizont profile four PNEs were made and only some chemical explosions spared irregularly without covering the eastern part of the profile.

The upper mantle velocity structure does not change strongly along the Globus profile (**Fig. 6b**). A regular increase of the velocities with depth is clearly observed from 8.15 beneath the Moho up to 8.3 km/s at the N1 boundary (depth of 70 km) and up to 8.4-8.5 km/s at the N2 boundary (depth of 120 km).

Along the Horizont profile the longest observations were carried out from the SP H1 and H4 with the offsets up to 1100 km. They served to describe the upper mantle structure to the depths of 140 km. In the western part of the profile the uppermost mantle velocities are 8.0 –8.1 km/s, they are slower than those beneath the central part of the Siberian craton (**Fig. 6c**). The N1 boundary with velocity of 8.35 km/s is determined at the depth of 100 km with the uplift up to 70 km beneath the northern edge of the Urals. The N2 boundary with the velocity of 8.4 km/s is observed at the depth of 110-130 km. A low velocity zone is distinguished above the N1 boundary in the cratonic area.

Along the Rubin profile the mantle waves from the PNE Ru are recorded up to 1500 km distance. The high amplitude reflections from the N1 and N2 boundaries are characteristic for this profile. They have anomalously high apparent velocities: more than 9.0 km/s. The ray-tracing has shown that this wave pattern may be explained by inclinations of the mantle reflectors from the Urals to the west (**Fig. 6a**). The L boundary is almost horizontal in this part of the profile.

Fennolora profile crosses the Fennoscandian Shield from the Barents Sea to the Baltic Sea (**Fig. 1**). This profile is a part of the European Geotraverse which was conducted by a group of European countries within the framework of one of the largest international project (Mueller and Ansorge, 1988; Guggisberg et al., 1991). The Baltic Shield is the geologically and geophysically most studied region of the East European platform. The shield comprises the Archaean part in the north-east, Karelian Craton, while the rest is Paleoproterozoic, Svekofennian domain.

The length of the Fennolora profile is 2000 km and 8 chemical explosions were shot with the interval of 25-30 km. Two explosions (SPs B and I) were made in seas and they were recorded along the whole profile.

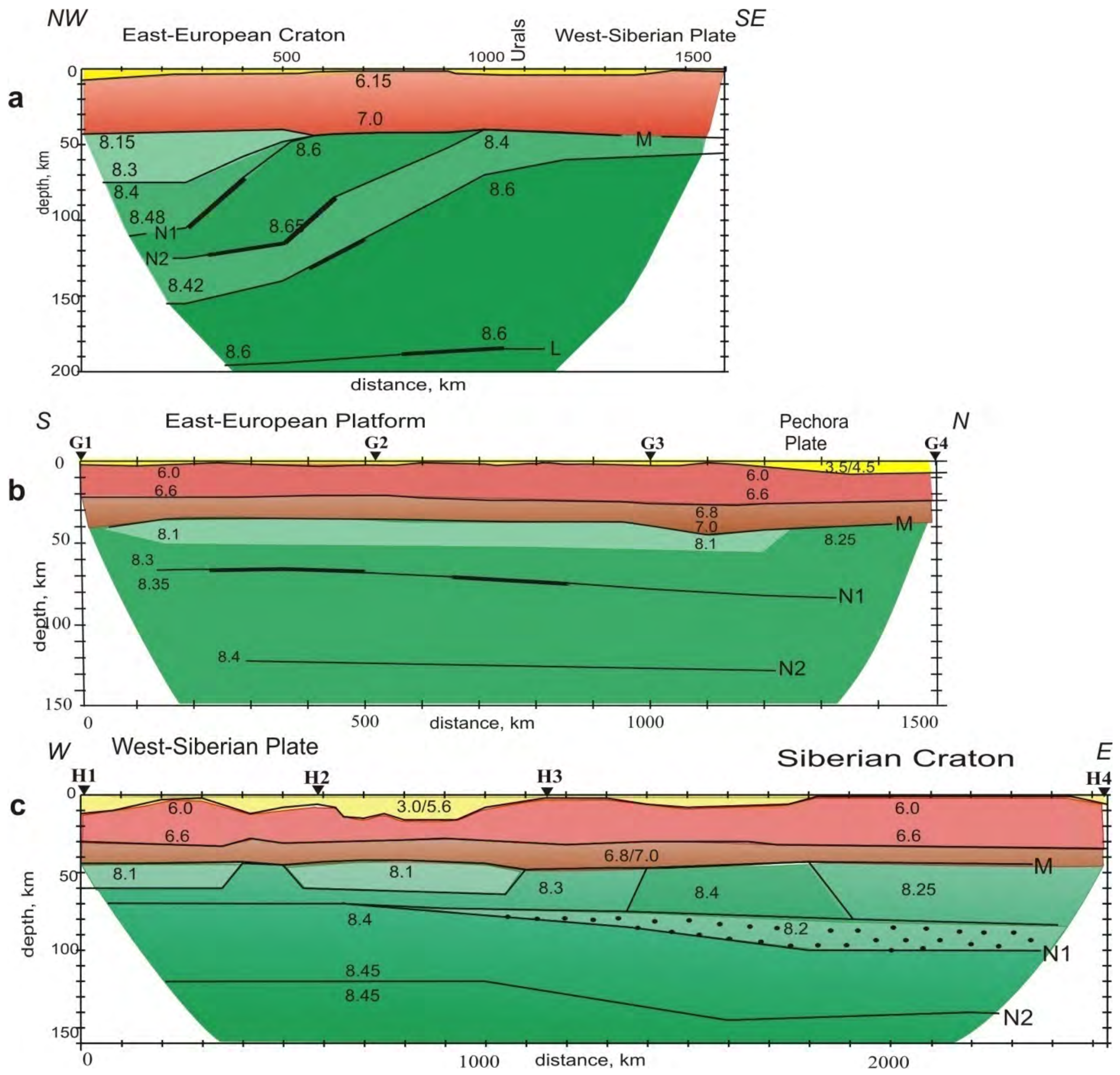

Fig. 6. Velocity cross-sections along the profiles Rubin (**a**), Globus (**b**) and Horizont (**c**) (Fig. 1). Legend is in Fig. 3.

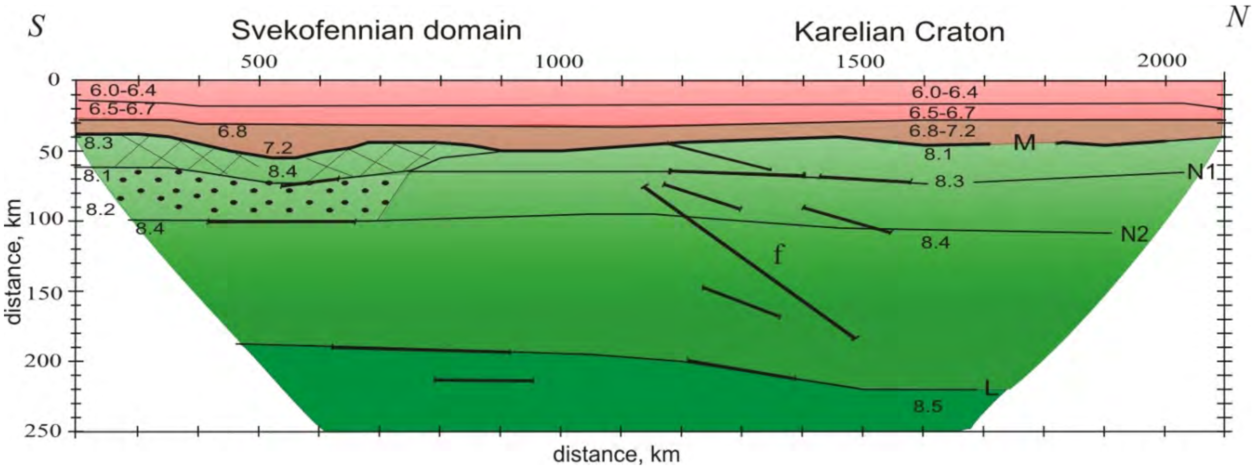

Fig. 7. Velocity cross-sections along the profiles Fennolora (Fig. 1). Legend is in Fig. 3.

The main structural feature of the upper mantle along the profile is the division of the mantle into two large blocks (**Fig. 7**). The deep subsidence of the Moho and the highest velocities (8.3-8.4 km/s) under this boundary are characteristic for the southern block of the profile. The mantle structure in the northern part is smoother and velocities in the uppermost mantle are lower (8.1 km/s). This velocity difference persists up to a depth of 80 km. A lower velocity layer observed at greater depths in the southern part virtually smooths out the lateral velocity variation in the mantle at a depth of about 100 km. The distinguished blocks are separated by a broad disturbed zone with numerous steeply dipping reflectors suggesting here a deep mantle fracture zone.

A certain interrelation is observed between the geologic history of the shield and the structure of the upper mantle along the Fennolora profile. The inferred mantle blocks correspond to the main tectonic domains of the Fennoscandia. The southern block is associated with the Svekofennian province, and the northern block, with the Karelian Craton.

3. The velocity modeling results and their petrophysical interpretation

The 3-D upper mantle velocity model.

The 3-D upper mantle model was compiled from the velocity cross-sections along the profiles. To describe the complicated velocity structure of the uppermost mantle, the map of the velocity distribution at depth of 60 km was constrained (**Fig. 8a**). Beneath the 60-km depth the 3-D model was presented by depth maps of the basic boundaries (**Fig. 8b, c & d**). The model includes three boundaries: N1 with the velocity V = 8.35 km/s, L (V = 8.5 km/s) and H (V = 8.6 km/s). As soon as the velocities are constant along the boundaries and they change linearly between them, such maps describe the velocity model in each point of the 3-D space.

The resulting model characterises the mantle structure of the Northern Eurasia in the following way. Beneath the Moho the velocities change from 8.0-8.2 km/s in the West Siberia to 8.3-8.4 km/s in some blocks of the Siberian Craton and the Urals. Four high velocity blocks are outlined in the uppermost mantle of the Siberian Craton. Three of them are determined from the reliable data of the reversed profiles: the Tunguss block in the area of the profile Meteorite, Rift and Kimberlite, the Vilyui block in the western part of the Vilyui Basin from the Craton and Kimberlite data and Pere-Baikal block in the southern part of the craton from the Rift and Meteorite data. The high velocities are distinguished also along the Horizont profile and in the Urals along Quartz and Rubin profiles. The East-European Platform mantle looks more homogeneous than that of the Siberian Craton. A local high velocity anomaly is observed only in the Fennoscandian Shield. The lowest velocities (8.0-8.1 km/s) are characteristic of the central part of the West Siberia and for the Timan-Pechora Plate. In all the other regions the normal velocities 8.1-8.2 km/s are observed in the uppermost mantle.

The velocity distribution looks otherwise at the depth of 100 km (**Fig. 8b**). The most of the local high velocity anomalies disappear and only two large anomalies are observed: the lower velocities in the central part of the West Siberia and the higher velocities in the Siberian Craton and in the Middle Urals. These structural features follow from N1 boundary depths. They are about 130 km in the central part of the West-Siberian Plate and only 60-70 km in the Middle Urals and beneath the Vilyui Basin in the Siberian Craton.

The depth map of the L boundary (**Fig. 8c**) shows the pictures similar to the map of N1 boundary. There are, however, some differences: L boundary clearly shows that the higher velocity area is concentrated in the central part of the Siberian Craton; the main uplift of the N1 boundary is observed in the eastern part of the craton (**Fig. 8b**).

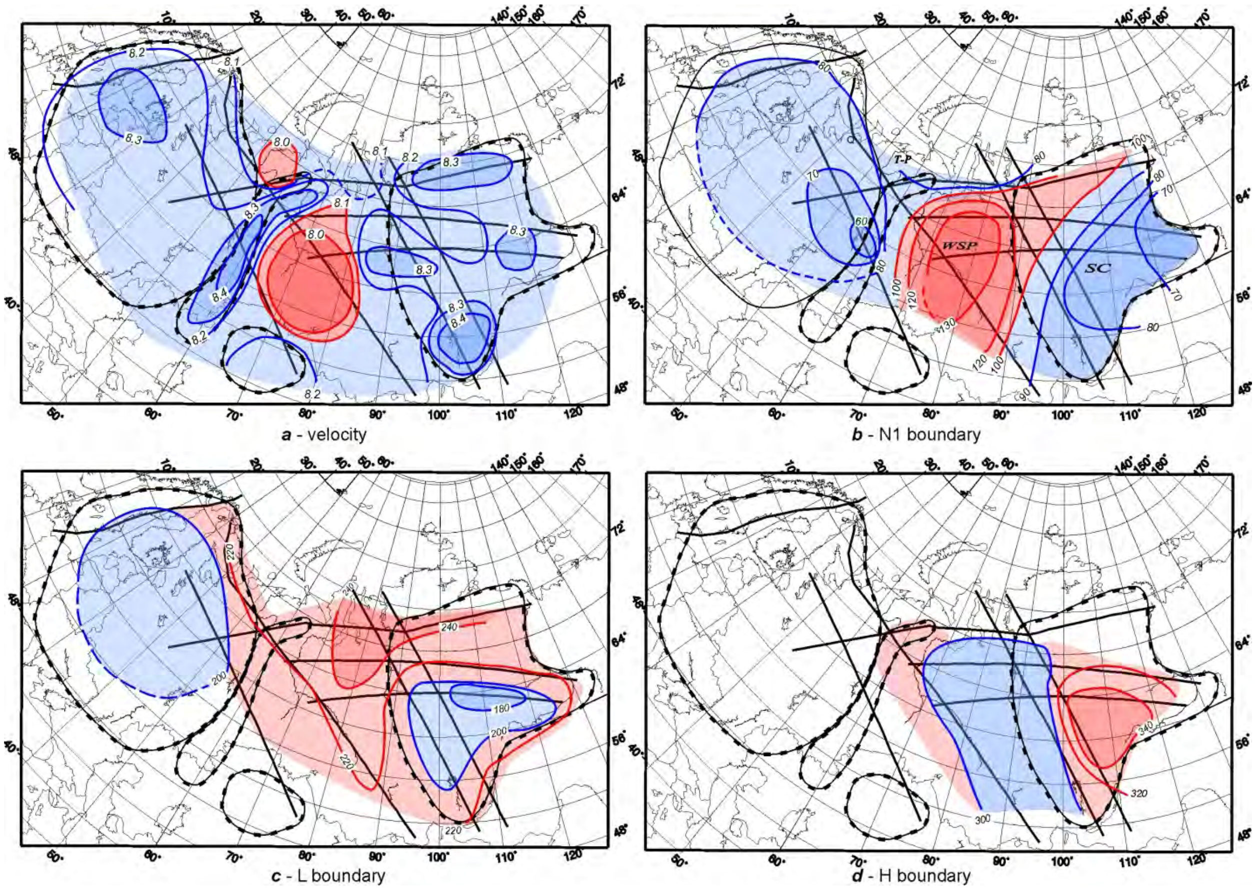

Fig. 8. 3-D velocity model of the upper mantle in the Northern Eurasia in a form of maps showing: **(a)** velocity (km/s) distribution at depth of 60 km; **(b-d)** depths of the mantle boundary N1 (boundary velocity is 8.35 km/s), L (8.5 km/s) and H (8.6 km/s). The tectonic structures (Fig. 1) are contoured by the dotted lines: WSP is the West-Siberian Plate, SC is the Siberian Craton.

The depth map of the H boundary (**Fig. 8d**) reveals an opposite picture: the higher depths beneath the eastern part of the Siberian Craton (330 km) and the depths of 300 km beneath the West-Siberian platform.

Some correlations of the uppermost mantle velocities with tectonics and with geophysical fields are noted. The lower velocities are observed in the areas of higher heat flow (**Fig. 1b**) and in the tectonic active areas. In the West -Siberian and Timan-Pechora Plates, likewise associated with young platforms, the mantle velocities are lower than in the adjacent ancient platforms. Such correlation has been also observed from seismological data (Koulakov and Bushenkova, 2010). This general regularity, however, is violated in the northern part of the Siberian Craton where the upper mantle is characterized by lower velocities although the heat flow is low here as in other parts of the craton. Possibly, the present-day mantle undergoes a high thermal activity in the northern part, but the deep heat has not reached the surface yet. The thermal activity might be related to the proximity of the Arctic shelf: that agrees with the general regularity of decreasing the upper-mantle velocities from the inner to peripheral areas of the continents. This might also be caused by the influence of the Yenisei-Khatanga active area, though the no less active Baikal Rift Zone does not exert such a serious effect on the mantle velocities. The described correlation, however, is not so visible for the deeper parts of the upper mantle, where there is a reverse correlation between the shallow and deep mantle boundaries.

The upper mantle petrophysical characteristics.

Seismic data include information on the composition of the crust and upper mantle, on their thermal regime and on the changes of the physical and mechanical properties of the matter. The main problem of the seismic data interpretation is to divide the effects of the composition and physical components using petrology data and data of other geophysical methods. Possibilities of such interpretation are different for the crust and the upper mantle. For the crust there is a lot of experimental data on its composition and on the physical parameters of the rocks at high PT condition. There are also the deep borehole data on the upper crust composition. Combine interpretation of these data with the geophysical fields enables to determine the detail petrophysical structure of the crust, its horizontal inhomogeneity and the nature of the seismic boundaries. It is presented that the seismic velocities and seismic boundaries characterize mainly the changes in the composition of the crustal rocks. Three basic layers of the consolidated crust demonstrate the changes of the rock composition with depth from the granite-gneiss to granulite-gneiss and to the basic composition. The block structure of the crust also corresponds to the tectonic domains of different composition.

The petrophysical interpretation of the seismic data is much more complicated for the upper mantle. The main difficulty is that the seismic velocities are almost the same for the mantle matter of the different composition (**Fig. 9a**). Another difficulty is the limited geological data on the mantle matter: there are only some mantle xenolith data mainly for the cratonic areas. At such condition the combined interpretation of the geological and geophysical data is necessary to constrain the petrophysical model of the continental upper mantle.

The first stage of the combined interpretation is estimation of the upper mantle composition from the xenoliths data. As follows from the chemical composition of xenoliths from kimberlites in the Siberian and other cratons**,** the lithospheric mantle beneath cratons is significantly depleted (relative to the primitive mantle) in CaO, Al_2O_3 and FeO (Ionov et al., 2010; Kuskov et al., 2014). The depletion of ultramafic rocks decreases with depth because beneath 150–180 km depths an increase in the fertility of mantle xenoliths is observed, i.e., the mantle material becomes gradually enriched with basaltic components. The Siberian xenoliths data show that the most of the sampled xenoliths are common peridotites such as harzburgite and lherzolite, and only a few samples have rather unusual compositions (Boyd et al., 1997; Griffin et al., 1996; Ionov et al., 2010). The laboratory studies of the xenoliths physical parameters at high temperature and pressure (**Fig. 9a**) show that the changes in the upper mantle composition from the fertile substance of the primitive mantle (PM) to the strongly depleted matter (Hzb, Lh, GP) have small effects on the seismic velocities. But the densities of the depleted matter are much lower than that of the primitive mantle (**Fig. 9b**).

As regards the mantle temperature the laboratory studies of the mantle rocks showed that the seismic velocities for the depleted and fertile mantles are very sensitive to temperature: the small changes in the temperature regimes between the heat flows of 35 and 40 mW/m^2 strongly influence both the velocities and densities (**Fig. 9a & b**). That agrees with the observed correlation between the seismic structure of the upper mantle and the heat flow. The high velocity lithosphere of the Siberian Craton is characterized by the low heat flow averaging 38-40 mW/m^2. In the northeastern and central areas of the craton where the mantle velocities increase, the heat flow is estimated at 20–30 mW/m^2.

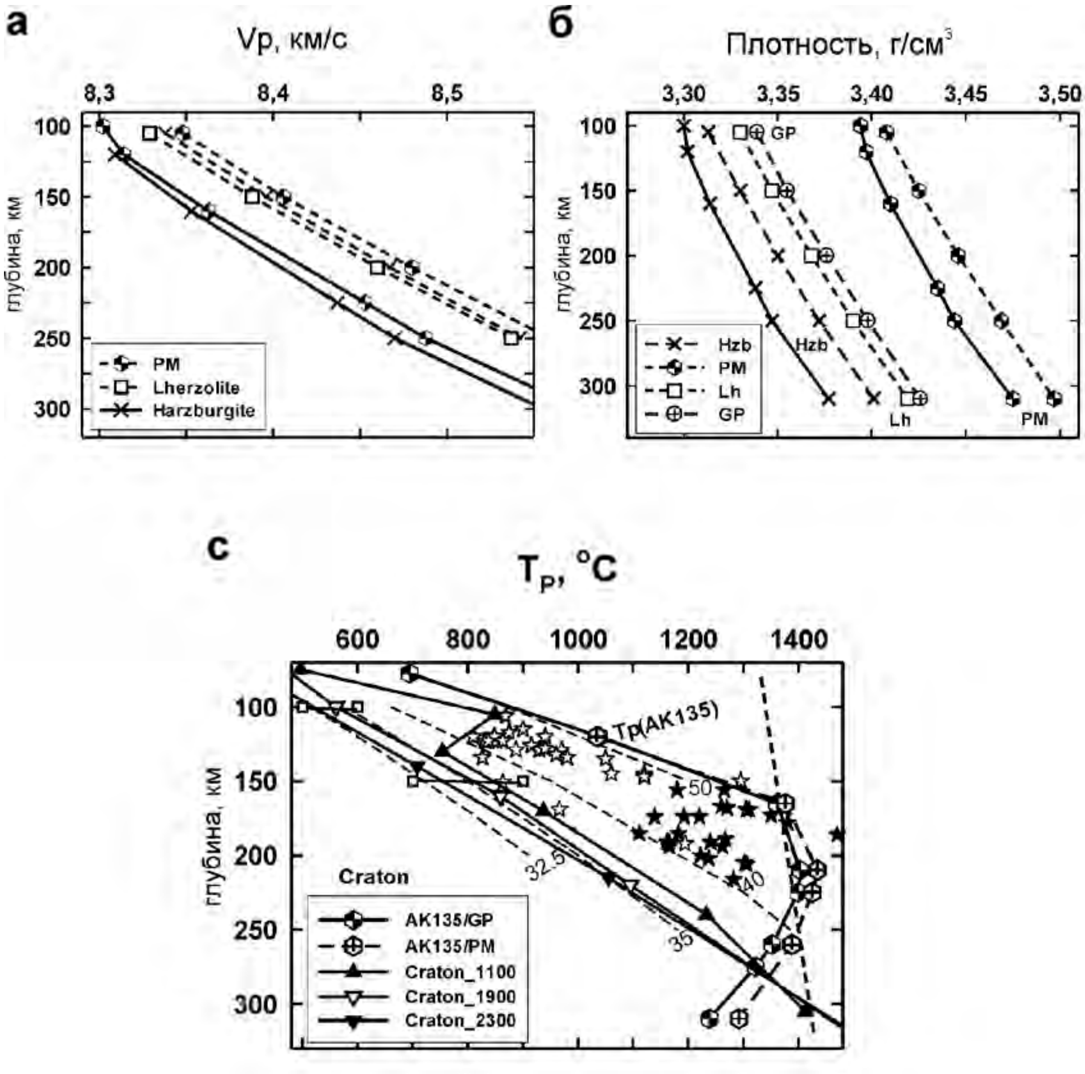

Fig. 9. Comparison of the P-velocities **(a)** and densities **(b)** for garnet harzburgite (Hzb), garnet lherzolite (Lh), average garnet peridotite (GP) and primitive mantle (PM) calculated along conductive geotherms 35 mWm^{-2} (dashed lines) and 40 mWm^{-2} (solid lines). **(c)** Upper mantle temperatures (T_P) beneath the Siberian Craton derived from P-velocity models along the Craton profile at the distance of 1100 km, 1900 km and 2300 km [Kuskov et al., 2014]. The light and dark stars are the P–T parameters for low- and high-temperature xenoliths of garnet peridotites from the kimberlite pipes. The stroke line is the1300°C adiabat. The line T_P(AK135) is an average continental geotherm. The thin stroke lines are the conductive geothermes for the heat flow of 32.5-40 mW/m^2.

Thus, the seismic velocities can be converted to temperature-depth function using the xenoliths data. For the Siberian Craton the deep temperatures were obtained by (Kuskov et al., 2014) from absolute values of velocities, taking into account phase transformations, anharmonicity, and anelastic effects. The bottom of the craton lithosphere was determined at the crossing of the determined temperature-depth curve with the adiabat ones. As a result the 2-D thermal state of the lithospheric mantle was estimated beneath the craton in both vertical and lateral directions by inverting P-velocities from the profiles Craton, Kimberlite, Rift and Meteorite taking into account geochemical constraints on depleted garnet peridotite xenoliths and primitive mantle composition. The temperature profiles present a substantial decrease in temperature beneath the craton with comparison to the average temperature in the surrounding mantle and paleotemperatures inferred from thermobarometry of xenoliths (**Fig. 9c**). The seismically derived temperatures allowed to constrain the thermal structure of the Siberian lithosphere mantle and to show that the craton center is about 50-70°C colder than its marginal parts.

The depth of the thermal lithosphere is close to the 1450°C isotherm and is estimated as 300–330 km thick for all the seismic profiles. The latter agrees with the results of the heat flow data interpretation which indicates that the cratonic lithosphere may be up to 350 km thick (Artemieva and Mooney, 2001).

Density models of the crust and upper mantle.

The next stage of the petrology-geophysical interpretation includes the density modeling. The combined seismic, gravity and surface heat-flow data provide some information about the composition of the deep interior because the fertile composition has significantly higher density than the depleted compositions (**Fig. 9b**).

The gravity field in the Siberian Craton is highly anomalous: against the background of slight negative Bouguer anomaly (~ -10 mGal) of the West-Siberian plate and the East-European platform, the Siberian Craton is clearly distinguished by a strong gravity minimum reaching -100 mGal (**Fig. 10**). This anomaly is a part of the global gravity ring around the Pacific (Choi and Pavlenkova, 2009).

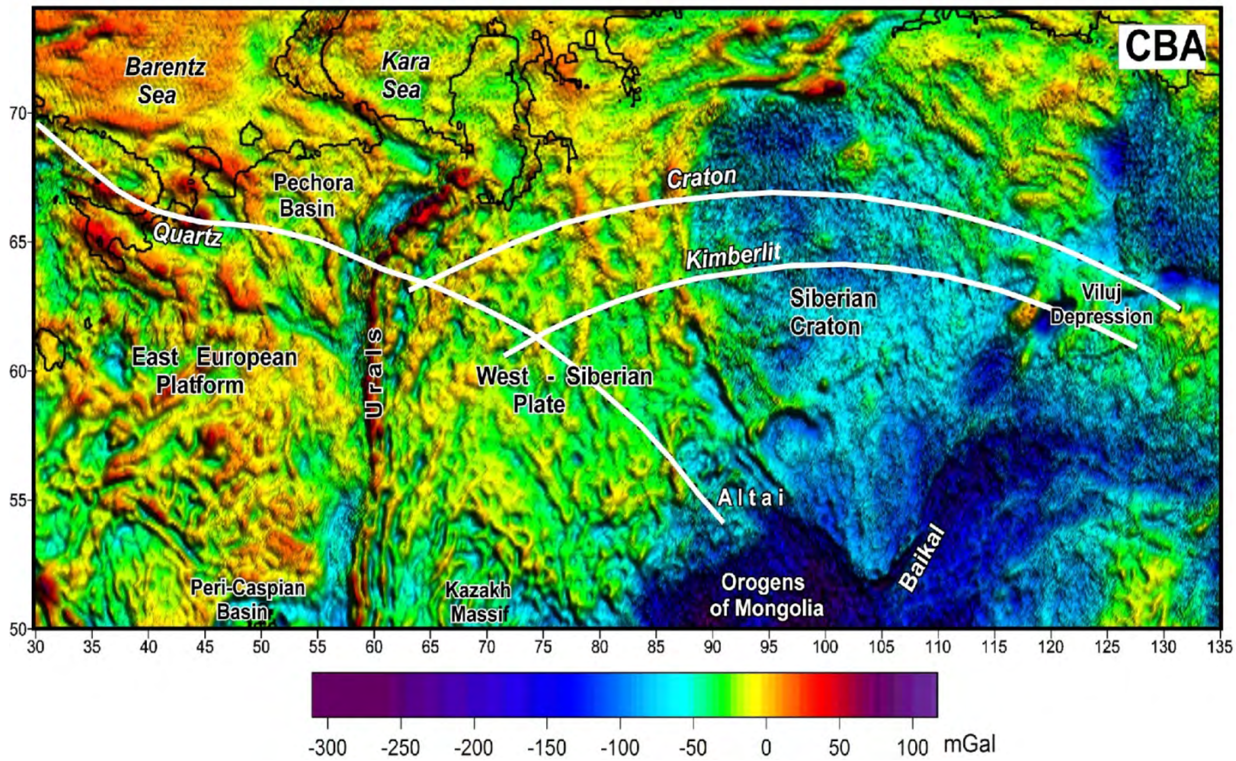

Fig. 10. Gravity field – model EGM2008 – Bouguer anomalies in the Northern Eurasia and the PNE seismic profiles.

The velocity-density modeling for the upper mantle was made for three long-range profiles Quartz, Craton and Kimberlite (Yegorova and Pavlenkova, 2014) (**Fig. 10**). Initial density models for the upper mantle and the mantle transition zone were set up using the relation between P-wave velocity and density of the PREM reference model. The gravity effects of such model were compared with the observed gravity field and if they disagreed the density models were corrected. The results of such modeling are shown in **Fig. 11** for the Craton profile.

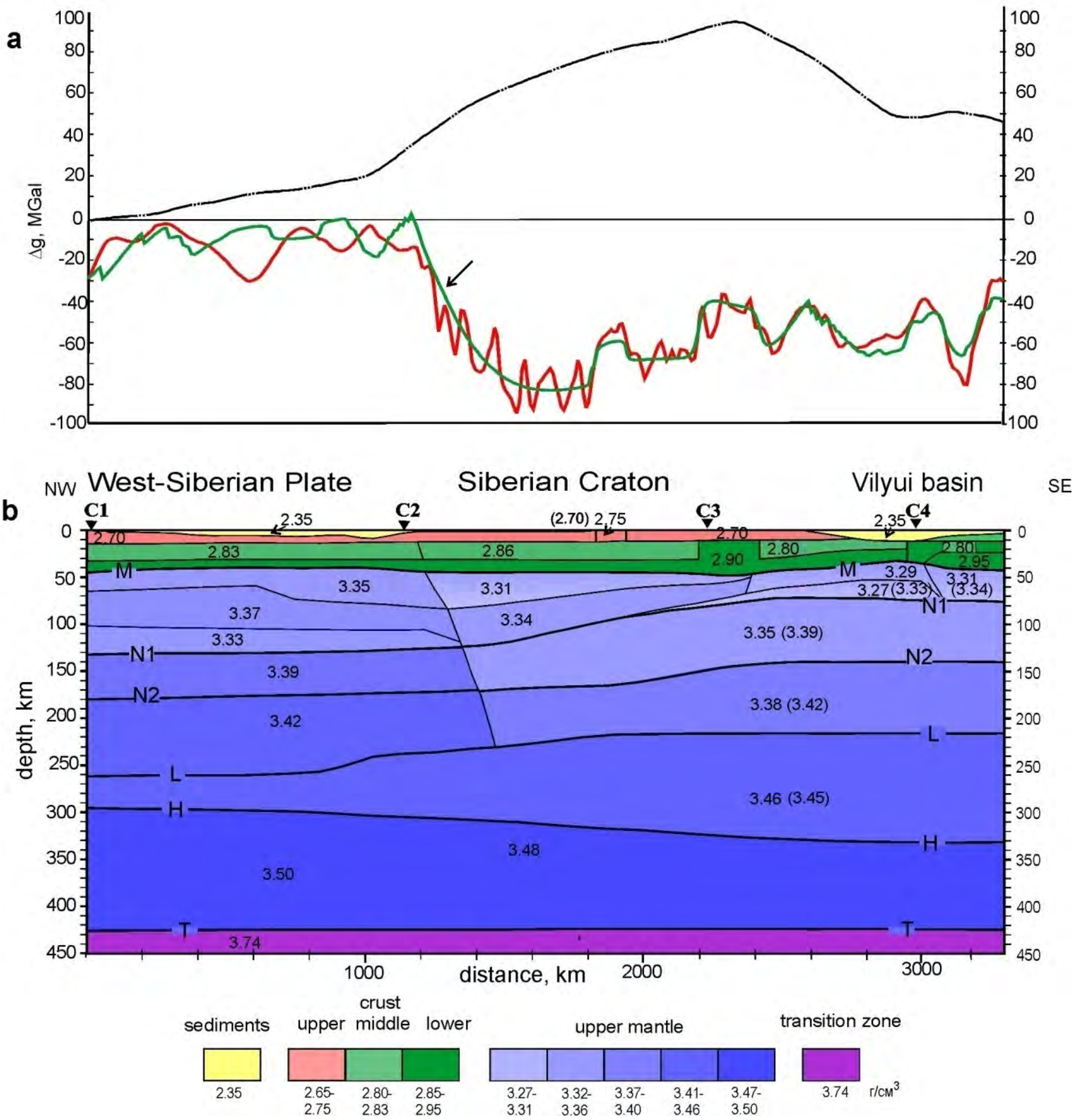

Fig. 11. Results of the gravity modeling along the Craton profile (Yegorova, Pavlenkova, 2014).

(a) Comparison of the observed gravity anomaly (red line) with the calculated ones for the initial model (black line) and the corrected model (green line).

(b) The resulted density model (g/sm^3) of the crust and upper mantle. The initial densities are in the brackets.

The gravity modeling for all the profiles has shown that the effect of the lower part of the upper mantle and transition zone at the depth of 300-670 km is small and can contribute only to regional background level. That is caused by the rather deep location of the seismic boundaries and, in particular, by their flat topography. The final density model for the Quartz profile shows that the thick crust of the East European platform is underlain by uppermost mantle of rather simple structure of 3.34 g/cm^3 density (Vp=8.25 km/s) down to the depth of 75 km (boundary N1). Deeper, a layer with 3.40 g/cm^3 occurred down to seismic boundary N2 at the depth of 130 km. The thick uppermost mantle layer of the lower velocity (8.0-8.1 km/s) occurred down to a depth of 130 km below the West Siberian plate could have, on the contrary, increased densities (3.35 g/cm3).

The velocity-density modeling for the Craton and Kimberlite profiles was more complicate. The calculations for the initial model have shown a strong discrepancy between the calculated and observed gravity fields in the area of the Siberian Craton. Instead of a gravity low above the craton (the red line in

Fig. 11a) an intense gravity maximum up to 100 mGal (the black line in **Fig. 11a**) was obtained. It became evident that without corrections with decreasing densities in the upper mantle of the craton it is impossible to explain the observed gravity low. Such density decrease was accepted down the L boundary at 210-250 km depth that could be related with variations in composition (from depleted to fertile mantle) (Kuskov et al., 2006 and 2014).

Thus, the gravity modeling, performed along the PNE seismic profiles revealed significant distinctions in the upper mantle of the Northern Eurasia. The upper mantle of the low heat flow Siberian Craton is characterized by the higher velocities and by the lower densities. The East-European Platform of the same age and of the same heat flow as the Siberian Craton is characterized by the higher upper mantle velocities and by the normal densities. Our modeling shows that the upper mantle below young West Siberian plate with the heat flow of 60 mW/m^2 has the decreased velocities and increased densities in comparison with the old platforms. That proposes decreasing of the depleted mantle thickness beneath the areas around the Siberian Craton.

The lithosphere-asthenosphere system.

The nature of lithosphere-asthenosphere system is complicate and unsolved problem [Fuchs, Froidevaux, 1987; Eaton et al., 2009]. The low velocity zone in the upper mantle was usually interpreted as zone of partial melting (“thermal” asthenosphere). As shown above, such interpretation is difficult for the old platform areas. Beneath the Siberian Craton a zone of partial melting was supposed from heat flow data at the depths of 250-300 km (Artemieva and Mooney, 2001), but the low velocity zones are not revealed at these depths. More over such zones are observed at depth of about 100 km (**Figs. 3-5**).

A question follows, what is the origin of these zones in the cold cratonic mantle? The most probable answer is that the decreasing of the velocity dues to changes of the mechanical properties of the mantle matter and increasing the fluids content (Willie, 1970; Pavlenkova, 1988, 1996 and 2011; Thybo and Perchuc, 1997). The sharp changes of physical or mechanical properties of the matter: porosity, permeability, fissuring, transition from solid state to liquid through creep, transition into the state of true plasticity and other physical transformations. An increase or a decrease in porosity is invariably followed by a change in fluid content, which may cause the beginning of different physicochemical matter transformation, such as new degrees of metamorphism, and stimulate partial melting of material at relatively low temperature. The laboratory study of the fluids transportation through the mantle rocks at the high pressure and temperature confirm such transformation (Lebedev et al., 2017). The matter transformation can also explain the nature of the N1 and N2 boundaries, observed usually beneath the low velocity layers

Comparison of the seismic data with other geophysical data confirms such origin of the lower velocity layers: in many regions such uppermost mantle layers are characterized by higher electrical conductivity (Jones at al., 2009).

The long-range seismic profiles put another question – what is an origin of mantle reflected boundaries L and H? May be they are lithosphere-asthenosphere boundary? The existence of the regional seismic boundaries in the upper mantle was an unexpected result because it looks unrealistic to find the regular and strong velocity contrasts in the upper mantle which velocities do not depend on the matter composition. No phase transitions were revealed at the depths where the boundaries are traced.

None of the reference boundaries is the first order discontinuity: the waves from these boundaries are of the complicated multi-phase groups with long coda (**Fig. 2**). The wave cross-section of the boundary constrained by migration of such multi-phase wide angle reflections shows that it is not a sharp boundary but the complicate reflective zones with alternating of high- and low-velocity layers. Average velocity contrasts are not high at the boundaries but they are high within the thin layering. The similar interpretation of the many phase reflections is given by the other authors: Egorkin et al. (1987) and Morozov et al. (1999) show the corresponding mantle boundaries as thin low velocity layers.

It may be proposed (Pavlenkova, 2011) that such upper mantle boundaries appear as the physical boundaries which are, like the low velocity layers, represented by sharp changes of mechanical properties of the matter and the change in fluid content, which may stimulate partial melting and mobility of material at relatively low temperature (Kern, 1993). The matter flow along these weak low velocity zones may assist the formation of the anisotropic high velocity intermediate layers. The Lehmann (L) discontinuity was often considered as the base of an anisotropic layer.

Another specific feature of the mantle complicated boundaries is revealed from the xenoliths data: the xenoliths from the Siberian Craton kimberlites taken from the depths of these seismic boundaries have indications of film melting. The generalization of the data all over the world shows that the most part of the xenoliths comes from the depths around 100, 150 and 200 km which are close to the average depths of the regional seismic boundaries N1, N2 and L. The latter characterize these boundaries as high strain zones.

Some other specific features may be noted for the mantle boundaries**.** The 2-D and 3-D seismic modeling reveals some peculiarities of these boundaries which may be interpreted as a change of the upper mantle rheology. The N1 and N2 boundaries, or N transition zone, divide the lithosphere in two portions with different inner structure. Above this zone the sub-Moho lithosphere has complex block structure (**Figs. 3-7**), beneath the blocks disappear. As noted above, in many regions these boundaries underline the low velocity layers. These characteristics indicate the N zone as a bottom of the brittle part of the lithosphere (the mechanical but the “thermal” lithosphere). Beneath this zone the lithosphere material is more plastic and cannot preserve its own inhomogeneity.

The change of the rheology, which may be interpreted as the lithosphere bottom, is visible beneath the H boundary. As mentioned above the waves from the boundary attenuate in many record-sections and the low velocity gradient may be proposed beneath the boundary. The Q factor which has been determined from the mantle wave spectrums decreases at depths of 250-300 km (Egorkin and Kun, 1978). These values agree with the lithosphere bottom determination from **Fig. 9c** (the Siberian craton geotherm crosses the 1300^o adiabat at depth 300 km). And finally, the increasing of the plasticity below these depths follows from structural features of the L and H boundaries. The H boundary has the reverse form relatively to the L boundary (**Figs. 3 and 4**), and it means that the matter at these depths can flow to create the isostatic equilibrium of the upper mantle.

Comparison of the deep earthquake distribution with depth indicates another peculiarity of the upper mantle boundaries. In different tectonic regions, inside the continents and in the continental margins, the most earthquakes are located at depths of around 100 and 200 km where we determine these regional seismic boundaries. For instance, the earthquake distribution in the Tian-Shan, Pamir and Kamchatka regions shows two maximums at depths of 100 and 200 km. The international projects ANCORP and CINCA show the same pictures in the earthquake distribution in the Benioff zones of the western margin of the American continents: two clusters of seismicity occur at 90-110 and 190-250 km depths.

The correlation the xenoliths origin depths and the earthquake clusters with the regional mantle boundaries (thin layering zones) is not an accidental correlation, and it shows that the depths of the regional boundaries are critical depths where some regular transformations of the deep fluids and mantle matter happen. The deep earthquakes which are concentrated around the depths of 100 and 200 km may be a result of deep fluids decompression and detonation at these critical PT levels.

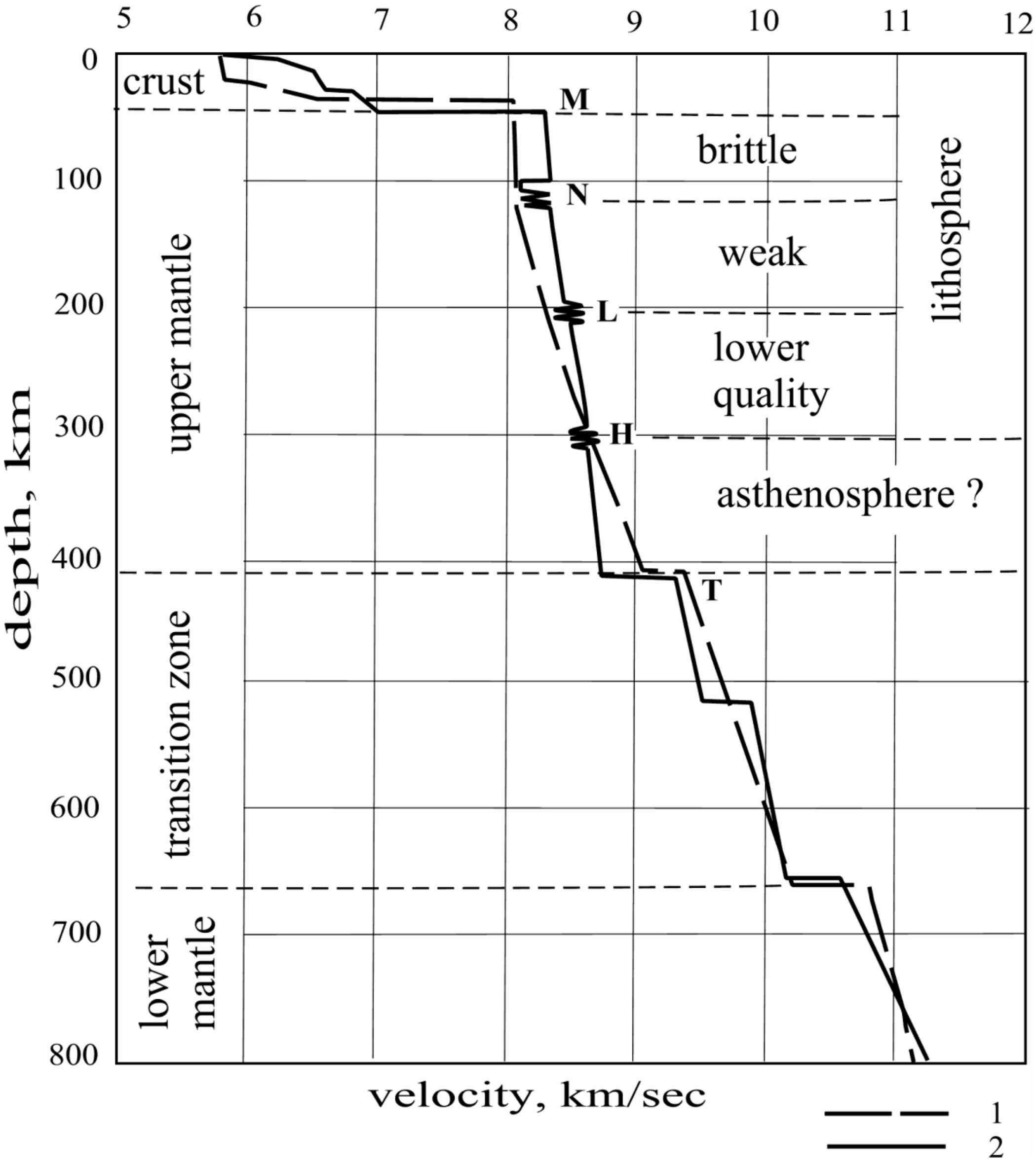

Fig. 12. Generalized 1-D velocity model of the Northern Eurasia upper mantle (1) in comparison with the model IASP91 (Kennett, Engdahl, 1991). (2). Seismic boundaries N, L and H are shown as the multi-layered zones.

Thus, the combined interpretation of the petrological and geophysical data gives a possibility to constrain the basic petro-physical models for the upper mantle of the Northern Eurasia and to explain the main tendencies of the seismic velocity changes with depth. These main results are presented in **Fig. 12** in form of the generalized 1-D velocity model. The model shows the upper mantle velocities to increase gradually with depth from 8.2 to 8.7 km/s. Only a little bit higher vertical velocity gradient is observed in the depth interval 50-200 km. Three main boundaries are identified in the upper–lower mantle transition zone the upper–lower mantle transition zone at depths 420, 520 and 640 km. The model differs from the IASP91 model by the higher velocities in the uppermost mantle and by the lower velocity at the depths of 300-400 km.

Conclusion.

The results of collection and analysis of seismic data received from the long-range seismic profiles in the Northern Eurasia reveal many new structure features of the continental upper mantle. All profiles with total length of more than 25000 km including 26 PNEs and many large chemical explosions were interpreted using the common methodology. The 2-D velocity models of the crust and upper mantle along the profiles

(**Figs. 3-7**) and a 3-D velocity model of the upper mantle (**Fig. 8**) were constructed. The main results of their interpretation are the following.

1. The crust and the upper mantle of the Northern Eurasia are significantly heterogeneous both vertically and laterally. This is expressed as variations in seismic velocities, topography of seismic boundaries, and a degree of layering and local heterogeneity. The lithosphere structure along the most of profiles may be described by a block-layered model which suggests a combination of almost horizontal stratification (layering) divided by several blocks. The block structure usually reflects the tectonics. The strongest changes in the crustal structure correlate with the large tectonic domains of different ages: the East-European Craton, the Urals, the young West-Siberian Plate and the Siberian Craton. Higher velocities in the uppermost mantle are typical for the cratons. The Urals is also characterised by high velocities beneath the Moho but its deeper structure is closer to the young platforms. The velocity differences between the small geostructures are observed down to 100-120 km and between the large tectonic domains - down to 200-250 km. The close correlation is determined between the uppermost mantle velocities and heat flows. In the areas with the low heat flow the upper mantle velocities are higher; higher heat flow regions are correlated with the lower mantle velocities.

2. Several regional reflecting boundaries are traced in the large areas of the Northern Eurasia. They are N1 boundary (the boundary velocity of 8.35 km/s, depths of 75-120 km), the N2 boundary (8.4 km/s, the depths of 140-170 km), the L boundary (8.5 km/s; 180- 240 km) and H boundary (8.6 km/s; 280-300 km). The waves from these boundaries are the complicated multi-phases groups with long coda which characterise the corresponding boundaries as high reflective zones with alternating of high- and low-velocity layers. Average velocity contrasts are not sharp at the boundaries (0.0- 0.1 km/s) but they are big within the thin layering. The nature of these boundaries and of velocity inversion zones may be explained as the high strain zones and as zones of deep fluids concentration at some critical depths.

3. The combined petrophysical interpretation of the seismic cross-sections, the xenoliths data and the geophysical fields provide the estimation of the upper mantle composition and the temperature regime (**Fig. 9**). The temperature profiles present a substantial decrease in temperature beneath the cratons as compared to the surrounding mantle. Comparison of the 3-D upper mantle velocity model with the gravity field shows a change of the composition beneath the Siberian Craton which is characterized by negative gravity anomaly (**Fig. 10**). The latter proposes the depleted upper mantle beneath the craton.

4. It is difficult to present the observed stratification of the upper mantle in the traditional lithosphere-asthenosphere model. According to the heat flow data in the northern Eurasia the “thermal” lithosphere is limited at the depth about 350 km (Artemieva and Mooney, 2001). The upper-mantle velocity models show the absence of lower velocities which could be related to the matter of the partial melting. The change of the rheology, however, may be proposed at this depth: the H boundary has a form reverse to L boundary. The latter means that the matter at these depths can flow to create the isostatic equilibrium of the upper mantle and it is possible to consider the H boundary as the lithosphere bottom (**Fig. 12**).

The presented data show the lithosphere to be rheologically stratified. At depths of 200-300 km beneath the L boundary the Q factor decreases. Strong changes of the rheology may be supposed at depth of 100-120 km where the lithosphere is divided into two portions with different inner structure: the sub-Moho lithosphere is complex, laterally inhomogeneous, and its structure appears to be less complex beneath 100-120 km.

5. The observed features of the upper mantle structure indicate a great role of the deep fluids advection for the formation of the thick continental lithosphere. The long process of the removal of the silica, alkalis, fluids and incompatible elements in the crust should lead to the depletion of mantle rocks and their crystallization. The longer this process continues - the thicker become the crust and the mantle lithosphere. Further gradual cooling makes the upper mantle more stable, promoting the formation of the less density lithosphere compared to the oceanic areas.

All these data were important for the development the new global tectonic conception described in Pavlenkova (2015).

Aknowledgements: I would like to thank David Pratt and Dong Choi for their consideration, useful advices and critical remarks to my papers.

References

Artemieva, I.M. and Mooney, W.D., 2001. Thermal thickness and evolution of Precambrian lithosphere: a global study // *Journal of Geophysical Research* 106 (B8), p. 16387-16414.

Benz, H.M., Huger, J.D., Leith, W.S., Mooney, W.D., Solodilov L.N., Egorkin A.V. and Ryaboy, V.S., 1992. Deep seismic sounding in Northern Eurasia. *EOS*, 73, p. 297-300.

Boyd, F.R., Pokhilenko, N.P., Pearson, D.G., Mertzman, S.A., Sobolev, N.V. and Finger, L.W., 1997. Composition of the Siberian cratonic mantle: evidence from Udachnaya peridotite xenoliths. *Contrib. Mineral. Petrol*., v. 128, p. 228-246.

Cermak, V., 1985. Thickness of the lithosphere of the USSR territory from geothermal data. *Geology and Geophysics*, № 5, p. 33-40.

Choi, D.R. and Pavlenkova N.I., 2009. Geology and tectonic development of the Pacific Ocean. Part 5. Outer low gravity belt of the Great Pacific Ring structure. *NCGT Newsletter*, no. 50, p. 46-55.

Cipar, J.J., Priestley, K., Egorkin, A. and Pavlenkova, N., 1993. From rift to rift: the Yamal Peninsula – Lake Baikal deep seismic sounding profile. *Geophys. Res. Lett*., v. 20, p. 1631-1634.

Eaton, D.W., Darbyshire, F., Evans, R.L., Grütter, H., Jones, A.G., Yuan X., 2009. The elusive lithosphere–asthenosphere boundary (LAB) beneath cratons. *Lithos*, v. 109, p. 1-22.

Egorkin, A.V., 1999. Study of the mantle by superlong geotraverses. *Izvestiya, Physics of the Solid Earth*, № 7-8, p. 114-130.

Egorkin, A.V. and Kun, V.V., 1978. P-wave absorption in the upper mantle of the Earth. *Isvestija, Physics of the Solid Earth*, № 4, p. 25-36.

Egorkin, A.V., Zuganov, S.K., Pavlenkova N.A. and Chernyshev, N.M., 1987. Results of lithosphere studies from long-range profiles in Siberia. *Tectonophysics*, v. 140, p. 29-47.

Fuchs, K. (ed.), 1997. Upper Mantle Heterogeneities from Active and Passive Seismology. NATO ASI series. Kluwer Academic Publishers, Dordrecht–Boston–London. V. 17, 366p.

Fuchs, K. and Froidevaux, C. (eds.), 1987. Composition, Structure and Dynamics of the Lithosphere-Asthenosphere Systems. Geodynamic Series, 16, International Lithosphere Program Contribution. Washington D.C. 327p.

Griffin, W.L., Kaminsky, F.V., Ryan, C.G., O'Reilly, S.Y., Win, T.T. and Ilupin, I.P., 1996. Thermal state and composition of the lithospheric mantle beneath the Daldyn kimberlite field, Yakutia. *Tectonophysics*, v. 262, p. 19–33.

Guggisberg, B., Kaminski, W. and Prodehl, C., 1991. Crustal structure of the Fennoscandian Shield, a traveltime interpretation of the long-range FENNOLORA seismic refraction profilev. *Tectonophysics*, v. 195. №s 2/4, p. 105-137.

Ionov, D.A., Doucet, L.S. and Ashchepkov, I.V., 2010. Composition of the lithospheric mantle in the Siberian Craton: new constraints from fresh peridotites in the Udachnaya-East kimberlite. *Jour. Petrol.,* v. 51, p. 2177–2210.

Jones, A.G., Evans, R.L. and Eaton, D.W., 2009. Velocity–conductivity relationships for mantle mineral assemblages in Archean cratonic lithosphere based on a review of laboratory data and Hashin–Shtrikman extremal bounds. *Lithos*, v. 109, p. 131-143.

Kennett, B.L.N. and Engdahl, E.R., 1991. Traveltimes for global earthquake location and phase identification. *Geophysical Journal International*, v. 105, p. 429-465.

Kern, H., 1993. P and S-wave anisotropy and shear wave splitting at pressure and temperature possible mantle rocks and their relations to the rock fabric. *Phys. Earth Planet. Inter*., v. 78, p. 245-256.

Koulakov, I. and Bushenkova, N., 2010. Upper mantle structure beneath the Siberian craton and surrounding areas based on regional tomographic inversion of P and PP travel times. *Tectonophysics*, v. 486, p. 81-100.

Kuskov, O.L., Kronrod, V.A., Prokofyev, A.A. and Pavlenkova, N.I., 2014. Thermal and density structure of the Siberian craton lithospheric mantle inferred from long-range seismic profiles Craton, Kimberlite, Rift and Meteorite. *Tectonophysics*, v. 615-616, p. 154-166.

Lebedev, E.B., Pavlenkova N.I. and Lukanin O.A., 2017. Experimental Study of the Influence of Water on Elastic Wave Velocities in Dunite and Serpentinite (on the Nature of the Low-Velocity Zone in the Upper Mantle of the Earth). *Doklady Earth Sciences*, v. 472, Part 1, p. 49–52.

Lehmann, I., 1964. On the velocity of P in the upper mantle. *Bulletin of the Seismological Society of America*, v. 54, p. 1097-1103.

Mechie, J., Egorkin, A.V., Fuchs, K., Riberg, T., Solodilov, L.N. and Wenzel, F., 1993. P-wave mantle velocity structure beneath Northern Eurasia from long-range recordings along the profile QUARTZ. *Phys. Earth Planet. Inter*., v. 79, p. 269-286.

Morozov, I.B., Morozova, E.A., Smithson, S.B. and Solodilov, L., 1999. Heterogeneity of the uppermost mantle beneath Russian Eurasia from the ultralong-range profile Quartz. *Jour. Geophys Res*., v. 104(B9). p. 20329-20348.

Mueller, St. and Ansorge, J., 1988. Deep seismic sounding of the mantle lithosphere . G. Nolet and B. Dost (eds.), European Geotraverse (EGT) Project, the upper mantle. ESF, Strasbourg, p. 63-76.

Nielsen, L. and Thybo, H., 1999. Seismic tomographic inversion of Russian PNE data along profile Craton. *Geophys. Res. Lett*., v. 26, № 22, p. 3413-3416.
Pavlenkova, G.A. and Pavlenkova, N.I., 2006. Upper mantle structure of the Northern Eurasia from peaceful nuclear explosion data. *Tectonophysics*, v. 416, p. 33-52.
Pavlenkova, G.A., Priestly, K. and Cipar, J.J., 2002. 2-D model of the crust and uppermost mantle along Rift profile, Siberian craton. *Tectonophysics*, v. 355, p. 171-186.
Pavlenkova, N.I., 1988. The nature of seismic boundaries in the continental lithosphere. *Tectonophysics*, v. 154, p. 211-255.
Pavlenkova, N.I., 1996a. Crust and upper mantle structure in Northern Eurasia from seismic data. Advances in Geophysics, Academic Press, Inc. (Eds. Dmowska, R. and Saltzmann, B.), v. 37, p. 1-133.
Pavlenkova, N.I., 1996b. General features of the upper mantle stratification from long-range seismic profiles. *Tectonophysics*, v. 264, p. 261-278.
Pavlenkova, N.I., 2011. Seismic structure of the upper mantle along the long-range PNE profiles ─ rheological implication. *Tectonophysics*, v. 508, p. 85-95
Pavlenkova, N.I., 2015. Degassing and expanding Earth: new model of global tectonics. *NCGT Journal*, v. 4, n. 4, p. 489-515.
Pavlenkova, N.I. and Pavlenkova, G.A., 2014. The Earth's crust and upper mantle structure of the Northern Eurasia from the seismic profiling with nuclear explosions. Moscow, GEOKART: GEOS.
Priestly, K., Cipar, J., Egorkin, A.V. and Pavlenkova N.I., 1994. Upper mantle velocity structure beneath the Siberian Platform. *Geophys. Jour. Int.*, v. 118, p. 364-378.
Ryberg, T., Wenzel, F., Egorkin, A.V. and Solodilov, L., 1998. Properties of the mantle transition zone in northern Eurasia. *Jour. Geophys. Res*., v. 103, № B1, p. 811-822.
Thybo, H. and Perchuc, E., 1997. The seismic 8^0 discontinuity and partial melting in continental mantle. *Science* v. 275, p. 1626-1629.
Wyllie, P.J., 1970. Low-velocity zone of the Earth's mantle: incipient melting caused by water. *Science,* v. 169, p. 764-766.
Yegorkin, A.V. and Pavlenkova, N.I., 1981. Studies of mantle structure of USSR territory on long-range seismic profiles. *Physics of the Earth and Planetary Interior*, v. 25, p. 12-26.
Yegorova, T.P. and Pavlenkova, G.A., 2014. Structure of the upper mantle of Northern Eurasia from 2-D density modelling on seismic profiles with peaceful nuclear explosions. *Tectonophysics*., v. 627, p. 57-71.

The saga of India's drift and supra-subduction origin of the ophiolites on its northwestern margin, Pakistan

Ghulam Sarwar* and Yasir Shaheen Khalil**

* Independent consultant, Houston, Texas, USA (gsarwar45@gmail.com)
** Geoscience Labs, Geological Survey of Pakistan, Islamabad, Pakistan (yasirshaheen2189@gmail.com)

(Since the dawn of humanity man has created myths about his world and beyond – he is still at it).

Abstract: According to Plate Tectonics theory (PT), it is believed that, in the aftermath of Gondwana rifting, India drifted northward across a vast Tethys and collided with the various Eurasian blocks and arcs. There are, however, serious geological arguments against India's drift across a supersized Tethys and its isolation from other landmasses for most of the Cretaceous period. This is not supported by the relevant stratigraphic and paleontological data.

Similarly, there are strong geological arguments against the idea that the ophiolites on the northwestern margin of Indian Plate at Bela (BO), Muslim Bagh (MBO) and Waziristan (WO) were formed in a Supra- Subduction Zone (SSZ) environment. The (SSZ) origin claims are based on mafic rock chemistry alone and pale in front of solid field observations, basin analysis and geodynamic considerations. There is hardly any evidence for the existence of a subduction zone where it is needed (i.e. east of the Chaman-Ornach-Nal faults). For example, the subophiolitic (Kanar) Mélange contains a multitude of mountain size blocks with little penetrative internal deformation, indicating that the mélange formed by tectonic deformation in shallow crustal conditions and not in any grinding deep subduction grade environment.

Also, the ophiolite belt seems to have been subjected only to garnet-amphibolite grade regional metamorphism - no proof for a subduction zone accretionary wedge metamorphism. The Waziristan, Muslim Bagh and Bela Ophiolites do not support the past existence or disappearance of a Tethys of colossal size. Instead they may simply be remnants of a much smaller Late Mesozoic oceanic basin - possibly a narrow linear trough running along the northwestern margin of India - that collapsed due to convergence between India and its neighboring blocks to the west along an otherwise transform margin.

Keywords: *India's drift, Tethys, ophiolites, supra-subduction, problems*

(Received 3 November 2016. Accepted 5 February 2017)

Introduction

The intent of this paper is to scrutinize the controversial application of plate tectonics (PT) to the movements of Indian Plate in the aftermath of Gondwana breakup. Related to India's northward drift is the problem of subduction of Tethyan oceanic crust and the origin of ophiolites and mélange deposits on the northwestern margin of the Indian Plate. Some of the field relationships, litho-stratigraphic and litho-tectonic aspects - crucial in determining mélange genesis and their lack of support for the (SSZ) models - are also discussed.

Northward drift of India and subduction of Tethys

Numerous PT enthusiasts (e.g., Cande and Stegman, 2011 and Cande et al., 2010) have discussed northward subduction of the Tethyan oceanic crust of the Indian Plate under Eurasia. Some have even invoked double subduction to explain high rate of subduction of as much as 140 mm per year (Jagoutz et al., 2015). So, let us take a cursory look at what we are supposed to believe when it comes to disappearance of Tethys due to subduction.

According to the proponents of PT, the Indian Plate - a part of the Gondwana Supercontinent (**Fig. 1**) during Permian through Middle Jurassic - gradually rifted and drifted northward, colliding first with the Kohistan-Laddakh Arc and finally with Asia, in the Early Eocene. So, all told, it is believed to have travelled some 9000 kms in 160 million years (Dietz and Holden, 1970; Chatterjee and Scotese, 1999, Chatterjee, et al., 2013). We are therefore led to believe, that nine thousand kms of Tethyan oceanic crust (**Fig. 1**) simply vanished by subduction, leaving only small ophiolitic remnants along its northern, northeastern and northwestern margins. This is simply too hard to swallow, especially considering all the physical problems involved in subduction (see Choi, 2006 and Pilchin, 2016, for example).

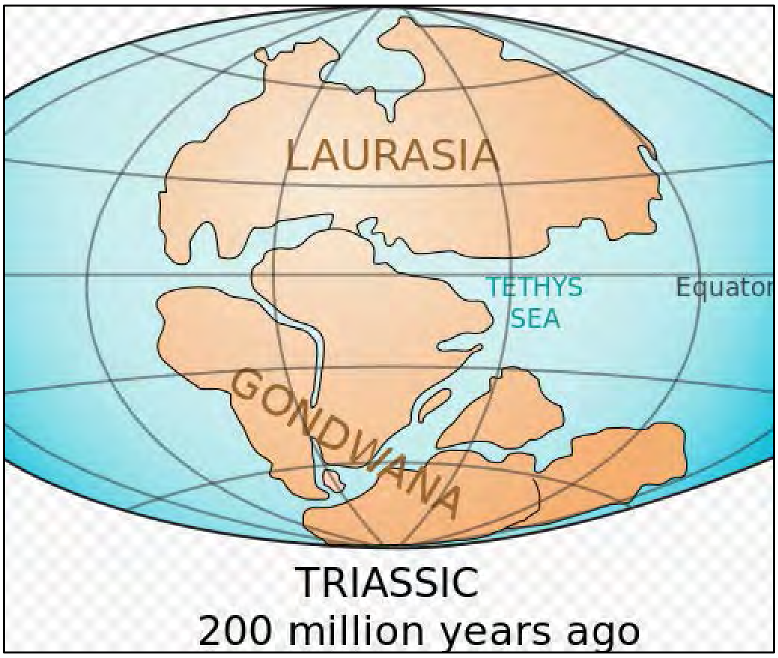

Fig. 1. According to the Plate Tectonic theory breakup of Permian supercontinent Pangaea resulted in Laurasia and Gondwana fragments with the vast Tethys Sea in between (Late Triassic map from Wikipedia).

Biotic evidence against long-term isolation of India

Long-term isolation of India, between its rifting and collision with Eurasia, is also not supported by the fossil evidence. Gondwana type Permo-Triassic vertebrate fossils have been reported from Tien Shan and the Turfan Basin in the Xinjiang province of northwestern China (Sun Ai-Lin, 1972). Several basins in India, such as the Satpura, Damodai, Son-Mahanadi and Pranhita-Godavari, have also yielded a rich assemblage of Gondwana vertebrate fauna of Permian-Middle Jurassic age from nine different horizons, showing that India was clearly a part of the Pangaean domain (Bandyopadhyay, 1999). Colbert (1973) noted the abundance of Early Jurassic and Late Cretaceous dinosaur fossils in India and commented that there had to be overland communication between India and other continental regions throughout these times. Similarly, the discovery of mammals, dinosaurs, and crocodiles in Late Cretaceous (Maestrichtian) of Madagascar that are closely related to forms in India, and South America (Krause et al., 1999), also negates isolation of India and points to overland communication.

The terrestrial faunal resemblance between India-Africa and India-Europe throughout the Mesozoic suggests that there were close terrestrial links between India, Africa and Europe during this vast span of time (Chatterjee and Scotese, 1999). Like these authors though, many other workers using the PT model have conveniently used several land bridges at various times to explain the faunal links of India with Africa, Asia and Europe. For example, Prasad et al. (2013), reporting the first Indian Simosuchus-like Notosuchian crocodile from the Cauvery Basin in southern India, wrote that their findings strengthened earlier evidence from other vertebrate groups for close biotic links between India and Madagascar in the Late Cretaceous - most likely through dispersal via the Seychelles Block, Amirante Ridge, and Providence Bank.

From the above, it is clear that there is a distinct lack of endemism among the Indian Mesozoic terrestrial vertebrates - suggesting the Indian landmass was not isolated enough to accomplish that. Looking at the biota of landmasses such as Australia, New Zealand, Socotra islands, and Madagascar, to name a few - that have been isolated for much of the Cenozoic - it is clear that diverse evolutionary trends kick in and take life in uniquely different directions within a matter of a few millions of years or far less. India should have acted no differently had it ever been totally isolated for any substantial length of time. Meyerhoff et al. (1996) showed in a comprehensive way how the Gondwana realm biotic elements (Lower Permian - Cretaceous) extended northward through India, China and Mongolia on to northeastern Siberia, and how the Tethyan biotas extended southward from southern India to Arabia, Australia and New Zealand – questioning the plate tectonic constructs of Tethyan evolution and isolation.

The question of land bridges

A solution to this problem has been suggested by building land bridges: For example, Chatterjee and Scotese (1999) have suggested that a greater Somalia promontory and the Late Cretaceous Kohistan - Dras Island Arc, developed along the northern margin of India, provided convenient land bridges (**Fig. 2**). This allowed migration of animals between India, Africa and Europe. Such mixing at least can explain why the Maestrichtian dinosaurs and other vertebrates of India do not show any convincing evidence of endemism. The main problem with this suggestion is that it is not clear as to where this greater Somalia promontory came from, what became of it after it collided with India, and what present day land mass represents this lost land. The suggestion that the Lut-Afghan Blocks may be the lost Somalian Block (Chatterjee and Scotese, 1999 and 2010) is not too convincing. The idea of the Kohistan-Dras island chain as a land bridge (**Fig. 2**) is also controversial, and seems to be just another convenient creation for trying to fit things in the poor PT model. According to Khan et al. (2009), India and Kohistan-Ladakh Arc collided in Early Paleocene, as indicated by the cessation of convergence-related calc-alkaline magmatic activity in Kohistan-Ladakh Arc.

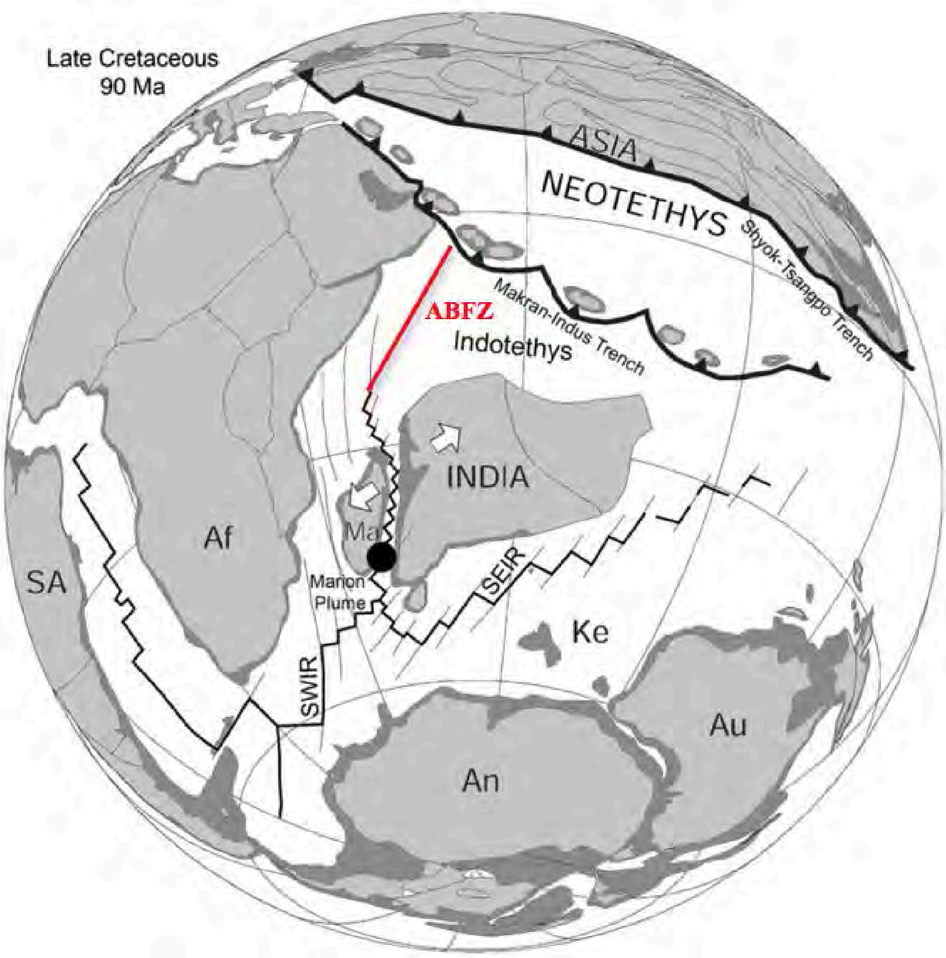

Fig. 2. Paleogeographic reconstruction of drifting Gondwana fragments during the Late Cretaceous, showing the evolution of Oman-Kohistan-Dras Arc (modified after Chatterjee and Scotese, 2010). ABFZ: Ancestral Bela Ophiolite Fracture Zone.

Paleomagnetic data from Teru Volcanics (64 Ma) of the Kohistan Arc yielded a paleo-latitude of 27.5º N+/- 6º (Ahmed et al., 2001). The apparent polar wander path analysis for the southern margin of Asia between 80-40 Ma located it at 30º - 35º N (Besse and Courtillot, 2002; Schettino and Scotese, 2005). Therefore, it appears that, in the Late Cretaceous, both India-Kohistan mass and the southern margin of Asia, were not far from each other.

Additional paleontologic and stratigraphic evidence against India's drift

Another problem for PT is the presence of equatorial and Tethyan nature of the Late Jurassic-Cretaceous fauna at the southern tip of India (Meyerhoff and Meyerhoff, 1974), which indicates that India has not moved since at least the Late Cretaceous. This would lend support to the argument that India has always been close to where it is today.

Kashfi (1988) had analyzed a vast range of geological data, from Iran and the rest of Middle East and concluded that nothing in the geological record supported a separation between Arabia-Africa and the Middle East in the Phanerozoic as there are strong stratigraphic and paleontological correlations throughout the region - even between Iran and Central Asia. In support of this assertion, he points to the facies continuity of the Pre-Cambrian-Cambrian salt deposits from western India, Pakistan, Iran, and Persian Gulf to Arabia. He also pointed out that lack of any solid correlation between the alleged present or past subduction zones with seismicity in the area. The random distribution of ophiolites and volcanics are also strong points against PT. To that, we can add, that in Pakistan also, south of the Kohistan Arc, there is little convincing evidence for a past or present subduction zone along the ophiolite belt (see below for further discussion of this point). Even the Makran subduction zone seems to be ill defined, as admitted by the authors themselves (Jacob and Quittmeyer, 1979), and thus contrived and wishful.

Northwestern ophiolites of the Indian plate: Are they subduction-related?

These ophiolites consist of three major outcrops exposed along the mountainous fold and thrust belt that runs in a general north south direction **(Fig. 3)** along the northwestern margin of the Indian Plate. From north to south, these are the Waziristan (WO), the Muslim Bagh (MBO) and the Bela ophiolites (BO) and there is a wide range of opinions about their origin, as follows:

No detailed ophiolite maps have so far been made for the various ophiolites. The WO is located in a remote and rather dangerous tribal belt that has seen plenty of violence and conflict. The MBO perhaps has drawn more workers because of its relative proximity to Quetta and mining of chromite deposits. The Bela Ophiolite, though the largest among the three, has been only sporadically mapped. A map covering the northern half of BO, based on remote sensing techniques (Xiong et al., 2011) has been published, however, it does not correlate well with observations made on high resolution satellite photos and also lacks appropriate field checks.

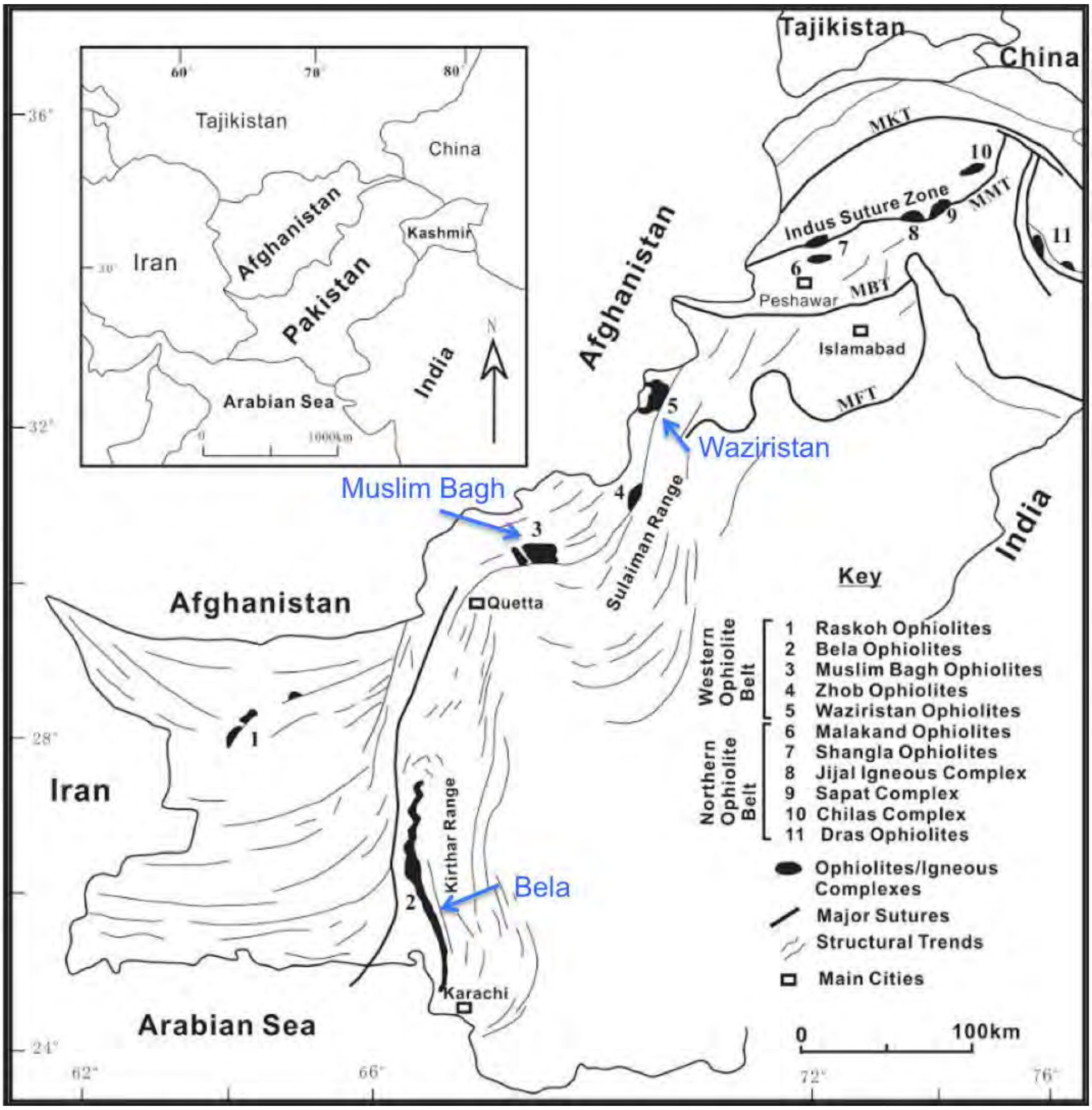

Fig. 3. Ophiolites in Pakistan: those discussed here are marked by arrows (after Asrarullah et al., 1979).

Waziristan Ophiolite

The northern most ophiolite (WO) covers about 1800 km^2 in area, second only to the Bela Ophiolite in Pakistan. In fact, it may well be an extension of the Khost Ophiolite exposed across the western border in Afghanistan (Jan et al., 2011). It is top most of the three major nappes derived from the oceanic and slope environments of the Tethyan regime to the west. The (WO) nappe itself can be further subdivided in three thrust sheets that involve a typical ophiolite suite with ultramafic rocks, gabbros, sheeted dikes, pillow lavas, plagiogranite and pelagic sedimentary rocks (Jan et al., 1985 and 2011).

The nappes are to a variable extent dismembered into a tectonic mixture but, unlike the Bela or Muslim Bagh ophiolites, there is no subophiolitic mélange involving ophiolitic and continental rocks. The age of associated radiolarian fauna (Tithonian- Valanginian), suggests a Late Jurassic or older age of formation for the ophiolite (Khan et al., 2004). According to them it formed in a back arc basin in a SSZ environment. However, the authors seem to have struggled with certain chemical traits of the analyzed rocks, transitional between Mid Oceanic Ridge Basalts (MORB) and Island Arc Tholeiites (IAT), before settling for a SSZ setting for the origin of WO. The ophiolite was initially obducted at 90 Ma due to an intra-oceanic convergence between Arabian and Indian plates (Gnos et al., 1997), but its subsequent eastward obduction on to the Indian shelf sequence took place in the Paleocene (Beck et al., 1996). A sequence of Early to Middle Eocene sedimentary rocks overlies the ophiolite with an unconformity.

Muslim Bagh Ophiolite

The Muslim Bagh Ophiolite consists of two large tectonic blocks named Jang Tor Ghar and Saplai Tor Ghar, underlain by green schist- garnet amphibolite facies metamorphic slivers (along the sole), thrusted over a mélange zone (Ahmad and Abbas, 1979). The ophiolites consist of ultramafic tectonites (harzburgites and dunites with chromite pockets), ultramafic and mafic cumulates and a sheeted dike complex. Pillow lavas are absent above the sheeted dikes but occur as blocks in the mélange under the ophiolite blocks. Ahmad and Abbas (1979) have described two kinds of mélange: the ophiolitic mélange containing exotic blocks of marble, radiolarite, basalt and gabbro wrapped in a foliated serpentinite matrix, and the other containing a mix of ophiolitic and continental blocks of all sizes embedded in a sheared shale matrix. Among the clasts found are pillow lavas, pelagic carbonates (of Maestrichtian age and older), serpentinite, and Jurassic platform carbonates – many of mountain size, interpreted as giant olistoliths. The mélange tectonically overlies the Mesozoic shelf carbonates of the Indo- Pakistan margin. The MBO is believed to represent Tethyan oceanic crust that was emplaced in Paleocene-Early Eocene (Ahmad and Abbas, 1979). The youngest rocks underlying the ophiolites are Maestrichtian in age and Early Middle Eocene carbonates unconformably overlie the ophiolites – thus they were emplaced at about the same time as the Bela Ophiolites (Alleman, 1979).

Kakar et al. (2014 and 2015), have not described any major mélange from under the MBO. Instead they seem to have lumped these rocks into a unit dubbed Bagh Complex – described as "an assemblage of Triassic-Cretaceous igneous and sedimentary rocks, containing tholeiitic, N-MORB-like basalts and alkali basalts with oceanic island basalt (OIB) type signature". Based on the whole rock chemical analyses of gabbros, sheeted dikes and other late mafic dikes, they suggested that MBO originated in a supra-subduction zone of Neo-Tethys during the Late Cretaceous. Earlier, Siddiqui et al. (2011) had suggested that sheeted dikes in MBO had a back-arc basin signature, related to a Cretaceous Ceno-Tethyan convergence zone.

The Muslim Bagh ophiolite (MBO) complex comprises two nappes of different ages, and lithology. However, there are many differing opinions about its tectonic setting by various workers. Kakar et al., 2014, have interpreted both MBO and BO as supra-subduction zone type ophiolites. On the other hand, the upper nappe has been interpreted as a supra-subduction zone ophiolite, whereas the lower nappe is believed to have formed along a mid-oceanic ridge (hot spot?) during separation of the Indian Plate from the African Plate (Khan et al., 2007). Thus the MBO seems to be a composite of both SSZ and MOR settings; it was also intruded by hot spot derived magmas (Khan et al., 2007). Siddiqui et al. (2011) assigned a back-arc origin to the sheeted dike complex of MBO, whereas Mahmood et al. (1995) were in favor of a MOR origin for the MBO.

Bela Ophiolite

The Bela Ophiolite, the largest in Pakistan, is exposed along a 200 miles (321 km) long belt in the Kirthar Mountains of Pakistan. They can be divided into two tectonic units representing the lower and upper part of a complete ophiolite sequence, stacked in reverse order: The tectonically higher but stratigraphically lower unit consists of peridotites, gabbros, sheeted dikes, some pillow lavas and is separated from the lower unit by a thrust fault (Gnos et al., 1998; Khan et al., 1998). It is exposed in the northern part of the belt whereas the stratigraphically higher part of the ophiolite sequence, as described by Sarwar (1981; 1992), is exposed in the southern half in a 3-5 km thick sequence of basaltic pillow lava, inter-flow sedimentary rocks (chert, argillite, limestone) and diabase-gabbro sills. Debris of serpentinite (up to many kilometer-sized blocks), serpentinite-carbonate breccia, and less commonly of basalt, gabbro, peridotite, pelagic limestone and their metamorphic equivalents occur throughout the ophiolite sequence and may form extensive horizons (Kunno Mélange of DeJong and Subhani, 1979; Sarwar, 1981).

The age of the ophiolite, as indicated by pelagic micro fauna associated with the lava flows, is Aptian-Early Maestrichtian. The lava flows belong to a spilite-keratophyre-basaltic andesite suite of tholeiites enriched in FeO, TiO_2 and other trace elements (Sarwar, 1981). The lava flows although similar to the E-type MORB differ in details such as La/Ta ratio ranges (9.62–18.04 for the Bela lavas versus 10–15 for the MORB). The diabase-gabbro sills are similar to the associated lava flows. However, due to their relative enrichment in certain elements (e.g., Fe, Ti, Hf, Th and Ta, etc.), they may represent more fractionated late melts.

A comparison of the stratigraphic and structural features of the Bela Ophiolite with modern oceanic environments reveals that these ophiolites probably originated in a large oceanic fracture zone (Sarwar, 1981 and 1992), that acted as a boundary between India and an oceanic basin (Tethys or Neo-Tethys?) during the Cretaceous - analogous to the present-day Owen Fracture Zone that separates the Indian and the Arabian plates. The ancestral fracture zone was destroyed when transform movement gave way to oblique convergence, culminating in the ophiolite obduction in Paleocene-Early Eocene time (Sarwar and DeJong, 1984). The ophiolites are unconformably overlain by Eocene reefal carbonates (Nal Limestone) that signify post-obduction marine transgression.

According to Gnos et al. (1998), the Bela Ophiolite contains a complete ophiolite-accretionary wedge-trench sequence and overlies an accretionary wedge. Earlier, their accretionary wedge was named the Kanar Mélange by DeJong and Subhani (1979) and Sarwar (1981 and 1992). They interpreted it as a sedimentary-tectonic mélange, resulting from oblique convergence along the Ancestral Bela Ophiolite Fracture Zone (ABFZ) – without invoking subduction (**Fig. 2**). The same process culminated in ophiolite obduction also (Sarwar, 1981). However, according to Gnos et al. (1998), the BO were emplaced onto the Indian continental margin when India-Seychelles Block ran over the active Reunion Hotspot 66 Ma ago.

Gnos et al. (1998) have claimed that the ophiolite emplacement occurred during the counterclockwise separation of Madagascar and India-Seychelles, which caused shortening and consumption of oceanic lithosphere between the African-Arabian and the Indian-Seychelles plates. So their model seems to require a west dipping intra-oceanic subduction zone (**Fig. 4**, Carmen et al., 2015) that supposedly developed due to a counter-clockwise rotation of India along its northwestern margin - otherwise a transform margin to this point - causing shortening and ophiolite obduction on to the Indian margin to the east. Again, it seems a little too convenient to believe that a transform margin became a convergent margin so subduction and ophiolite obduction could take place, and afterwards, the same margin was allowed to go back to transform status - as if by magic and remains as such to this day.

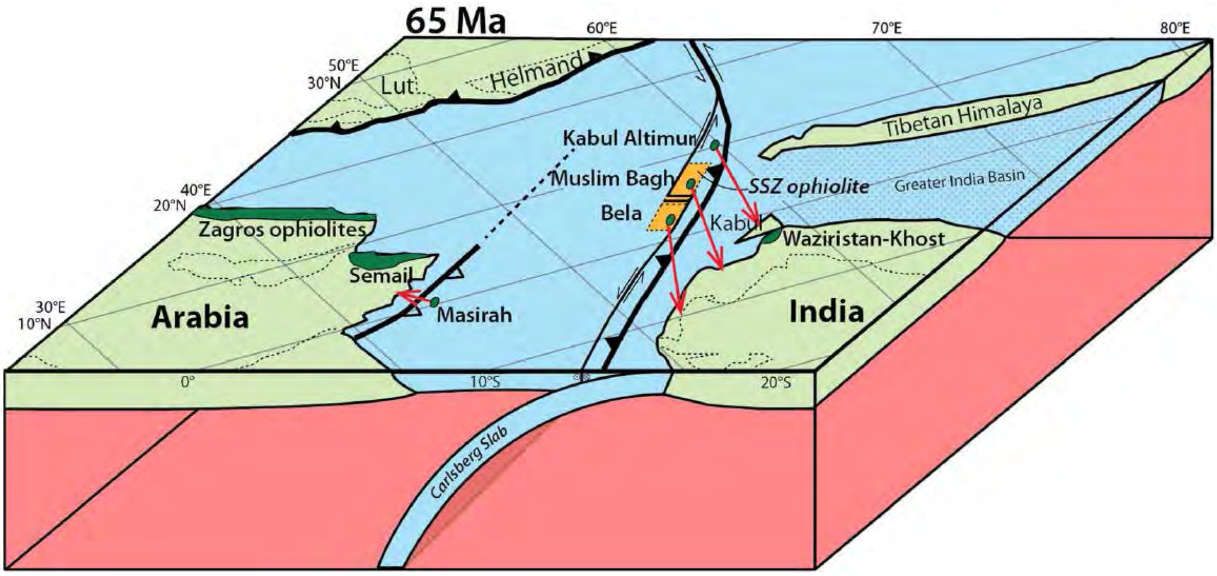

Fig. 4. The supra-subduction zone (SSZ) model showing Late Cretaceous-Early Eocene plate configuration between India and Arabia (Carmen et al., 2015). They proposed that oblique convergence between the two plates was partitioned into overriding plate strike-slip with a pull-apart basin above a subduction zone that consumed Indian oceanic crust. Continued convergence ultimately resulted in the obduction of the SSZ ophiolites (Bela and Muslim Bagh) that formed in the pull-apart basin above the subduction zone. Please compare with figure 5 and see text to learn why this model is not favored here (after Carmen et al., 2015).

The ophiolite obduction in the Baluchistan belt of the northwestern Indian continental margin was preceded by alkaline (WPB) volcanism, represented by the Bibai Lavas (Kazmi, 1979), Porali and the Deccan

Basalts (Sarwar, 1981). It is important to note that this volcanic arc was not related to the ophiolites (DeJong and Subhani, 1979) and represented northward extension of the continental (within plate basalt – WPB type) Deccan volcanism of India (Sarwar, 1992), the origin of which is also controversial (Sheth, 2005).

Chemical discrimination of ophiolitic basalts

The use of chemical diagrams based on the geochemistry and petrology of oceanic and ophiolitic basalts and associated plutonic rocks has been a common practice for discriminating rocks from various tectonic environments. All workers in favor of SSZ origin for the WO, MBO and BO (Gnos et al., 1998; Ahmed and Ernst, 2000; Kakar et al., 2014) have based their verdict on basalt chemistry and chemical discriminant diagrams, with complete faith in the PT story that India had to have drifted north during much of the Cretaceous, as a vast stretch of the Tethyan crust was subducted under various oceanic island arcs and Eurasian blocks.

Regardless of the difficulties of subduction (Pilchin, 2016) and a vanishing super-sized Tethys, this is not acceptable for other reasons also: Recently, several workers (Sheth, 2008; Vermeesch, 2006) have evaluated most of the available discrimination diagrams, based on log ratios and linear discriminant analysis (LDA) of major oxides, for their ability to distinguish between such tectonic environments as oceanic island basalts (OIB), continental rift basalts (CRB), island arc basalts (IAB), and mid-ocean ridge basalts (MORB). It appears that their performance is not so satisfactory when applied to the ophiolitic basalts such as those exposed in the Tethyan regime that includes the ophiolites of northwestern Indian Plate.

Considering the fact that the ophiolitic basalts are frequently altered, resulting in mobility of most major elements, these diagrams are deemed unreliable (Sheth, 2008; Verma and Agrawal, 2011). Analysis employing a large data set of geochemically immobile major elements during alteration, like (Ti), and trace elements (e.g. Nb, Y, Zr) may have better success in discriminating tectonic settings of ophiolitc basalts. However, there are additional requirements of LDA analysis using immobile major elements that have to be met for a valid and meaningful analysis (see Verma and Agrawal, 2011, and references therein).

The BO has a well-developed sheeted dyke complex exposed on its northern side (Lat. 27º 6′ N) that indicates a high spreading rate, characteristic of mid-oceanic ridges of large basins because of readily available magma supply (Robinson et al., 2008). In the relatively smaller marginal basin type environments (including supra-subduction zone in PT jargon), the magma generation and supply is relatively poor, resulting rarely in large well-developed sheeted dike complexes.

From the above, it is clear that there is disagreement among the workers on the origin of these ophiolites. There can be inconsistency even in the chemical analysis of a particular unit by different workers, as there can be a number of diverse reasons behind chemical differences. However, the bottom line is that chemical discrimination of ophiolitic rocks is problematic, and, doing so without any regard to the litho-stratigraphic, litho-tectonic, field relationships, and regional geodynamic considerations of the sequence involved, is reckless and hazardous. So, with that in mind, let us take a look at whether a supra-subduction origin can be justified for the Pakistani ophiolites under discussion here.

Geodynamic considerations

According to PT, the northwestern margin of Indian Plate was part of a transform margin during much of its northward drift in the Cretaceous (**Fig. 2**). However, due to a counter-clockwise rotation of India, convergence caused a west dipping subduction zone to develop along the Baluchistan margin, which resulted in the formation of an accretionary wedge above the subduction zone (Gnos et al., 1998) that was thrusted over by ophiolite nappes from the west. Since the evidence for rotation of India and convergence was not revealed by Gnos et al. (1998), the question arises what was the basis for their claim. Carmen et al. (2015) have argued that the ages of the metamorphic soles of the Bela and Muslim Bagh ophiolites, (circa 65 Ma: Mahmood et al., 1995) somehow demonstrated that subduction was active between India and Arabia at that time, which seems to be just another example of model-driven thinking and wishful argument. The date of metamorphic soles marks the time of movement of the nappes and that might have been caused not by subduction but simply by oblique convergence, as suggested by Sarwar and DeJong (1984; **Fig. 5**).

Let us see if we can find any other evidence or hints for a Cretaceous island arc west of the subduction zone (marked currently by the Ornach-Nal-Chaman fault transform boundary) or for an accretionary wedge east of it. There is no known island arc related rocks east of the Chaman-Ornach-Nal fault zone – the current transform boundary of Indian Plate – anywhere within the ophiolite belt along the western margin of the Indian Plate. However, that is not a problem since it would have developed above (and west of) the west dipping subduction zone (Fig. 4, Carmen, et al., 2015). According to the PT model, any such island arc would have been left behind as India resumed its northward drift after ophiolite obduction in the Paleocene. So, the only other physical evidence still available for scrutiny should be the alleged accretionary wedge of Gnos et al. (1998), represented by the mélange that underlies the Baluchistan belt ophiolites. Let us take a look at this mélange and see if it contains any physical evidence that supports the assertion of Gnos et al., 1998, that it was formed as an accretionary wedge.

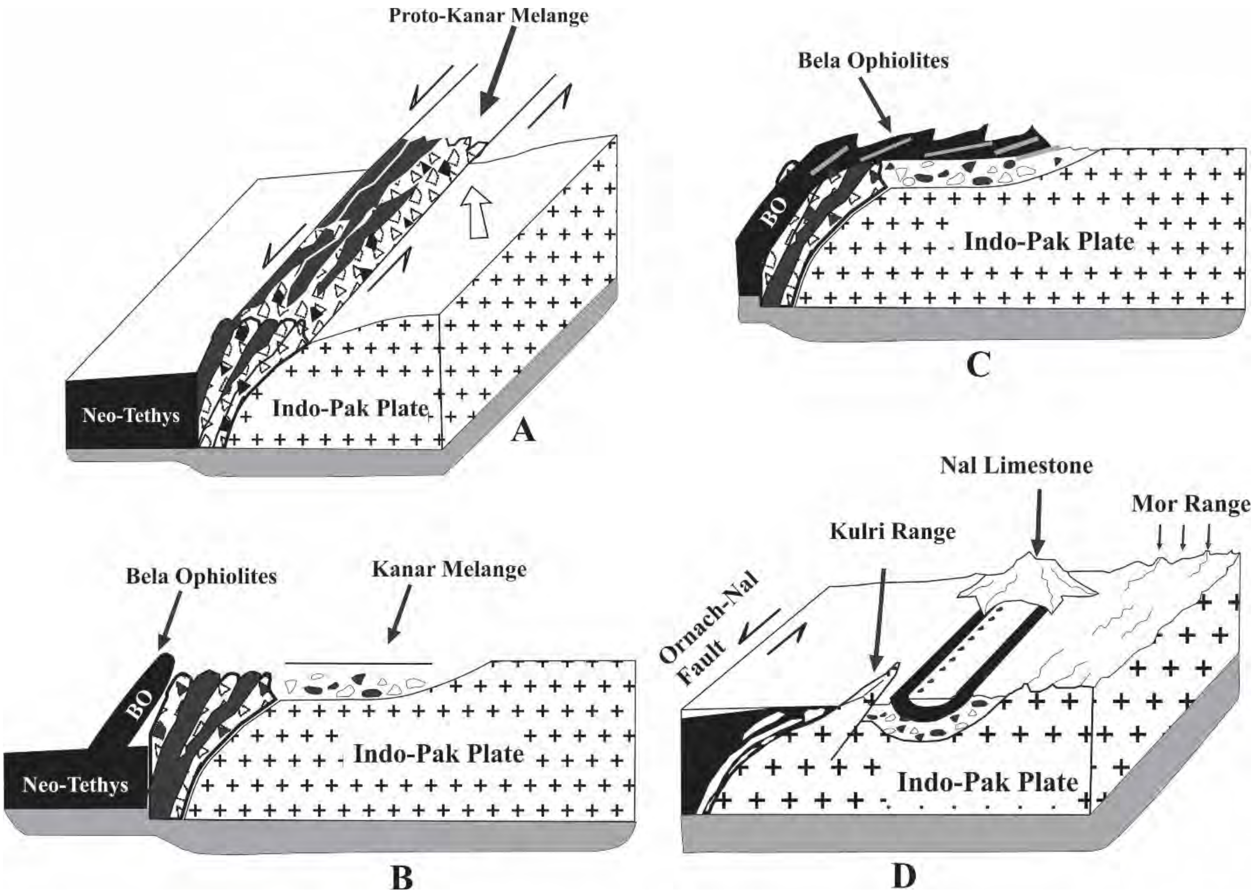

Fig. 5. Model for the formation of Kanar Mélange: (A): Paleocene oblique convergence between the Indian Plate and the Neo-Tethys, along a Cretaceous transform boundary, creates an emergent belt of tectonic mélange (Proto-Kanar Mélange). (B): Debris derived from the tectonic mélange belt is deposited as Kanar Mélange in a tectonic foredeep on the Indian continental margin. (C): Progressive oblique convergence leads to obduction of Bela Ophiolites above the Kanar Mélange, inducing a tectonic fabric. Ophiolite obduction is complete by the Early Eocene. (D): Further convergence results in folding of the mélange-ophiolite belt and upthrusting of the Kulri Range. Nal Limestone is neo-autochthonous, deposited by marine transgression in the Middle Eocene-Oligocene on the folded and eroded surface of the ophiolites (revised after Sarwar and DeJong, 1984).

Testimony of the sub-ophiolitic mélange

No sub-ophiolitic mélange has been reported from the Waziristan (WO) area. The ophiolitic mélange under the MBO nappes consists of two kinds (Ahmad and Abbas, 1979), one with serpentine matrix and the other with an argillaceous matrix. The serpentinite matrix mélange (up to 1000 feet thick) contains metamorphic clasts such as garnet amphibolite, green schist, radioliarite, marble, basalt, and gabbro etc. Below the ophiolitic mélange is the mélange with highly sheared argillaceous matrix containing a wider variety of clasts of all sizes including many exotics. Among the rock types reported are pillow basalt, serpentinite, and pelagic carbonates with Maestrichtian and older micro-fauna (Alleman, 1979). Mountain size clasts of Jurassic platform type carbonates, interpreted as Olistoliths by Alleman, are also present (pers. comm. to Ahmad and Abbas, 1979).

The mélange under the Bela Ophiolite has been described by DeJong and Subhani (1979) and Sarwar and DeJong (1984). It is exposed along both flanks of the regional northwest-southeast oriented synclinal structure of the southern BO belt (DeJong and Subhani, 1979; Sarwar and DeJong, 1984; Sarwar et al., 1988).

They describe the sub-ophiolitic mélange as a chaotic mixture of continental and ophiolitic clasts, a millimeter to tens of kilometers in size, including some exotics, set in a dominantly argillaceous matrix. Among the clasts of continental affinity are those from the underlying Jurassic-Cretaceous shelf sequence (Shirinab and Sembar-Goru formations), debris and blocks of gray basaltic conglomerate, and boulders of pink granite resembling that of the Indian Shield. Among the very large hill size blocks, some measuring up to tens of kilometers, are the Jurassic carbonate blocks and dark basaltic conglomerate blocks (**Fig. 6**; see also Sarwar and DeJong, 1984, figures 2-5). Some of the Jurassic carbonate blocks contain barite mineralization (**Figs. 7-10**) characteristic of the equivalent rocks exposed in the Kulri Range to the west and the Mor Range far to the east. The basaltic conglomerate (Porali Agglomerate of DeJong and Subhani, 1979) blocks show a thick (up to 1.5 kilometers) monotonous bedded sequence or thick (up to tens of meters) horizons, locally inter-layered with pelagic marl horizons. Monotonous lithology, unsorted nature and tremendous thickness of the basaltic conglomerate (**Figs. 11-12**) are indicative of a source relatively nearby and quick deposition from mass transport processes like debris flows. The ophiolitic clasts in the mélange, many measuring up to several hundred meters, consist of serpentinized ultramafic rocks, serpentinite breccia (ophicalcite), gabbro, massive and pillowed basalt, chert and pelagic sedimentary rocks.

The matrix of the mélange consists of variegated shale, mudstone and marl; the matrix to clast proportion is generally low. At places blocks are all jumbled up together with thin screens of matrix filling spaces in between the blocks. The deformation within the matrix varies from mild to severely folded and may be foliated enough to the extent that it obliterates bedding. However, distinct beds are present within the matrix (**Fig. 13**; see also figures 6-7 in Sarwar and DeJong, 1984). The deformation within the continental blocks varies from brecciation to shearing and folding in limestone and mudstone blocks (**Figs. 8, 9, and 10**). The volcanic conglomerate blocks are surprisingly undeformed or mildly deformed internally (Figs. 11-12). Most of the ophiolitic blocks of pillowed lava, associated sediments and gabbro are also relatively mildly deformed, with the exception of serpentinized blocks that can be brecciated to severally foliated (**Fig. 14**).

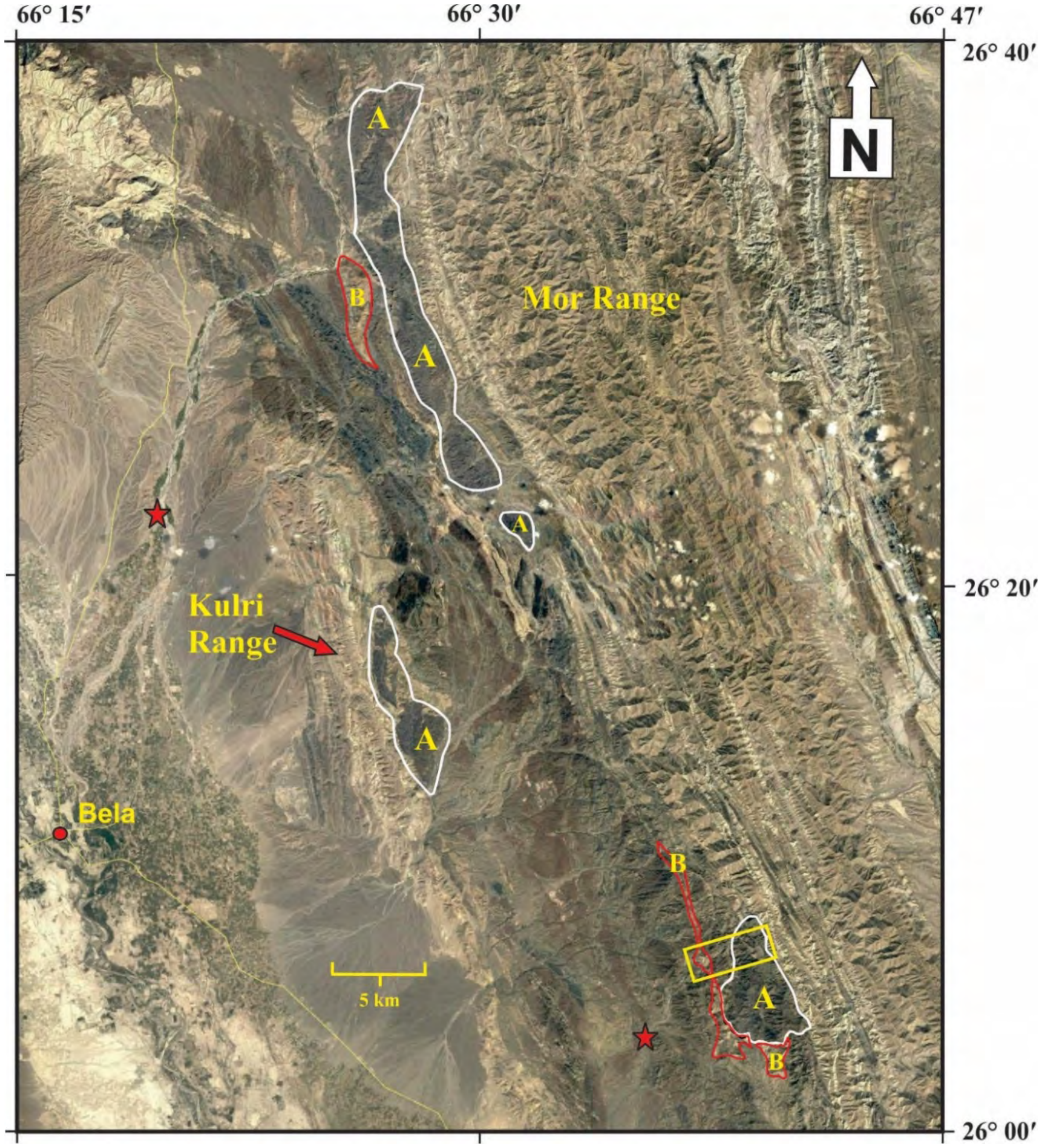

Fig. 6. Satellite view of part of the southern Bela Ophiolites east of Bela – showing several of the mountain size blocks (outlined in white and red) in the Kanar Mélange that underlies the ophiolite nappes. All blocks have been field checked: A: Porali Conglomerate blocks. B: Jurassic Carbonate blocks - many with horizons with barite-fluorite-lead-zinc mineralization characteristic of the Jurassic of the Mor Range in the area. Most mélange blocks show a distinct lack of internal deformation (see text). Red stars mark the location of two samples of river sand analyzed for heavy mineral concentrates with the aim of determining the extent of metamorphism suffered by the ophiolite belt. Yellow rectangle marks the approximate location of (Fig. 7) in the mélange zone.

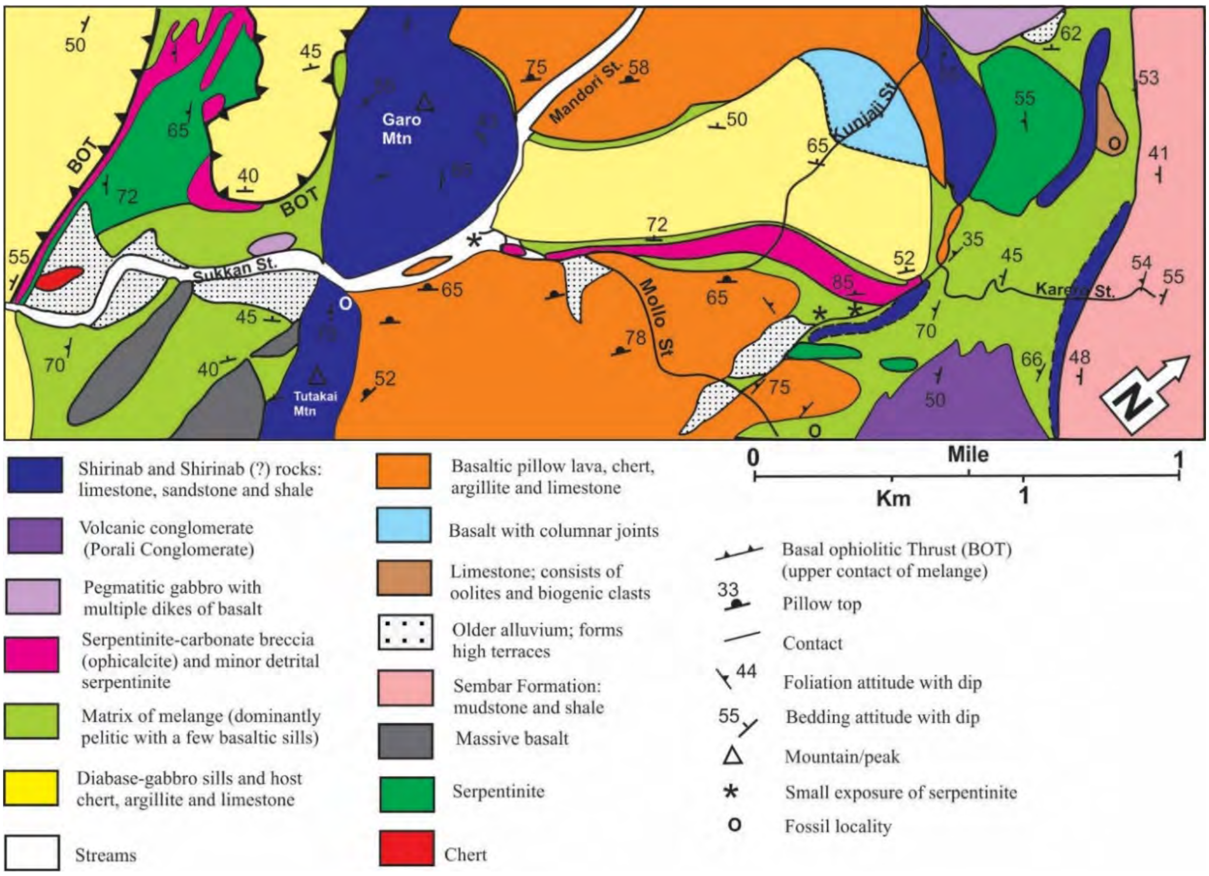

Fig. 7. Geological map of a part of the Kanar Mélange (location shown on Fig. 6; modified after Sarwar and DeJong 1984).

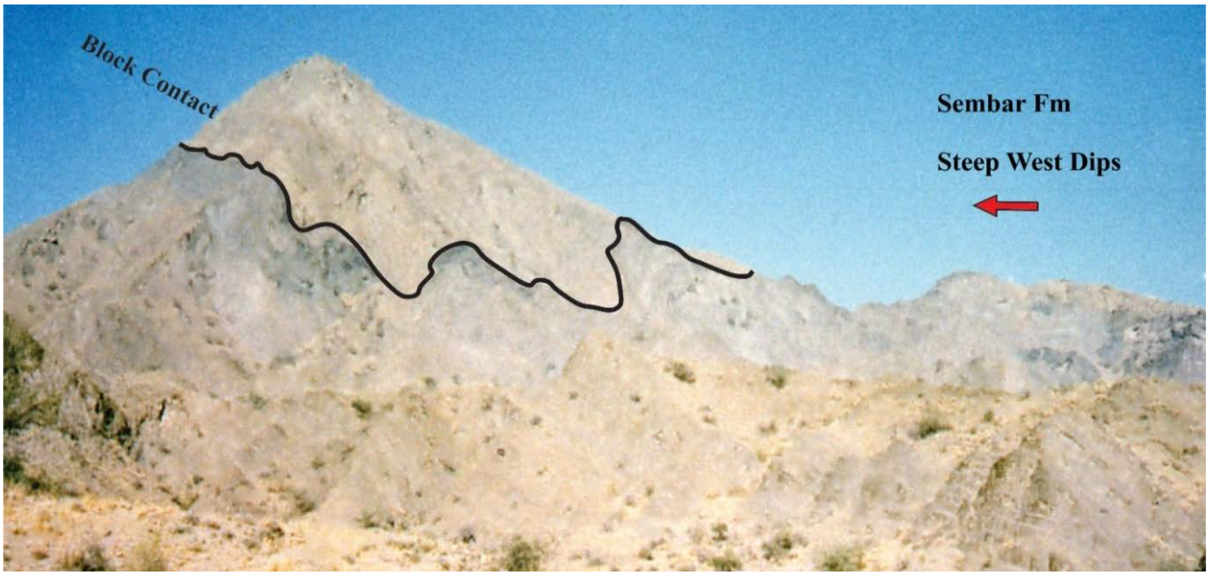

Fig. 8. Mountain size block of folded Jurassic Shirinab limestone in undeformed (except under the block) shales above Sembar Formation. This is the southern end of block B shown in southeastern part of (Fig. 6). There are numerous huge Shirinab type blocks scattered throughout the mélange belt.

Fig. 9. Barite–fluorite- lead – zinc mineralization in a large Shirinab carbonate block found in the mélange. Numerous such blocks are scattered throughout the mélange belt where some locals mine them at small scale. Note broken but distinct beds and lack of any severe deformation.

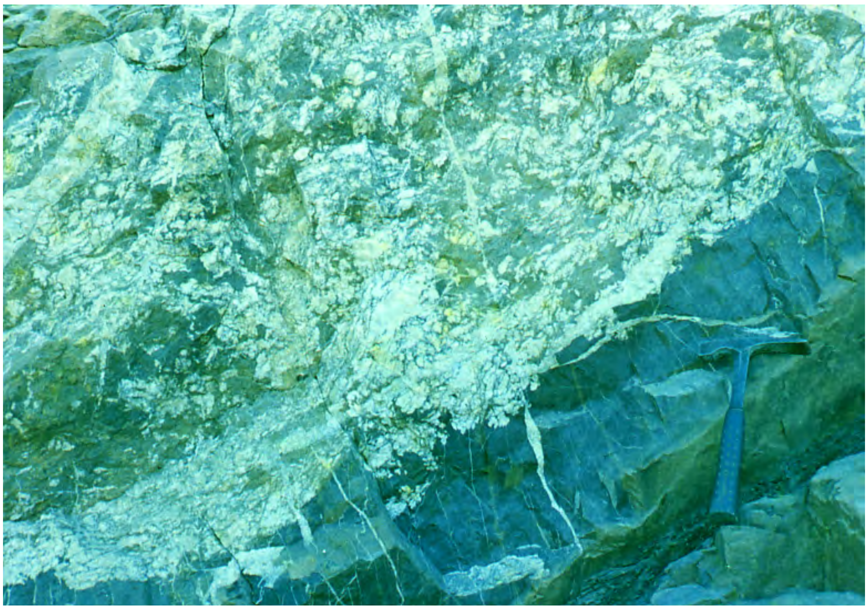

Fig. 10. Barite in the Jurassic Shirinab Limestone, note sharp nature of the replacement front and late fractures filled with calcite.

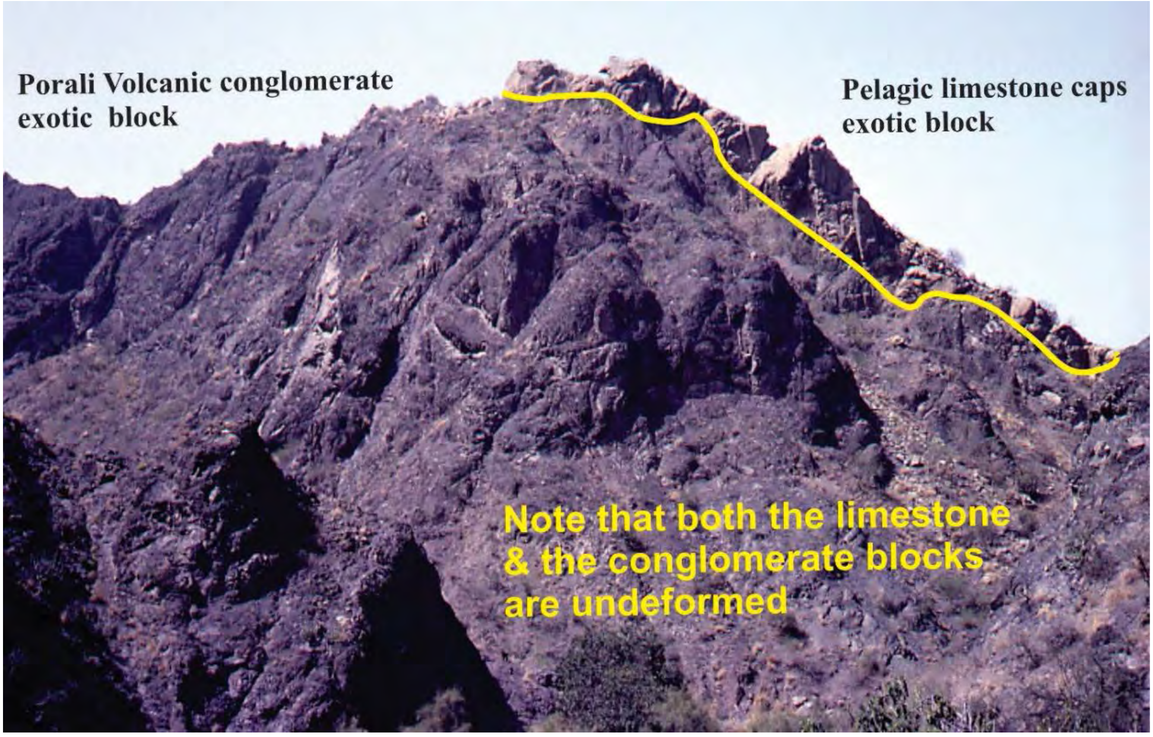

Fig. 11. A Maestrichtian foraminiferal limestone bed caps this three miles long Porali Volcanic Conglomerate block in the Kanar Mélange. This conglomerate is chemically very similar to the continental alkaline Deccan flood basalts exposed in India hundreds of miles to the south. This is block 'A' shown in the southeastern corner of figure 6.

Considering the field relationships, rock chemistry and geodynamic considerations, a leaky transform model still seems to be the best fit for the origin of Bela Ophiolites (Sarwar, 1981 and 1992), so this margin probably had been a transform margin through much of the Cretaceous. However, to allow for the ophiolite obduction and mélange formation in the Paleocene-Early Eocene, some convergence might have occurred. Yet in the absence of such features as blueschist-eclogite in the mélange, calc-alkaline volcanic piles and volcanogenic flysch in the ophiolite belt, no major convergence can justifiably be advocated. The alkaline magmatism recorded by the Porali Conglomerate blocks and many mafic intrusives in the sub mélange shelf sequence was of within plate type related to the Deccan Basalts. So, considering all aspects, an oblique convergence model along a transform zone is still the best fit as proposed by Sarwar (1981) and Sarwar and DeJong (1984).

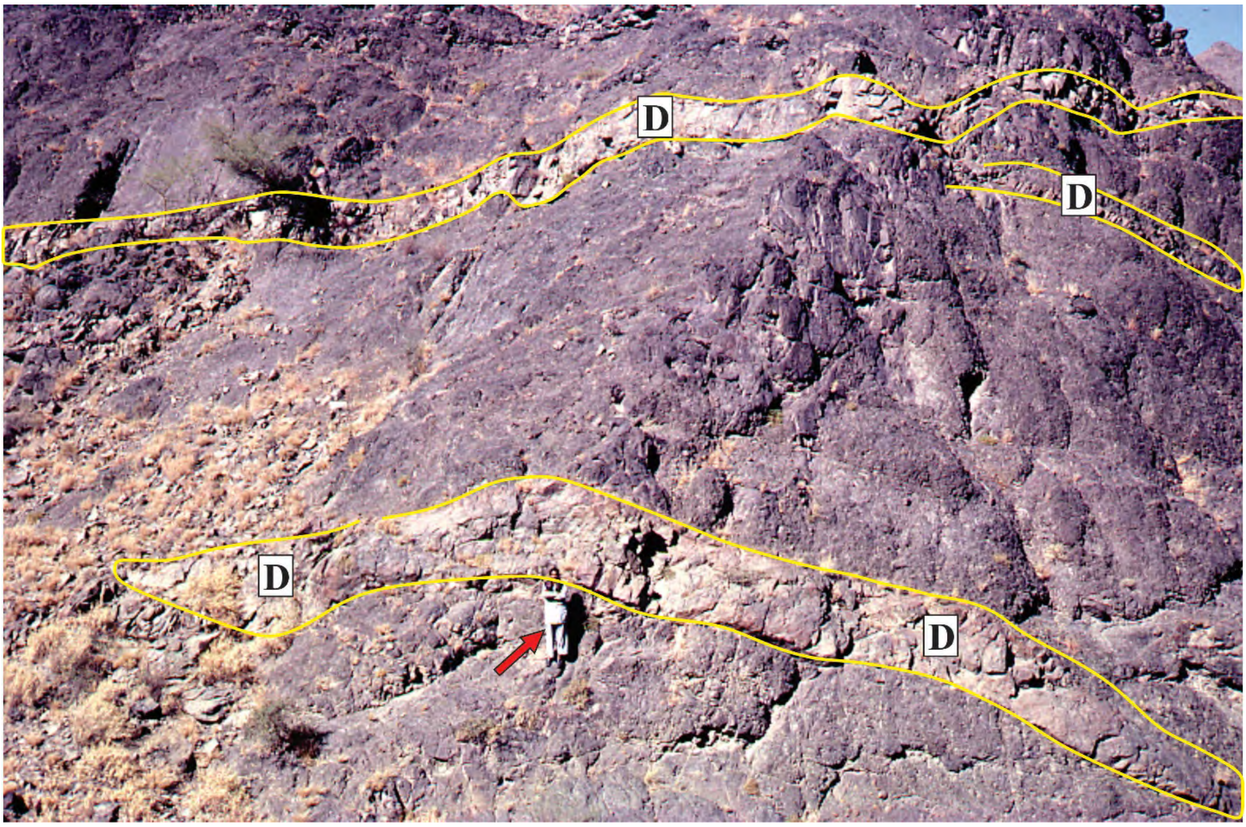

Fig. 12. Mountain size Porali Conglomerate block cut by basaltic dikes (D). Both rocks are alkaline and chemically related. Note man for scale (arrow) and lack of internal deformation within the massive conglomerate beds as well as in the dikes

There are distinct clues within the Kanar Mélange also that point to its origin: for example, its basal contact with underlying Sember Formation, although locally disturbed because of thrusting, appears to be depositional (see figure 10 in Sarwar and DeJong, 1984). Many of the ophiolitic and continental blocks such as serpentinite, pelagic rocks and Jurassic limestone, are far more severally deformed than the enclosing bedded but sheared matrix, indicating that their deformation predated their final inclusion in the mélange as olistoliths (**Figs. 8 & 13**).

Thus according to the oblique convergence model (**Fig. 5**), the Kanar Mélange developed in an elongated trough on the continental margin in front of the eastward moving ophiolite nappes in a marginal marine environment. The tectonic mixing of oceanic and continental rock types was achieved due to convergence along an otherwise transform margin that resulted in closure of this part of the (Tethyan?) oceanic basin. The tectonic mélange was subjected to erosion, influenced by sedimentary processes in the trough and finally run over by the ophiolite nappes, as convergence culminated in folding, thrusting and uplift (**Fig. 5**).

Fig. 13. The matrix of Kanar Mélange can be from distinctly bedded (bottom right) to sheared and foliated (bottom left). Note a large lenticular block of foliated serpentinite in front of the man.

Therefore, the Kanar Mélange of BO is a tectonic-sedimentary mix of oceanic and continental rocks, with well-preserved sedimentary fabrics. It is largely clast-supported and matrix poor. Numerous clasts of gigantic proportions (up to 22 km long and 6 km wide) are present - many of these are exotic, such as the Porali Conglomerate. No appreciable regional metamorphic overprint is present, so there is little evidence of deep burial or grinding in any tectonic hellhole like a subduction zone. Although both clasts and the mélange matrix are deformed to various degrees - from brecciation and shearing to foliation at places - there is no reported occurrence of any high-pressure metamorphic rocks like eclogites and garnet blue schists, believed to be found in the so called subduction related mélanges such as the Fransiscan of California (Ernst, 2015).

Regional metamorphic aspects of Bela – Muslim Bagh Ophiolites

In order to get a better feel for the degree of metamorphism in BO belt, including the mélange, two samples of river sands were analyzed for heavy minerals. The samples came from major streams that cut across the ophiolite belt (**Fig. 6**). The pan-concentrate heavy mineral suite consisted of magnetite, amphibole, epidote, zircons (both abraded and fresh), and chromite, in decreasing order of abundance along with an accessory amount of olivine, pyroxene, garnet, chlorite and gold etc. From this observation it also appears that the degree of metamorphism achieved by the BO and mélange did not exceed the garnet-amphibolite grade. Xiong et al., 2011, had also noted amphibolite facies as the highest metamorphic grade in BO. One would expect to see a higher grade if the BO and the mélange had been subjected to the subduction zone metamorphism. Similarly, the highest metamorphic grade reported from the Muslim Bagh ophiolites, is also garnet-amphibolite (Kakar et al., 2014).

Fig. 14. Exotic iron rich serpentinite-carbonate breccia (ophicalcite) in the mélange is believed to have formed by serpentinization in the oceanic regime and obducted as such. Note lack of shearing within the breccia clasts. White material is mostly calcite.

The Porali Conglomerate blocks are internally not deformed and volcanic pebbles, boulders, and beds are all internally intact (**Figs. 6, 7, 11 and 12**). Similarly, many of the Jurassic carbonate blocks measure up to 10 kilometers and are only brecciated or folded with a conspicuous lack of shear (**Figs. 6 -10**) that would be expected under deep intense shearing metamorphism in a subduction environment. It is only the serpentinite blocks of all sizes that show various degrees of brecciation and alteration with or without extreme foliation (**Figs. 13-14**), but these are often wrapped in pelitic matrix that may or may not be deformed. So their deformation seems to be largely inherited from the oceanic regime and not a result of subduction or obduction process. Lack of internal deformation also was noticed in the pillow lava (**Fig. 16**) and gabbro blocks. Preservation of bedding and other sedimentary fabrics such as slumping was also noticed throughout the mélange matrix (**Figs. 13 and 15**). Such features do not necessarily support a subduction related accretionary wedge origin for the Kanar Mélange.

Fig. 15. This slump fold is an example of well-preserved sedimentary fabrics in the Kanar Mélange.

Fig. 16. This undeformed pillow lava is exposed in a hill size block in a stream cut within the Kanar mélange. Even the cooling cracks are pristine, implying no severe deformation since its birth in the oceanic regime.

The NW margin of Indo-Pakistani block thus appears to have been a transform continental margin that was subjected to Deccan-Porali type alkaline volcanism along the coastal belt and then oblique convergence with another block located to its west on the other side of Tethys, resulting in mélange formation and ophiolite obduction (Sarwar, 1981; Sarwar and DeJong, 1984). With continued convergence and transpression in the Cenozoic, this margin became an oblique collision margin as seen today.

Conclusions

The application of PT model to the dispersal of Gondwana fragments has been controversial in that India's incredibly long drift, both in space and time, has not been backed by any credible field, stratigraphic, paleontologic, paleogeographic or petrochemical data. Instead, the whole story of India's northward drift and collision with the Eurasian blocks is based on various aspects of the controversial PT model and other wishful constructs such as land bridges, plate rotation and Pangaean reconstructions based on a globe of present day Earth volume (as argued by Crawford, 1979).

The northwestern ophiolites of the Indian Plate do not support the past existence or disappearance of a Tethys of colossal size. Maybe they simply represent the remnants of a Late Mesozoic oceanic basin - possibly a narrow-elongated trough located next to the northwestern margin of India - that collapsed due to convergence between India and its neighboring blocks to the west and north. There is no credible evidence either for any accretionary wedge in the sub-ophiolitic mélange or for an island arc east of the Chaman-Ornach-Nal faults. Also, there is no evidence for subduction. The subduction model, based largely on chemistry of mafic ophiolitic rocks, is not supported by any field data and geodynamic considerations.

The "leaky fracture zone" model of Sarwar (1981), however, may survive as the fracture zones remain an integral part of the oceanic crust – even under an expanding Earth model, or any other theory worth its salt (see Carey, 1988, for example). If India has always been close to where it is today (as argued by many), then, may be Tethys was only a small linear oceanic basin that once opened between India and the Afghan-Iran blocks and subsequently closed when the major basins of Indian Ocean and Arabian Sea opened south of India.

We do not pretend to know as to how exactly these and other major ocean basins formed on our planet, but as a parting thought, consider the following: There is mounting evidence for the presence of Archaean continental crust under many Indian Ocean islands, such as Mauritius and Seychelles (Ashwal et al., 2017). In fact, there are numerous older reports of the presence of continental rocks within the Pacific, Atlantic and Indian oceans. Such occurrences of continental rocks, especially those along the mid-oceanic ridges, are strictly incompatible with the plate tectonic sea-floor spreading model and lend support to competing hypotheses of oceanization and micro-expansion of earth (please see Yano et al., 2011, for a comprehensive review).

Acknowledgements: The authors thank Dr. Dong Choi for his editorial comments and encouragement to scrutinize the supra-subduction origin claims for the ophiolites discussed here. Also, an anonymous reviewer helped us better focus our thoughts.

References

Ahmed, M.N., Yoshiki, F. and Paudel, L.P., 2001. Remagnetization of igneous rocks in Gupis area of Kohistan arc, northern Pakistan. *Earth, Planets & Space*, v. 53, no. 5, p. 373–384.

Ahmad, Z. and Abbas, S. G., 1979. 'The Muslimbagh Ophiolites in Geodynamics of Pakistan'. Farah A. and DeJong, K., eds., p. 243-249.

Ahmed, Z. and Ernst, W.G., 2000. Island Arc related, back-arc basinal, and oceanic island components of the Bela ophiolite mélange complex, Pakistan. In: Ernst, W.G. and Coleman, R.G. (eds.) 2000. Tectonic Studies of Asia and the Pacific Rim. A Tribute to Benjamin M. Page (1911–1997). *International Book Ser.*, v. 3, 328p. Columbia, MD: Bellwether Pub. Co. for Geol. Soc. America.

Alleman, F., 1979. Time of emplacement of the Zhob Valley ophiolites and Bela ophiolites, Baluchistan: in Geodynamics of Pakistan, Farah A. and DeJong, K.A. (eds.), p. 215-242.

Ashwal, L.D., Weidenbeck, M. and Torvik, T.H., 2017, Archaean zircons in Miocene oceanic hotspot rocks establish ancient continental crust beneath Mauritius: Nature Communications. Article no.14086. DOI: 10.1038/ncomms 14086. Pub. on line Jan. 2017.

Asrarullah, Ahmad, Z. and Abbas, S., 1979. Ophiolites in Pakistan. In Geodynamics of Pakistan: Abul Farah and Kees DeJong edit. Geol. Survey of Pakistan, Quetta, p. 181-192.

Bandyopadhyay, S., 1999. Gondwana vertebrate faunas of India: PINSA, v. 65, no. 3, p. 285-313.

Beck, R.A., Burbank, D.W., Sercombe, W.J., Khan, M.A. and Lawrence, R.D., 1996. Late Cretaceous ophiolite obduction and Paleocene India-Asia collision in the westernmost Himalaya. *Geodinamica Acta*, v. 9, p. 114-144.

Besse, J. and Courtillot, V., 2002. Apparent and true polar wander and the geometry of the geomagnetic field in the last 200million years: Jr. Geophy. Res. v. 107. (B11), 2300, doi:10.1029/2000JB000050.

Cande, S.C. and Stegman, D.R., 2011. Indian and African plate motions driven by the push force of the Reunion plume head. *Nature,* v. 475, p. 47-52.

Cande, S.C., Patriat, P. and Dyment, J., 2010. Motion between the Indian, Antarctic and African plates in the Early Cenozoic. *Geophys. Jr. Int.* v. 183, p 127–149.

Carey, S.W., 1988. Theories of the Earth and Universe. Stanford Univ. Press, Stanford. 413p.

Carmen, G., Hinsbergen, D.J.J.V. and Spakman, W., 2015. Tectonic interactions between India and Arabia since the Jurassic reconstructed from marine geophysics, ophiolite geology, and seismic tomography. *Tectonics*, v. 34, p. 875-906.

Chatterjee, S. and Scotese, C. R., 1999. The breakup of Gondwana and the evolution and biogeography of the Indian plate. *Proceedings of the Indian Science Academy*, v. 65, no. 3, p. 397-425.

Chatterjee, S. and Scotese, C.R., 2010. The wandering Indian plate and its changing biogeography during the Late Cretaceous–Early Tertiary period. In: Bandopadhyay, S. (ed.), New Aspects of Mesozoic Biogeography. Springer-Verlag, Berlin Heidelberg, Germany, p. 105–126.

Chatterjee, S., Goswami, A. and Scotese, C.R., 2013. The longest voyage: Tectonic, magmatic and paleoclimatic evolution of the Indian plate during its northward flight from Gondwana to Asia. *Gondwana Res*., v. 23, p. 238-267.

Choi, D.R., 2006, Where is subduction under the Indonesian Arc? *NCGT Newsletter,* no. 39, p. 2-11.

Colbert, E.H., 1973. Continental drift and the distributions of fossil reptiles. In: Tailing D.H., Runcorn S.K., eds. Implications of continental drift for the Earth sciences. London: Academic Press. p. 395–412.

Crawford, A.R., 1979. The myth of a vast Oceanic Tethys, the India-Asia problem and Earth expansion. Petroleum Geol., v. 2, no. 1, p. 3–9.

Deitz, R.S. and Holden, S.C., 1970. The breakup of Pangaea. Sci. Amer. v. 223, p. 30-41.

DeJong, K.A. and Subhani, A.M., 1979. Note on the Bela ophiolites with special reference to the Kanar area. In: Farah, A. and DeJong K.A., eds. Geodynamics of Pakistan. Geol. Sur. Pakistan. p. 263-270.

Ernst, W.G., 2015, Franciscan geologic history constrained by tectonic/olistostromal high-grade metamafic blocks in the iconic California Mesozoic-Cenozoic accretionary complex. *American Min*., v. 100, p. 6-13.

Gnos, E., Immenhauser, A. and Peters, T., 1997, Late Cretaceous/Early Tertiary convergence between the Indian and Arabian plates recorded in ophiolites and related sediments. *Tectonophy.* v. 271, p. 1-19.

Gnos, E., Khan, M., Mahmood, K., Shafique, A.S. and Villa, I.M. 1998. Bela oceanic lithosphere assemblage and its relation to the Reunion hotspot. *Terra Nova*, v.10, no. 2, p. 90-95.

Hunting Survey Corporation (HSC), 1960. Reconnaissance geology of part of western Pakistan: Toronto, Government of Pakistan, 550p.

Jacob, K.H. and Quittmeyer, R.L., 1979. The Makran region of Pakistan and Iran: Trench-arc system with active plate subduction, Geodynamics, in Farah, A. and DeJong, K.A., (eds.), Geodynamics of Pakistan, Geological Survey of Pakistan, p. 305–317.

Jagoutz, O., Royden, L., Holt, A.F. and Becker, T.W., 2015. Anomalously fast convergence of India and Eurasia by double subduction. *Nature Geosci. Lett.,* v. 8, p. 475-478.

Jan, M.Q., Windley, B. and Khan, a., 1985, The Waziristan ophiolite, Pakistan: general geology and chemistry of chromite and associated phases. *Econ. Geol*. v. 80, no. 2, p. 294-306.

Jan, M.Q., Khan, S.M. and Khan, A.M, 2011. Petrology of the ultramafic rocks from the Waziristan Ophiolite, NW Pakistan: 26th Himalaya-Karakoram-Tibet workshop, Canmore, Canada, July 12-13, 2011.

Kakar, M.I., Mahmood, K., Arif, M., Khan, M., Kerr, A.C., Mohibullah M. and Kasi, A.M., 2015. Petrology and geochemistry of mafic dykes from the Muslim Bagh Ophiolite (Pakistan): implications for petrogenesis & emplacement. *Turk. Jr. Earth Sci*., v. 24, p. 1404-1424.

Kakar, M.I., Kerr, A.C., Mahmood, K., Collins, A.S. and Macdonald, I., 2014. Supra-subduction zone tectonic setting of the Muslim Bagh Ophiolite, north western Pakistan: Insights from geochemistry and petrology: Online accepted manuscript. May 2014. *Lithos* 3302.

Khan, M., Gnos, E., Khan, A.S. and Mahmood. K., 1998. Genetically two different types of basaltic rocks from Bela Ophiolite, Balochistan, Pakistan. *Acta Mineralogica Pakistanica*, v. 9, p. 27-36.

Kashfi, M.S., 1988. Evidence for non-collisional geology in the Middle East. *Jr. Petrol. Geol.*, v. 11, p. 443-460.

Kazmi, A.H., 1979. The Bibai and Gogai nappes in the Kach-Ziarat area of northeastern Baluchistan. In: Farah, A. and DeJong K.A., Eds. Geodynamics of Pakistan. Geol. Sur. Pakistan. p. 333-340.

Khan, M., Kerr, A.C. and Mahmood, K., 2007. Formation and tectonic evolution of the Cretaceous–Jurassic Muslim Bagh ophiolitic complex, Pakistan: Implications for the composite tectonic setting of ophiolites. *Journal of Asian Earth Science*, v. 31, p. 112-127.

Khan, S.D., Walker, D.J., Hall, S.A., Shah, M.T. and Stockli, L., 2009. Did the Kohistan-Ladakh arc collide first with India. *GSA Bull*., v. 121, nos.3/4, p. 366-384.

Khan, S.R., Jan, Q.M., Khan, T. and Khan, M.A., 2004. Waziristan ophiolite: A back arc basin caught in continental collision, Waziristan, NW Pakistan. *Himal. Jr. Sci*., v. 2, no. 4 (spec. issue), p. 176-187.

Krause, D.W., Rogers, R.B., Forster, C.A., Hartman, J.H., Buckley, G.A. and Sampson, S.D., 1999. The Late Cretaceous vertebrate fauna of Madagascar: Implications for Gondwanan paleobiogeography. *GSA Today*, v. 9, p. 1–7.

Mahmood, K., Boudier, F., Gnos, E., Monié, P. and Nicolas, A., 1995. 40Ar/39Ar dating of the emplacement of the Muslim Bagh ophiolite, Pakistan. *Tectonophysics*, v. 250, p. 169-181.

Meyerhoff, A.A. and Meyerhoff, H.A., 1974. Tests of plate tectonics. In: Cahle, C.F. (ed.), Plate tectonics – assessments and reassessments. *AAPG Mem*. 23, p. 43-145.

Meyerhoff, A.A., Boucot, A.J., Meyerhoff-Hull, D. and Dickins, J.M., 1996. Phanerozoic faunal and floral realms of the Earth: the intercalary relations of the Malvinokaffric and Gondwana Faunal realms with the Tethyan faunal realms. *Geol. Soc. America Memoir* 189, 69p.

Prasad, G.R., Verma, O., Flynn, J.J. and Goswami, A., 2013. A Late Cretaceous vertebrate fauna from the Cauvery Basin, South India: Implications for Gondwanan paleogeography. *Jr. Vertebr. Paleont.* , v. 33, no. 6, p. 1260-1268.

Pilchin, A., 2016. Critical analysis of the plate tectonics model and causes of horizontal tectonic movements. *NCGT Journal*, v. 4, no. 1, p. 204-272.

Robinson, P.T., Malpas, J., Dilek, Y. and Zhou, M., 2008. The significance of sheeted dike complexes in ophiolites. *GSA Today*, v. 18, issue11, p. 4-10.

Sarwar, G., 1981, Geology of the Bela ophiolites in the Wayaro area, Las Bela District, South Central Pakistan. Ph.D. Dissert. Univ. of Cincinnati, Ohio, 375p.

Sarwar, G. and De Jong, K.A., 1984. Composition and origin of the Kanar Melange, Southern Pakistan. In: L.A. Raymond (Editor), Mélanges: Their nature, origin and significance. Geol. Soc. Amer. Spec. Paper 198. P. 128-138.

Sarwar, G., Qureshi, M.J., Bhagwandas, Mukhtar, S., Zaid, A., Taggar, M.A. and Ahsan, S.N., 1988. Geological map of Wayaro Quadrangle, Las Bela District, Baluchistan, Pakistan: Topographic sheet no. 35 J/12 - a 15-minute quad. at 1: 50,000. Pub. by Geol. Survey, Pakistan.

Sarwar, G., 1992, Tectonic setting of the Bela Ophiolites, Southern Pakistan. *Tectonophysics*, v. 207, p. 359-381.

Schettino, A. and Scotese, C.R., 2005. Apparent polar wander paths for the major continents (200 Ma to present day): a paleomagnetic global frame for global plate tectonic reconstructions. *Geophys. Jr. Interntl*. v. 163, p. 727-759.

Sheth, H., 2008. Do major oxide tectonic discrimination diagrams work? Evaluating new log-ratio and discriminant-analysis-based diagrams with Indian Ocean mafic volcanics and Asian ophiolites. *Terra Nova*, v. 20, no. 3, p.229-236.

Sheth, H.C., 2005. From Deccan to Reunion: no trace of a mantle plume. In: Foulger, G.R., Natland, J.H., Presnall, D.C. and Anderson, D.L. (eds.). Plates, Plumes, and Paradigms. Geological Society of America, Special Papers 388, p. 477-501.

Siddiqui, R.H., Mengal, J.M., Hoshino, K., Sawada, Y. and Brohi, I.A., 2011. Back-arc basin signatures represented by the sheeted dykes from the Muslim Bagh Ophiolite complex, Baluchistan, Pakistan. *Sind Univ. Res. Jr.* v.43, no.1, p. 51-62.

Sun, Ai-Lin, 1972, Permo-Triassic reptile of Sinkiang. *Scientia Sinica* (notes), v. 16, p. 152-156.

Verma, S.P. and Agrawal, S., 2011, New tectonic discrimination diagrams for basic and ultrabasic rocks through log-transformed ratios of high field strength elements and implications for petrogenetic processes: Revista Mexicana de Geologicas, v. 28, no. 1, p. 24-44.

Vermeesch, P., 2006, Tectonic discrimination diagrams revisited: *Geochem. Geophys. Geosyst.*, v. 7, Q06017. doi: 10.1029/2005GC001092.

Xiong, Y., Khan, S.D., Mahmood, K. and Sisson, V.B., 2011. Lithological mapping of Bela ophiolite with remote-sensing data. *International Journal of Remote Sensing*, v. 32, no. 16, p. 4641-4658.

Yano, T., Vasiliev, B.I., Choi, D.R., Miyagi, S., Gavrilov, A.A., and Adachi, H., 2011, Continental rocks in the Indian Ocean. *New concepts in global tectonics newsletter*, no. 58, p. 9-28.

Application of mobile and direct-prospecting technology of remote sensing data frequency-resonance processing for vertical channels of deep fluids migration detection

Sergey Levashov[1-2], Nikolay Yakymchuk[1-2], Ignat Korchagin[3] and Dmitry Bozhezha[2]
[1]Institute of Applied Problems of Ecology, Geophysics and Geochemistry, Kiev, Ukraine. slevashov@mail.ru
[2]Management and Marketing Center of Institute of Geological Science NAS Ukraine, Kiev, Ukraine. admin@karbon.com.ua
[3]Institute of Geophysics of Ukraine National Academy of Science, Kiev, Ukraine. korchagin@karbon.com.ua

Abstract: The results of testing the advanced direct-prospecting method of frequency-resonance processing and decoding of RS data on a large Shebelinka Gas and Condensate Field, GCF (Ukraine) are analyzed. Vertical channels of deep fluids migration within the hydrocarbon fields and mapped anomalous zones of the "deposit of hydrocarbons" type have been detected and localized in various regions of the world: the Dnieper-Donets (DDB) and Pripyat Basins (PB), Western Siberia, the Gulf of Mexico and Mediterranean Sea, Republic of Kazakhstan.

Mobile technology of satellite images frequency-resonance processing was used for the collection of field data. It is based on the principles of "matter" paradigm of geophysical studies which allows the deection and mapping of the anomalous zones of "deposit of hydrocarbons (oil, gas and gas condensate)" type. A separate method of this technology allows within the contours of detected anomalous zones at the resonance frequencies of gas to estimate the maximum value of the fluid pressure in the reservoirs at different intervals (including depth) of cross-section.

In the region of the Shebelynka GCF location the anomalous zone of 224.5 km^2 area of the "gas+condensate" type with reservoir pressures in the range of 20.4-25.8 MPa has been mapped. In the north-western and south-eastern parts of the field two vertical channel of fluid migration with reservoir pressure of 280 and 272 MPa were found. Within the vertical channels areas anomalous responses at resonant frequencies of oil, gas, condensate, helium, hydrogen and carbon dioxide have been registered. Within the larger area (2220 km^2) seven separate anomalous zones with total area of 259.9 km^2 have been detected and mapped. In relation to the observed area all anomalous zones make up 21.82%. Vertical channel with a pressure of 42.5 MPa was also found within the structure of "vortex" type in Western Siberia and two additional channels (95.0 MPa and 110.0 MPa) within Machuhskoye gas field in the DDB. The vertical channel with largest area was detected in the region of emergency well location in the Gulf of Mexico. The maximum value of the formation pressure within its contour was estimated at 165 MPa. Within two anomalous zones of the "Oil&Gas" type, found in the vicinity of Zohr large gas field in the Mediterranean Sea, the vertical channel of depth fluids migration with the reservoir pressure of 141.0 MPa have been mapped also. Local site in the areas of vertical channels location, identified within the contours of the anomalous zones, should be considered as the most promising for a detailed study by geophysical methods and location of prospecting wells.

The results of these studies indicate the presence within the hydrocarbons fields and mapped anomalous zones of the "deposit of hydrocarbons" type of local areas with anomalously high formation pressure of fluids in the reservoirs of cross-section – the vertical channels of the deep fluids migration. Mobile and direct-prospecting methods allow the identification and mapping of these channels by the results of anomalous responses registering the resonant frequencies of helium, hydrogen, and carbon dioxide. The proven methods of the vertical channels of fluid (HC) migration detecting and of reservoir pressures on different depths of cross-section evaluation can be widely used for the operational assessment of hydrocarbon potential of deep horizons of the cross-section. These facts of the vertical channels of fluid migration detection, as well as the presence of a significant number of anomalous zones of the "Oil and Gas deposit" type at different levels (depth including) of the cross-section can be regarded as important evidence in favor of the abiotic origin of hydrocarbons.

Keywords: *vertical channel, oil & gas, well, satellite data processing, direct prospecting, mobile technology*

(Received 19 January 2017. Accepted 19 March 2017)

Introduction

For over 15 years, the authors conducted actively and purposefully the research and experiments on the problem of development and implementation for exploration of mobile and low-cost technologies of direct prospecting and exploration of mineral resources – oil, gas, gold, uranium, water (drinking, mineral, geothermal), etc. At present, we have developed and tested in various regions of the world the mobile ground-based geoelectric methods using short-pulsed electromagnetic field (FSPEF (SCIP)) and vertical electric-resonance sounding methods (VERS) (Levashov et al., 2006, 2009, 2011and 2012; Shuman et al., 2008; Yakymchuk et al., 2008; Yakymchuk, 2014), as well as a super-mobile (super-operative) method of frequency-resonance processing and interpretation (decoding) of remote sensing (RS) data (satellite images) (Levashov et al., 2010, 2011 and 2012; Yakymchuk, 2015). The results of testing and practical application of individual direct-prospecting methods, and technologies as a whole are shown in numerous published articles and materials (proceedings) of scientific and practical conferences, seminars, symposia (Levashov et al., 2006, 2009, 2010, 2011, 2012, 2013, 2014, 2015 and 2016; Shuman et al., 2008; Solovyov at al., 2011; Yakymchuk et al., 2008 and 2015).

It is also appropriate to note that the testing of the developed methods have also been repeatedly performed on the known deposits of hydrocarbons (HC), including one of the largest in the Ukraine – the Shebelinka gas condensate field (Shebelinka GCF) (Levashov et al., 2011; Shuman et al., 2008; Yakymchuk et al., 2008).

Throughout this time, research was carried out constantly and purposefully to improve the theoretical justification of these mobile methods and the development of guidelines and techniques for their practical application. It is clear that for this (past) time the developed methods have been significantly upgraded. In 2015 the method of estimating the fluid pressure in the collectors by frequency-resonance processing and decoding of RS data was significantly improved. This fundamentally important component of direct-prospecting technology was "supplemented" by a separate operating mode, which allows one to estimate the fluid pressure in the reservoirs at different (including deep, as well as a priori given) horizons of cross-section.

Due to the fact that the improved modifications (components) of technology were not tested, it was decided to carry out further experimental work at the Shbelinka GCF, and within the surrounding areas of the Shebelinka GCF. It was also planned, based on the field work from earlier years, to prepare an article (publication), where at a particular practical material to demonstrate as a process of direct-prospecting methods improving, so and the new possibilities that these techniques can provide for potential users during the specific exploration tasks (problems) solving. These additional investigations were performed during February 2016.

However, during remote sensing data frequency-resonance processing in the Shebelynka GCF area, local specific structural elements in the deep part of the cross-section which suggest the presence of vertical channels of deep fluids migration have been discovered. These led to the need for additional experimental investigation within the known deposits of hydrocarbons and specific structures in other oil and gas regions. All this, as a whole, predetermined the completely different format, and the main purposes of this article. Materials of the conducted research allow us to formulate the main purposes (tasks) of the article in a following way:

– Development of methods for detection and localization of vertical channels of deep fluid migration based on the results of frequency-resonance processing and decoding of remote sensing data (satellite images) and its validation in the known hydrocarbon fields and promising structures in different regions of the world;

– To conduct additional testing of the advanced modification of the frequency resonance method of the satellite images processing and interpretation the commercial oil and gas accumulations searching and prospecting in reservoirs of various types;

– Once again to demonstrate for the specialists of oil and gas and service geophysical companies the expediency of more active application of mobile and direct-prospecting geophysical methods with the purpose of accelerating and optimizing exploration for oil and gas;

– To draw attention of the scientific community and technical experts on the accumulated (in large amounts) data of remote sensing of the Earth, which, with application of effective methods and technologies of their decoding and interpretation, may be successfully used for exploration and prospecting of ore minerals, accumulations of hydrocarbons and water;

– A demonstration of the direct-prospecting methods and technologies possibilities in the essential problem solving – justification of concept of deep (endogenous) hydrocarbon synthesis in the process of large-scale hydrogen degassing of the Earth.

To the above, we add that problems with the existence of vertical channels of deep fluids migration, as well as their detection and localization by geophysical methods, have long been given due attention by researchers. In particular, in the "geosoliton" concept of hydrocarbon formation (it supplements the abiogenic theory of the hydrocarbon genesis) the "geo-soliton tubes" are the proposed supply channels for oil and gas fields (Bembel et al., 2003 and 2013). The authors of the article (Muslimov and Trofimov, 2012) believe that "each oil field consists of three main components: a) a trap proper, filled with oil; b) a certain deep reservoir – a supplier of hydrocarbon fluids; and c) an oil supply channel, connecting the deep reservoir and the trap". It is also noted the occurrence of anomalous high production rates of hydrocarbons in wells that were drilled into such channels zones. However, such supply channels (or "geo-soliton tubes") were detected by high-precision seismic surveys, the use of which has been tested on a number of oil fields in the Western Siberia. Given the high cost of high-precision seismic studies, the problem discovering more economic and effective techniques for detecting and locating the vertical channels of deep fluids migration is quite urgent and deserves strong attention.

Below the graphics materials (data) of frequency-resonance processing and decoding of satellite images of eight areas (including areas of known oil and gas fields location) in different regions of the world are presented and analyzed. Almost all the experimental works have been conducted operatively in February-March 2016.

About deep (endogenous) origin of hydrocarbons

Many years of experience in the practical application and testing of mobile direct-prospecting technologies on known hydrocarbon deposits and prospecting areas and blocks compelled the authors to draw attention to the enough actual problem of hydrocarbons origin (genesis). The following circumstances (points) served as basis for this.

Firstly, the anomalies (anomalous zones), mapped by direct-prospecting methods, can be considered in a first approximation as integral projections of the contours of all deposits in the cross-section to the surface. This makes it possible to form some idea about the deposits form (structure) and their correlation with the known structural and tectonic elements of the investigated (studied) areas and local sites. And first of all – their location relative tectonically weakened zones (tectonic faults).

Secondly, the active use since 2010 in the search process of a super-mobile and direct-prospecting technology of frequency-resonance processing and decoding of satellite images provides an opportunity to purposefully conduct experimental research in all oil and gas regions in the laboratory.

In particular, in recent years a significant amount of targeted research of experimental nature was made in the areas of shale distribution (Levashov et al., 2014c), rocks of the Bazhenov formation (Levashov et al., 2014a), impact structures in the various regions of the world, within the crystalline shields (Levashov et al., 2013 and 2014b), as well as in offshore areas (Levashov et al., 2015; Yakymchuk, 2015). The received results allow the authors quite reasonably support many arguments and positions of the supporters of abiotic synthesis of hydrocarbons.

So, in their articles and demonstration documents the authors consistently noted that the structure and characteristic features of anomalous zones, mapped with the use of the direct-prospecting methods and technologies, can find a logical explanation from the standpoint of deep (abiotic) hydrocarbon synthesis and their subsequent vertical migration to the top part of the Earth's crust and in the atmosphere as part of the global process of the Earth degassing.

Numerous studies on the problem of deep origin of hydrocarbons set out in the list (far from exhaustive) of research publications (Bagdasarova, 2014; Bembel at al., 2003 and 2013; Valyaev, 2012; Krayushkin, 1986; Kusov, 2011; Kutcherov and Krayushkin, 2010; Kucherov, 2016; Larin, 2014; Lukin, 2015; Megerya et al., 2012; Timurziyev, 2013 and 2015 and 2016), mentioned in the references. A huge number of various information on this issue can also be found in many documents and articles on the “Deep oil” site (www.deepoil.ru).

The authors strongly support fundamental "Deep oil" project and its organizers with their participation (full-time and by correspondence) in conferences "Kudryavtsevskiye reading" and the publication of research results in the electronic journal "Deep oil" (Korchagin at al., 2014; Levashov et al., 2013 and 2014a and 2014b).

The basic postulates of the endogenous concept of hydrocarbons synthesis are described in Kutcherov (2013). So, in the article introduction Kutcherov states the following: “The theory of the abiogenic deep origin of hydrocarbons recognizes that the petroleum is a primordial material of deep origin (Kutcherov and Krayushkin, 2010). This theory explains that hydrocarbon compounds generate in the asthenosphere of the Earth and migrate through the deep faults into the crust of the Earth. There they form oil and gas deposits in any kind of rock in any kind of the structural position. Thus the accumulation of oil and gas is considered as a part of the natural process of the Earth’s outgassing, which was in turn responsible for creation of its hydrosphere, atmosphere and biosphere”.

Kutcherov (2013) states that the theoretical aspects of abiogenic hydrocarbon synthesis are considered and analyzed in the following directions: a) “milestones of the theory of abiogenic deep origin of hydrocarbons; b) experimental results of hydrocarbon synthesis; c) formation of oil and gas deposits in the light of the abiogenic deep origin of hydrocarbons; d) natural gas and oil in the recent sea-floor spreading centers; e) bitumen and hydrocarbons in native diamonds; f) petroleum in meteorite impact craters; g) oil and gas deposits in the Precambrian crystalline basement; h) deep and ultra-deep petroleum reservoirs; i) supergiant oil and gas accumulations; j) gas hydrates: the greatest source of abiogenic hydrocarbons”.

For the given above let us just note the following. The numerous anomalous zones of the "deposit of hydrocarbons" type (or "projection on the Earth's surface contours of projected hydrocarbon accumulations in the cross-section"), as described below, and the discovered and mapped accumulations by mobile geophysical methods in different regions of the world, allow us to rightly argue about the possibility of their formation only through vertical (sub-vertical) migration of deep fluids. It should be added that the structure and nature of location of the mapped anomalous zones of the "hydrocarbon deposit" type on the whole can be explained by the mechanism of hydrocarbon accumulation and formation, which is described in Krayushkin (1986, p. 582) and Kutcherov and Krayushkin (2010, p. 5) as follows: "... The formation of oil and gas deposits occurs differently. Rising from sub-crustal layers abiogenically synthesized oil and gas move along the fault and its feathering fractures and are "injected" under tremendous pressure from the mantle into porous and permeable host rocks, producing a mushroom-like cloud hydrocarbon and gas. They remain relatively fixed, and do not migrate to any anticline or syncline or in an inclined or horizontal formation untill the new portions of oil and gas are depleted. This is indicated by experiments and practice of construction of underground gas storage facilities in the horizontal and inclined water-saturated layers of sand or sandstone".

Unfortunately, in most cases the described mechanism is not taken into account during the choice of objects and structures for drilling, prepared by the seismic data. This may, to some extent, influence the success of drilling. According to Zapivalov (2013), "the success of exploration in the world is kept at an average of 30%".

Let's also pay attention to the publications of Rusakov and Kutas (2014) and Rusakov (2016). Based on generalization of literary sources, these articles show that there is not enough biogenic methane in the Black Sea to form large industrial accumulations of oil and gas. Areas of intensive gas seeps are recommended by authors for future prospecting of deep origin gaseous hydrocarbons.

The following results of the additional practical testing of an improved methodology of the reservoir pressure values assessing in different (including depth) horizons of the cross-section, as well as the facts of the detection and localization of vertical channels of deep fluid (hydrocarbon) migration can be regarded as additional (and rather weighty) arguments in favor of the deep origin of oil and gas.

Methods of investigation

Mobile and direct-prospecting technology that includes a method of frequency-resonance processing and interpretation of satellite images (Levashov et al., 2010 and 2011 and 2012) and the ground-based geoelectric methods FSPEF (SCIP) and VERS (Levashov et al., 2006 and 2009 and 2012; Shuman et al., 2008; Yakymchuk et al., 2008; Yakymchuk, 2014) is widely used during conducting the experimental studies of various character. The individual components of the technology have been developed on the principles of "substance" ("matter") Paradigm of Geophysical Research (Levashov et al., 2012), the essence of which is to search for a specific (desired in each case) substances (matter) - oil, gas, gas condensate, gold, iron, water, etc. Distinctive features of these methods are described in many publications and studies on completed reports, including in list of literature (Levashov et al., 2006 and 2009 and 2010 and 2011and 2012 and 2013 and 2014 and 2015 and 2016; Shuman et al., 2008; Solovyov at al., 2011; Yakymchuk et al., 2008 and 2015). In this article, we are characterizing in more detail the stages of prospecting and results that can be obtained at each stage.

Prospecting investigation by mobile method of frequency-resonance processing of remote sensing data and ground-based geoelectric methods FSPEF (SCIP) and VERS may be conducted in three main phases: 1) frequency-resonance analysis of satellite images of the major search areas and blocks in a relatively small scale (*the study of regional character*); 2) a detailed frequency-resonance analysis of satellite images of individual areas (sites) of anomalous zones, allocated at the first stage (*work of detailed character*); 3) field geoelectric works on the most promising local areas, identified at the second phase of the work (*ground-based studies*).

Regional studies.
At this stage the search areas are evaluated for the presence of hydrocarbon deposits. Research carried out in the following sequence: 1) the selection and follow-up on the area of linear zones of tectonic fractures; 2) registration of anomalous responses on the resonance frequencies of gas, oil and condensate in order to detect anomalous zones of the "deposit of gas," "oil reservoir", "gas-condensate deposit" type; 3) the contours of search objects fixing and their areas defining; 4) determining the intervals of reservoir pressure of oil and gas for each selected anomalous zone; 5) the maps of the anomalous areas constructing in isolines of maximum reservoir pressure values for each anomalous zone.

At the regional stage of research the frequency-resonance analysis of satellite images is conducted in the scale of 1: 200 000 - 1: 150 000. The processing time of one tablet (satellite image in A3 format) is about 2-3 days.

The works of detailed character within the contours of the most promising areas (anomalous zones), detected at the first stage of works, are carried out with using the method of frequency-resonance interpretation of satellite images. The criterion of the promising sites selection for detailing can be the size of the anomalous zones and the availability of reservoir pressures intervals in each anomalous zone. Depending on the size of anomalous zones, for detailing may be used the scales in interval of 1: 60000 - 1: 15000.

At this stage of the work it is carried out:

1) Detecting and tracing of tectonically weakened zones and tectonic faults, which were not be detected on the small-scale tablet.
2) Detailing and clarifying the anomalous zones contours, the calculation of their areas and the definition of the boundaries of oil-water contact.
3) The detailed maps of the anomalous area in isolines of maximum values of reservoir pressure constructing.
4) Conducting the vertical scanning of the geological cross-section at the point of maximum reservoir pressure in order to highlight the depth interval of anomalous polarized layers (APL) of the "oil", "gas", "water", "water+gas", "solid rocks" type occurrence. As a result of the scanning the construction of the vertical columns of anomalous polarized layers (APL) is carried out.
5) Through the point with the maximum value of the anomalous zone the several profiles are laid, along which the additional points of the vertical scanning are placed. As a result of scanning at these points the columns and vertical cross-sections of APL are constructed for the anomalous zone.
6) For the thickest layers formation the pressure of APL is estimated (APL layer is considered promising provided that the obtained estimate of its formation pressure exceeds the hydrostatic pressure at that depth).

7) Constructing the maps of the total thickness of the APL of "deposits of oil" and "gas deposits" type.
8) The volumes of reservoirs, containing oil and gas, are estimated.
9) If the prospective APL layer is traced at the all scanning points, it can be taken as a marker horizon. In this case, the structural map of depths for the reservoir occurrence can be built.
10) Due to the constructed structural map, the assumptions may be make about the type of hydrocarbon trap (anticline, tectonically shielded, lithologically limited).
11) Further analysis of the results of second phase of the work allow to determine the optimal volume of geoelectric field research. If necessary, the recommendations to carry out seismic surveys along certain profiles or within the entire anomalous area can be formulated.

The detailed investigation within one anomalous zone takes 4-5 days.

Field works.
According to the results of the second phase of the study the most promising anomalous zones for the field measurements are identified. A survey of isolated (local) areas is carried out with the ground-based geoelectric methods of FSPEF (SCIP) (the forming of short-pulsed electromagnetic field) and VERS (vertical electric-resonance sounding).

At the stage of field work the following can be carried out:
1) Within the surveyed anomalous zones the small tectonic faults, which can divide anomaly (anomalies) into separate units, are detected and traced.
2) The size of each block and the contours of oil-water contacts are specified.
3) The anomaly area is covered by a network of vertical sounding points. At each point the intervals of the APL of the "oil", "gas", "gas+water", "water" type are determined and specified
4) For each reservoir of the hydrocarbon deposit the formation pressure is determined (estimated).
5) The vertical columns and vertical geological and geophysical cross-section for the projected field are constructed.
6) The maps of total thickness of the APL of "oil" and "gas" type and maps of thickness of the most promising oil and gas reservoirs are constructed.
7) The structural maps for several marker horizons are constructed.
8) The overall potential of oil and gas resources are evaluated.
9) The optimal points for the exploration wells laying are defined.
10) In the recommended points of the wells locations the binding of detected APL intervals to the lithological elements of geological cross-section is carried.

The time of field work conducting is 15-20 days. Processing of the field studies results and the report materials preparation take 20-30 days.

Focusing on the fact that the processing and interpretation of satellite images of search areas, taken from sources (sites) of free access, are performed quickly (operatively) in the laboratory conditions, without the field research organizing and conducting. In this connection, this technology can be considered a super-rapid (super-operative), allowing for a very short time to perform an assessment of hydrocarbon potential (ore content, water content) of exploration blocks at any point of the globe.

Some developments in terms of the theoretical justification of applied research methods in thesis form are set forth in paper (Yakymchuk, 2014). Additional information about this direct-prospecting method, as well as numerous examples of its practical application during operative solving the various search problems can be found at the site (http://www.geoprom.com.ua/index.php/ru/).

For the frequency-resonance processing, the multispectral images are used from different satellites. In most cases, these are in the public domain. For reconnaissance surveys of large areas and during the processing of remote sensing data on a scale of 1:50,000 and smaller, the images of Landsat 5 and Landsat 7 with a resolution of 30 m/pixel can be used. When looking for small objects, the remote sensing data processing should be done on a larger scale and requires high-resolution images, 2.5-1.0 m/pixel.

In the course of the studies the satellite images from Landsat 5-7-8 were used from site (http://glovis.usgs.gov/).

Geography of technology application.
In Ukraine, the geophysical works were carried out for various minerals searching – gas, gas condensate, crude oil, coal, drinking, mineral and geothermal water, uranium, and gold. Geotechnical engineering works were carried out during the construction of highways, subway lines, residential buildings and industrial complexes, survey of landslide areas, dams, searching for underground cavities, and others.

The authors have actively conducted the geophysical surveys for various minerals in foreign countries in different continents. These are: Russia – oil, gas, gas condensate, gas hydrates, diamonds and gold; Belarus – oil, gas and gas condensate; Republic of Kazakhstan – oil, gas, gold and zinc; Turkey – oil, gas, gas condensate, gold, platinum and geothermal water; Colombia – oil, gas, gas condensate and coal; Antarctic Peninsula region (Ukrainian Antarctic station on Galindez Island, expeditions in 2004, 2006 and 2010) – gas hydrates, oil, gas, glaciers mapping, and ice deposits thickness determination; offshore Falkland Island – oil and gas; Mongolia – oil, gas, iron ore, uranium, and geothermal water; Bulgaria – oil and gas; US – oil and gas; England – oil and gas; Australia – copper and gold; Mexico – gold; Chile – copper; Ecuador – oil and gas; Guyana – gold and manganese; Sudan – oil, gas and gold; Iran – oil and gas; Uzbekistan – oil and gas; Turkmenistan – oil and gas; Indonesia – oil and gas (offshore); Portugal – gold; Libya – oil and gas (offshore and onshore); Afghanistan – oil and gas; Ghana – oil and gas (offshore); Tunisia – oil and gas; Cameroon – gold; South Africa – oil and gas (offshore and onshore); Namibia – oil and gas; Madagascar – gold; Slovakia – geothermal water; UAE – oil and gas; Lithuania – oil and gas; Poland – oil, and gas; Romania – oil and gas; Armenia – oil and gas; Georgia – oil and gas; shelf in the Arctic region – oil and gas; Norway – oil and gas (offshore); Venezuela – oil and gas (offshore); Trinidad and Tobago – oil and gas (offshore); Gulf of Mexico – oil and gas hydrates; Vietnam – titan magnetite; Thailand – oil and gas (offshore).

It is advisable to focus on the fact that the technology of remote sensing data frequency-resonance processing was developed and continues to be improved by an experimental way. At the moment, a complete theoretical substantiation of separate technology methods does not exist. In this regard, the authors continue to purposefully conduct experiments to explore the potential of the frequency-resonance method of remote sensing data processing during solving a variety of problems, including those of environmental and monitoring nature. Results for each additional experimental study are making their specific contribution to further establish and develop this original technology.

The Features of Mobile Direct-Prospecting Methods
The ground-based geoelectrical methods of FSPEF and VERS make it possible to efficiently and accurately determine a geologic model beneath the sounding site. The original FSPEF and VERS methods are based on studying the geoelectrical parameters of the medium in pulsed transient geoelectrical fields, as well as of the quasi-stationary electric field of the Earth and its spectral features over hydrocarbon reservoirs (Levashov et al., 2006 and 2012; Yakymchuk et al., 2008 and 2014).

Ground survey by FSPEF method can be performed in two ways: on the car and by pedestrian. In the automotive embodiment, the antennas are mounted outside the vehicle. The survey is conducted at a speed not more than 20-30 km per hour. The signals of field formation are registered every 50-60 meters or through a priori specified time interval.

In the pedestrian embodiment, the equipment, including the batteries, is transferred by the operators (weight of apparatus: up to 10 kg). The survey is performed by two operators.

The results of FSPEF survey are used for selecting optimal profiles for the VERS method, which are implemented at individual points. VERS profiles intersect anomalous zones mapped during the FSPEF survey. The time required for sounding at one point within the depth interval up to H = 1.0 km is about 2 hours. The sounding is performed by three operators.

The main difference between the used geoelectrical methods from classic electric prospecting is that in the electric prospecting methods the surface-to-air boundary is considered a conductor and an insulator. In geoelectrical method the near-surface part of the atmosphere is considered as weakly ionized plasma. The frequency generation occurs in the space charge of near-surface part of the atmosphere.

In the natural quasi-stationary electric field Ez, the anomalous object, located at a depth H, forms with the ground-air interface the polarized dipole of H thickness. During the natural or artificial changes (excitation) of the primary polarizing field Ez, the dipole radiates electromagnetic waves with frequencies f = C/L, where C is the speed of light and L is the length of the waves, which is equal to L = 2H.

Feature of measurement by VERS method is following. The natural field Ez is distorted over exploratory geological object by short electromagnetic pulses, and at this point the frequency responses are measured. When the frequency response is known, we can determine the depth of the object: H = C/2f.

The generator of rectangular impulse with the frequency of 3.0 kHz is used for generating perturbing field. The registering of the natural electromagnetic field is carried out by using broadband antennas. Signals are recorded in the frequency range from hundreds of hertz to tens of megahertz. Spectral signal processing is carried out further; the results of processing are compared with the reference spectra of searching objects.

The distinctive features of the FSPEF and VERS geoelectrical methods, used by the authors, are described in articles by Levashov et al. (2012) and Yakymchuk et al. (2008 and 2014). The principle of vertical sounding was done by Shuman (2012). A technique similar to the VERS method of sounding is described in the patent from Weaver and Warren (2004). For more information about the features of mobile technologies and the results of their application, visit the EAGE site, www.earthdoc.org/.

The Frequency-Resonance Processing of Remote Sensing Data. Currently, there are methods of remote sensing data processing and interpretation that are developed and improved within the framework of the "substantial" ("matter") paradigm of geological and geophysical studies. The essence of this paradigm is "direct" searching and prospecting for specific substances such as oil, gas, gold, silver, platinum, zinc, iron, water, etc. (Levashov et al., 2012). Among such technologies may be Infoskan (http://www.infoscan.ru), Tomko (Rostovtsev et al., 2011), Poisk (Kovalev et al., 2010 and Pukhliy et al., 2010), etc. The effectiveness of geophysical methods, based on the principles of this paradigm, is higher than traditional.

A phenomenological description of features of the Tomko technology is the following (Rostovtsev et al., 2011, p. 61): "It is based on the latest advances in astrophysics, mathematics, and knowledge about electromagnetic radiation, modern laser, computer hardware and software. It became possible due to the phenomenological approach to the study of the phenomena observed. Technology of quantum-optical filtering of satellite imagery allows, in most cases, anywhere in the world to identify the boundaries of projected oil and gas fields and record the density distribution of reserves within them.

Theoretical justification for this technology may be the ideas of E. I. Tarnovskiy, which are based on the fact that all atoms in molecules have a certain spatial position and its own electro-magnetic field with the characteristic spatial frequency intensity distribution.

The spatial-frequency structure of electromagnetic fields of any substance is determined by the chemical composition and molecular structure, or spatial lattice material. A large number of homogeneous substances will create a collective characteristic for the substance electromagnetic field radiation, whose power is proportional to the concentration of a substance in a given direction. We may assume that the linear polarized wave with the specified frequency response carries information about the structure of the substance, is not absorbed by the medium, and their intensity does not decrease with distance. In this case, a homogeneous substance at an arbitrary depth of the Earth will create a field, as if this substance were on the surface.

It was found that the characteristic of an electromagnetic wave of large quantities of oil and gas is fixed in a certain way on the satellite image; this is already used for opening and identifying yet-unknown fields. We pay attention to the phrases "a large number of homogeneous material", "radiation power which is proportional to the concentration of the substance," and "will create a field, as if it were a substance at the surface" in the above quotation.

In the Tomko technology, the useful signal separation is conducted by the quantum-optical filtering of satellite images. In this method, used by the authors, the separation of the useful signal from the satellite images is provided by the frequency-resonance method. For the various minerals (oil, natural gas, uranium, gold, water, zinc, etc.), their characteristic resonance frequencies have been identified on the minerals samples, and these are used during the remote sensing data processing and decoding.

Table 1 below gives the values of the resonance frequencies for water of different mineralization. For other minerals, the resonance frequencies are fixed in a wider range.

Table 1. Resonance frequencies of water of different salinity

Number	Mineralized water	Mineralization (g/dm^3)	Resonance frequencies, kHz
1	Structured (Alpine sources)	< 0.1	**717.6**
2	Weakly mineralized (Morshynskiye sources)	0.1 -0.4	**643.8**
3	Average mineralization	0.5 - 1.0	**615.7**
4	Strong mineralization	5.0 – 15.0	**551.5**

Assessment of the Values of Fluid Pressure in the Reservoir

Within the frequency-resonance technology of remote sensing data processing in general, a special place occupies a method of maximum values of fluid pressure assessment in the reservoir (Levashov et al., 2011a). First, it allows researchers to significantly narrow the areas for hydrocarbon deposit search and, consequently, the sites for the exploratory wells. Second, the result of its application for the fluid pressure assessment in reservoir can help to form an initial hypothesis about the depth of hydrocarbon deposits. Third, the lack within detected and mapped anomalous zones of the reservoir with relatively high values of fluid pressure in reservoir allows researchers to exclude such anomalies from the list of objects that deserve priority for a detailed study and drilling. Assessments of maximal values of fluid pressure in reservoir, in which the anomalous zones of oil/gas reservoir type are constructed, involves complex parameters that depend on the pressure of the gas in the fluid or in the free form in reservoir, as well as its amount, i.e., porosity of the rocks. Therefore, at the edges of the anomalous zones, a decrease of this parameter value is fixed. In areas of gas absence, the pressure is not defined, so here this parameter value is zero.

When research was conducted in 2015, the authors started testing the improved method of estimating the values of fluid pressure in the reservoirs. A distinctive feature of the improved method is that it allows to obtain the estimates of fluid pressures in the predicted hydrocarbon reservoirs within a given interval of cross-section (from the surface to a depth of 6 km, for example). In this situation, the process of anomalous response registration does not stop even in the case of their absence within certain intervals of the cross-section. The experiments showed that such a methodological procedure is justified; the anomalous responses within many detected anomalous zones were fixed at various intervals (segments) of the resonance frequencies. Therefore, an improved method of estimating fluid pressure allows researchers to detect the predicted hydrocarbon deposits in the various horizons of the cross-section and to assess approximately the depths of their occurrence.

Shebelinka gas and condensate field

During the testing of new and improved methods and technologies of special interest are the known deposits and prospective areas, within which the studies have been already carried out with using earlier versions of search methods. In these cases, there is a real opportunity to compare research results at different times, as well as by different methods. These objects include Shebelinka GCF (Atlas of…), the largest in Ukraine. The peculiarity of this field is that it is fairly well investigated.

Reconnaissance work with the methods FSPEF (SCIP) and using VERS has been held on Shebelinka GCF in February 2008. The obtained results (**Fig. 1**) allowed to state that (Levashov et al., 2011; Shuman et al., 2008; Yakymchuk et al., 2008):

a) mapped anomaly of the "deposit" type (DTA) well coincides with the contour of the structure; within its limits the areas of high and low values of anomalies were fixed;
b) within the Western Shebelinka area, as well as in the western part of the very Shebelinka structure the DTA are not fixed, which casts doubt on the usefulness of the further geological and geophysical surveys and drilling there;
c) a small anomaly was identified within the Northern Shebelinka area;
d) in the center of East Shebelinka area an anomaly of "deposit" type was recorded, to the south – an

intense anomaly was revealed, which is a continuation of the anomaly over the Shebelinka structure, it is not fully delineated;

e) within the Southern Shebelinka area the route FSPEF survey was not carried out;

f) to the north of Shebelinka structure two anomalous zone of "deposit" type were discovered by the separate routes of survey (**Fig. 1**);

g) within the anomalous zone over field by the VERS sounding at the point V1 (**Fig. 1, 2**) in the range depths of 1100-6500 m three gas-bearing interval (1385-1466 m 3 APL "gas", Hs=23 m, 1584-1772 m 3 APL "gas", Hs=28 m, 1860-2150 m, 22 APL "gas", Hs=118 m) were detected, the latter of which can be classified as interval of intense gas saturation. The massive layer deposit of Shebelinka GCF is fixed by 22 APL on the sounding diagram. APL of "salt" type is fixed at a depth of 5140 m, it is traced to 6500 m - the lower limit of the salt is not achieved (**Fig. 2**).

h) within the northern anomalous zone by the VERS sounding at the point V2 (**Fig 1, 3**) in the range depths of 1000-6600 m two gas-bearing interval (2639-3039 m 3 APL "gas", Hs=10 m; 5510-6600 m, 8 APL "gas" and "oil", Hs=160 m) were detected. In the lower range for the APL "gas" - Hs=57 m, and for APL "oil" - Hs=107 m, it is not tracked deeper (see **Fig. 3**). The total thickness of APL at this point is 170 m and is practically comparable to that at the point V1.

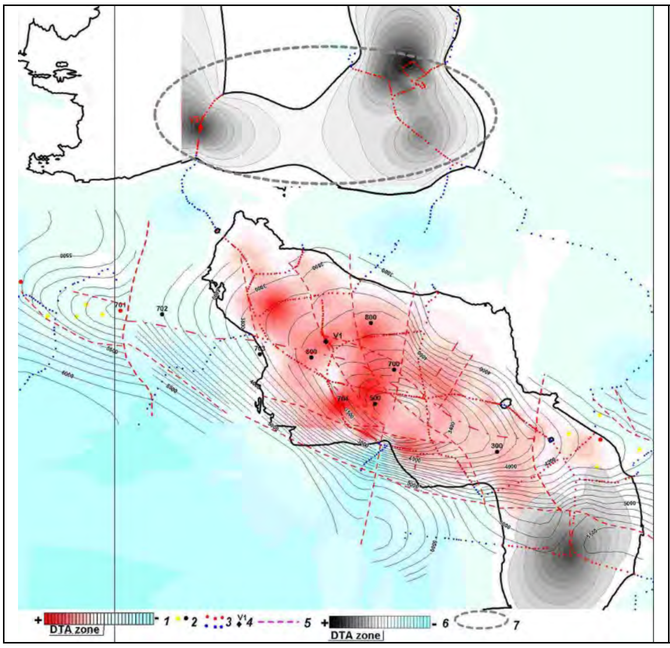

Fig. 1. A map of "deposit" type geoelectric anomaly on a structural map of horizon Vb_1^{1-n} (C_2m) of Shebelinka field. *1* – scale of FSPEF field values (DTA of gas+condensate type); *2* – wells; *3* – points of the FSPEF survey (positive values - red, negative - dark blue); *4* – VERS point; *5* – tectonic fractures; *6* – scale of FSPEF field values (DTA of gas+oil type); *7* – the probabilistic contour of northern anomalous zone.

Testing of the first modification of frequency-resonance technology of remote sensing data processing over area of Shebelinka GCF location was held in January 2010, at the beginning of its application. The results are shown in **Fig. 4**. In general, the identified anomalous zones of the "hydrocarbon deposit" type satisfactorily correlated with the anomalous geoelectric zones, mapped by ground-based FSPEF (SCIP) survey. Comparison of these results has allowed to focus on the following points (Levashov et al., 2010 and 2011):

1. The maximum values of anomalous responses are recorded in the central part of Shebelinka structure.
2. According to the results of decoding two anomalous zones are recorded to the north of the structure, as well as the anomalous zone to the south of the structure (by a ground-based FSPEF (SCIP) survey also).
3. Within the north-western part of the structure the anomalies of the "deposit" type are absent (similar to a ground-based FSPEF (SCIP) survey).
4. The small in size and intensity anomalous zone showed in the western part of the area. The ground-based FSPEF (SCIP) survey on this site has not been conducted.
5. Do not exclude the possibility that in the areas of elevated values of anomalous responses may be wells with high inflow of fluids. There also may be the areas of additional hydrocarbon inflow. However, this question requires more detailed study.

Methodology of evaluating the maximum value of fluids pressure in the reservoirs (Levashov et al., 2011) on Shebelinka GCF was not tested. In this regard, it was decided to carry out the processing of the field satellite image with this technique. The main task of investigation was an assessment of the prospects of detection of industrial hydrocarbon accumulations in the deep horizons of the cross-section.

Furthermore, it was also planned to examine the located in close proximity to the field sites with the aim of detecting and mapping the objects (anomalous zones), promising for HC industrial accumulation detection. Additional research in the area of deposits was held in February 2016.

Given previous research the satellite image processing of field locations area was carried out in a scale of 1: 100,000 (**Fig. 5**), as well as the image of a larger area at a scale of 1: 150,000 (**Fig. 9**). In the course of the image frequency-resonance processing the method of estimating fluid pressures in different levels (intervals) of the cross-section, including the deep intervals, was applied. In the graphical form the part of the results is shown in **Figs. 5-9**. Discovered anomalous zones are also shown on the field structural map (**Fig. 6**), as well as on satellite images.

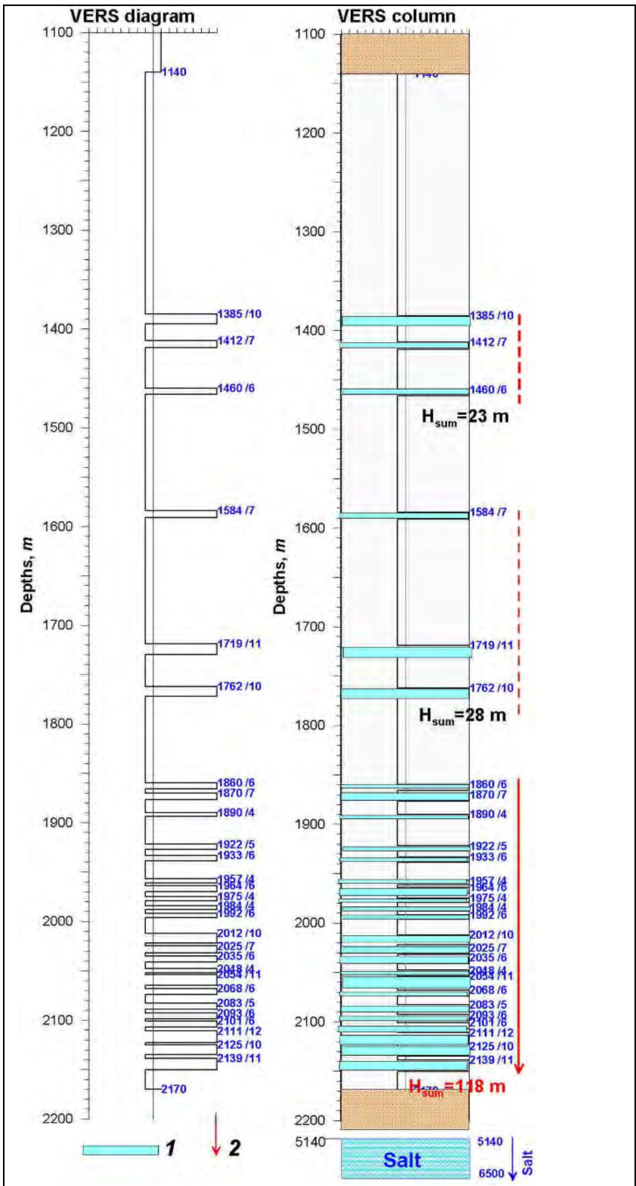

Fig. 2. The VERS data in an anomalous zone within the Shebelinka structure boundary. *1* – APL of "gas" type; *2* – interval of intensive gas content.

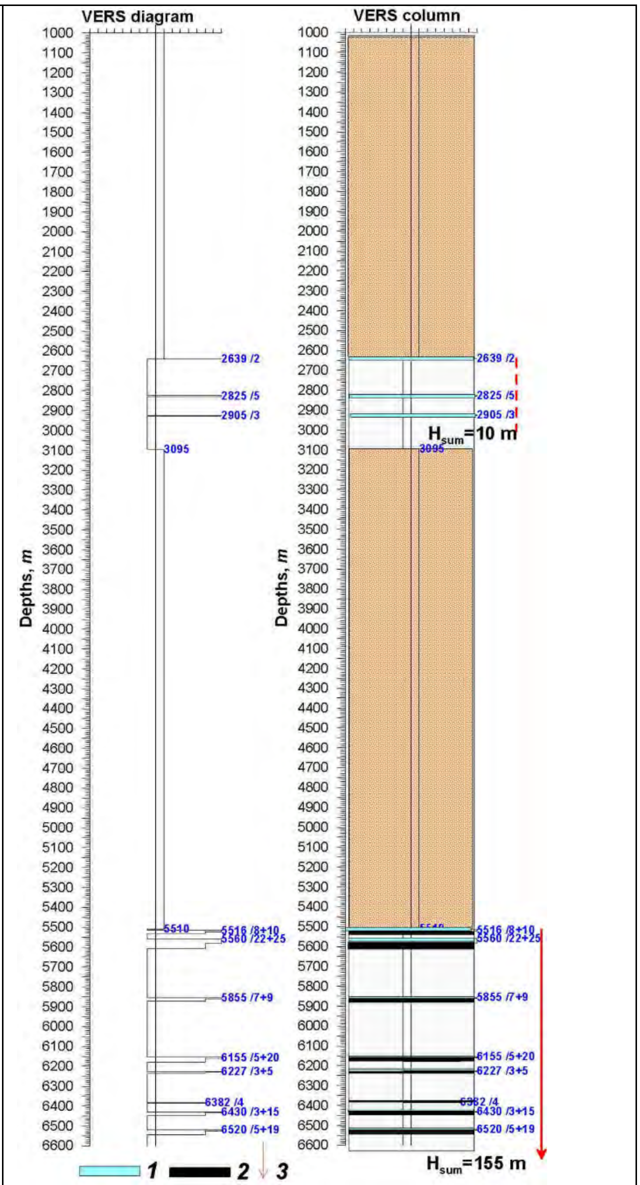

Fig. 3. The VERS data in an anomalous zone outside the Shebelinka structure boundary. *1* – APL of "gas" type; *2* – APL of "oil" type; *3* – interval of intensive HC content.

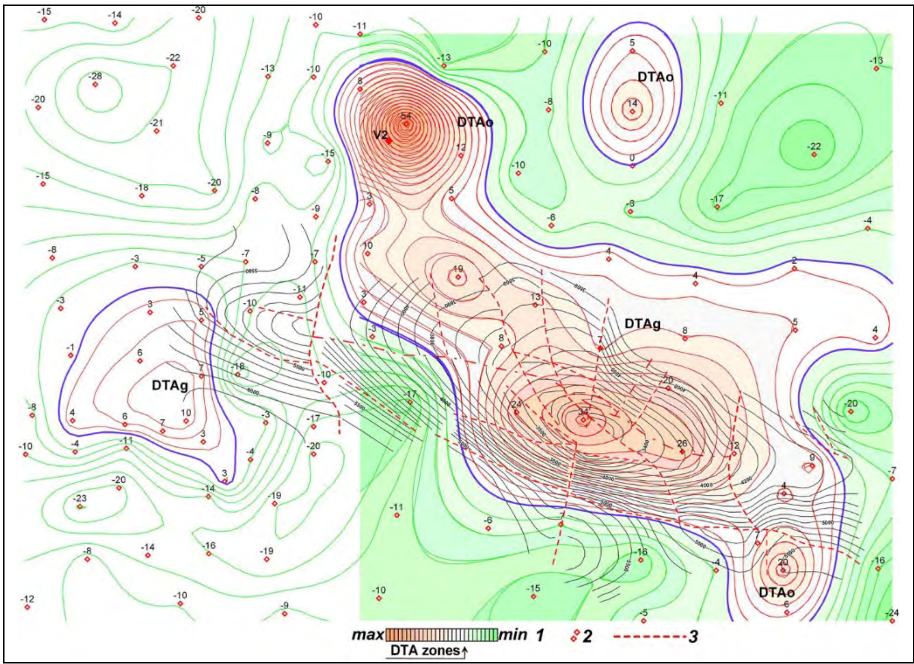

Fig. 4. The results of satellite data special processing on a structural map of horizon Vb_1^{1-n} (C_2m) of Shebelinka gas-condensate field. *1* – scale of the signal amplitude values that are determined during data processing, *2* – points of the signal amplitudes determination, 3 – tectonic fractures on seismic data. DTAg – anomalous zone of "gas" type, DTAo – anomalous zone of "oil+gas" type.

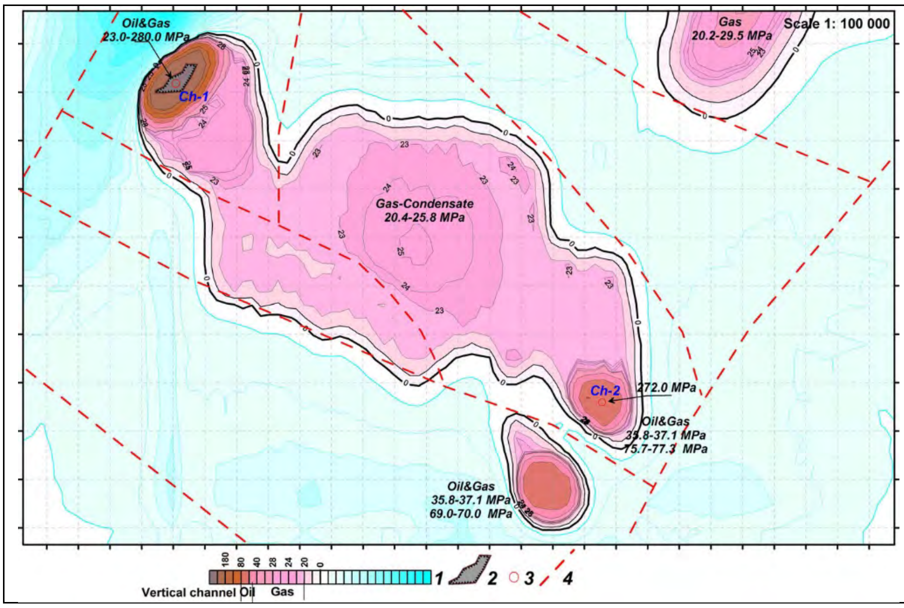

Fig. 5. Map of the geoelectric anomalous zone of "Oil-Gas" type in the area of Shebelynka gas-condensate field (According to the frequency-resonance analysis of satellite images). *1* – scale of the maximum values of reservoir pressure, MPa; *2* – the projected area of the vertical channel; *3* – coordinates of the central points of the vertical channels #1 - X=36.4415168º, Y=49.5036848º and #2 – X=36.7102815047º, Y=49.3714168274º; *4* – tectonically weakened zones (fractures).

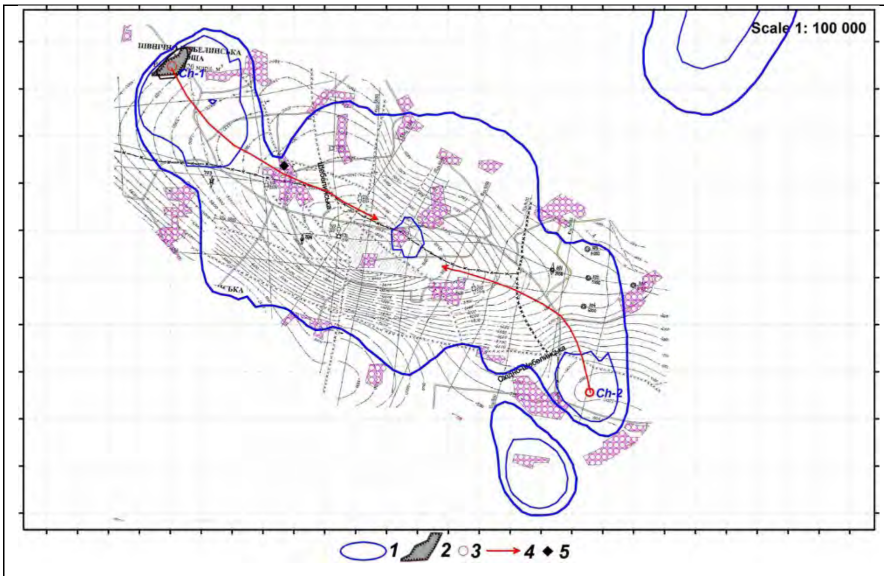

Fig. 6. A schematic map of the predicted migration of HC from the depth vertical channels in the zone of Shebelinka GCF (on the map of the field seismic borders on one of the reflectors). *1* – contours of geoelectric anomalous zone; *2* – the projected area of the vertical channel; *3* – coordinates of the central points of the vertical channels #1 - X=36.4415168º, Y=49.5036848º and #2 – X=36.7102815047º, Y=49.3714168274º; *4* – the expected paths of hydrocarbon migration from a vertical depth channel; *5* – point of vertical sounding VERS V1 in 2008.

Paying attention to the fact that during the areal satellite image processing at the scale of 1: 100,000 the local anomalous zone with a very high value of the reservoir pressure has been detected in the northwestern part of area – 280 MPa (**Figs. 5 and 6**). Earlier, during the analogical works in other regions such pressures on the local sites were not recorded. Most likely due to the fact that these areas are very small in size and during the images processing at a small scale, such small anomalies are usually skipped (not fixed). It is possible, in principle, to state that the local zone with a reservoir pressure of 280 MPa in the area was detected by accident.

In this situation, it was necessary to survey this anomalous area on a larger scale. Additional processing of satellite images of the local area was carried out on a scale of 1: 15000 (**Fig. 7**). As a result, the contours of the anomalous zone with high pressure reservoir were localized. Within their contours the anomalous responses at resonant frequencies of oil, gas, condensate, helium, hydrogen, and carbon dioxide have been registered.

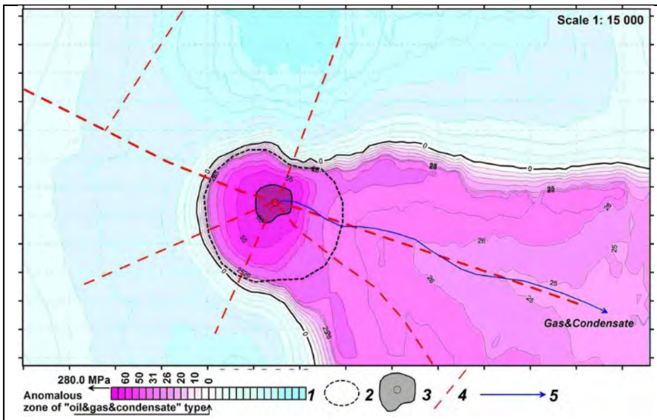

Fig. 7 Geoelectric anomalous zone in the vicinity of the vertical channel of hydrocarbon migration on Shebelinka gas condensate field. *1* – scale of the maximum values of reservoir pressure, MPa; *2* – zone of anomalies of "Oil" type; *3* – zone of the vertical channel (recorded at the resonant frequencies of oil, gas, condensate, helium (He), hydrogen (H_2), carbon dioxide (CO_2)); coordinate of the vertical channel center: X=36.4423111071º, Y=49.4989071944º; *4* – tectonic faults; *5* – predicted direction of hydrocarbon migration.

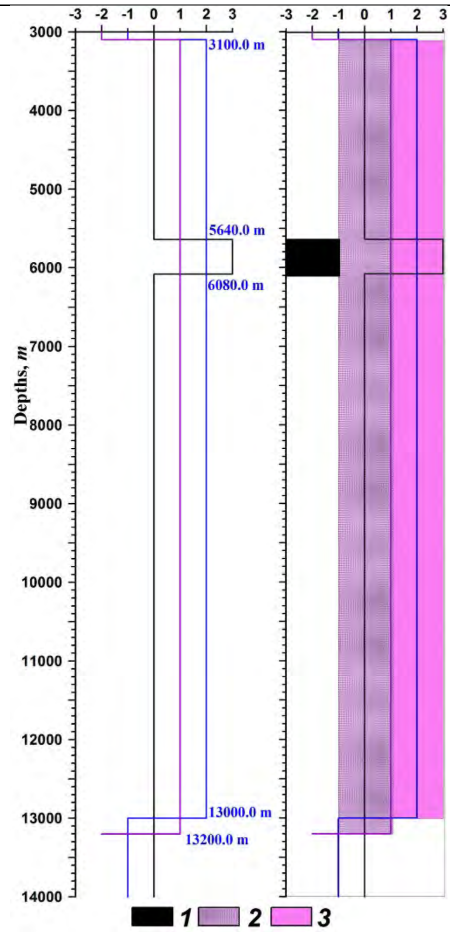

Fig. 8 (right). The results of vertical scanning of cross-section in the area of vertical channel of hydrocarbon migration on the territory of Shebelinka gas and condensate field. Anomalous polarized layers of following types: *1* – "Oil"; *2* – "Condensate"; *3* – "Gas".

In the center of the local anomalous zones the vertical scanning of cross-section was held to assess the depth of occurrence of possible accumulations of oil, gas and condensate (**Fig. 8**). In the process of scanning the anomalous responses at the resonant frequencies of oil were recorded in the depth interval of 5640.0-6080.0 meters, at gas - 3100.0-13000.0 m, at condensate - 3100.0-13200.0 m. Registered anomalous responses at the resonance frequencies of gas and condensate in a considerable depth range can be considered as additional (for high values of reservoir pressure) evidence in favor of the presence within the local area of a vertical channel of deep fluids (including HC) migration.

In the process of work it is quite naturally a question has arisen: whether there is within the field the similar zones in other parts of field. In this regard, additional analysis of satellite image was carried out within the local anomalies with high pressure value, located in the southeastern part of Shebelinka structure (**Figs. 5 and 6**). In its contours on a small area the anomalous responses on the resonant frequencies of the helium were recorded. By area, the anomaly in this part of the site is still less than that found in the north-western part. In the center of this local area the maximum reservoir pressure was estimated at 272 MPa (**Figs. 5, 6 and 9**).

In general, targeted search and detection of the second vertical channel of deep fluids migration allows to ascertain the development of instructional techniques (principles, approaches) for the detection and localization of such structural elements of the cross-section. In the future, these methodological techniques have been successfully used for the purpose of searching the vertical channels of deep fluids migration in the contours of the anomalous zones in other regions of the world.

The results of processing a larger area image at a scale of 1: 150,000 are shown in **Fig. 9**. The total surveyed area of the block in the region of Shebelinka GCF is 2220 km^2. The area of the large anomalous zone, mapped on the Shebelinka structure (field), is 224.5 km^2. Within the investigated site seven distinct anomalous zones with total area of 259.9 km^2 were further found and mapped. In relation to all investigated area the anomalous zones (over the field including) constitute 484.4/2220=21.82%. Additionally, for the shown in **Figs. 5, 6 and 6** materials the following conclusions can be formulated briefly.

1. Above the deposit directly large anomalous zone of the "gas" type was mapped. Almost in the center of this anomaly the assessments of reservoir pressure were recorded in the range of 20.4-25.8 MPa.
2. In the southeastern part of the field two local anomalous zones of the "oil and gas" type were found, within which during the reservoir pressures evaluation the anomalous responses were recorded in two horizons of the cross-section.
3. In the northwestern part of the surveyed area the anomalous zone of the "oil and gas" type with very high values of reservoir pressure has been detected - 280 MPa. In the southeastern part of the field a second local area with reservoir pressure of 272 MPa was found. These values of the pressure estimates are recorded for the first time!

These local anomalous zones can be considered as vertical channels of deep (abiogenous) fluids (hydrocarbons) migration in the upper part of the cross-section. Possible ways of gas migration from a vertical channel in the Shebelinka structure direction are shown in **Figs. 6 and 9**.

4. To north of the deposit four anomalous zones of the "oil and gas" type have been discovered and mapped with estimates of reservoir pressure in two intervals of the cross-section (**Fig. 9**). The anomalous zone of the "gas" type in the north-eastern part has been contoured fully. In the south-western part of the surveyed area a relatively large anomalous zone of the "gas" type with estimates of reservoir pressure in one range of depths has been found.

It is also appropriate to note that paper (Lepigov et al., 2013) discusses the possibility of forming the Shebelinka field from the standpoint of abiotic origin of hydrocarbons within “geosoliton” concept of theirs formation (Bembel at al., 2003 and 2013; Megerya et al., 2012). This fact determined the choice of the next test object – the structure of “geosoliton” (vortex) type.

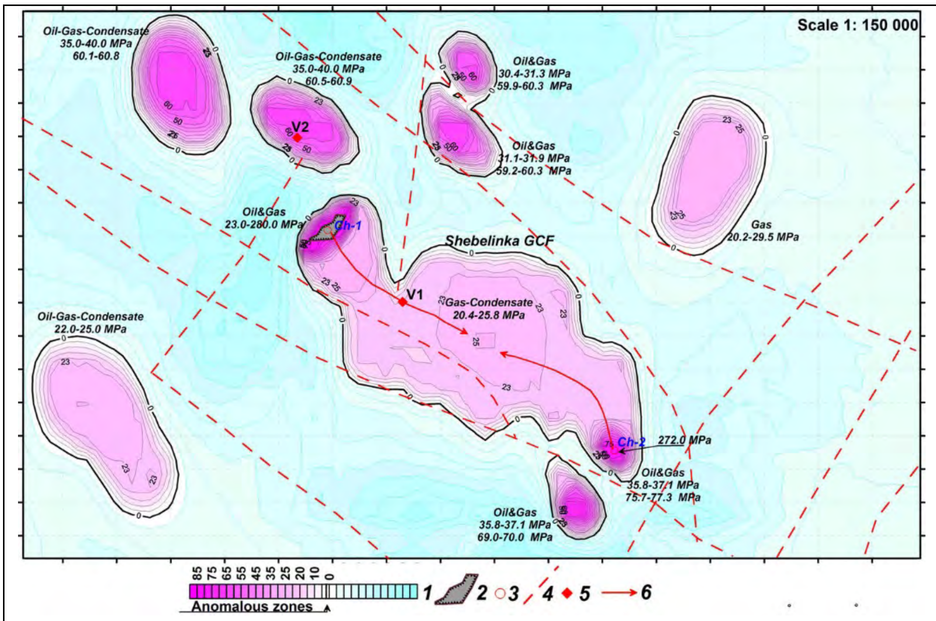

Fig. 9. Map of the geoelectric anomalous zone of "Oil-Gas" type in the area of Shebelynka GCF (According to the frequency-resonance analysis of satellite images). *1* – scale of the maximum values of reservoir pressure, MPa; *2* – the projected area of the vertical channel; *3* – coordinates of the central points of the vertical channels #1 - X=36.4415168º, Y=49.5036848º and #2 – X=36.7102815047º, Y=49.3714168274º; *4* – tectonically weakened zones (fractures); *5* – points of vertical sounding VERS V1 and V2 in 2008; *6* – the expected paths of hydrocarbon migration from a vertical depth channel.

Pulytyinskaya area in Western Siberia

After the start of the practical application of methods of the relative and maximum reservoir pressure values assessing the authors began to pay attention to the near-isometric structure of allocated anomalies of "hydrocarbon deposit" type. In this regard, it became clear that the "geosoliton" mechanism of oil and gas formation (Bembel at al., 2003 and 2013) may explain to some extent the structure of the mapped by mobile methods anomalies of this type.

To study the nature of the location of "geosoliton tubes" (structures of "vortex" type) in relation to the hydrocarbon deposits in November 2011the remote sensing data processing was performed of the area of the Iusskoye and Kotylninskoye oil deposits location, as well as Pulytyinskaya area, within which the object of this type was detected by seismic data. Satellite image of this structure location area is shown in **Fig. 10**, some of the cross-section of the wave field, based on 3D seismic survey - in **Fig. 11**, a schematic plan of Iusskoye oil and gas deposits - in **Fig. 12**.

As a result of the area image processing at the small scale of 1:200,000 within the surveyed area, anomalies of the "deposit of hydrocarbons" type were found and mapped within the Iusskoye and Kotylninskoye field location directly (**Fig. 13**) (Megerya et al., 2012). A small anomaly of the same type has been found in the south-western corner of the area. The anomaly of the "gas deposit" type with relatively low values of the gas pressure in reservoir was fixed in area of same "tube" location. Another anomaly of the same type was found in the northeastern part of the area. Presented in **Fig. 13** materials allow to suggest that: a) the trap cover in the area of "tube" is destroyed, resulting in hydrocarbon deposits not forming; b) the migration of fluids from the "tube" location area took place in the north-eastern direction; c) it can not be ruled out from consideration the possibility of fluid migration in the south-western direction.

In general, the obtained results allow to form an idea about the possible nature of the hydrocarbon deposits formation in the areas of fluids vertical migration. It should be added that the same relationships between the zones of vertical migration and traps were recorded during the technogenic gas deposits mapping in one of the fields in DDB, as well as in the area of the Djau Tepe mud volcano (Kerch Peninsula) (Korchagin at al., 2014).

We draw attention to the fact that the frequency-resonance processing of satellite image of the site was made in a relatively small, reconnaissance scale - 1:200,000. In this regard, in February 2016, a satellite image of the local area of "vortex" structure location was directly processed on a large, detailed scale of 1:15,000 (**Fig. 14**). As a result, in the center of this structure a small local area (on the anomalous responses at resonant frequencies of helium) with sufficiently high (relative to the whole structure) values of reservoir pressure was revealed - 42.5 MPa. Additionally, around this local anomaly the concentric zones of the positive and negative charges have been highlighted, which also favors into the "vortex" nature of this structural formation.

Fig. 10. Satellite image of the vortex structure on the Polytinskaya area (Bychkov, 2011).

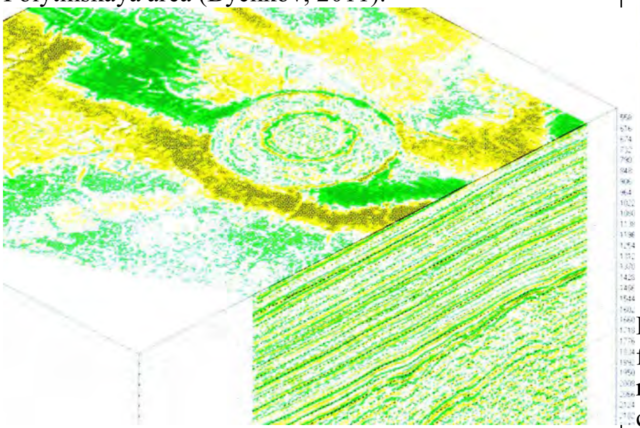

a)

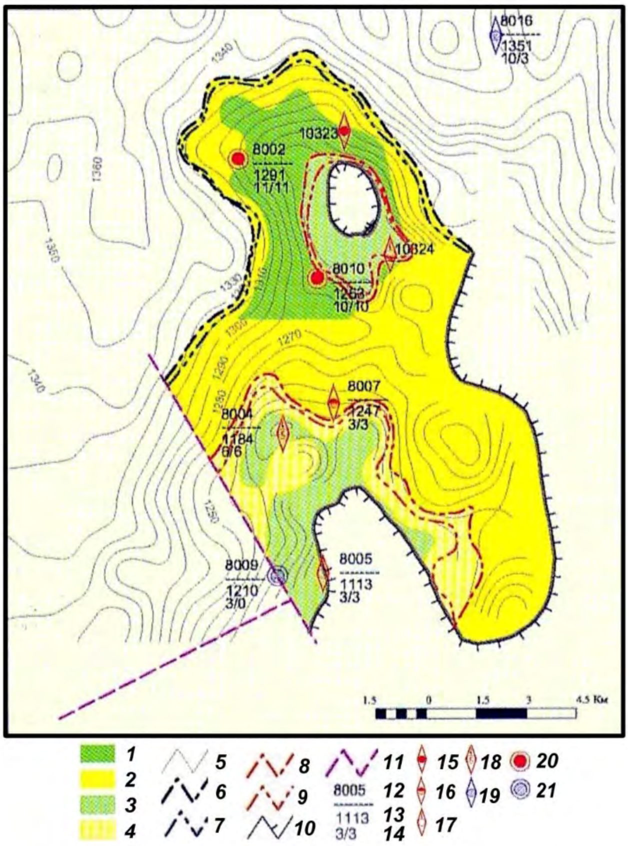

Fig. 12. Schematic map-plan of Iusskoye oil and gas field. *1* – C1 category reserves of oil; *2* – C2 category reserves of oil; *3* – C1 category reserves of gas; *4* – C2 category reserves of gas; *5* – isohypses of seam roof; *6* - OWC outer contour; *7* – OWC inner contour; *8* – GWC outer contour; *9* – GWC inner contour; *10* – line of tiling; *11* –lines of tectonic fractures; *12* – number of wells; *13* – the absolute elevation of the roof; *14* – thickness of gas reservoir / thickness of the oil reservoir; exploratory wells: *15* – inflow of oil; *16* – inflow of oil with water; *17* – inflow of gas; *18* – inflow of gas with condensate; *19* –inflow of water; exploration wells: *20* – inflow of oil; *21* – water inflow.

Fig. 11. Various cross-section of the wave field based on 3D seismic : *a)* composition of vertical and horizontal wave field; *b)* a vertical cross-section of the wave field through a “geosoliton tube” (Bychkov, 2011; Megerya et al., 2012).

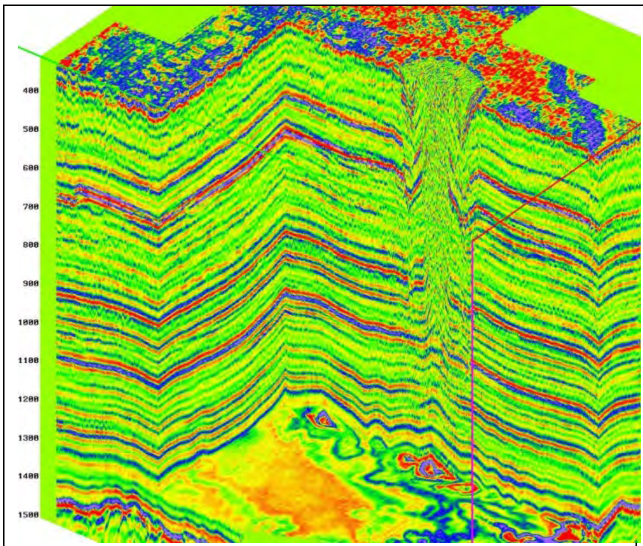

b)

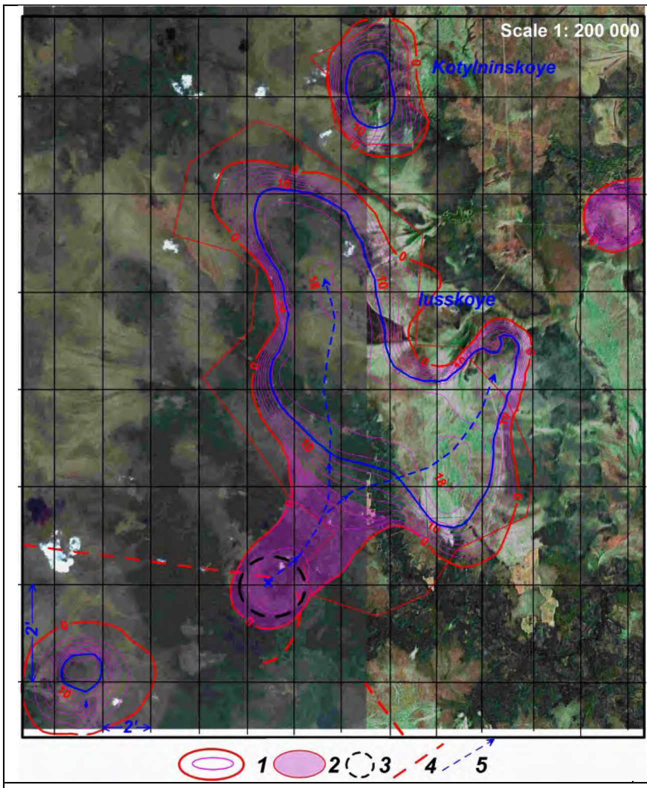

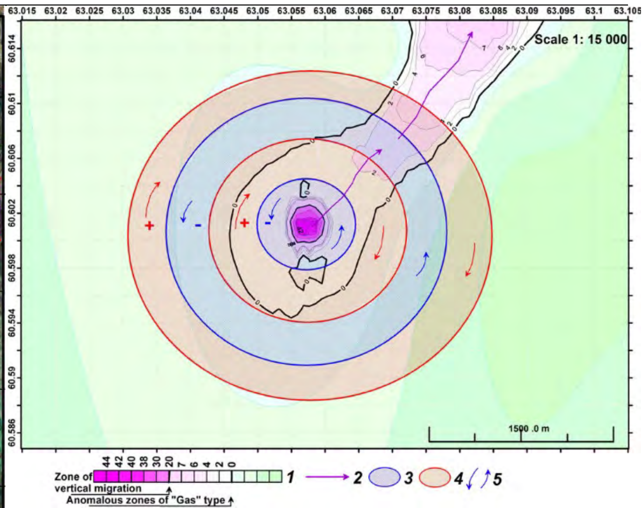

Fig. 14. Geoelectrical anomalous zones in the region of “geosoliton” structure location on Pulytinskaya area (Shaimsky oil and gas region, Russia). *1* – scale of gas pressure values in the reservoir, MPa; *2* – the projected direction of gas migration; *3* – zone of concentration of negative charges; *4* – zone of concentration of positive charges; *5* – direction of vortical rotation of the charges in a magnetic field of the Earth.

Fig. 13. Map of anomalous zones of "hydrocarbon deposit" type within the Pulytinskaya area, Iusskoye and Kotylninskoye hydrocarbon fields on the satellite image of area. *1* – isolines of anomalous response (in terms of reservoir pressure, MPa); *2* – anomalous zone of the "gas" type; *3* – position of Iussky object (geosoliton); *4* – tectonic faults; *5* – the possible ways of fluid migration.

It should be noted that in the area of this vortex structure a significant amount of geophysical and geochemical studies was made. For example, the article (Bychkov, 2011) describes the results of gravimetric and magnetometric measurements along two perpendicular profiles, laid across the structure center. Position of profiles is shown on the structure satellite image (**Fig. 10**), and the graphics of the measured values of the gravitational and magnetic fields - in **Fig. 15**. Note attention on the following interesting fact: Comparison of local anomalies of the gravitational field (**Fig. 15**) with concentric zones of the positive and negative charges indicates a very good correlation between these components of geophysical fields.

Within this area a significant amount of geochemical studies was also made. The obtained results in (Bembel at al., 2013, p. 40) are characterized as follows: "... the content of methane in the axial region of the tube exceeds the background value in 70 times; Helium - 40 times, hydrogen - 39 times. Extremely high concentrations of helium, hydrogen, and methane indicate a connection of degassing with the lower mantle. In the axial part of geosoliton tube at a depth of 1.5 m from the surface the increased concentration of rare microelements were revealed: mercury, niobium, cobalt, nickel, bismuth, yttrium, ytterbium, copper, zinc, etc. The concentration of rare microelements exceeded the background level at 2-5 times. Many of these chemicals have long been known as the accompanying deposits of oil and gas. These rare minerals fall into the upper layers, where the deposits are formed, along the system of geosoliton tubes coming from the very great depths (a sign of a great deep of faults is the high content of helium and mercury)".

Authors' of geo-soliton concept of HC formation in their publications (Bembel at al., 2003 and 2013) have repeatedly mentioned that getting well in such vertical channels ("geo-soliton tubes") can lead, on the one hand, to the "hurricane" inflows of hydrocarbons in wells. On the other hand, it may also be the cause of accidents on the wells. This circumstance led to the next object of research.

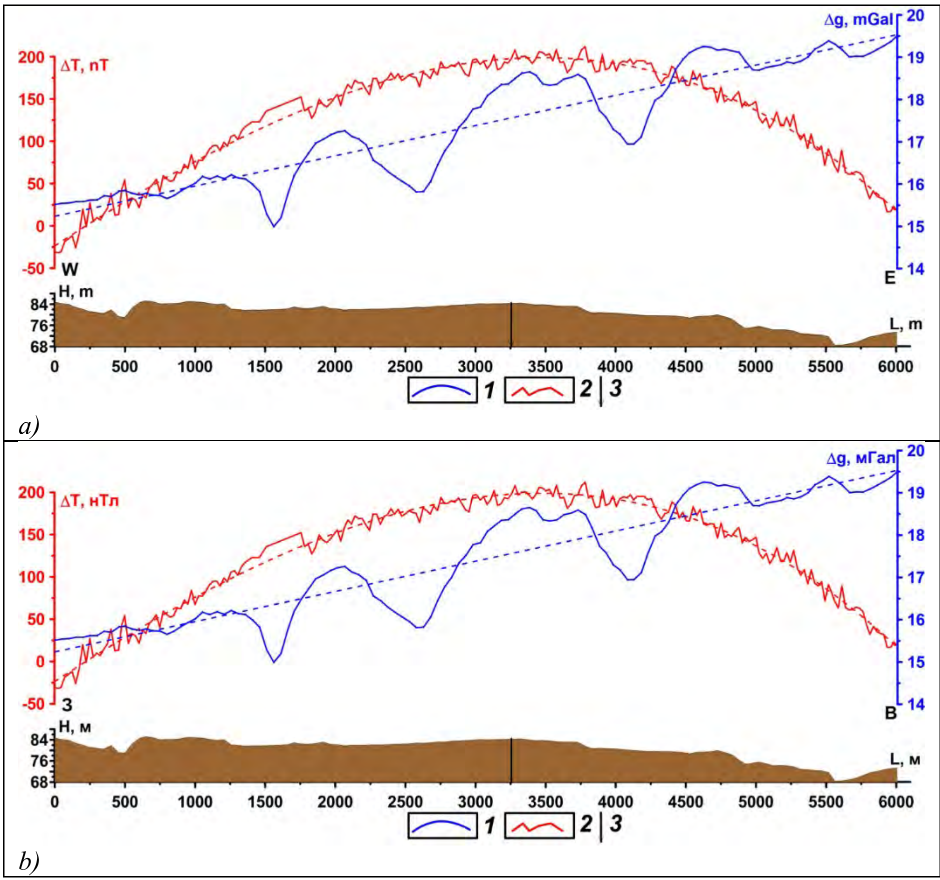

Fig. 15. Gravity (1) and magnetic (2) field of Pulytinskaya anomaly along east-west (a) and north-south (b) profiles (Bychkov, 2011). *1* – a graph of the gravitational field; *2* – a graph of the magnetic field; *3* – point of the profile intersection. Position of profiles is shown on the areal satellite image (Fig. 10).

Area of emergency well in the Gulf of Mexico

Since the vertical zones of fluids migration with very high values of pore pressure can create emergencies during drilling within them, the attempt was made to find such a zone in the area of emergency well location in the Gulf of Mexico.

Frequency-resonance processing of satellite image of emergency wellsite area in the Gulf of Mexico was made in June 2010, in a small reconnaissance scale of 1: 250,000 (**Fig. 16**) (Solovyov at al., 2011). At that time, in the course of processing within the detected anomalies only the relative values of reservoir pressure have been determined. Prior to this, by the experimental measurements the dependence of the anomalous response values from the reservoir gas pressure was installed. From these data, the scale was formed of the relative pressure values ranging from 0 to 6. This dependence (scale) was used at that time when satellite data processing to estimate the relative values of reservoir pressure. Thus, in the area of emergency well the relative value of pressure was determined as 6, i.e. pressure in the well area is the maximum in comparison with that at other sites examined. In principle, the highest values of the reservoir pressure may be indicative of a higher probability of commercial inflows of fluids.

In 2010, it has also been suggested that an emergency situation on the well could also trigger gas from gas hydrate deposits. In this connection, a satellite image of the area was also processed to detect and map the gas hydrate deposits (**Fig. 17**). In carrying out this work, we used the same values "of the characteristic parameter" (resonant frequency) of gas hydrates as in the Antarctic region, and on the Messoyakhskoye field. The research results of 2010 were published in Solovyov at al. (2011).

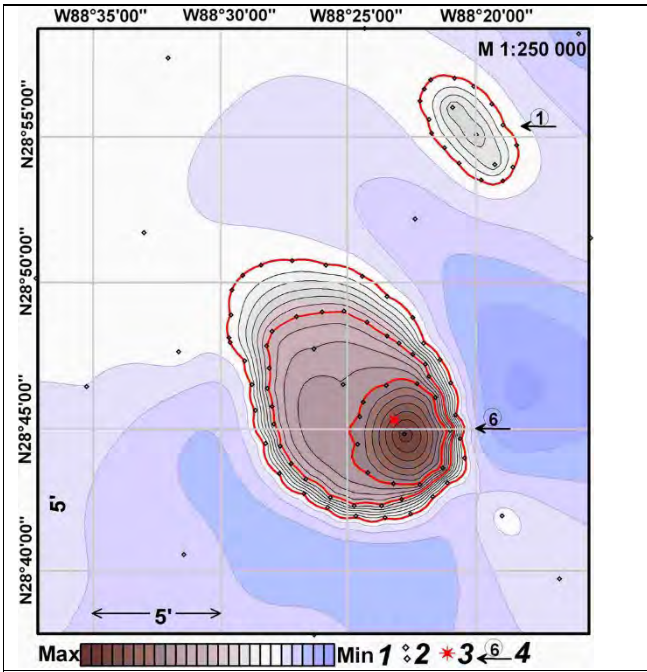

Fig. 16. Map of anomalies of the "oil deposit" type in the area of the emergency well in the Gulf of Mexico, based on the satellite data processing results. *1* – scale of the reservoir pressure relative values; *2* – points of the anomalous response registration; *3* – emergency well location; *4* – relative values of reservoir pressure in the anomalous zone.

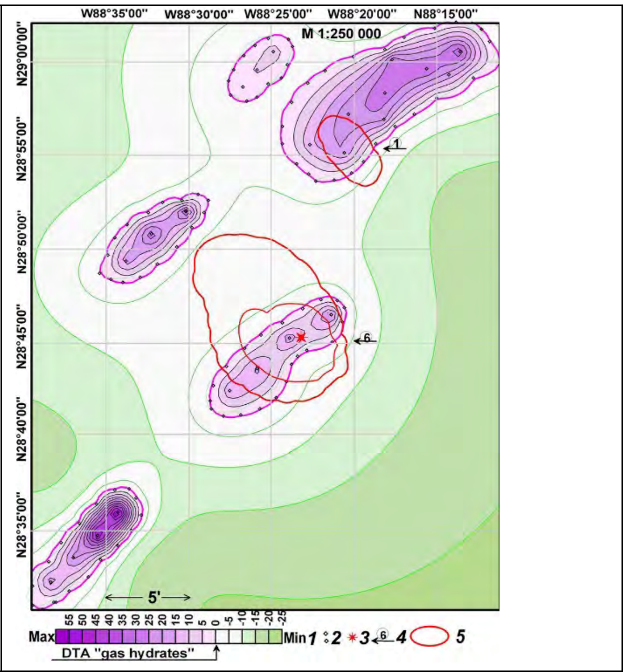

Fig. 17. Map of anomalies of “gas-hydrate deposits” type in the area of the emergency wells in the Gulf of Mexico, based on the results of satellite data processing. *1* – scale of intensity values of the anomalous response; *2* – points of the anomalous response registration; *3* – emergency well location; *4* – relative values of the reservoir pressure in the anomalous zone; *5* – contours of the anomalous zone "oil pool" type, based on satellite data.

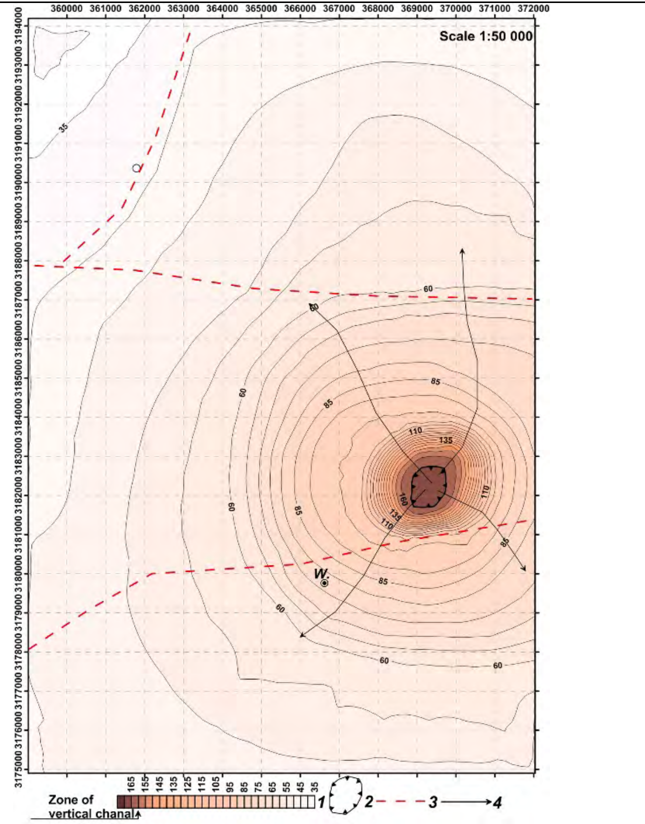

Fig. 18. Map of the maximum values of the fluid pressure in oil reservoirs at the field in the Gulf of Mexico (region of emergency well in 2010). *1* – scale of the maximum values of reservoir pressure, MPa; *2* – area of the vertical channel; *3* – tectonically weakened zones; *4* – direction of hydrocarbon (fluids) migration. The precise location of emergency well is shown by symbol W.

In order to search for possible vertical channels of fluid migration the further research in the area of emergency wells was held in March 2016. For the frequency-resonance processing the satellite image of the well site location has been prepared in the relatively large, detailed scale of 1:50,000. The position of the well in the image was clarified by data from various Internet sites.

The main purpose of further processing was the detection and delineation of small local areas with very high values of the reservoir pressure. And such local site was detected and delineated by the anomalous response on the resonant frequencies of the helium (**Fig. 18**). The maximum values of pressure within the reservoir of the local area were estimated at 165 MPa.

The obtained results allow to suggest that the emergency situation on a drilling platform in 2010 could be caused (triggered) by the pulse of fluid (HC) pumping in the detected deposits along the detected vertical channel.

Region of Zohr gas field in the Mediterranean Sea

Fact of detection of vertical channel of deep fluids migration (local area with very high values of reservoir pressure) in the area of emergency wells in the Gulf of Mexico, quite naturally set before the authors the question of the existence of similar channels within the contours of anomalous zones in other regions, as well as the possibility of their detection and localization. To answer these questions further experimental studies were required.

To carry out these experiments the authors chose the Mediterranean Sea, where within the local areas of Block 9 (Shorouk, Egypt shelf) (**Figs. 19 and 21**) and Block 11 (Cyprus shelf) (**Fig. 21**) in 2015 three anomalous zones of «Oil&Gas» type have been found and mapped, on the Zohr structure (field) including (**Fig. 20**) (Levashov at al., 2015b).

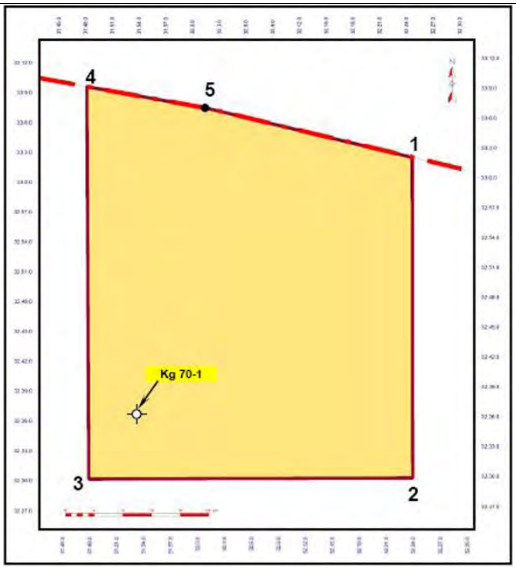

Fig. 19. The coordinates of the corner points of the Block 9 contour on the Egypt offshore and the drilled well Kg 70-1 (6014 m) location within it (Block 9…, website **)**.

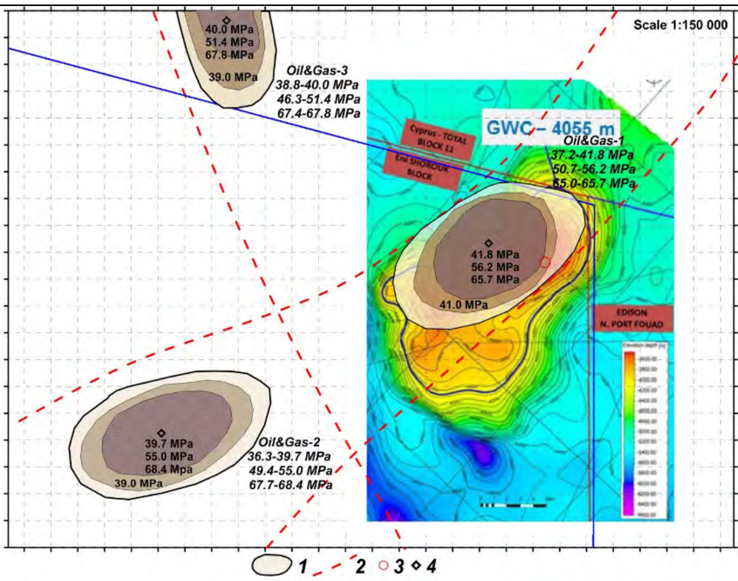

Fig. 20. Map of geoelectric anomalous zones of the "hydrocarbon deposits" type in the area of the Zohr structure and drilled well Zohr 1X NFW location (SHOROUK license block, offshore Egypt). *1* – outline of the anomalous zones of the "hydrocarbon deposits" type; *2* – tectonically weakened zones; *3* – position of Zohr 1X NFW well (floating drilling platforms); *4* – central points of anomalous zones (in which the maximum value of reservoir pressure in three interval of oil and gas saturation are indicated).

Note also that in 2016 the authors have received some additional materials on Zohr deposit and the Mediterranean region - this is an article (Esestime at al., 2016) and presentations (Golia Field Trip…, website). It provided an opportunity to compare the results of the frequency-resonance processing of satellite images, published in Levashov at al. (2015b), with the materials of geological and geophysical studies in the region. In particular, in **Fig. 20** an anomalous zone «Oil & Gas-1", found on the Zohr deposit, is shown on the structural map of this field, taken from a presentation (Goliat…). We also add that on the seismic cross-sections, presented in (Esestime at al., 2016; Goliat…, website), we can see the anticlinal structures at the areas of anomalous zones «Oil & Gas-2» and «Oil & Gas-3"» location.

Additional studies in this area were also due to the following circumstances:

1. The results of previous works, presented at site www.researchgate.net online and in the paper (Levashov at al., 2015b), did not receive enough attention (reaction) of the managers and specialists of oil and service companies, which are involved in carrying out prospecting and drilling in the region. It can be noted that these materials, in most cases, are not taken into account.
2. Processing of satellite image of Zohr field location area (**Fig. 20**) (Levashov at al., 2015b) has been performed in a small (reconnaissance) scale of 1:150000. It is suitable on materials of the region to demonstrate the potential of mobile technology, when the satellite images processing in a large (detailed) scale.
3. Discovered within the shelf of Cyprus anomalous zone "Oil&Gas-3" was not fully delineated (**Fig. 20**).
4. Within a SHOROUK block the dry hole Kg 70-1 was drilled (6014 m) (**Fig. 19**). Moreover, earlier in the deep part of the Mediterranean Sea (within the license block Nemed, including block SHOROUK) 9 dry wells were drilled. Traditionally, the wells are placed in the central parts of structures, identified by seismic surveys.

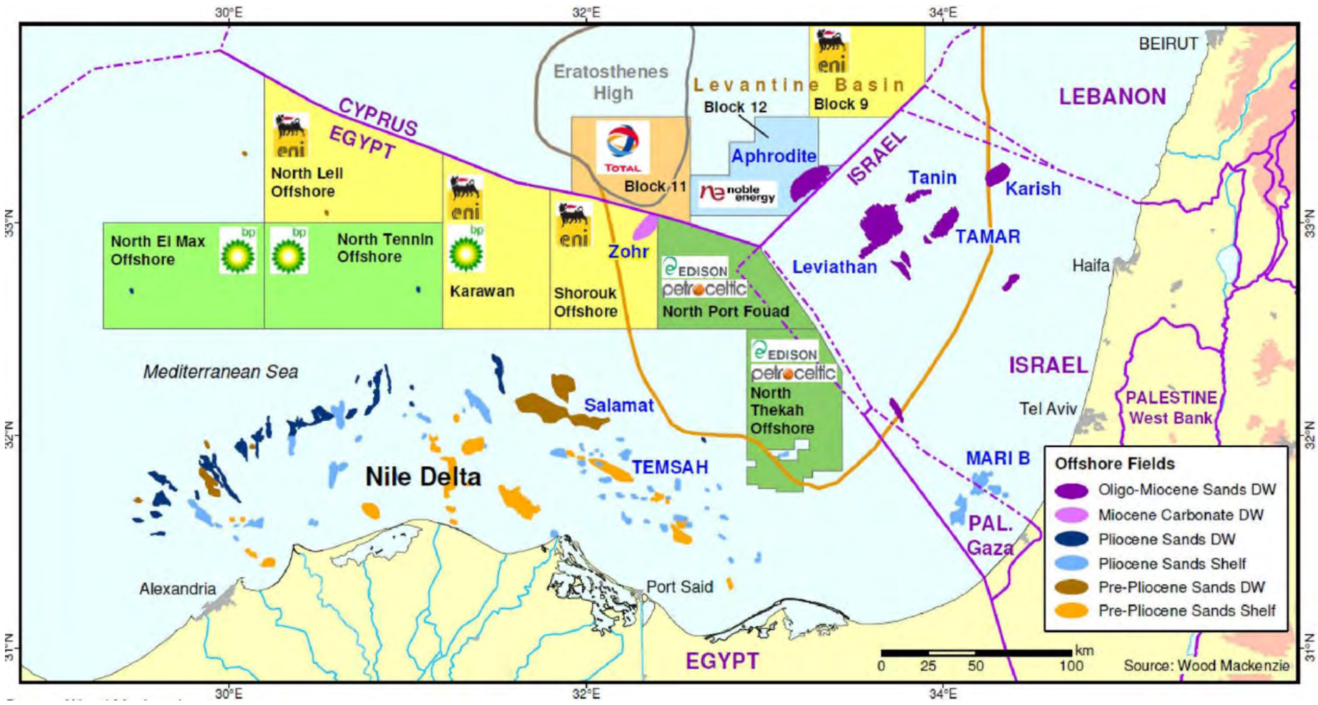

Fig. 21. The HC deposits in the eastern Mediterranean, the contours of the license blocks and names of companies.

As mentioned above, for further research in this region two local area were adopted - the area of the anomalous zone “Oil&Gas-3” on Cyprus offshore (**Fig. 20**) (Levashov at al., 2015b) and a drilled deep well Kg 70-1 within the Shorouk block (**Fig. 19**) (Levashov at al., 2015b). The main objective of the additional processing of satellite images of these areas was detecting of local vertical channels of the deep fluids (hydrocarbons) migration within them. Additionally, on an area of “Oil&Gas-3” anomalous zone location was planned to follow its stretch to the north, as well as to clarify the contours of the anomaly. We also add that within the drilled well area on the initial stage of work was planned to detect the anomalous zone of Oil&Gas type, or several such zones.

Satellite images of these sites have been processed by frequency-resonance method in the small detailed scale of 1:50,000. The results are shown in **Figs. 22 and 23**. Brief information on the results of the work is as follows.

Anomalous zone “Oil&Gas-3” (**Fig. 22**). The area of surveyed sea site is 230 km^2. Anomalous zone “Oil&Gas-3” was contoured to the north. Its area along the contour of 0 MPa is 46 km^2, and along contours of 60 MPa - 10.5 km^2. With respect to the area of the surveyed site the mapped anomaly area is 46/230=20%.

It is worth noting that the area of fully traced and contoured anomalous zone did not substantially change. This is due also to the fact that increasing the processing scale increases the accuracy of determining the contours of anomalies.

Within this anomalous zone the search of vertical channels of deep fluids migration has been carried out specifically. And such a channel was found in almost the central part of the anomalous zone. Estimation of the maximum values of reservoir pressure within this small local area amounted to 141 MPa.

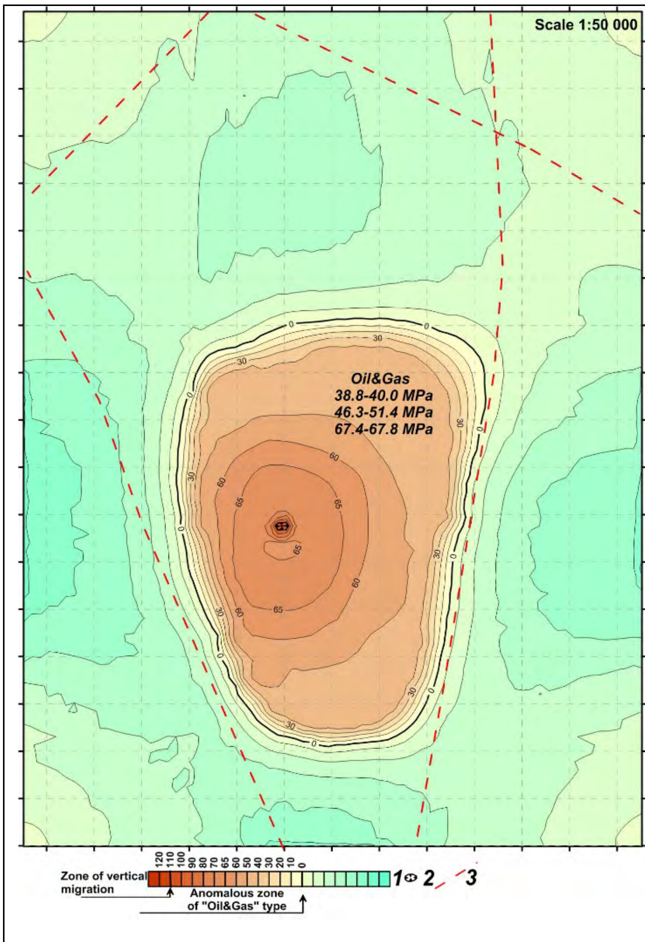

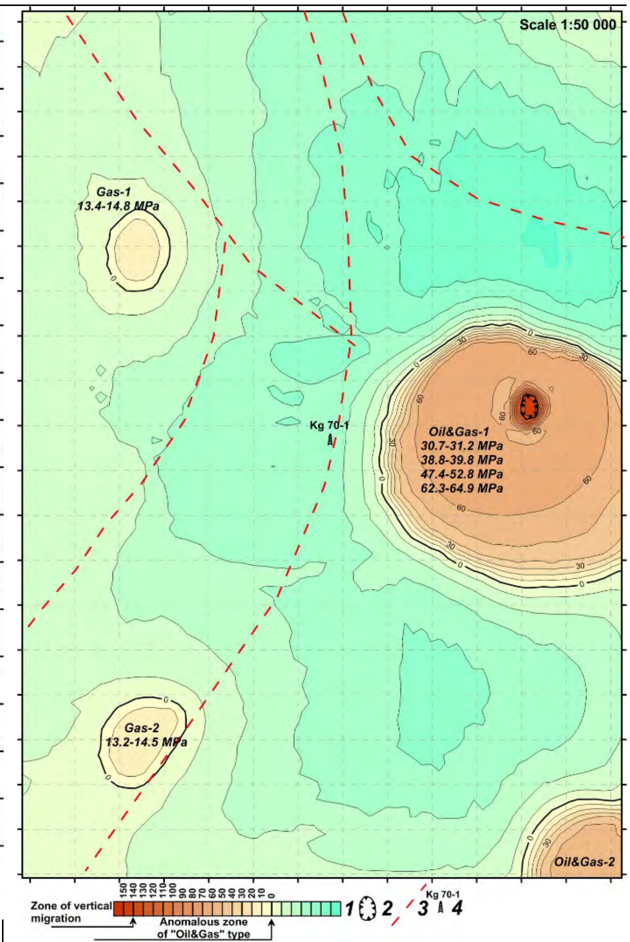

Fig. 22. Map of geoelectric anomalous zones of the "Oil&Gas" type in Mediterranean Sea (the southern part of Block 11, Zone of Cyprus) (according to the frequency-resonance analysis of satellite images). *1* – scale of the maximum values of reservoir pressure, MPa; *2* – location of the vertical channel of fluids (hydrocarbons) migration (maximum reservoir pressure – 141.0 MPa); *3* – tectonically weakened zones.

Fig. 23. Map of geoelectric anomalous zones of the "Oil&Gas" type in Mediterranean Sea (the south-western part of Block 9 (SHOROUK), Egypt Zone) (according to the frequency-resonance analysis of satellite images). *1* – scale of the maximum values of reservoir pressure, MPa; *2* – location of the vertical channel of fluids (hydrocarbons) migration (maximum reservoir pressure – 141.0 MPa); *3* – tectonically weakened zones; *4* – approximate position of unproductive well Kg 70-1 (6014 m), drilled by Shell.

*Area of Kg 70-1 drilled well location (**Fig. 23**).*

The area of surveyed sea site is 258 km^2. In the area of the drilled well, situated practically in the site center, the anomalous responses on the resonance frequencies of gas and oil were not fixed. However, approximately at 1.5 km to east from the well the relatively large anomalous zone Oil&Gas-1of isometric shape was found and almost completely mapped. The area of this anomaly along the contour 0 MPa is 25.5 km^2, and along contour of 60 MPa - 13.3 km^2. Within it there are four intervals of reservoirs pressures, and a small local vertical channel of deep fluids migration was found. In his contour the maximum values of fluids pressure in reservoirs was estimated at 141 MPa.

Also in the lower right corner of the site another anomalous zone “Oil&Gas-2” was found, which is not fully delineated in the south-eastern direction. Two other small anomalous zones Gas-1 and Gas-2 have been found in the western part of the surveyed area. The low values of reservoir pressure in one interval were set up within these anomalies.

The area of all anomalous zones along the isoline of 0 MPa is 33.5 km^2. In relation to the area of the whole site this is 33.5/258=12.98%.

In general we can say that within two operatively surveyed sites in the deep eastern Mediterranean two relatively large anomalous zones have been detected and mapped, promising for the industrial accumulation of oil and gas detecting. Within the contours of recorded anomalies the small local area with very high values of the fluid pressure in reservoirs (141 MPa) were confidently fixed. It can be reasonably assumed that these local areas are zones of deep (endogenous) fluids vertical migration.

We draw attention to **Fig. 21**. From this figure follows that in this region of the Mediterranean Sea the geophysical prospecting works and drilling are actively underway. Naturally, in order to avoid a repetition of the accident, which occurred in the Gulf of Mexico, it is appropriate to detect and map the vertical channels of deep fluids migration for the safe laying of prospecting and exploration wells.

Machuhskoye gas field in the Dnepr-Donets Basin (DDB)

The field is located in the Poltava region, at 8 km from the city of Poltava. In tectonic terms, it is in the southern side zone of DDB (Atlas of…, 1999). The author's interest in this deposit is due by information (Atlas of…, 1999) of the very high value of reservoir pressure, set in one of the wells: in Tournaisian sediments at a depth of 5209 m is set an area with anomalous high pressure of 94.9 MPa. In this regard, it was decided to try to discover the area of vertical migration within this field.

It should be noted that in January 2012 the frequency-resonance processing of satellite image on a scale of 1:100,000 of relatively large search area at northeast of Poltava (DDB, Ukraine) was made. Within the contour of the surveyed area there are known deposits of hydrocarbons: Selyuhovskoye; Makartsevskoye; Abazovskoye; Machuhskoye (**Fig. 24**). A separate site in the center of this area was processed in a larger scale of 1:35,000 (**Fig. 25**). As a result, at the site of Machuhskoye gas field location two anomalous zones of the "gas" type with the maximum values of fluids pressure of 50.0 and 48.0 MPa have been detected (**Fig. 24**).

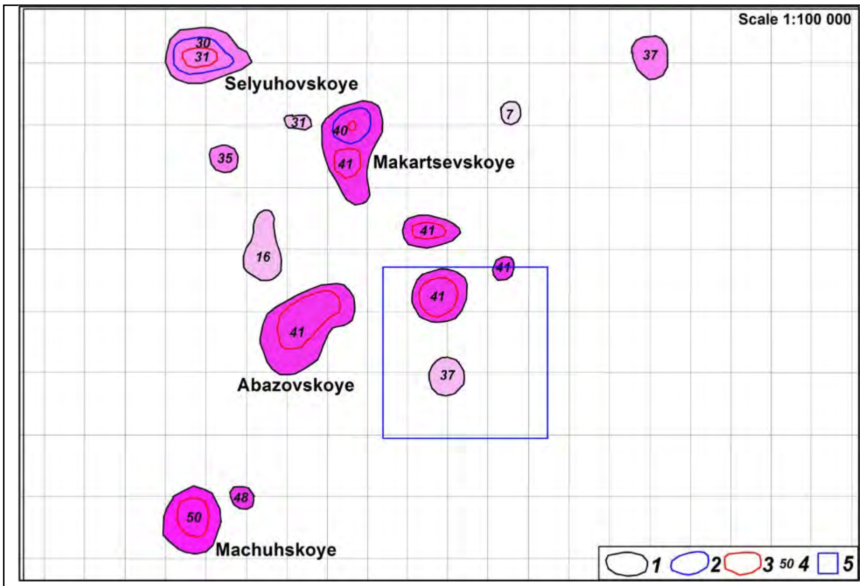

Fig. 24. Map of the anomalous zones of the "hydrocarbon deposits" type on oil and gas area, located northeast of Poltava. *1* – the general outline of the anomalous zone; *2* – contour with the reservoir pressure values above 30 MPa; *3* – contour with the reservoir pressure values above 40 MPa; *4* – assessments of the maximum values of reservoir pressure (in MPa) in the anomalous zones contours; *5* – location of the local area of satellite image processing in the scale of 1: 35,000 (see Fig. 25).

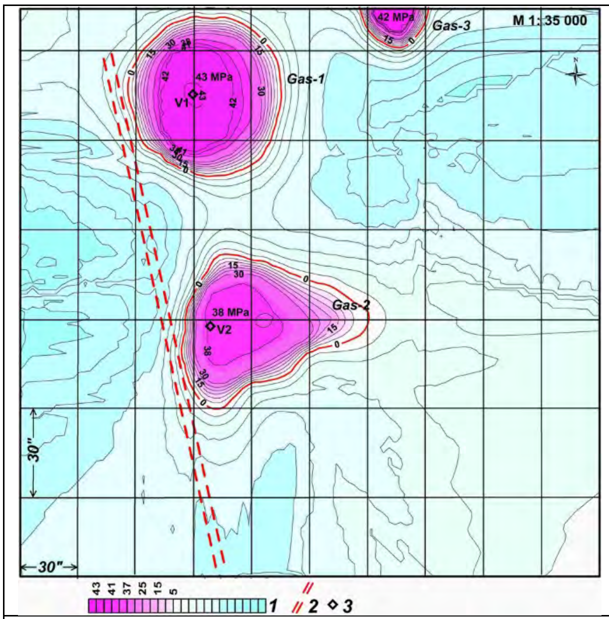

Fig. 25. Map of the anomalous zones of the "gas-condensate" type in the area of work in the Poltava region (central part of the areat on Fig. 25). *1* – a scale of the anomalous response intensity (in the values of reservoir pressure, MPa); *2* – tectonic faults; *3* – the central points of the anomalous areas.

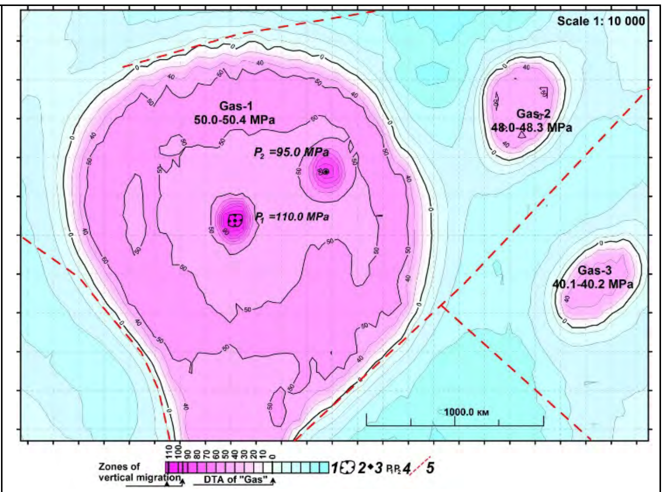

Fig. 26. Map of geoelectric anomalous zones of "gas deposit" type on the "Machuhskoe" gas field in Poltava region (According to the frequency-resonance analysis of satellite image). *1* – scale of the maximum values of reservoir pressure, MPa; *2* – area of the vertical channel; *3* – central point of the vertical channel; *4* – coordinates of the central points: P_1 – N49.5687645925º, E34.3043190539º; P_2 – N49.5712777721º, E34.3115022134º; *5* – tectonically weakened zones.

In March 2016, during the experimental studies to search for vertical channels of fluid migration the satellite image of the site of Machuhskoye deposit location was processed on a very large scale – 1: 10000 (**Fig. 26**). Materials of works in 2012 were used during the processing. Within the surveyed area three anomalous zones of the "gas" type were found and mapped - a relatively large and two small (**Fig. 26**). Reservoir pressure within the large anomalous zone was estimated in the range of 50.0-50.4 MPa.

The search for the vertical channels of deep fluids migration has been conducted in the future within a large anomalous zone contour. As a result, within this anomaly two small local areas with relatively high values of the reservoir pressure were detected: 95.0 and 110.0 MPa (**Fig. 26**). These local areas can be considered as vertical channels of deep fluids (including HC) migration.

On the area of Machuhskoye gas field the geochemical studies were also carried out. **Fig. 27** shows the schematic map of the of hydrogen distribution in the surface sediments (Koryukin and Kulbachenko, 2014; Hydrogen echo…, website), and **Fig. 28** – a schematic map of the distribution of the intensity of complex geochemical anomalies (Hydrogen echo…, website).

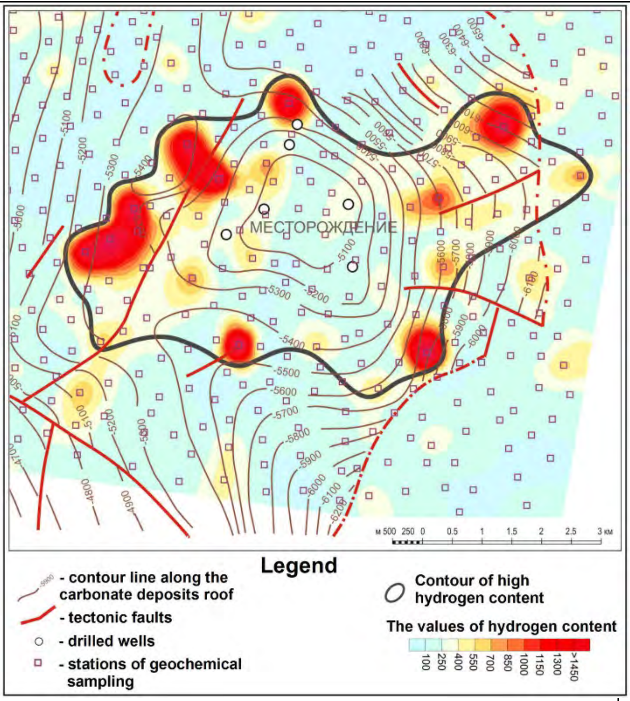

Fig. 27. Schematic map of the hydrogen distribution in the surface sediments on the "Machuhskoe" gas field (Koryukin and Kulbachenko, 2014; Hydrogen echo…).

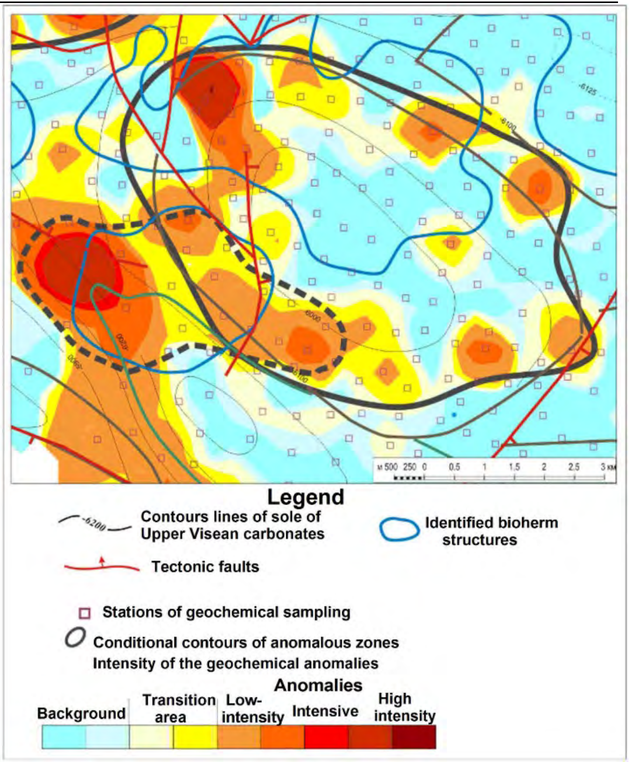

Fig. 28. Schematic map of the distribution of the intensity of the complex geochemical anomalies on the "Machuhskoe" gas field (Hydrogen echo…).

Area of Predrechitskaya-1 deep well drilling in the Pripyat Trough

To demonstrate the potential of direct-prospecting technology the authors repeatedly conducted studies of monitoring character within the areas of exploratory wells drilling. This kind of research has a monitoring character, because they are carried out on a one search site several times. In particular, such monitoring was carried out for the drilling of two wells for gas in tight sands in the DDB by Shell Company. The results of these studies (and some others) are presented in (Levashov at al., 2015a).

We carried out the same kind of research and on the site of Predrechitskaya-1 deep well drilling in the Pripyat Trough. The well was drilled to search for hydrocarbon deposits in the sediments of inter-salt complex and for evaluation of oil and gas potential of subsalt and Upper Proterozoic complexes within Predrechitskaya inter-salt trap.

The actual depth of the drilled Predrechitskaya-1well is equal to 6755 m (design depth of the well – 6680 m). The planned duration of well drilling amounted to 527 days, but the drilling was conducted for 901 day. Project drilling cost was $ 27.5 million. It can be assumed that with an increase of the drilling duration the real costs at its holding were significantly higher.

Experimental studies on the drilling site (frequency-resonance processing of satellite images) were carried out in three phases – in October 2013, July 2015 and March 2016.

At the first phase of works in October 2013 the different by area sites of the well locations have been processed at the scale of 1:20,000 and 1:30,000. At the well site area the anomalous zone of the "gas+condensate" type with a maximum reservoir pressure of 58.0 MPa was discovered and mapped (**Fig. 29**). The very well hit the contour outline of 55 MPa. This allowed the authors to conclude about the high probability of commercial hydrocarbon inflows receiving after the completion of well drilling (Levashov at al., 2015c).

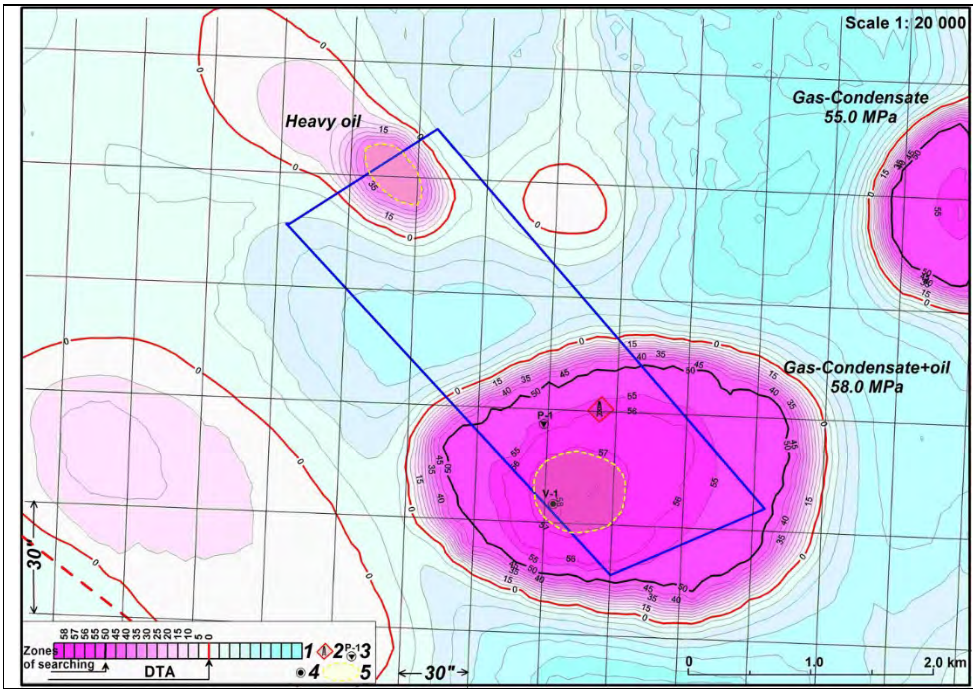

Fig. 29. Map of the anomalous zones of the "hydrocarbon deposit" type on a "Predrechitskaya" prospecting area (Republic of Belarus) (based on the frequency-resonance processing of remote sensing data. *1* – the scale of the maximum values of fluid pressure in the reservoirs, MPa (complex parameter); *2* – well; *3* – projected point of the target horizon opening; *4* – "central" point of the anomalous zone; *5* – area of oil detecting.

However, the industrial inflows of hydrocarbons in the well were not received after the completion of well drilling. In this regard, in July 2015 at the site of the well location the additional studies have been conducted to determine the causes of the erroneous prediction.

Practical experience of the application of frequency resonance technology of RS data processing and decoding on numerous examples showed that with the increase of satellite image processing scale the area of mapped "deposit of HC" type anomalies can be reduced (in some cases significantly), or individual large anomalous zones are "broken up" into several smaller ones. Such a reduction is particularly noticeable when the projected or installed by drilling hydrocarbon deposits are located at greater depths. In these cases, they are mapped (identified) by relatively high values of fluid pressure in reservoirs.

Given this feature of the technology, it was decided to carry out processing of satellite image of area of the mapped anomaly location in the scale of 1:20000 in a larger scale – 1: 10,000. This processing was conducted in July 2015. The obtained results showed that:

1) The area of the anomalous zone has decreased significantly (as in many other cases).
2) The site of drilling and projected point of the target horizon opening appeared at the edge of the anomalous zone, in the field of low values of fluids pressure in the reservoirs.
3) On the "central" part of the anomalous zone a maximum values of reservoir pressure was recorded: 58 MPa. This point (zone) is the best for laying the exploratory well.
4) The "central" point (part) of the anomalous zone has moved relative to the site of the well drilling to the east. In principle, such peculiarities during the remote sensing data processing on a larger scale have been recorded previously.
5) At the center of the anomalous zone, in the area of reservoir pressures values of 57 MPa and higher the anomalous responses at resonant frequencies of oil have been recorded (anomalous zone Gas+Oil).
6) Within the main part of the anomalous zone the anomalous responses at resonant frequencies of oil are absent (anomalous zone Gas).

In March 2016 it was decided to "search" the areas of fluids vertical migration within the detected anomalous zone in the area of Predrechitskaya-1 well. To this the frequency-resonance processing of satellite images of the well site location on a scale of 1:10000 was further carried out (**Fig. 30**). As a result of focused work within the mapped anomaly a small local area with relatively high values of the fluids pressure was found: 118.0 MPa. This local area can also be considered as a vertical channel of deep fluids (including HC) migration.

The results of the research of monitoring nature in the area of Predrechitskaya-1 deep well drilling in the Pripyat Trough allows stating the following:

1. According to the results of remote sensing data processing the attempt to make definitive predictions (close to 100%) on the prospects of hydrocarbon inflows obtaining (and, even more so, the commercial ones) from the drilled wells are wrong.
2. Such predictions can be made (and then only with low probability values) in those cases, when the drilling site falls into the zone of "central" anomaly point location.
3. The locations of the wells should be selected based on the results of detailed studies with geoelectric methods FSPEF (SCIP) and VERS using! By this it is advisable to add that in the case of the target horizons location at the big depths the ground-based research with FSPEF (SCIP) and VERS methods using should be super-detailed (!), and perhaps even with an estimate of the projected hydrocarbon resources in the target horizons.

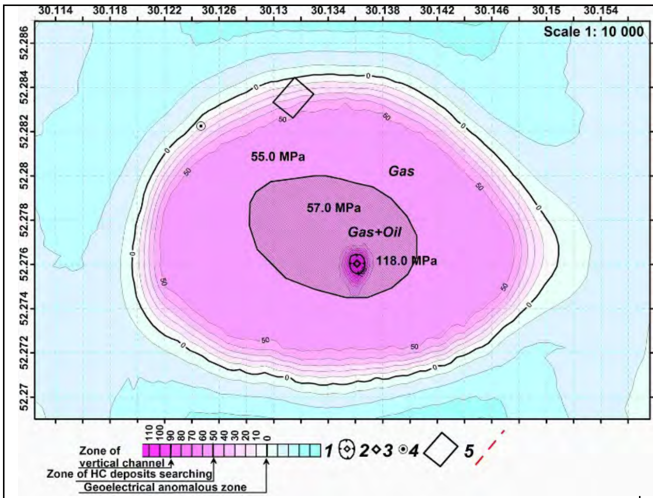

Fig. 30. Map of the anomalous zones of the "hydrocarbons deposits" type in the area of 1-Predrechitskaya deep well drilling (Republic of Belarus) (based on the frequency-resonance analysis of remote sensing data in the scale of 1: 10,000). *1* – scale of gas pressure in collectors, MPa; *2* – vertical channel area: 118.0 MPa; *3* – central part of the vertical channel: coordinates - X 30.1360740º, Y 52.27604354º; *4* – point to the target horizon opening (-4950); *5* – site of 1-Predrechitskaya well drilling on the satellite image.

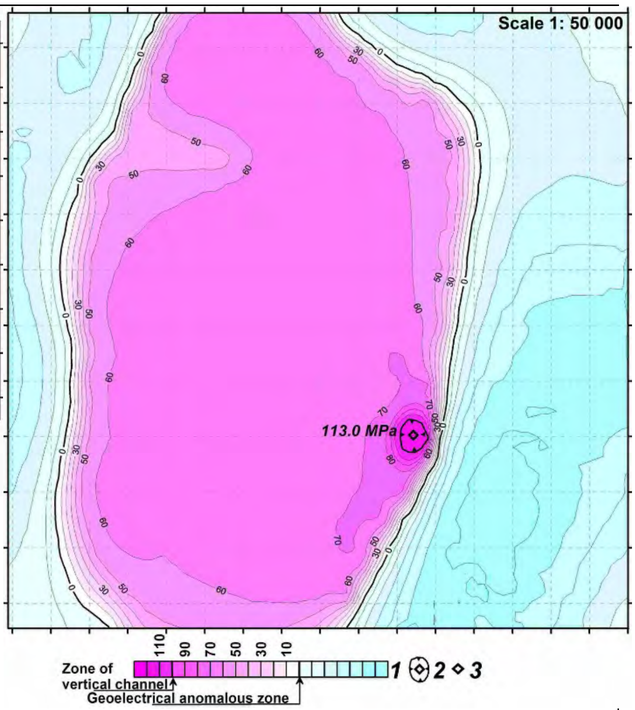

Fig. 31. Map of geoelectric anomalous zone of "oil and gas deposits" type on the "Tengiz" oil field area in the Republic of Kazakhstan (according to the frequency-resonance analysis of satellite image). *1* – scale of the reservoir gas pressure values, MPa; *2* – vertical channel area: 113.0 MPa; *3* –central part of the vertical channel: coordinates – X 53.43414046º, Y 46.14028904º.

Tengiz oil field (Republic of Kazakhstan)

In 1985, at the Tengiz oil field major accident occurred during the drilling of exploration well number 37 – from a depth of 4467 m oil and gas spewed into the atmosphere and a few hours later opened fountain of oil and gas blowout on fire. As a result of the accident, a pillar of fire broke out on land, with a height of 300 m and a width of 50 m. The temperature around the well reached of thousands degrees of Celsius. The fire was lasted for 398 days - from June 23, 1985 to July 27, 1986.

It is worth noting that in the Tengiz field area location the experimental studies have been conducted by the authors previously. However, the frequency-resonance processing of satellite image of field location was carried out in a relatively small scale. Satellite image processing results at a scale of 1:100,000 are presented in Levashov at al. (2015c).

In connection with the incident that occurred at the well number 37 authors also planned to process a satellite image of the site of its location on a larger scale in order to assess reservoir pressure values in this area. However, due to lack of a coordination, such work was not carried out.

We have already noted that in 2016 it was developed a method of detecting and locating areas with high reservoir pressures – vertical channels of deep fluids migration. The process of such zones detection significantly accelerated when at the first stage of the work to search for anomalous zones at helium resonant frequencies. This technique has been used also at the Tengiz field. For the survey in this region a fragment of deposit was taken, a satellite image of which will fit on a sheet of A3 format on the scale of 1: 50,000 (**Fig. 31**). As a result of image frequency-resonance processing on the edge of the mapped anomalous zone (in the eastern part) an anomaly of helium resonant frequencies has been discovered. Within its contour the assessment of reservoir pressure values amounted to 113.0 MPa. In view of the above materials, it is good reason to believe that this local site is a vertical channel of deep fluids migration.

Again, pay attention to the fact that coordinates of emergency wells number 37 locations at the image processing time were not known for performers. If the well number 37 is located within another part of the field, then in the area surrounding this well a search of vertical channels of fluid migration through the satellite image processing on a larger scale would have been carried out.

About the causes of technogenic deposits formation at the gas field (Korchagin at al., 2014)
In the area of one of the wells in the gas-condensate field in the DDB the sources of water with the gas have been found. Therefore, it was discussed about the possibility of gas entering the upper horizons of cross-section and its accumulation (i.e. formation of "man-made" deposits) in the water-bearing reservoir formations. A significant increase in pressure in aquifers could lead to the water with gas extrusion onto the surface.

The resulting non-standard situation at the field has set a number of tasks that had to be solved quickly. There are following problems: a) the establishment of the gas entering paths in the upper horizons of the cross-section; b) detection and mapping of gas penetration area into aquifers; c) determination of the depth and the total area of the gas distribution in the upper water-bearing reservoirs.

To solve these tasks the operative field surveys within the problem area by geoelectric methods FSPEF (SCIP) and VERS (Levashov at al., 2006; Yakymchuk at al., 2008) were carried out four times: after 4(1), 10(2), 36(3) and 72(4) days after the start of the event. Survey by FSPEF (SCIP) method was used for the detection and mapping of anomalous zone in the area of detected sources of water with gas (**Fig. 32**). Note that mapped anomalous zone, likely, is due to increased migration of water flow in the upper layers of the cross-section. The depths of the anomalous polarized layers (APL) of the "gas" and "aquifer" type were determined by VERS method. The VERS results are presented by the columns and diagrams of sounding, by vertical cross-sections of gas penetration zone, by map of thickness of technological gas "deposits" (Levashov at al., 2009).

According to the materials of field work with FSPEF (SCIP) and VERS methods using on the 4th day in the well number 37 (**Fig. 32a**) the perforation at depths of 450 and 310 m were held. From the depths of 450 and 310 m the inflows of water with gas were received.

During re-examination after ten days the detailed sounding were held in the area of projected wells ## D1, D2, D3 (**Fig. 32b**) to remove the "man-made" gas from the aquifers. A sounding has been conducted also near the wellhead of well number 37.

At the third stage of work (36 day) within technogenic deposits three degassing wells ## D1, D2, D3 were drilled (**Fig. 32c**) to a depth of about 340 m. From a depth of 330 m the gas inflows were obtained. There has been drilling of degassing well # D4.

Compared with previous surveys by the FSPEF (SCIP) method (**Fig. 32**), the anomaly area has been decreased by almost half. So, on the 4th day the total anomaly area was S=20.7 hectares, on the tenth day – S=19.7 hectares, and on the thirty-sixth – S=10.5 hectares. Repeated VERS sounding have shown that the thickness of APL of "gas" type in the area of degassing wells decreased by 4-5 times in comparison with the data on the tenth day.

When working through the 72 days the sources of water and gas in the area of well number 08 were not observed. From degassing wells D1-D4 the gas outlet were produced. The drilling of wells #D5 and #D6 have begun (**Fig. 32d**). The area of the anomaly from the man-made reservoir, built according to detailed FSPEF (SCIP) survey, fell to S=7.5 hectares (**Fig. 32d**).

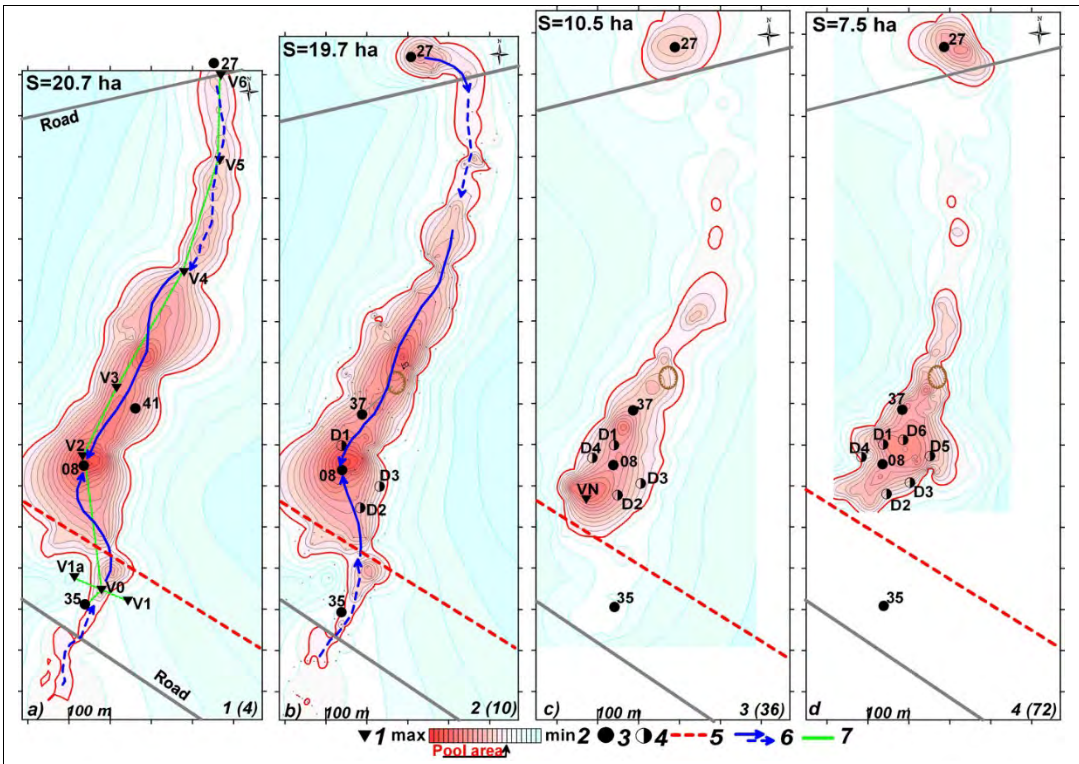

Fig. 32. Maps of the anomalous zone of techno-genic deposits of gas in the borehole #08 area for 4, 10, 36 and 72 days after the start of the event. *1* – VERS points; *2* – intensity scale of FSPEF (SCIP) field; *3* – wells; *4* – drilled degassing wells; *5* – tectonic fracture by seismic data; *6* –direction of ground water flow migration in the depth interval of 425-460 m; *7* – line of cross-section.

In the area of the well number 27 APL of "gas" type with a total thickness of 15 m are defined in following intervals: 1) 465- 474 m (9 m); 2) 662-665 m (3 m); 3) 1008-1011 m (3 m). Therefore, according to geophysical data the depth interval of 465-474 m can be considered as the main, from which the penetration of gas from the well number 27 has been passed into the upper horizons of cross-section.

Imposition of the mapped "technogenic" deposits on the technologic scheme of gas and condensate field development (**Fig. 33**) and the subsequent analysis of all available information allow to state the following:

1. The injection of "technologic" gas was carried out in the well #77 (**Fig. 33**) (designated as 27 in **Fig. 32**) in order to increase inflows in producing wells.
2. Unfortunately, the injected gas does not hit the target horizon. He along the well annulus of emergency well 77 rose up, got into a zone of the aquifer, and formed a man-made reservoir of gas.
3. Pay attention to the fact that the "technologic" gas not formed the local isometric deposit around the well 77, but an extended in the south-south-easterly direction tectonically screened accumulation in the weakened area, the location of which is fixed on the surface by the ravine. The shielding tectonic fracture is shown in **Fig. 33**.
4. When the pressure in the water-bearing reservoirs with anthropogenic deposit significantly increased, gas and water along the annulus of emergency borehole #58 (**Fig. 33**) (designated as 08 in **Fig. 32**) "broken" to the surface, thereby creating a technogenic emergency situation on the gas field.

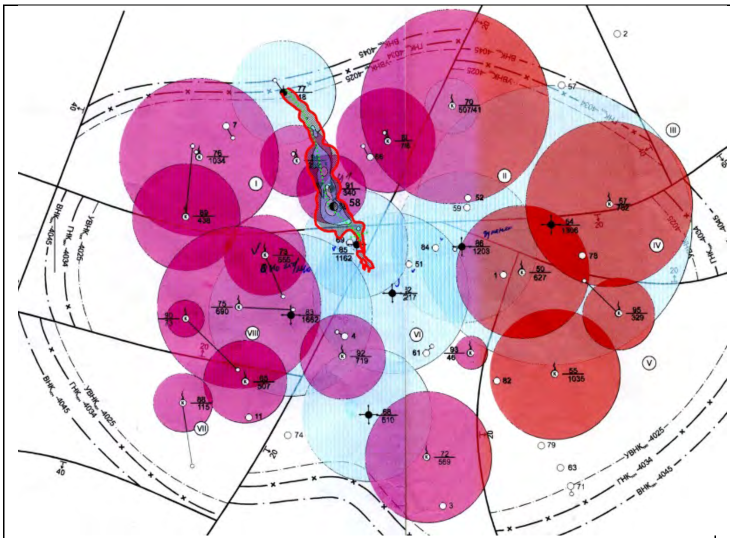

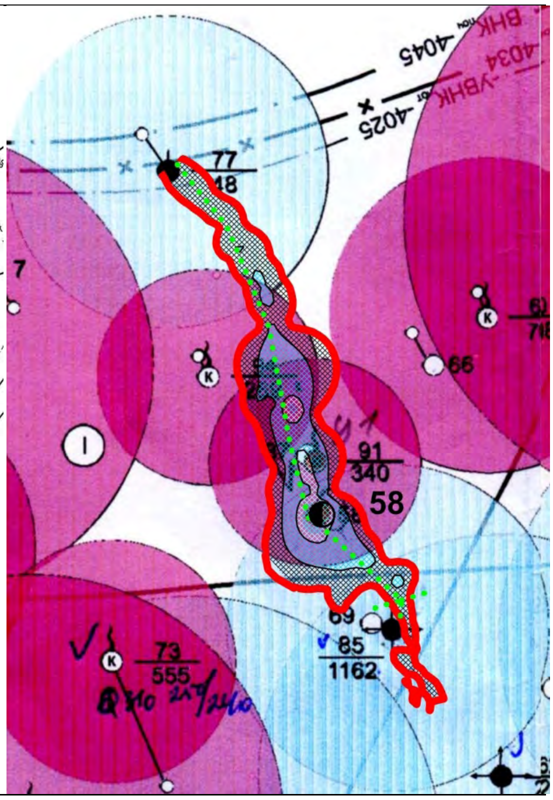

Fig. 33. Location of techno-genic deposits of gas on the sketch-map of Timofeevskoye gas and condensate field development (on the right survey site is shown in a large scale). In the center of the blue circle the wells are shown into which the gas is pumped to increase inflows in producing wells, designated by purple circles. The circles size show the volume of gas (extracted or injected) into the well.

In general, we can say that the materials of this section demonstrate quite clearly the process of hydrocarbon deposits forming in the conditions of the fluid discharge under a lot of pressure along the vertical (sub-vertical) channels.

Detection of the vertical channels of deep fluids migration on other research areas

Proven on the above given areas (sites) of survey methodology of detection and localization of vertical channels of deep fluids migration are now purposefully used during the search (prospecting) operations in various regions of the world. We describe briefly the some results of additional application of this technique.

1) While working on the article, the authors were informed of the approximate location of the emergency wells number 37 in the area of Tengiz oilfield. It was found that it is outside the anomalous zone, shown in **Fig. 31**. In this regard, the processing of a larger area in this region on the scale of 1:100,000 were further carried out. As a result, within the surveyed area three anomalous zones "Oil&Gas-2", "Oil&Gas-3" and "Oil&Gas-4" were revealed with maximum values of reservoir pressure of 74.5, 75.0 and 73.0 MPa, respectively. Anomalous zones "Oil&Gas-2" and "Oil&Gas-4" were not fully delineated in the south direction.

Well number 37 hit in "Oil&Gas-2" anomalous zone. Next to this zone a vertical channel of fluid migration was detected and located, the maximum reservoir pressure within which amounted to 105.0 MPa.

Third vertical channel with reservoir pressure of 93.0 MPa was detected within the contours of anomalous zone "Oil&Gas-3".

To this we add that in the Caspian Sea a relatively large anomalous zone "Oil&Gas-5" with a reservoir pressure of 71.5 MPa and two minor anomalies with low pressure of about 35.0 MPa were also found.

2) At the beginning of 2016 an independent evaluation of hydrocarbon potential of major search area (approximately 8000 km^2) in Central Asia has been conducted by a result of the frequency-resonance processing and decoding of remote sensing data (Levashov at al., 2010, 2011 and 2012). In the surveyed

area 27 anomalous zones were found: 16 anomalies of the "oil and gas" type, 10 – of the "gas" type, and one of the "gas and condensate" type. In view of the identified anomalous zones areas, the maximum reservoir pressure and the number of search intervals along the depth 15 prospective areas for detailed examination were allocated by the results of reconnaissance studies.

A little later, with the use of frequency-resonance method of RS data decoding the detailed research were conducted within all 15 anomalous zones, recommended for examination. Within the contours of three anomalies the vertical channels of fluids migration – local areas with significantly increased values of the fluids pressure in the reservoirs – were detected.

In the course of detailed works in the central points of the anomalous zones (with maximum values of reservoir pressure) a vertical scanning of the geological cross-section at depths up to 3500 m was carried out in order to determine the depth and thickness of anomalous polarized layers (APL) of the "oil", "gas", "water+gas", "water" type. Scanning was also conducted in areas of identified vertical channels.

Naturally, the detection of anomalous areas of the "helium" and "hydrogen" type refers to the deep source of identified in cross-sections of anomalous zones of the "anomalous polarized layers (APL) of oil and gas type". In this situation, there is an additional question: whether the helium and hydrogen can also accumulate in the APL of the "oil" and "gas" type, selected by the scanning at certain points?

To answer this question, it was held an additional scanning in one of the points of the individual intervals of cross-section (APL of "oil" and "gas" type) for the purpose of anomalous responses registration on the resonant frequencies of hydrogen and helium. As a result of additional scanning the anomalous responses on the resonant frequencies of hydrogen were fixed in the two gas layers, and at the resonant frequencies of the helium – in one gas layer. This suggests that one of the selected layers have a gas with hydrogen and helium, and in the other – only hydrogen.

The results of experimental studies allow us to state that mobile and direct-prospecting technology of RS data frequency-resonance processing and decoding can also be used for exploration and delineation of significant accumulation of helium and hydrogen in the cross-section.

We have already noted that the searches for the vertical channels of deep fluids migration were conducted within all 15 surveyed in detailed mode anomalous zones. The vertical channels – high reservoir pressures areas – were found only within three anomalous zones. In this regard, we call attention to the following circumstance. Numerous results of the frequency-resonance processing of satellite images in a different oil and gas regions give reason to assume that the channels of deep fluids migration must may exist within almost all fields contours (anomalous zones, including). However, these areas are not always active. By the anomalies of helium and hydrogen, as well as high values of reservoir pressure the currently active channels, as well as those, whose activity has been ceased relatively recently, are detected and localized enough confidently. Within the contours of the inactive vertical channels for a long time, the high values of reservoir pressure equalized with the pressure in the reservoirs and it is quite difficult to detect them by this criterion.

3) In 2016, there was also an attempt to find a vertical channel of deep fluids migration during the works at the site of underground petroleum storage location. To do this, at the intersection of detected tectonic faults with very small step the registration of anomalous responses on the resonant frequencies of hydrogen and helium has been conducted. As a result, a small (local) anomaly was detected at these frequencies. Estimates of the reservoir pressure in the contours of this anomaly yielded a value of 32.0 MPa. These results allowed to assume reasonably that at the point of tectonic faults intersection there is a vertical channel of deep fluids (including hydrocarbons) migration, along which the gas and the "easy oil" are (may be) "injected" under a high pressure into the collector (clastic intercalations in salt) on the territory of an underground facility.

We add to the above that on the storage territory near the individual wells for many years the gas exiting to the surface were fixed. In some places the liquid (very similar to oil) leaked on the surface also.

4) In 2016, with the evaluation of oil and gas potential of a small exploration block in the United States (20 km^2) the vertical channel of deep fluid migration has also been detected and localized in the fault zone of

crystalline rocks protrusion.

Anomalous responses registration on the resonant frequencies of hydrogen and carbon

When searching for oil and gas with the use of direct-prospecting technology of RS data frequency-resonance processing and decoding the resonant frequency of the gas, oil and condensate are traditionally used. These frequencies are determined on oil samples. They can also be matched (selected) on the known hydrocarbons deposits, if there will be sufficient information on the reservoir depths location.

Practical experience has shown that the information content, detail and accuracy of the frequency-resonance method of satellite images processing significantly increases if the samples of oil and condensate from the area of work, as well as detailed information about the location of productive horizons depths are provided for the performers of works. This information is used later to determine (and refinement) of the resonant frequencies of oil and condensate.

At the absence of such information during the images processing the average value of the resonant frequencies, mounted (determined) on HC samples from other research areas, are used. In this situation, for more reliable detection of anomalous zones of the "oil" and "condensate" type during the decoding process it is necessary to use a set of resonant frequencies. Unfortunately, these sets of resonant frequencies for liquid hydrocarbons from different regions may vary. In this regard, at the poor choice of resonant frequencies for satellite images processing, some promising objects (anomalous zone) may be skipped.

The main chemical elements of hydrocarbons are hydrogen and carbon. Therefore, a substantial interest may be to study the possibility of using the resonant frequencies of these common chemical elements during the frequency-resonance processing of satellite images to detect and map the anomalous zones of the "oil reservoir", "gas reservoir", "condensate deposit" type.
Research in this direction has already begun. The resonance frequency of hydrogen and carbon are determined. When processing the satellite images of areas of some hydrocarbon deposits location the anomalous responses were recorded at these resonant frequencies. For a final decision on the possibility and feasibility of a hydrogen and carbon resonant frequency using during the search for oil and gas with the use of frequency-resonance processing technology the large-scale studies on a representative set of known hydrocarbon deposits in various parts of the world are planned.

Fig. 34 represents a fragment of a satellite image of the local area in the north of the Republic of Kazakhstan with the evidence of the hydrogen degassing of the Earth, taken from a presentation (Larin at al., 2013). Frequency-resonance processing of this image was performed with using hydrogen and carbon resonant frequencies. In all contours of areas of the visible hydrogen degassing in this image the anomalous responses at these frequencies have been recorded.

Please also note that the structural elements of the relief, characteristic for the hydrogen degassing area, can be seen at the images of some search sites near the detected and mapped anomalous zones of the "deposit of hydrocarbons" type. In this connection it can also be concluded that the areas of the territory with visible evidence of hydrogen degassing deserve priority attention during the oil and gas deposits prospecting and exploration in poorly studied areas.

The new field in Belarus

In December 2016, a new oil field appears on the oil map of Belarus (The new …., website). It is open within the intermediate block of regional Rechitsa-Vishansky fault of Pripyat Trough. This field was named Ugolskoye. During exploration drilling of Ugolskaya subsalt structure the exploration well number 1-Ugolskaya with depth 5218 m given inflow of oil with gas to about 39.5 tons per day, when Semiluki horizon development. Oil of Ugolskoye deposit is classified as inaccessible reserves. It is located in deep horizon and in low-permeability reservoirs. A positive factor for the development will be the anomalously high formation pressure.

Geological reserves of the new field are estimated at 1 million 695 thousand tons of oil. A more accurate estimate can be made after drilling in the 2017 of exploration well number 2-Ugolskaya.

In January 2017 a satellite image of a small area of new oilfield location has been processed on a relatively large scale – 1: 20000 (**Figs. 35 and 36**). The main objective of this work was the detection of vertical channel of deep fluids migration within the contour of new field.

Fig. 34. The degassing structures in the Northern Kazakhstan (Tokushy, Petropavlovskaya region) (Larin at al., 2013).

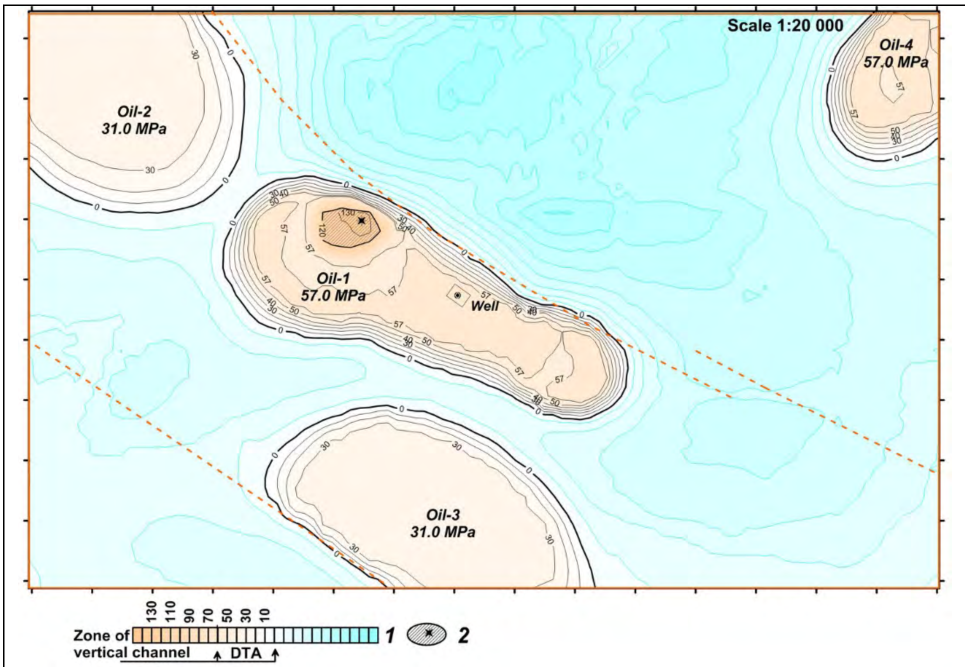

Fig. 35. Map of the anomalous zones of the "Oil" type in the area of Ugolskoye oilfield, the Republic of Belarus (according to the frequency-resonance analysis of satellite images). *1* – scale of the maximum values of reservoir pressure, MPa; *2* – area of the projected vertical channel location with a maximum reservoir pressure of 135 MPa.

As a result of the image processing four anomalous zones of the "Oil" type have been found and mapped on the surveyed area. Anomalous zone "Oil-1" is detected in the area of a new field (**Figs. 35 and 36**). Within this anomaly contour a small local area with the maximum value of the reservoir pressure of 135 MPa was fixed. This zone is a vertical channel of deep fluids migration. In the vicinity of this area it is advisable to drill a second exploration well number 2-Ugolskaya. The higher oil inflows can be obtained in this area.

The anomalous zone “Oil-2” was mapped on the known oil field.

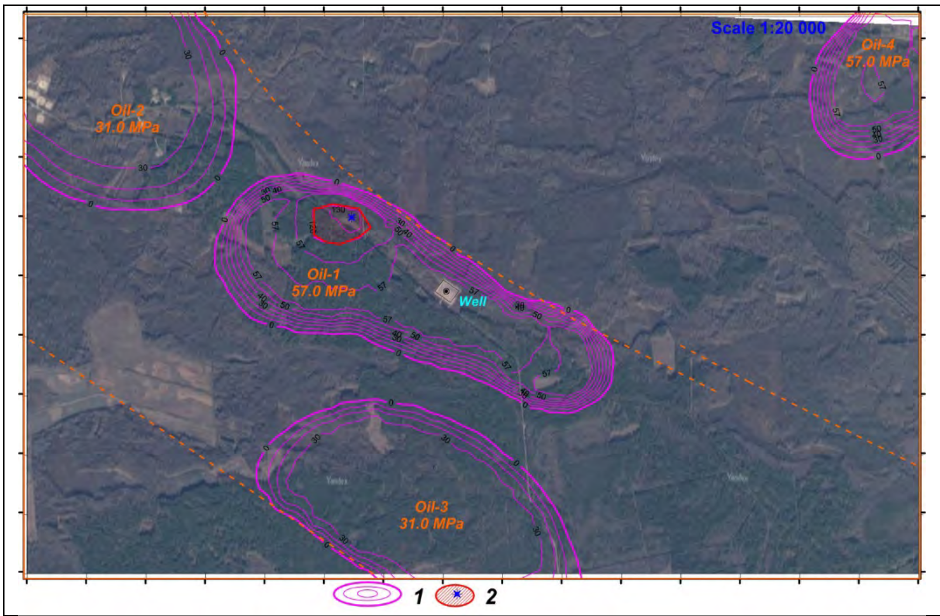

Fig. 36. Map of the anomalous zones of the "Oil" type in the area of Ugolskoye oilfield on the satellite image of survey area, the Republic of Belarus (according to the frequency-resonance analysis of satellite images). *1* – izolines of the maximum values of reservoir pressure, MPa; *2* – area of the projected vertical channel location with a maximum reservoir pressure of 135 MPa.

Summary of findings, comments and discussion

Evaluating, on the whole, the results of experimental studies within investigated areas in different regions of the world it can be stated that on the one hand, they were some unexpected for authors and at the same time to some extent predictable, on the other. To the above the following may be added in thesis form.

1. Of fundamental importance are the facts of detection and localization within the surveyed areas of vertical channels of deep fluids (hydrocarbons) migration – local areas with very high values of the reservoir pressure. In total, eleven such channels have been found within all surveyed areas. It is possible that during detailed research within the surveyed areas the others vertical channel can be detected also.

2. It can also be argued that in the process of research the methodological principles (approaches) of the operative (targeting) detection and localization of vertical channels of fluid migration were formulated (outlined) in the first approximation. The main element of this technique consists of anomalous responses registration at the resonance frequencies of hydrogen and helium at the initial stage of the search. Further, within the anomalous zones of the "helium" ("hydrogen") type the assessment of maximum values of reservoir pressure is performed. This methodical approach has been tested on almost all surveyed areas. Add to this that recently the approved methods of detection and localization of vertical channels of deep fluids migration have been applied purposefully during the oil and gas potential evaluation of the major prospecting blocks and local areas.

3. We note that within the first vertical channel on the Shebelinka GCF the anomalous responses at resonant frequencies of oil, gas condensate, helium, hydrogen and carbon dioxide were fixed.

We have already noted that by the results of the geochemical survey in the Pulytyinskaya area the percentage of methane near the centerline of the tube exceeds the background value at 70 times; helium – 40 times, hydrogen – 39 times.

Results of frequency-resonance processing of satellite images of a specific object on the Pulytyinskaya areas at a large scale (**Fig. 14**) confirmed a "vortex" nature of this structure, and the presence within it of the vertical channel of deep fluids migration – a "geo-soliton tube" according to the ideas of the authors (Bembel at al., 2003 and 2013).

To this we add that the vertical channel of deep fluids migration has been found and fixed at the resonant frequencies of the helium. In principle, such channels can also be detected during the anomalous responses registration and resonant frequencies of hydrogen.

4. On the adjoining to Shebelinka GCF areas seven distinct anomalous zones (**Fig. 9**) with a total area of

259.9 km^2 (larger than that of the anomalous zone at field himself) were detected and mapped additionally. With respect to the surveyed area in this region the area of all anomalous zones (above the field including) is approximately 21.82%. Discovered anomalous zones deserve of the detailed study and drilling.

5. In the region of emergency wells in the Gulf of Mexico the largest by area vertical channel of fluid migration with high reservoir pressure of 165.0 MPa has been found quite predictably (**Fig. 18**). These new materials increase further the likelihood of initiating an emergency on a drilling platform by triggering of pulse of fluid pumping through the channel (similar to the emissions of mud volcanoes or seeps).

And for another thing we pay attention. Satellite image of this area was processed at the scale of 1:50000 (**Fig. 18**). The images of two segments in the Mediterranean Sea (**Figs. 22 and 23**) and also in the area of Tengiz oilfield (**Fig. 31**) were processed at the same scale also. A comparison of **Figs. 18, 22, 23 and 31** shows that anomalous zone in the Gulf of Mexico is considerably bigger than those in other sites; the contour line of 40 MPa does not fit in **Fig. 10**.

This comparison may indicate an enough large deposit in this area. And when you consider that it could still be replenished through the detected vertical channel, the predicted (projected) oil reserves at the field may be enormous.

6. The previously detected (Levashov et al., 2015b) oil and gas in the territorial waters of Cyprus anomalous zone have been fully delineated in the northern direction. In **Fig. 22** it is presented in isolines of reservoir pressure. As a result of the satellite image purposeful processing on a larger scale of 1: 50,000, a small local zone of the fluids (HC) vertical migration was found within anomaly contours; evaluation of reservoir pressure within this zone amounted to 141.0 MPa. By area this zone is substantially smaller than the corresponding zone in the vicinity of the emergency well in the Gulf of Mexico (**Fig. 18**).

7. Quite projected materials were obtained by a result of satellite image processing of the local area in the vicinity of drilled Kg 70-1 well (**Fig. 23**). Note that within the NEMED large block in the Mediterranean deep-waters 9 wells were drilled in which the commercial inflows of hydrocarbons were not received. Zohr 1X NFW well (Levashov et al., 2015b) is the tenth in this block, and the first productive. Traditionally, in most cases, the wells are laid on the seismic surveys results in the central parts of detected and mapped anticline structures. In its publications, the authors repeatedly referred to the article (Karpov, 2012), which shows that the structural (anticlinal) principle of the wells laying did not justify itself in the Western Siberia. Following Karpov (2012) we see that it does not justify itself and in the Mediterranean Sea (only a tenth well in the deep-water was productive).

The results of satellite image processing of well location area (**Fig. 23**) demonstrate once again that the objects (anomalous zones), promising for the detection of commercial hydrocarbon accumulations, may not be located in the center of the detected structures.

Another fundamentally important feature of the image processing results in this area - we obtain the estimates of fluid pressures in reservoir within four intervals of cross-section.
And finally, in the contours of the mapped anomaly the local zone of fluid vertical migration was again detected; the reservoir pressure within this zone was estimated at 141.0 MPa.

8. The experimental results (including at two areas in the Mediterranean Sea) suggest that the same local zones of fluids vertical migration can also be detected in contours of anomalous zones Oil&Gas-1 (Zohr field) and Oil&Gas-2 (**Fig. 20**) within the SHOROUK block on the Egypt shelf (Levashov et al., 2015b) during a frequency-resonance processing of satellite images of these anomalies location areas at a larger scale.

9. We mentioned of 9 wells, drilled within the NEMED block. The satellite images processing of 8 other wells location areas (analogous to those in the area of Kg 70-1 well location, `**Fig. 23**) will allow us to discover other objects (anomalous zones), promising for the detection of commercial hydrocarbon accumulations.

To this can be added that, in principle, no need for additional research within anomalous zones, which can be detected. For the already drilled wells laying, such studies have been conducted earlier.

10. Discovered in the Mediterranean two vertical channel of fluid migration are medium in size. And, therefore, the probability of getting a well in such a channel is quite low. However, given that in this region of Mediterranean a lot of hydrocarbon fields have opened, as well as the significant amounts of prospecting operations and exploration drilling are conducted (**Fig. 21**), then it is better to identify such areas and contour them during the prospecting and exploration works conducting. It will further substantially reduce the probability of accidents. And besides, the wells location at a safe distance from the vertical channels will allow to receive in them a larger inflows of hydrocarbons.

11. The experimental study within small areas in the deep part of the Eastern Mediterranean support, in principle, the high oil and gas potential of the region. This is also evidenced by the numerous submarine volcanoes and seeps, discovered and mapped by detailed geophysical investigations from the vessel board (Dupré at al., 2010). The use of mobile and direct-prospecting technologies and methods provides a real opportunity to detect operatively, in a short time period the perspective objects (anomalous zones) for detailed study and drilling.

12. At Machuhskoye gas field the high values of reservoir pressure have been recorded in one of the wells (Atlas of …, 1999). As a result of the processing of the field satellite image two vertical channel of deep fluids migration were identified and localized within the mapped anomalous zone of "gas" type (**Fig. 26**). In this situation, we can say that the existence of areas with high reservoir pressure is confirmed by drilling.

13. As predicted, a local channel of fluids migration has been found also at the site of Predrechitskaya-1 deep well drilling in the Pripyat Trough (**Fig. 30**). The huge investment of time and material resources in the drilling of this well did not lead to positive results – for the commercial inflows of hydrocarbon receiving. Understandably, this well was also pawned based on seismic surveys. And again, as in many other cases, the most promising according to direct-prospecting method object turned out to be a little bit away from the place of well location. But there is nothing surprising to the authors, if you remember the paper (Karpov, 2012) again, the reference to which has been repeatedly cited.

14. Pay attention to the following circumstance. Satellite images of areas of Machuhskoye field (**Fig. 26**) and a Predrechitskaya-1 deep well location (**Fig. 30**) were processed in one and the same large enough scale of 1: 10,000. The anomalous zones of very similar in size (by area) were found and mapped within the surveyed areas. Only the fixed maximum values of reservoir pressure are higher within the Predrechitskaya anomaly contour. Given this "likeness" of detected anomalous zones on the two areas we can conclude that within Predrechitskaya anomaly the commercial inflows of hydrocarbons can be obtained also. It is only necessary to locate the well, taking into account the materials of direct-prospecting methods.

15. The authors of the article are not pioneers in the formulation of the problem of search and localization of vertical channels of deep fluids migration. Much earlier, many researchers have focused their attention on the importance of this problem. In particular, V.A. Trofimov in one of his articles (Trofimov, 2009, p. 48) states that "geophysical methods of hydrocarbon traps searching can be supplemented by the refilling channels forecasting, which will help improve the efficiency of oil exploration drilling".

The electronic publication (Kucherov, 2016) on this issue states the following: "The main search feature of methods of oil and gas accumulations detection is to find possible traps – the porous and fractured rock, that can accommodate hydrocarbons, covered with a layer of impermeable rock. Now we can add a new search feature – the identification of possible channels of fields feeding. Using two of these search features will significantly increase the probability of detection of new, primarily giant oil and gas fields".

To the above, we add that **by extra (and rather important) search features may also be considered the mapped by direct-prospecting geophysical methods anomalous zones of the "oil reservoir", "gas reservoir", "condensate deposit" type, as well as the anomalous polarized layers of "oil", "gas", "condensate", "water", etc. type, allocated by these methods in the cross-section.**

On the importance of the natural filtration channels other publications (Gluhmanchuk at al., 2014 and 2015) should be brought to attention. In Gluhmanchuk at al. (2015, p. 32), in particular, the following is stated: "Features that characterize the specificity of hydrodynamic and geomechanical properties of rocks, give grounds to assert that the most cost-effective production of the Bazhenov oil can be achieved through the use of natural filtration channels. The experience of domestic oil production from Bazhenov Formation shows that, for the development system designing it needs a full integration of wells layouts to filter channels as a prerequisite for effective drainage of reserves".

In one of his articles Timurziyev states (2016, p. 137): "In the context of convergence of the extreme points of view on the hydrocarbons genesis and development of a unified concept of the hydrocarbon deposits formation as a form of manifestation of the "cold" branch of deep degassing of the Earth, on the agenda there is a practical question to develop the methods of forecasting and mapping of centers of hidden deep fluids unloading in the crust. The solution of this problem brings us not only to the question about the sources and forms of hydrocarbon migration, but also to the direct forecast of oil and gas potential of subsoil".

16. Facts of the vertical channels of deep fluids migration which is detectable allow also in more justified manner to talk about the reality of the process of developed oil and gas fields replenishment. In this regard, noteworthy the interviews of experts, submitted in electronic documents on the sites (Larin, 2014; Polevanov, 2015), where sufficiently substantiated from the standpoint of large-scale hydrogen degassing of the Earth argued the processes of recovery of oil and gas resources.

In the same interview (Larin, 2014; Polevanov, 2015) the attention also is drawn to the urgent need of using as a fuel the hydrogen that is in the Earth. Due to the hydrogen the oil and gas reserves continue to recover. Numerous facts of large-scale hydrogen degassing of the Earth are given in paper (Larin at al., 2013 and 2014; Zgonnik at al., 2015). In the area of the Chernobyl Exclusion Zone (Ukraine) the evidences of hydrogen degassing are presented in Shestopalov and Makarenko (2013) and Shestopalov (2016).

The problem of hydrogen degassing ("gas breathing") of the Earth is analyzed in detail in paper (Shestopalov and Makarenko, 2013). The scale of degassing in this paper is characterized as follows (Shestopalov and Makarenko, 2013, p. 22): **"The discovery of the mass decontamination through continental and marine depressions, line and other forms within the continents, continental slopes and vast areas of the ocean floor indicates the existence of a single huge extensive network of multi-million underneath depressions and linear channels, providing a much larger volume of degassing, than was rated in accordance with the previously executed assessments".**

Note also that the characteristic for areas of intensive hydrogen degassing structural features of relief, similar to those in Larin at al. (2013 and 2014) and Zgonnik at al. (2015), the authors have found within the survey area in the Shebelynka GCF region (**Fig. 9**). However, due to limitations on the scope of this article, the graphic illustrations are not presented here.

And the most important point – **mobile technology of frequency-resonance processing and decoding of remote sensing data can be used successfully for operative detection and mapping of possible accumulations (large) of hydrogen in the areas (sites) of intensive hydrogen degassing.**

17. We have already referred to the interview of Larin (2014) and Polevanov (2015), which focuses on the use of hydrogen as a fuel, as well as from the standpoint of large-scale hydrogen degassing of the Earth argued the processes of recovery of oil and gas resources.

Since the vertical channels of deep fluid migration can be detected and localized as anomalous zones of the "hydrogen" type, the authors considered it appropriate to give for this element (gas) more information. In this article references are Koryukin and Kulbachenko (2014), Novikov; Perevozchikov (2012) and Shevchenko and Silkin, 2015, website) are added. Experts, interested in detailed information on these materials, may download them from the web sites.

In Koryukin and Kulbachenko (2014, p. 3) it is noted that "on the reference areas (known deposits of hydrocarbons) the hydrogen markers were obtained within the near-surface sediments, showing hydrogen yield in almost all the studied deposits of oil and gas. Near hydrocarbon deposits – in the upper part of the sedimentary cover the anomalous geochemical field of hydrogen concentration are formed, which by their configuration are differentiated at: a) areal anomalous zones of hydrogen; b) ring – focal manifestations of hydrogen; c) hydrogen "windows", characterized by hurricane hydrogen values; d) linear near-fault hydrogen anomalies; d) diapir type hydrogen stream exits.... Analysis of the performed work showed a significant impact of hydrogen "breathing" of the Earth's bowels on the geochemical processes in the lithosphere, including the formation of oil and gas fields.

Schematic map of the hydrogen distribution in the surface sediments of Machuhskoye gas field from the article (Koryukin and Kulbachenko, 2014) is shown in **Fig. 27**.

Perevozchikov in his article (2012, p. 11) concludes: "As a result of the research it was found that the Gazly oil and gas field has been formed in the area of a stationary sub-vertical flow of deep hydrogen, which, probably, is a consequence of the processes leading to the formation of liquid and gaseous hydrocarbons in the subsurface. At least, the hydrogen halos fix the ways of useful components transit along deep faults in structural traps, arranged in layers with favorable capacitive-filtration properties in the sediments of Cretaceous and Jurassic age. Deep faults are laid at depths – no higher than the zones of active seismic-tectonic events and from sources of oil and hydrocarbon gas generation under the influence of endogenous processes in the interior of the Earth's crust. If the theory of hydrocarbon formation in the hydration process with the participation of endogenous hydrogen stream is valid, then in the Gazly field, the growth of unaccounted reserves of oil and gas can be observed ... ".

In the Shevchenko and Silkin paper (website, p. 1), the data of the hydrogen distribution in the cross-section of several successful exploration wells were studied. They revealed certain patterns of hydrogen distribution in the studied sedimentary cover, taking into account the depth, stratigraphic and lithologic confinement of anomalies and hydrogen concentration distribution in the cross-section, which indicates a high likelihood of deep origin of hydrogen.

The findings led to the tentative conclusions about the possible role of deep hydrogen and the fluid flow in general in the processes associated with the formation of oil and gas deposits in the study area".

18. The authors have good reason to believe that the observed vertical channels of deep fluids migration are, in fact, by "geo-soliton tubes" in the geo-soliton concept of HC formation (Bembel at al., 2003 and 2013; Megerya, 2012). The authors of the concept say that only the results of high-resolution 3D-seismic survey can guarantee successful hit of exploration and production wells in the small-size deposits of hydrocarbons, which are controlled by separate vertical channels ("tubes").

The above results show that, for such local and small objects detection the mobile and direct-prospecting techniques, frequency-resonance technology of satellite images processing and decoding including, can also be used successfully. Moreover, the practical application at the initial stages of prospecting of mobile geophysical methods provides a real opportunity to accelerate and optimize the process of prospecting for oil and gas.

In this situation, the high-resolution 3D-seismic survey using at the second stage of prospecting works (after the discovery and mapping of anomalous zones of the "hydrocarbon deposit" type) allows you to: a) significantly reduce the area of the seismic survey, and, consequently, periods of prospecting of specific areas and sites; b) within the mapped anomalous zone to hold only 3-D seismic studies of increased detail; c) to study in detail the small-size and low contrast objects, which are essential to recharge (increase) the hydrocarbon reserves; d) to form according to the high-resolution 3-D seismic the detailed model of site, based on which the optimal model of development as of individual deposits of oil and gas, so and the entire field as a whole, could be built.

19. During the period of studies in the Mediterranean the satellite image of a relatively small area of Israel territory, within which the Heletz oil field is located, was processed at a scale of 1: 80000. Within the study area several anomalous zones of the "reservoir of oil and gas" type were revealed.

It is clear that the search and exploration for the oil and gas accumulations and the development of discovered resources within onshore are significantly cheaper than on offshore. Given the detected anomalous zones in the Heletz field area, it can be assumed that within whole Israel territory of such prospective sites may be a significant amount. Since Israel's small area (27,000 km^2), the satellite images of the whole country can be operatively processed in a suitable scale for the detection and mapping of the most promising sites (anomalous zones). In the future, the companies that will carry out detailed work and drilling on the Israel territory will receive substantial economic benefits, compared to working on the offshore and in the deep part of the Mediterranean.

Studies on local areas in the eastern Mediterranean and Israel are purely of demonstration character. The authors hope that the obtained materials will help to attract potential investors and professionals to more active search for hydrocarbons on onshore in the region. However, after the reading the Sokolin (website) paper the authors' rosy illusions in this respect were completely dispelled. The article presents the shocking material – in Israel for 50 years of searching 400 wells were drilled and only two fields have been opened!

This article demonstrates quite clearly that even the "super disappointing" results of searching for the HC industrial accumulations for many years can not to shake the established principles of organization and methods of search operations carrying out, which are traditionally used in the oil and gas sector of the world economy.

However, this is not surprising. Foreign experience shows that such "rejection" of innovative technologies and methods (mobile and direct-prospecting including) phenomenon in the world, most likely, regular than exclusive. So, Ken Feather, Vice President of Marketing at EMGS, which also took the difficult path of development and has been recognized by the representatives of the oil and gas community only after receiving in 2003 of World Oil magazine award for the development of the method of Sea Bed Logging (SBL) (www.emgs.com), writes (Feather 2007, p. 37): "For all benefits that successful game-changing technologies generate, history shows that they often have a relatively difficult time to start with. In fact, the user community tends to reject them, sometimes out of ignorance, sometimes out of fear, **but mostly because they generally upset the status quo.** They are often, in the best sense of the word, disruptive technologies".

Conclusions

The research, operatively carried out at the beginning of 2016 within many areas (sites), located in different regions of the globe, have provided a considerable amount of additional and independent information as of petroleum prospects of the surveyed areas, so and of methodological features of practical application of mobile and direct-prospecting technology for the specific prospecting tasks solving. To carry out such volume of research in such a short time (within two months) allows only the super-mobile and super-operative frequency-resonance technology of RS data processing and decoding. The above experimental results once again demonstrate the feasibility of this technology using in the search and exploration process. More active and purposeful use of different technologies components to solve specific practical problems will significantly speed up, streamline and reduce the cost of exploration process for industrial (commercial) oil and gas accumulations prospecting and exploration in reservoirs of traditional and non-traditional type. During the sharp drop of oil prices in the world, this problem is extremely urgent.

Testing of advanced techniques and methodological procedures of remote sensing data processing and interpretation (decoding) on the fields and promising areas in different regions (onshore and offshore), and the received results provide additional evidence (arguments) for the understanding of the oil and gas genesis and the nature of their industrial accumulations formation. Thus, numerous data on the existence within the surveyed areas of anomalous zones with multiple intervals of reservoir pressure and of the vertical channels of deep fluid migration can be considered as powerful arguments in favor of the endogenous (deep) origin of hydrocarbons.

Authors' of the geo-soliton concept of HC formation (Bembel at al., 2003 and 2013; Megerya, 2012) has repeatedly drawn attention to the fact that getting the wells into vertical channels of fluid migration ("geo-soliton tube ") can lead, on the one hand, to the "hurricane" inflow of HC in wells. On the other hand, it may also initiate the emergencies at wells with heavy environmental consequences. Emergency situations on well number 37 on Tengiz field in 1985, as well as in the Gulf of Mexico in 2010 could easily be provoked by triggering of pulse of fluid (HC) injection in deposits along the vertical channels, detected near these wells. In this regard, noted the problem of detecting and locating of small areas of fluids vertical migration (areas with anomalously high pressure of fluid in reservoir) deserves attention during the exploration for oil and gas.

The results of numerous experimental studies in various regions indicate that the use of mobile and operative methods of "direct" searching for hydrocarbon accumulations in areas of non-conventional and conventional reservoirs spreading will significantly increase drilling success rate (an increase in the number of wells with commercial hydrocarbon inflows). The wells laying within areas of vertical channels of fluids migration location may lead to an increase in hydrocarbon inflows.

Proven direct-prospecting technology of remote sensing data frequency-resonance processing is recommended to be used for the preliminary assessment of large petroleum potential areas (remote and inaccessible) which are poorly studied. Application of this technology can bring significant impact during the search for commercial hydrocarbon accumulations in unconventional reservoirs (including the areas of shale, rocks of the Bazhenov formation, coal-bearing formations and crystalline rocks). Mobile technology can also be successfully used during studies within the poorly studied areas and blocks in the known oil and gas-bearing basins.

Acknowledgements: The authors are deeply grateful to Dong Choi, Louis Hissink and an anonymous reviewer, whose comments, correction and suggestions helped improve the manuscript structure and contents.

References

Atlas of oil and gas in Ukraine. Eastern oil and gas region. 1999. Lviv: Centr Evropi, vol. III, 484p. (in Ukrainian).

Bagdasarova, M.V., 2014. Degassing of the Earth - a global process of fluidogene minerals forming (oil and gas including). *Glubinnaja neft'* (RUS), vol. 2, no. 10, p. 1621-1644. Available at: http://journal.deepoil.ru/images/stories/docs/DO-2-10-2014/5_Bagdasarova_2-10-2014.pdf (Accessed 25 March 2016) (in Russian).

Bembel, R.M., Megerya, V.M. and Bembel, S.R., 2003. Geosolitons: functional system of the Earth, the concept of exploration and exploitation of hydrocarbons. Tyumen': Vektor Buk, 2003, 344p. (in Russian)

Bembel, R.M. and Bembel, M.R., 2013. Ideas of V.A. Obruchev, M.A. Usov, and N.N. Urvantsev in modern geology of fossil fuels. DEVELOPMENT OF MINERAL RESOURCES BASE OF SIBERIA: FROM Obruchev V.A., Usov M.A., Urvantsev N.N. TO THE PRESENT DAYS. Materials of All-Russian forum with international participation, dedicated to the 150th anniversary of academician V.A. Obruchev, the 130th anniversary of Academician M.A. Usov and the 120th anniversary of Professor N.N. Urvantsev. p. 37-40. Available at: http://www.lib.tpu.ru/fulltext/c/2013/C38/003.pdf (Accessed 25 March 2016) (in Russian).

Bychkov, S.G., 2011. The gravitational and magnetic fields of Pulytyinskaya Area. Deep structure, geodynamics, thermal field of the Earth, interpretation of geophysical fields: six scientific reading for memory of Yu.P. Bulashevich. Yekaterinburg, IGF UrB of RAS, 2011, p. 55-58 (in Russian).

Dupré, S., Woodside J., Klaucke, I., Mascle, J. and Foucher, J-P., 2010. Widespread active seepage activity on the Nile Deep Sea Fan (offshore Egypt) revealed by high-definition geophysical imagery. *Mar Geol.*, 275(1-4):1±19. doi:10.1016/j.margeo.2010.04.003

Esestime, P., Hewitt, A. and Hodgson, N., 2016. Zohr – A newborn carbonate play in the Levantine Basin, East-Mediterranean. First break, 34, no. 2, p. 87-93.

Feather, K., 2007. The rapid adoption of seabed logging. *Scandinavian Oil and Gas magazine*. – # 5/6, p. 37-38. http://www.emgs.com/content.ap?thisId=228&TPYear=2007&DocumentTypeId=2&ContentParents=228&SiteId=1

Gluhmanchuk, E.D., Krupizkyi, V.V. and Leontyevskyi, A.V., 2014. Fracture-block structure of deposits as the main reason of low efficiency of geological and hydrodynamic models. Nedropol'zovanie XXI vek, 2014, no. 3, p. 64-67 (in Russian).

Gluhmanchuk, E.D., Krupizkyi, V.V. and Leontyevskyi, A.V., 2015. Oil of Bazhenov stratum – "oil shale technology" and domestic experience in production. Nedropol'zovanie XXI vek, 2015, no. 7(57), p. 32-37 (in Russian).

Karpov, V.A., 2012. Status and prospects of oil and gas exploration in Western Siberia. *Oil and gas geology*, no. 3, p. 2-6. (in Russian)

Korchagin, I.N., Levashov, S.P. and Yakymchuk, N.A., 2014. On the vertical migration of fluids: some results of mobile geoelectric and remote sensing methods application. 3rd All-Russian conference on the deep genesis of oil "Kudryavtsevkiye reading." Russia-Moscow-CGE, Oct. 20-23 – 2014, 6c. Available at: http://conference.deepoil.ru/images/stories/docs/3KR/3KR_Theses/Korchagin-Levashov-Yakymchuk_Theses-2.pdf (Accessed 25 March 2016) (in Russian).

Koryukin, G.L. and Kulbachenko, L.V., 2014. Hydrogen echoes of Earth and their reflection in subsurface sediments above oil and gas fields. Geomodel 2014 - 16th EAGE science and applied research conference on oil and gas geological exploration and development. Available at: http://www.earthdoc.org/publication/publicationdetails/?publication=77937 (in Russian).

Kovalev, N.I., Goh, V.A., Ivashchenko, P.N. and Soldatova, S.V., 2010. Experience in the practical use of the "Poisk" equipment for the detection and delineation of hydrocarbon deposits. *Geoinformatika*, no. 4, p. 46-51 (in Russian).

Krayushkin, V.A., 1986. Oil and gas deposits of deep genesis. *Zhurnal Vsesoyuznogo khimicheskogo obshchestva im. D.I. Mendeleeva,* vol. 31, no. 5, p. 581-586 (in Russian).

Kusov, B.R., 2011. The genesis of some carbon-containing minerals (from methane to diamond): Monograph. Vladikavkaz, IPO SOIGSI, 2011, 195p. (in Russian).

Kutcherov, V.G. and Krayushkin, V.A., 2010. Deep-seated abiogenic origin of petroleum: From geological assessment to physical theory. *Reviews of Geophysics*, 48, RG1001. Available at: http://onlinelibrary.wiley.com/doi/10.1029/2008RG000270/pdf (Accessed 25 March 2016).

Kutcherov, V.G., 2013. Abiogenic deep origin of hydrocarbons and oil and gas deposits formation. Hydrocarbon. Dr. Vladimir Kutcherov (Ed.), InTech, DOI: 10.5772/51549. Available from: http://www.intechopen.com/books/hydrocarbon/abiogenic-deep-origin-of-hydrocarbons-and-oil-and-gas-deposits-formation

Larin, N.V., Larin V.N., Zgonnik, V.A. and Rodina, S.N., 2013. Remote data and direct observation of the hydrogen degassing of the Earth's interior as a justification of lakes formation mechanism in the Yana-Indigirka lowland. Conference on permafrost mapping Geological Faculty of Moscow State University. 2013. (Presentation). Available at: http://geo.web.ru/db/msg.html?mid=1187400&uri=pdf/larin_et_al_2013.pdf

Larin, N.V., Zgonnik, V., Rodina, S., Deville, E., Prinzhofer, A. and Larin, V.N., 2014. Natural molecular hydrogen seepage associated with surficial, rounded depressions on the European craton in Russia. *Natural Resources Research*, no. 24(3), p. 369–383. doi:10.1007/s11053-014-9257-5

Lepigov, G., Guliy, V., Poberezhs'ka, I. and Loktev, A., 2013. Geosoliton conception of hydrocarbon origin under geological conditions of Ukraine. *Visnyk of the Lviv University. Series Geology.* no. 27, p. 94-103. Available at: http://nbuv.gov.ua/UJRN/VLNU_geol_2013_27_11. (in Ukrainian).

Levashov, S.P., Yakymchu, N.A. and Korchagin, I.N., 2006. Express technology of "direct" prospecting and exploration for hydrocarbon accumulations by geoelectric methods: results of practical application in 2001-2005. *Geoinformatika* (Ukraine), 2006, no. 1, p. 31-43. (in Russian).

Levashov, S.P., Yakymchuk, N.A., Korchagin, I.N. and Sinyuk B.B., 2009. Practical experience of the operative detection, mapping and monitoring for technogenic "deposits" of gas by geoelectric methods. *Geoinformatika*, no. 1, p. 23-33 (in Russian).

Levashov, S.P., Yakymchuk, N.A. and Korchagin, I.N., 2010. New possibilities for the oil-and-gas prospects operative estimation of exploratory areas, difficult of access and remote territories, license blocks. *Geoinformatika,* no. 3, p. 22-43 (in Russian).

Levashov, S.P., Yakymchuk, N.A. and Korchagin, I.N., 2011a. Assessment of relative values of reservoir pressure of fluids in collectors: results of conducted experiments and prospects of practical application. *Geoinformatika*, no. 2, p. 19-35 (in Russian).

Levashov, S.P., Yakymchu,k N.A., Korchagin, I.N. and Bozhezha, D.N., 2011b. Approbation of mobile geophysical technologies on the large gas-condensate fields of Ukraine. 73nd EAGE Conference and Technical Exhibition. Vienna, Austria, 23-26 May 2011. Available at: http://earthdoc.eage.org/publication/publicationdetails/?publication=50479 (Accessed 25 March 2016).

Levashov, S.P., Yakymchuk, N.A. and Korchagin, I.N., 2012. Chastotno-rezonansnyj princip, mobil'naja geojelektricheskaja tehnologija: novaja paradigma geofizicheskih issledovanij. *Geophysical Journal*, vol. 34, no. 4, p. 166-176 (in Russian).

Levashov, S.P., Yakymchuk, N.A. and Korchagin, I.N., 2013. Mobile geophysical technologies: experience of application for the hydrocarbon deposits searching in crystalline rocks. *Glubinnaja neft' (RUS)*, vol. 1, no. 8, p. 1117-1141. Available at: http://journal.deepoil.ru/images/stories/docs/DO-1-7-2013/3_Levashov-Iakimchuk-Korchagin_1-8-2013.pdf (in Russian)

Levashov, S.P., Yakymchuk, N.A., Korchagin, I.N., Bozhezha, D.N. and Pidlysna, I.S., 2014a. Mobile geophysical technology: the possibility of their use for the hydrocarbon accumulations exploration in the areas of the Bazhenov Formation distribution. *Glubinnaja neft' (RUS)*, vol. 2, no. 3, p. 341-382. Available at: http://journal.deepoil.ru/images/stories/docs/DO-2-2-2014/3_Levashov-Yakymchuk-Korchagin-Bozhezha-Pydlysna_2-3-2014.pdf (in Russian)

Levashov, S.P., Yakymchuk, N.A., Korchagin, I.N., Bozhezha, D.N. and Shust, D.R., 2014b. Mobile geophysical technologies: detailed studies for hydrocarbon accumulations searching within the Ukrainian crystalline shield *Glubinnaja neft' (RUS)*, vol. 2, no. 6, pp. 862-898. Available at: http://journal.deepoil.ru/images/stories/docs/DO-2-6-2014/3_Levashov-Yakymchuk-Korchagin-Bozhezha-Shust_2-6-2014.pdf (in Russian)

Levashov, S.P., Yakymchuk, N.A., Korchagin, I.N. and Bozhezha, D.N., 2014c. Mobile geophysical technologies: experimental study of possibility of application for hydrocarbon accumulations prospecting within areas of shale spreading in eastern Europe. *Geoinformatika,* no. 4, p. 5-29 (in Russian).

Levashov, S.P., Yakymchuk, N.A., Korchagin, I.N. and Bozhezha, D.N., 2015a. Mobile technologies of direct prospecting for oil and gas: feasibility of their additional application in selecting sites of well drilling. *Geoinformatika,* no. 3, p. 5-30 (in Russian).

Levashov, S.P., Yakymchuk, N.A., Korchagin, I.N. and Bozhezha, D.N., 2015b. Operative assessment of hydrocarbon potential of area in region of Zohr gas field on the Egypt offshore in the Mediterranean Sea by the frequency-resonance method of remote sensing data processing and interpretation. *Geoinformatika*, no. 4, p. 5-16. (in Russian).

Levashov, S.P., Yakymchuk, N.A., Korchagin, I.N., Bozhezha, D.N. and Prylukov, V.V., 2015c. Experience of mobile and direct technologies using for oil and gas prospects assessment of deep layers of cross-section. *Teoreticheskie i prikladnye aspekty geoinformatiki, Kyiv*, p. 4-24 (in Russian).

Levashov, S.P., Yakymchuk, N.A., Korchagin, I.N. and Bozhezha, D.N., 2016. High-frequency electromagnetic emission in the earthquake epicentral areas detected by the remote sensing frequency-resonance data processing. *NCGT Journal*, v. 4, no. 3, December 2016, p. 601-614. www.ncgt.org

Lukin, A.E., 2015. The system "superplume – deep-lying segments of petroliferous basins – an inexhaustible source of hydrocarbons. *Geological journal,* no. 2, p. 7-20 (in Russian).

Megerya, V.M., Filatov, V.G., Starostenko, V.I., Korchagin, I.N., Lobanov, A.M., Glasko, Y.V., Volotskov, M.Y. and Skachkov, S.A., 2012. Opportunities and prospects of non-seismic methods application for the hydrocarbon

accumulations searching and geosoliton concept of theirs generation. *Geophysical Journal*, vol. 34, no. 3, p. 4-21 (in Russian).
Muslimov, R.Kh. and Trofimov, V.A., 2012. Drilling of the special parametric well bores for the predicted oil supply channels is the optimal way to obtain evidences of the existence of oil fields current inflow by deep hydrocarbon fluids. *Georesursy,* no. 5 (47), p. 41-44 (in Russian).
Perevozchikov, G.V., 2012. Geochemical research of hydrogen accumulation in Gasli gas field. Oil and gas geology. – Theory and practice. 2012. -v.7. - #1. 13p. Available at: http://www.ngtp.ru/rub/1/5_2012.pdf (in Russian).
Pukhliy, V.A., Pukhlii, J.A. and Kovalev, N.I. 2010. Nuclear magnetic resonance. Theory and Applications. Textbook. Sevastopol: Publisher "Cherkasky CSTEI ", 670p (in Russian).
Rostovtsev, V.V., Laynveber, V.V. and Rostovtsev, V.N., 2011. To great oil deposits of Russia. *Geomatics,* no. 1, p. 60-63 (in Russian).
Rusakov, O.M., 2016. Chasing the phantom of biogenic hydrocarbons in the Black sea. *Geology and mineral resources of the World Ocean,* no. 4, p. 118-127 (in Russian).
Rusakov, O.M. and Kutas, R.I., 2014. Fata morgana of biogenic doctrine of hydrocarbons in the Black Sea. *Geophysical Journal*, vol. 36, no. 2, p. 3-17 (in Russian).
Shestopalov, V.M. and Makarenko, A.N., 2013. Some research results, developed the idea of V.I. Vernadsky on the "gas breathing" of Earth. *Geological Journal.*, no. 3, p. 7-25. (in Russian)
Shestopalov, V.V., 2016. On the possible geological and geophysical risks and prospects of the Chernobyl Exclusion Zone. *Geophysical Journal*, vol. 38, no. 1, p. 3-16. (in Russian)
Shevchenko, I.V. and Silkin S.A., 2015. The study of the distribution of the hydrogen concentration in the sedimentary cover of the south-western part of the Volga-Ural oil and gas province. *Exposition Oil & Gas magazine*, no. 6 (45), p. 49-517. Available at: http://geovers.com/base/files/gr15/papers/pp_32_2015_ShevthenkoIV.pdf. (in Russian)
Shuman, V.N., Levashov, S.P., Yakymchuk , N.A. and Korchagin, I.N., 2008. Radio Wave Sounding Systems: Theoretical Postulates, State, Prospect. *Geoinformatika,* no.2, p. 22-50. (in Russian)
Shuman, V.N., 2012. Electromagnetic-acoustic conversion and high-sounding system, new opportunities and new formulations of old questions. *Geophysical Journal,* vol. 34, no. 3, p. 32-39 (in Russian).
Solovyov, V.D., Bakhmutov, V.G., Korchagin, I.N., Levashov, S.P., Yakymchuk, N.A. and Bozhezha, D.N., 2011. Gas Hydrates Accumulations on the South Shetland Continental Margin: New Detection Possibilities. Hindawi Publishing Corporation. *Journal of Geological Research*, Article ID 514082, 8 pages. doi:10.1155/2011/514082.
Timurziyev, A.I., 2013. Mantle pockets of hydrocarbon generation: geological and physical characteristics and prognostic search criteria mapping; patterns of subsurface oil and gas potential as a reflection of unloading in the crust of mantle hydrocarbon systems. 2nd Kudryavtsevkiye Reading. All-Russian Conference on the genesis of deep oil and gas. M.: *CGE,* p. 333-379. (in Russian).
Timurziyev, A.I., 2015. Mantle pockets of hydrocarbon generation: geological and geophysical signs and forecast-search mapping criteria; patterns of subsurface oil and gas potential as a reflection of the unloading in the crust of mantle hydrocarbon systems. *Tectonics and stratigraphy*, issue 42, p. 114-159. (in Russian).
Timurziyev, A.I., 2016. Structural indicators and fluid dynamics of the deep pockets of HC-fluids unloading in the earth's crust. Materials of the All-Ukrainian scientific-practical conference with international participation "Modern Problems of Petroleum Geology", June 16-17, Kyiv: Institute of Geological Sciences of Ukraine, p. 137-140. (in Russian).
Trofimov, V.A., 2009. Refilling Channels and Modern Refilling of Oilfields: Hypothesis and facts. *Georesources.* no.1(29), p. 46-48. (in Russian)
Valyaev, B.M., 2012. Nature and characteristics of the spatial distribution of unconventional hydrocarbon resources and their accumulations. Gazovaja promyshlennost'. Netradicionnye resursy nefti i gaza, 2012, p. 9-16 (in Russian).
Weaver, B.W. and Warren, R.K., 2004. Electric power grid induced geophysical prospecting method and apparatus. International Patent No WO 2004/106973 A2, Dec. 9, 2004.
Yakymchuk, N.A., Levashov, S.P. and Korchagin, I.N., 2008. Express-technology for direct searching and prospecting of hydrocarbon accumulation by geoelectric methods. International petroleum technology conference, 3-5 December 2008. Kuala Lumpur, Malaysia. Paper IPTC-12116-PP. Conference CD-ROM Proceedings. 11 pages. Available at: https://www.onepetro.org/conference-paper/IPTC-12116-MS (Accessed 25 March 2016).
Yakymchuk, N.A., 2014. Electric field and its role in life on Earth. *Geoinformatika*, no. 3, p. 10-20 (in Ukrainian).
Yakymchuk, N.A., Levashov, S.P., Korchagin, I.N. and Bozhezha, D.N., 2015. Mobile Technology of Frequency-Resonance Processing and Interpretation of Remote Sensing Data: The Results of Application in Different Region of Barents Sea. *Offshore Technology Conference Arctic Technology Conference*, 23-25 March, Copenhagen, Denmark, 2015. doi:10.4043/25578-MS. Available at: https://www.onepetro.org/conference-paper/OTC-25578-MS (Accessed 25 March 2016).
Zapivalov, N.P., 2013. Geological and environmental risks in the oil exploration and production. *Georesursy*, no. 3, p. 3-5 (in Russian).
Zgonnik, V., Beaumont, V., Deville, E., Larin, N.V., Pillot, D. and Farrell, K. M., 2015. Evidence for natural molecular hydrogen seepage associated with Carolina bays (surficial, ovoid depressions on the Atlantic Coastal Plain, Province of the USA). *Progress in Earth and Planetary Science,* no. 31(2). doi:10. 1186/s40645-015-0062-5.

Websites

Block 9. Shorouk offshore. Available at: http://www.egas.com.eg/BidRound2012/block009.pdf
Goliat Field Trip. Available at: http://www.eni.com/en_IT/attachments/investor-relations/presentation/2015/goliat-field-trip/Goliat_FINAL_Website.pdf
Hydrogen echo of the Earth and its reflection in the upper part of the sedimentary cover of the oil and gas fields: Available

at: http://geo-sphera.com/publicacii/41-vodorodnoe-ekho-zemli-i-ego-otrazhenie-v-verkhnej-chasti-osadochnogo-chekhla-nad-mestorozhdeniyami-nefti-i-gaza

Kucherov, V. G., 2016. Renewable oil: myth or reality? [Electronic resource]. Available at: http://www.ng.ru/energy/2016-02-09/14_oil.html (in Russian)

Larin, V.N., 2014. "Oil in the world does not end. Burn as you want" (Interview). – Available at: http://ptel.cz/2014/02/vladimir-nikolaevich-larin-neft-na-zemle-ne-zakanchivaetsya-zhgite-skolko-xotite/ (in Russian). (Accessed 25 March 2016)

Novikov, O.N. Hydrogen deposits. (in Russian). 8 p. Available at: http://www.fpst-klg.kalg.ru/page14.html (in Russian).

Polevanov, V.P., 2015. "Oil is not expensive, because restored as a forest" (Interview). – Available at: http://www.business-gazeta.ru/article/148000 (in Russian). (Accessed 25 March 2016)

Sokolin, H.G. Features of the national oil exploration. – Available at: http://elektron2000.com/sokolin_0111.html (in Russian). (Accessed 25 March 2016)

The new field. Available at: http://www.belorusneft.by/sitebeloil/ru/addUp/mediaCenter/newsDetail/novoe-mestorozhdenie-00001/ (Accessed 11 January 2017). (in Russian)

The seismic sequence in Central Italy (2016-2017) II - Problem solving and decision making on geodynamic interpretation

Giovanni P. Gregori[(a)(b)(c)(d)], Gabriele Paparo[(a)], Maurizio Poscolieri[(a)], Claudio Rafanelli[(a)], Giuliano Ventrice[(e)], Gianpaolo Garilli[(a)], Luca Imperatori[(a)], Fabio Lo Castro[(a)], and Giovanna Zimatore[(a)(f)]

(a) – *IDASC – Istituto di Acustica e Sensoristica Orso Mario Corbino (CNR)*, Roma (Italy)
(b) – *IEVPC (International Earthquake and Volcano Prediction Center)*, Orlando (Florida)
(c) – *IASCC (Institute for Advanced Studies in Climate Change)*, Aurora (Colorado)
(d) – *ISSO (International Seismic Security Organization)*
(e) – *PME* srl, Roma (Italy)
(f) – *Department of Health Sciences, University of Rome "Foro Italico"*, Roma (Italy)
Corresponding author: giovanni.gregori@idasc.cnr.it

Abstract – The seismic sequence in Central Italy begun in August 2016, and still in progress in the Spring 2017, is a useful experiment in the natural environment, suited to check the effectiveness of *AE* (acoustic emission) monitoring in order to diagnose the state of the crust preceding an earthquake. It has been envisaged (Gregori, 2016) that seismic catastrophes can be operatively and effectively managed in terms of a 4 level approach. The focus of a previous paper ("paper I") was on the interpretation of *AE* records. The present paper ("paper II") deals with a geodynamic interpretation of the Italian peninsula. A critical analysis is considered of some different proposed geodynamic models, with reference to no "generally agreed" paradigmatic scheme. An innovative perspective is thus found on the basis of a "top-down" approach. That is, only a straight application is considered of the fundamental laws of physics applied to a structural model of Italy, independent of the occurrence or not of seismic events. The target is to interpret phenomena in a self-consistent planetary framework. A subsequent paper ("paper III") is focused on the physical meaning and heuristic perspective of some seemingly observed seismic (and volcanic) transmigration. Altogether, this approach shows how catastrophe mitigation and management can be practically improved by means of a "humble" and understating realistic approach to observations, also relying on some unprecedented monitoring techniques and by appealing to no preconceived "generally agreed" paradigm.

Keywords: *seismic catastrophes, acoustic emission, the Amatrice-Norcia earthquakes, the Emilia earthquake, geodynamics of Italy and of the Tyrrhenian Sea, warm mud tectonics*

(Received 3 March 2017. Accepted 12 March 2017)

Acronyms

AE – acoustic emission	*INGV – Istituto Italiano di Geofisica e Vulcanologia*
ALB – asthenosphere-lithosphere boundary	*IGS - International GNSS Service*
CMB - core-mantle boundary	*l.o.d.* - length of the day
GNSS - Global Navigation Satellite System	*LF* – low frequency
GPS – Global Positioning System	*LN* - Lowes-Nevanlinna
GWT - global wrench tectonics	*MOR* – mid-ocean ridge
HF – high frequency	*SHE* – spherical harmonic expansion
IC – inner core	*WMT* - warm mud tectonics
ICB – inner core boundary	

1 - Introduction

From August 24th 2016 through the early months of 2017, Central Italy was struck by a series of earthquakes. Even though their magnitude was reasonably limited, they resulted particularly destructive. The *AE* (acoustic emission) monitoring and interpretation has been discussed by Gregori et al. (2016), to be quoted henceforward as "paper I". Its main focus was on crustal stress phenomena. A 4-level approach was envisaged to the mitigation and management of seismic catastrophes. The present paper is rather concerned, specifically, with the geodynamic interpretation that is the prerequisite in order to plan the correct needed preventive actions. An accompanying "paper III" discusses some empirical evidence related to some seemingly observed seismic transmigration.

In "paper I" the crucial difference was stressed between the operatives' roles of the geologist, of the seismologist, of the geophysicist, of the applied mathematician, of the statistician, and of the seismic engineer: their very different and substantial responsibilities have to be stressed, and also the incompatibility of their roles deriving from their professional competence. In fact, their respective background, expertise and viewpoint must be clearly separated – mainly due to strict deontological concern, upon considering the huge number of causalities, damages, and sufferance.

A primary gnoseological difference deals with the separation of a "bottom-up" approach, i.e. a seismic event is investigated *after* its occurrence by making reference to what preceded it. This is similar to the job of a coroner who analyzes a body after its death. This approach is typical of a geologist or of a seismologist. As a standard, the geologist relies on some "simple", intuitive attempt to correlate several observed effects, eventually leaving unexplained some apparent relationship. The seismologist exploits some complicated statistical analysis and its role ought to be considered as being akin to a statistician (see below) that, on the other hand, ought not to be confused with the role of the applied mathematician.

In fact, the applied mathematician is sometimes asked to implement a numerical model aimed to simulate some guessed mechanism, although the logical content of a model is only concerned with the *a priori* assumption of its guessed mechanism. That is, a numerical model is excellent in order to exploit the confirmatory analysis (Tukey, 1977), while it is unsuited for the exploratory analysis, which is mandatory for the physical interpretation of phenomena.

In contrast, also the statistician relies on a "bottom-up" approach, although he appeals to a rigorous formal approach, based on seismic catalogues, and on the set of the whole multidisciplinary information that is available concerning phenomena that preceded the occurrence of every earthquake.

The effectiveness of this approach is related to the empirical constraint. That is, the natural system has a huge number of degrees of freedom. We can detect and/or measure only a very limited set of parameters. Hence, we are "blind" for the largest number of degrees of freedom of the system. The prize of every statistical analysis is therefore its capability to extract "all" information that is physically contained inside the available observational dataset. But, algorithms *must* also avoid to give any inference that relies on some more or less unconscious, though implicit, assumption related to the formal implementation of the analysis.

A serious bias, however, is the unknown non-homogeneity of the dataset. That is, one can formally compute a mean between a fish and a bird, although the concern is about its meaning. Similarly, often we cannot be aware whether our statistical analysis is being carried out on a set of mutually non-compatible elements that thus lead to incorrect results.

According to an opposite viewpoint, the approach of the geophysicist is "top-down", as he starts from consideration of the structure and composition of the natural system, and he applies the known laws of physics, independent of the occurrence or not of a seismic event. Then, he envisages the evolution of the system towards a possible eventual earthquake that, however, has to be considered only as an accidental occurrence. That is, one can correctly state that the geophysicist tries to *diagnose* the state of the Earth, *before* - and independent of - the occurrence or not of the earthquake. Similarly, a medical doctor observes and attempts to interpret the evolution of the health of his patient, independent of whether the patient is going to die or not: the concern is about recognizing the precursors of an unwanted evolution of the health of his patient.

The role and responsibility of the seismic engineer is obviously completely different.

An unwise overlapping of different competences, based on "extrapolation" proposed by some non-specific specialist - or on some hearsay learned from some colleague - generally leads to useless or sometimes even nonsensical misunderstanding and debate. This must be avoided.

The present paper is focused on the geophysicist viewpoint, i.e. it deals with a strictly "top-down" approach. We show that there is need to appeal to some substantial innovative inference, in contrast with the standard fashionable and "generally agreed" geodynamic models that rely on the "bottom-up" approach of the geologist. The key issue is therefore to re-discuss several presently "generally reported" interpretations that can find no objective support from observations.

2 - Geodynamic background

The XVIII and XIX centuries were characterized by a well-known harsh debate – which is a classical topic in the history of Earth science - between Uniformitarians and Catastrophists, and/or between Neptunists and Plutonists. Those debates were nonsensical, because during the history of the Earth both kinds of phenomena – e.g. uniform transformations and catastrophic events – always occurred and eventually overlapped each other. Those debates appear now childish and remind about stadium hooliganism, rather than about a truly scientific controversy.

In addition, some *basic deontological obligation* should be *always* clearly taken into account. That is, the geodynamic interpretation of the 2016-2017 Central Italy seismic crisis is not a simple matter of academic debate, because the fatalities, damages, and sufferance that are potentially associated to a future earthquake require a responsible and sound discussion with no reference to any kind of paradigm or "taken for granted" "generally agreed" "fashionable" "hear-said" model. It should be emphasized that it is not a matter of being either pro or con either one interpretation or another. A realistic and responsible, open-minded, strictly scientifically based, debate is the necessary prerequisite for a real progress of understanding and for an effective catastrophe management.

Natural reality is very complicated, while a "model" must be suited for the limited capability of the human mind. Hence, a "simple" model is said to be "beautiful" (according to Dirac and others). But, a "simple" geodynamic model can intrinsically explain only some facets of the very complicated and multifaceted natural system.

Therefore, different models that focus on different observational facets can be equally acceptable altogether, even in the case that they eventually appear incompatible or controversial. In fact, every model holds *only* as far as it is applied inside the *constraints* of its implicit approximation. But, whenever "for simplicity" it is extrapolated behind these constraints, it often unavoidably leads to some controversy with other models.

It is well known that – as it is often stressed – every author likes to point out every observation that fits with the expectation of his preferred model, while he considers as an "irrelevant exception" or "perturbation" or "scatter" or "error" or "unreliable datum" all features that seem to disagree with it. This psychological bias is amplified whenever a specialist - who has an inadequate background and expertise - deals with a model envisaged by a colleague of different specialization. This well-known drawback has devastating consequences, as it is shown here below.

One author of this paper (GPG) attempted to carry out a critical, objective and unselfish comparison between the different proposed geodynamic models.[1] All models ought to be - first of all - distinguished between "bottom-up" and "top-down". In addition, a clear distinction must be made between a working hypothesis and a real logically structured and self-consistent "model" (refer to "paper I").

But, in general, all various working hypotheses and/or models can be accepted according to their respective viewpoint. In fact, every proposal can always find some observational support, although this support is not a "proof" (see "paper I"). In this respect, it is unfortunate that, as mentioned below, one model, which is often assumed like a paradigm, definitely results to be inconsistent with observations and therefore it must be rebutted.

At present, the most fashionable and "generally agreed" model is plate tectonics. It speculates that the lithosphere drifts on the mantle, which is conceived like a Newtonian fluid, over which it floats (isostasy).

[1]At present an 8-volume set is in the process of final editing. See a preliminary invited short account in Gregori (2014).

The primary drivers are some fluid-dynamical cells - of suitable and debated size - that ought to be responsible for upwelling plumes and subduction zones. Historically, this model derived mainly from geological evidence according to a "bottom-up" viewpoint.

Two other well-known models are "surge tectonics" and "global wrench tectonics" (*GWT*). They are "bottom-up".[2] They rely on an accurate analysis of a huge amount of geological and palaeontological observations. The concern is about the physical assumptions that each model implies.

"Surge tectonics" assumes the existence of a return flow of matter underground. In this respect it reminds about the fluid-dynamical cells of plate tectonics, although – compared to plate tectonics – the cell geometry is constrained by some less compulsory requirement. The greatest difficulty is about the impossibility to get evidence for underground flow. That is, this model envisages some real close cycles. The model is 3D, while the observational evidence deals only with the 2D Earth's surface. This is just a matter of empirical constraint. A similar difficulty is also shared by plate tectonics.

GWT assumes large displacements of huge fractions of some outer layer of the Earth. Even though its difficulty relies on the need for some energy source, in principle, an energy source can certainly be envisaged, though it is difficult to explain its detailed mechanism.

Earth's expansionism has been recently supported by several authors. Similarly to other models, also this model has pro and con evidences. In any case, it cannot be "proven" (some supporting observation cannot be considered a "proof"), although it cannot be disproved. It might be an optional mechanism coexisting with other drivers.

However, an aspect - which has been neglected by all authors - deals with the implication of state-transformations of matter between different generally poorly known states of matter, or maybe between still unknown states. In fact, the solid, liquid, gas and plasma state are the unique four states of matter that we know in our environment. But several other states of matter certainly exist in some other natural environment, neither they can be reproduced in a manmade laboratory.[3]

One case history is represented, e.g., by the process of serpentinization that occurs deeply underground (e.g. Judd and Hovland, 2007, and references therein). It is an explosive phenomenon, although - whenever the medium is eventually strongly confined - it ought to produce some very large volumetric variation.

But in principle also other - eventually still unknown - transformations can originate large *local* volumetric variations. This item ought to be discussed in detail, although no study seems to have ever been carried out on it.

These processes can be likened to the Earth's expansionism model, although - unlike in the standard expansionism - the key focus is *not* on volume variations of the *whole* Earth and of its mean radius, rather one should be concerned only with some specific region at a time, and during some limited time span. That is, volumetric variations occur. The debate is on whether it makes sense to extrapolate the process synchronously on the planetary scale, or rather one should more realistically consider only its local or regional effects, depending on the specific tectonic setting at every site.

It is very unfortunate, however, that in general the debate between pros and cons either one model or another often reminds about the worst hooliganism, rather than about a concrete scientific discussion.[4]

---

[2]These are classical items. A large amount of literature exists. But, owing to brevity purpose it cannot be here quoted.

[3]Owing to brevity purpose, no discussion can be here given of these items. Reference ought to be made to the 8-volume set mentioned in a previous footnote. Some mentions are given in Gregori (2013). Note that, in general, the state of matter deep inside a planet, or inside stars etc., is of concern for the so-called high-energy-density physics that is investigated for inertial confinement fusion etc. (see e.g. the short authoritative review by Drake, 2010 and references therein).

[4]This is one aspect of the often-complained sociological problem of media conditioning. It is surprising how excellent people become unconscious victims of true servility. In the case here of concern, the "weapon" of mass media is the impact factor, although sometimes somebody seems to be aware of this. For instance, the US Senate - after the Tōhoku-Oki earthquake (M_w=9) that on 11 March 2011 severely damaged the Fukushima Dai-ichi nuclear

Every conscience driven scientist must rather consider every model as a possible explanation of some facets of the multifaceted natural reality. Every model can be a sound explanation for some observation. But a few observations cannot prove the general validity of model. No model can be extrapolated to be a "universal" paradigm.

When the aforementioned deontological issues are considered, the so-called scientific debate often appears childish, ridiculous, naïve, irresponsible. The present paper wants to avoid to enter into any discussion of this kind. No "war" is here made against any model of any kind.

The approach which is here considered relies on a mere "top-down" geophysical viewpoint. The starting point is the known structure of the Earth, and the physical laws are applied independent of any geodynamic or seismological concern. Natural catastrophes are rather eventually derived as a byproduct of a general - and physically sound and as far as possible rigorous - approach. In general, every previous proposed model can well fit into the logical scheme which is here considered, as every model focuses on different facets of observations.

But, it is very unfortunate that plate tectonics - which is the well-known "generally agreed" and most fashionable model extensively quoted by the largest amount of literature – results to be incompatible with observations. It is impossible, however, to synthesize here by a few statements alone a huge amount of discussion.[5] Only a few highlights can be here given.

Continental drift is an observed matter of fact. The basic dilemma is about deciding whether continents "float" inside a fluid, or rather they "slide" over some solid surface underneath. For instance, consider a book posed on your desk. The concern is about whether you claim that the book floats on the desk, or rather you claim that the book is a solid object posed over another solid object, while the crystalline bonds of the two bodies are responsible for their respective elastic response.

The "floating" continent hypothesis derives from a subconscious historical heritage dating back to the very early ancient Greek thinkers (Gregori, 2006e, 2009). In addition, this concept reminds about the experiments - by investigating the cooling of bronze cannon balls - carried out by Georges-Louis Leclerc, Comte de Buffon (1707-1788). Even at present, the Earth is generally conceived like a hot ball that is cooling in space on the billion-year time-scale, and nobody seems to reconsider critically this totally unproven unconscious historical heritage.

The difficulties are well known that have often been reported concerning the plate tectonic model. An endless literature can be found on these classical items, such as the concern about the viscosity of the mantle, the absence of any signature at the Earth's surface of convection cells in the mantle, the unbalance between upwelling plumes and subduction zones, the Africa and Antarctica paradoxes, as they are surrounded by mid-ocean ridges (*MOR*s) with no subduction zone, etc.

Let us rather focus on the well-known excessive flattening of the Earth when it is compared to an ideal fluid Earth body. According to arguments that can be found in several old authoritative papers and college textbooks, if the "floating" hypothesis is correct, the continents ought to move towards the equator due to a force, which is conventionally called *Pohlfluchtkraft*. The argument derives from the resultant force of gravitation, plus centrifugal force, plus buoyancy force. An older term for this same force is "Eötvös force".

---

power plant - invited for an audience some of the best known and authoritative specialists in geodynamics (Showstack, 2011). The concern was about a possible strong earthquake in the Aleutian Islands that could trigger a tsunami with devastating consequences for the whole US west coast. The scientists officially stated that they must have a greater "humility" (*sic*) in front of natural phenomena, and that their understanding is not as satisfactory as they generally believe. It is embarrassing to assess how some skilful and learned scientists are victims of the impact factor worshipping. The consensus by others has a top priority, even above every sound critical feeling and deontological responsibility. In his autobiography, Max Planck (1956) wrote that a new scientific truth can emerge only after the death of its opponents. This has also practical and severe consequences on the selection of young scientists. Thus, people are often selected with better attitude to servility. It is unbelievable that, while talking privately, some important science managers - such as rectors of important universities - are well aware of this drawback. But, they claim that this is the way to proceed and nobody can change it.

[5]This is one of the leading items discussed in the aforementioned 8-volume set in preparation.

In contrast, if the continents slide on a solid surface, the excessive Earth's flattening can be corrected if continents experience a poleward force, according to the scheme that is known as "Pekeris force". That is, some excess mass at the equator must slide poleward.

No observational evidence seems to exist that supports the *Pohlfluchtkraft*. In contrast, the poleward motion of Alaska - or of Antarctica, which is therefore at present a seismically exceptionally quiet continent - or maybe also the opening space of the Gulf of Mexico - are likely to support the "Pekeris force". But, this whole concern ought to require a much longer discussion, as it is multifaceted.

A merely "top-down" model has been proposed by Gregori (2002). It is very briefly synthesized in Gregori (2006e and 2009). It should be stressed that this model was *not* addressed to explain geodynamics. Rather its concern was about the origin of the geomagnetic field. Owing to brevity purpose, only a few basic reminds can be made about some physical matters of fact.

Since a long time it is well known that the lunar tide originates a slowing down of the spin rate of the Earth, i.e. the length of the day (*l.o.d.*) is steadily increasing.[6] Since several decades it is also known that the leading trigger and mechanism of this phenomenon is associated to the tidal action on the ocean water. Unlike the solid Earth's tides - which imply only a mainly elastic strain - ocean tides imply some large dynamic displacement of huge water volumes. Hence, the ocean water piles up on the eastern continental shelves, and its weight causes the so-called "loading tide". This originates a violent stress on continental shelves, being responsible for the "polarized tectonics", extensively investigated and reviewed by Doglioni and Panza (2015).

That is, a stress applied to the Earth's crust slows down the observed spin rate of the whole planet, as it can be monitored by an observer located at the Earth's surface. Therefore, a conspicuous stress certainly permanently affects the whole Earth's crust.

Since the Earth is not a unique and compact solid object, different subvolumes of the Earth's body move relative to one another. The final effect is therefore a dynamo. This effect is the leading concern of Gregori (2002) (see also Gregori, 2006e; 2009). The dynamo is called "tide-driven dynamo" or *TD* dynamo. Its energy balance has been the central item for discussion in Gregori (2002).

The available energy is enormous and it raises very serious problems of energy balance. The conclusion is that all endogenous energy phenomena of any kind are the result of the release of this huge endogenous energy. The *TD* dynamo generates huge electric currents that almost entirely decay by Joule heat, and only <<1% of them justifies the geomagnetic field.[7]

The Earth operates like a battery, as its endogenous energy is generated and released at different times, and also by a conspicuous spatial gradient. The largest percent energy release occurs through geothermal heat (with an order of magnitude of ~60%).

The geomagnetic evidence *per se* envisages the location of three mean "equivalent" spherical shells that can be associated with the location of electric currents that originate different parts of the so-called space-spectrum of the geomagnetic field (**Figure 1**). Every "shell" of currents is located, respectively, at the asthenosphere-lithosphere boundary (*ALB*), at the core-mantle boundary (*CMB*) and at the inner-core boundary (*ICB*), respectively. [8]

[6]The literature is huge. The observed trend displays some lesser scatter that has relevant physical meanings and implications. But these items are outside the framework of the discussion in the present paper.

[7]The standard geodynamo model reported in the literature assumes a practically infinite conductivity of the outer core, and searches of some tiny effect that ought to originate the geomagnetic field, which has a comparably feeble total amount of energy. The *TD* dynamo considers rather a huge amount of generated energy, while the observed geomagnetic field is only what remains after the almost entire Joule heat decay of the dynamo currents. It should be stressed that the standard geodynamo model is physically strictly inconsistent – hence it must be rebutted - due to the same reason by which the operator of a hydroelectric power plant, during night time - when the user absorption is reduced - must reduce the water volume falling on the turbines. See Gregori (2002, 2006e and 2009) for details.

[8]In reality, the *ICB* source is not a shell of electric currents, although – as far as the present logical purpose is concerned – the "equivalent" picture, in terms of a shell of electric currents, can be formally shown to be energetically rigorous. The state of the *IC* is not "solid", as it is generally stated. This is physically totally nonsensical. Several other states of

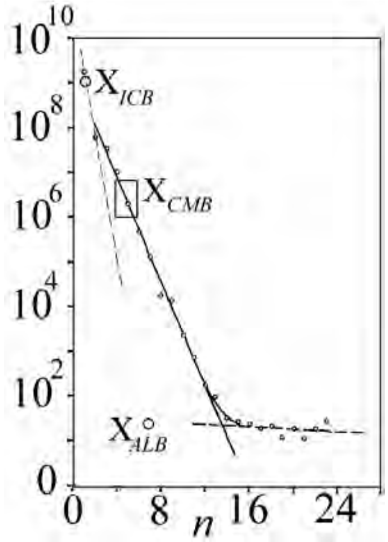

Figure 1 - Lowes-Nevanlinna's (*LN*'s) plot. The **B** observed at the Earth's surface (i.e. at $r = a$) is described by means of a potential, when air-earth currents are neglected. This potential is expressed in terms of a spherical harmonic expansion (*SHE*), every term of which is denoted by a couple of indices (i.e. degree *n* and order *m*). Its coefficients g_n^m and h_n^m can be arbitrary. In contrast, from a physical viewpoint their trend *vs. n* and *m* reflects the physics of the dynamo. Their trend *vs. m* depends on the choice of the frame of reference, unlike that one *vs. n* , which is invariant. The present plot displays on abscissas the degree *n* and on ordinates its corresponding associated fraction of $\mathbf{B}^2$, measured at $r = a$ and averaged over the entire planet (i.e. it is proportional to the mean magnetic energy density). See text for other details. Figure redrawn after Gregori et al. (1993, 2000c). Units are $nT^2\ m^{-3}$.

Concerning **Figure 1**, the fraction of $\mathbf{B}^2$, measured at $r = a$ and averaged over the entire planet, is defined by considering once at a time every contribution by all g_n^m and h_n^m for every fixed *n* and summing up over all $m=0, 1, ..., n$. The *SHE* here considered in **Figure 1** is based on the **B** records collected by the *MAGSAT* satellite, epoch *1979.85.* All points result to be aligned along *3* straight lines. One line through $n=1, 2$ is called Nevanlinna's line, and it is denoted by an index $k=0$. The line $k=1$ is called first Lowes' line and it goes through points with $n=3, 4, ..., 13$. The third line, $k=2$, is called second Lowes' line and it goes through points with $n=14, ...$ The tilt of every such line corresponds to the lower bound for the (seismically determined) radii R_{ICB}, R_{CMB}, and R_{ALB}, respectively, of *ICB* ($k=0$), *CMB* ($k=1$), and *ALB* ($k=2$). When considering *SHE*s that refer to different epochs, it is found that the tilt of every line changes *vs.* time, even by some relevant amount. However, every such a "historical" line always results to cross through some fixed cross-point here denoted as X_{ICB}, X_{CMB}, and X_{ALB}, respectively. This implies that every line ought to be associated to some relevant change of the internal structure of the Earth, though always allowing for one specific *n*, and also for a corresponding energy contribution by that given *n*, which is found to be invariant in time.

The total energy of the three internal sources of geomagnetic field can be shown to be, respectively, of the order of $\sim 10^{20}\ J$ (at the *ICB*), $\sim 10^{18}\ J$ (at the *CMB*), and $\sim 10^{10}\ J$ (at the *ALB*). However, the large energy of the *ICB* source ought to be better explained by means of the specific state of matter of the inner core (*IC*), but this is not pertinent for the present discussion. The tenuous *ALB* source is very likely to be originated by a feeble percent of electric currents that leak off from the *CMB* and decay at the *ALB*.

The location of the *ALB* is an observational matter of fact. But it is reasonable to enquire why it occurs at a given depth rather than at another. According to the discussion of serpentinization (Judd and Hovland, 2007) it is found that the *ALB* is the locus of deepest penetration of the serpentosphere. The conspicuous amount of fracturing causes the observed reduction of the propagation speed of seismic waves, and this effect is claimed by seismologists to be the evidence of the asthenosphere. In addition, the lithosphere slides on the asthenosphere, and friction heat is thus generated. The electric currents that leak off from the *CMB* find the conditions for expansion in space until they find a resistive environment where they decay of Joule heat. The whole phenomenon results therefore into a lubrication for the drift of the overlying lithosphere.

Consider one approximately spherical shell of electric currents. If a lesser bump exists on its surface, the electric currents tend to concentrate in regions of the shell of comparatively higher curvature (i.e. a loop of currents tends to expand in space as much as possible; this classical college-physics result is equivalent to the formal Hamilton's variation principle). This implies that the larger amount of Joule heat is released right on top of the bump. The result is that the bump propagates upward, while its cross-section shrinks

---

matter exist, other than solid, liquid, gaseous and plasma, that cannot be reproduced in our laboratories. This item is not of direct concern of the present discussion. See a previous footnote, and some mentions in Gregori (2013), and also e.g. Drake (2010).

(**Figure 2**). The final pattern is the generation of a conducting feature that reminds about a sea-urchin spike.

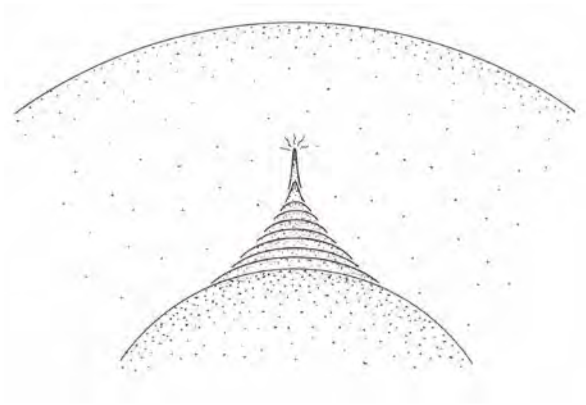

Figure 2 – Let a spherical shell inside the Earth have some minor bump with respect to perfect spherical symmetry. Owing to the Hamilton's principle, the electric currents **j** concentrate on the top of this bump, where they release a comparatively larger amount of Joule heat. But a local heating cannot easily propagate by conduction. Rather, the local temperature increases, and also the local electrical conductivity σ, by which, owing to Hamilton's, an additional and ever increasing amount of **j** concentrates on the bump. The process is self-amplifying, the bump penetrates upward and it shrinks, reminding about a sea-urchin spike. See text After Gregori (2002).

Concerning **Figure 2,** the entire Earth is depicted - in terms of the mass density - almost like an onion, and - in terms of the electrical conductivity - like a "sea-urchin" or an "octopus". This propagation, through **j** currents and Hamilton's principle, strictly implies no transport of matter (no magma, no ions, etc.), rather only and strictly only of conduction charges (electrons). That is, the process is merely electrodynamic, rather than thermodynamic. When such a "spike" of the sea-urchin approaches the Earth's surface, as soon as it finds some fluids (water, oil, methane, geogas, etc.), these fluids transport heat by advection and eventually ensure the energy balance. But, whenever they are insufficient, the local system warms up and the "spike" further propagates upward, until it reaches some comparatively shallow depth where the equation-of-state permits melt, in which case a new fluid is formed, i.e. magma. Magma can now work much like any other fluid, in the fact that it transports heat by advection through a magmatic effusion.

Summarizing, the former concern about the origin of the geomagnetic field leads, as a byproduct, to the explanation of the origin of the endogenous energy of the Earth.[9]

Thus, unlike the Buffon's cooling cannon ball, the Earth unexpectedly results to operate like a battery that recharges and discharges at different times, with large gradients in both space and time. This implies the temporary uplift (up to continental size) of large superswells originated by thermal volumetric expansion of the mantle - i.e. they are some continental-size huge "hills" – crossed by bunches of sea-urchin spikes. The lithosphere slides down the slope of these superswells (or, on a smaller spatial scale, of "geotumors").[10] Oppositely directed lithospheric slabs converge into huge megasynclines where overthrust occurs. The lubrication for sliding is provided by some leakage electric currents from the *CMB* that produce the partial melt observed at the asthenosphere (*ALB*).

In particular, just to mention only an example, at present a huge superswell is uplifting inside a wide region roughly around the Kerguelen Island, and it is responsible both for the poleward drift of Antarctica and for the northward push of Arabia and India. Another region of an ever-increasing release of endogenous heat in the whole northern polar cap. Several different evidences combine and provide with the same final conclusion. But, the best known effects deal mostly with the climatic implications being the likely main cause of the global change, of CO_2 and CH_4 injection into the atmosphere etc. (Gregori, 2015b).

A pattern of the present location of the largest superswells is shown in **Figure 3**.[11]

---

[9]Note that all other sources of endogenous energy (such as radioactivity, state transformation, friction heat, etc.) are optional, as the *TD* dynamo alone is certainly sufficient to justify all observed phenomena. that *must* be supplied by it just in order to get a correct energy balance of the system. That is, geodynamics, seismicity, volcanism, geothermal flow, etc. are strictly needed requirements due to energy balance of the system where the *TD* is active. All endogenous phenomena are no more a target of some *ad hoc* focused model. The same model is confirmed in all other planetary objects, including the very peculiar case history of the Pluto/Charon system (see Gregori, 2016a).

[10]The term "geotumor" was formerly proposed by van Bemmelen (1972).

[11]Credit: *http : www_app2:gfz_potsdam:de=pb1=op=grace=results=index RESULTS:html*; gravity field model *EIGEN-GRACE01S* released on July 25, 2003.

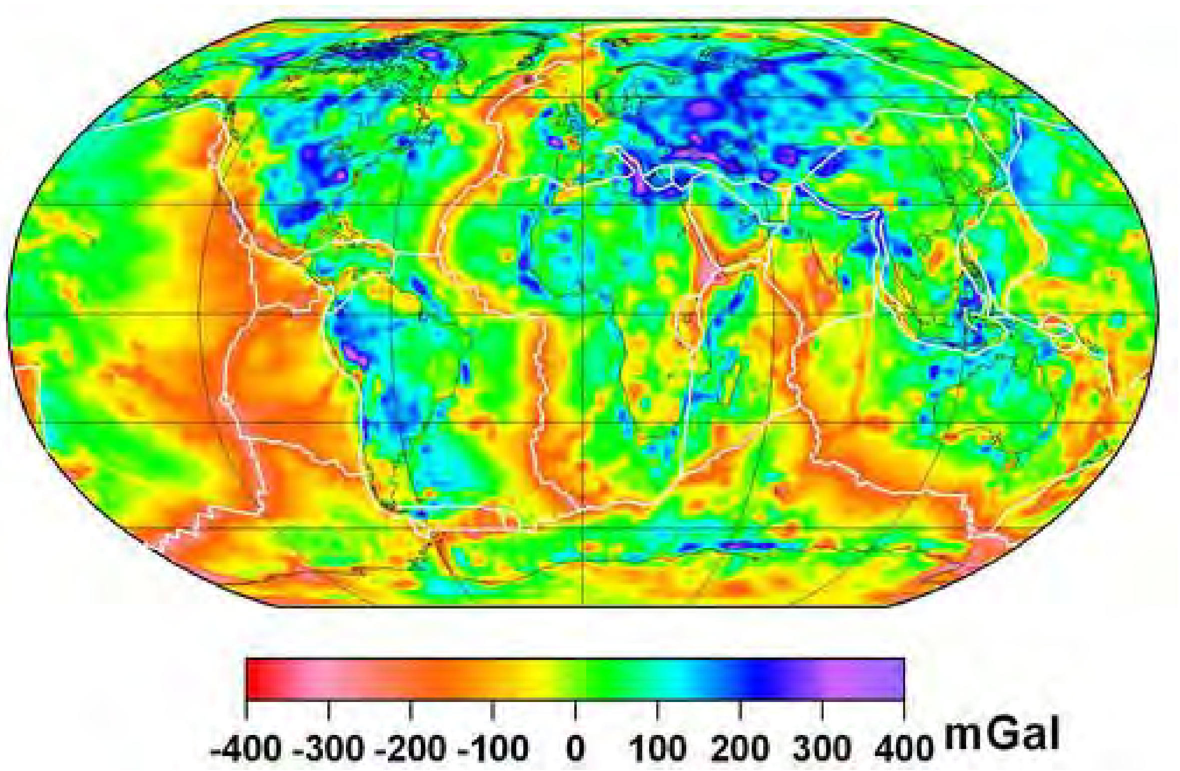

Figure 3 – Gravity anomalies according to the *GRACE* model after subtracting the contribution by matter above the Moho.

Note that the lithosphere is a unique deformable cover that envelops the whole Earth and it slides on the asthenosphere reminding about some kind of mud heated underneath. Hence, this "top-down" model can be called "warm mud tectonics" (*WMT*). The interested reader ought to refer e.g. to Gregori (2006e, 2009 and 2013) for a brief illustration of some details.

Other proposed mechanisms, such as "surge tectonics", *GWT* and expansionism, are consistent with *WMT*, as every interpretation represents different facets of natural reality. Every speculated mechanism can thus be complementary, or sometimes optional, inside the *WMT* model. In contrast, plate tectonics and isostasy, which do require the *Pohlfluchtkraft*, are incompatible as they are excessively one-sided and paradigmatic. In this respect, plate tectonics seems to be a surviving remnant of the Buffon's cooling cannon-ball concept.

It should be very clearly stressed that no "crusade" is here made against any model. All geodynamic models are welcome and considered upon referring to their specific observational and logical framework and concern. Every model was derived based on a learned and very prolonged study by geologists who carried out a huge amount of observations in the field. Every model deserves therefore our most serious consideration. Its database is a basic observational information, a great wealth for understanding. Every sound physical discussion must rely on observational datasets, including their criteria envisaged to organize in some organic way the available observations.

In this respect, it is sad and very unfortunate that plate tectonics results to be incompatible with some basic premises of the observational evidence. Hence, plate tectonics must to be rebutted.

3 – The Mediterranean region

Let us begin and consider the role of the loading tide by the water of the Pacific Ocean on the eastern Eurasian continental shelf. Its effect in the Mediterranean area was detected by Poscolieri et al. (2006a) who show **Figure 4**.[12]

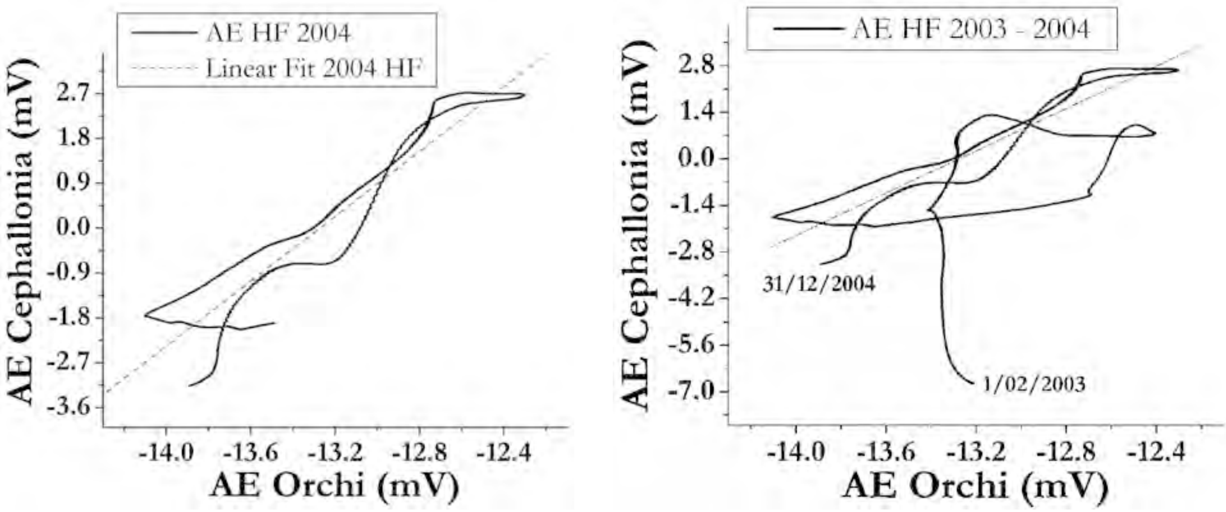

Figure 4 – Simultaneous *HF AE* records - collected at the Raponi site (Orchi, Foligno) and at Kefallinìa Island (or Cephallonia) - are used for drawing the Lissajous figure for 2004 in figure *(a)* [left]. Detrended data are used, respectively, at Raponi site on abscissas and at Kefallinìa Island on ordinates. The same for 2003-2004 is shown in figure *(b)* [right]. The almost perfect synchronism is observed in 2004, not in 2003. See text. Note that the amplitude of the *AE* signal at each site depends on unknown local rheological features and on the local "natural probe". Hence, in general there is no reason to expect an identical intensity at any two given sites. After Poscolieri et al. (2006a).

Note that it is important to avoid to make statistics (as statisticians generally like to do) including all kinds of physically non-homogeneous data - much like it is nonsensical e.g. to make a mean by including birds, fishes, insects and snakes ….. That is, the tectonically quiet condition of **Figure 4a** cannot be investigated altogether with the geodynamically very perturbed condition of **Figure 4b** as they refer to physically non-homogeneous and non-equivalent conditions.

The interpretation of **Figure 4** is according to **Figure 5** that shows the dependence on season - and likely also on the Moon's orbit - of the amount of water that loads on the Pacific continental shelf of Eurasia. The remarkable correlation and synchronism has to be emphasized between the *HF AE* records at the Raponi site ("Orchi") and at Kefallinìa Island. A physical confirmation ought to require *HF AE* records collected somewhere between the China Sea coast and the Mediterranean area. In this way, one could measure the propagation speed of the stress-wave that crosses through the entire span of Eurasia. According to a reasonable guess, this speed ought to result to be of the order of *~10 cm/sec*, i.e. the speed of the "domino effect" (see "paper I"). See, however, a warning deriving from the conclusions of "paper III". In any case, note that this speed is also responsible for the duration of a "crustal storm" (see "paper I" or Gregori et al., 2010; Gregori, 2013).

[12]Note, however, that **Figure 4a** refers to a period of comparably "stable" or "quiet" condition. In fact, during other periods of time (**Figure 4b**) when the Kefallinìa Island area is subject to intense geodynamic activity, the associated local tectonic evolution overwhelms the "quiet" time planetary-scale phenomenon. In fact, Kefallinìa Island is at a triple junction of three very active faults, and its tremendous seismicity is well known. Note that **Figure 4** refers to *HF AE* records, while (see "paper I") the seismic activity is much better represented by the *LF AE* that, indeed, can hardly display any regular trend comparable to this tectonically unperturbed *HF AE* trend.

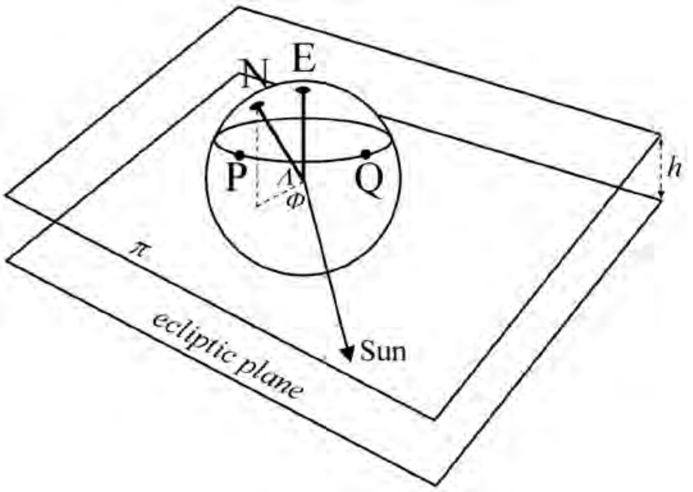

Figure 5 - Position and orientation of the Earth, and the mechanism of the loading tide. Consider two planes, i.e. the ecliptic plane and the plane π parallel to it and located at a distance h from it. The sphere is the Earth's surface. The North Pole is denoted by N, and the perpendicular to the ecliptic plane crosses the Earth's surface at E. Two angles Λ and Φ denote the orientation of the Earth relative to the Sun and to the ecliptic plane. The point P is along the Eurasian coast, and the point Q is along the Pacific North American coast. It is supposed that the loading tide, which pushes on the continental shelf at P, is proportional to the linear extension of the arc PQ along the circle that is the intersection of plane π with the Earth's surface. The total loading tide on Eurasia is an integral of such effect at every point along the Eurasian coast. The lunar effect is computed in a much similar way, where however the direction of the Sun has to be substituted by the position of the Moon. The solar variation gives a seasonal oscillation, the lunar variation gives a ~ 29 days' period oscillation. However, at some large distance along the Earth's surface, the shorter period oscillation is damped off due the greater plastic behaviour of the Earth's crust. In fact, in response to the seasonal variation the crust behaves like an elastic body. Hence, the final result which has to be expected is a seasonal variation of the stress that propagates through the crust. After Poscolieri et al. (2006a).

As far as the Mediterranean region is concerned, an often-reported statement is that it appears very difficult to apply plate tectonics in this area. In particular, a concern deals with the so-called “Adriatic plate” or “Adria plate”. For instance, Viti et al. (2011) exploit a clever analysis of the correlation of seismic activity in different circum-Adriatic regions. That is, they study the interaction between "*the Aegean-Balkan system and the Adriatic/Ionian domain (Hellenic trench, Cephalonia fault, Epirus, Albanides and Southern Dinarides)*", and "*the kinematics of the Adria plate (a large block encompassing the Adriatic continental domain, the northern Ionian zone and Hyblean-Adventure block).*" But they comment the fact "*that in our scheme Adria moves almost in connection with Africa.*" This "*is consistent with the lack of an active decoupling zone between Adria and Africa, an evidence that can hardly be reconciled with the kinematics so far proposed for these two plates.*" Hence, they "*adopt an Africa-Eurasia relative motion different from that implied by the popular* NUVEL-1 *global solution . . .* "[13]

That is, since no lithosphere separation is observed between Africa and the Adriatic Sea, in order to save plate tectonics, a somewhat "strange" feature is speculated, i.e. some kind of northward narrow "tongue" of the African plate extended until the eastern Alps and with west boundary right at the Apennines divide.

This assumption, however, appears perplexing to several other authors. Indeed, note that, unlike all other plates of plate tectonics, the Adria plate is very peculiar in the fact that it displays no real signature at its boundary phenomena. It is speculated to be bounded by the Apennines divide and by the Balkans peninsula, but no other similar or analogous plate seems to be reported from all over the world. The assumption of the Adria plate seems therefore to be definitely *ad hoc* and its real existence unproven.

In addition, concerning the Apennines, they are arbitrarily speculated to be similar to some island-arc phenomenon, with a hypothetical Wadati-Benioff plane deep towards the Tyrrhenian Sea. Some plots are sometimes observed of this plane drawn where also all earthquakes are included that occur in the Aeolian Island region. But, it appears arbitrary - and also inconsistent with all observational evidence - to treat Apennines and Aeolian Islands like similar physical systems.

[13]*NUVEL-1* is a standard “fixed” reference frame defined and used for computations of geodynamic kinematics.

That is, plate tectonics has to be rebutted in this general tectonic framework, and in particular it appears completely *ad hoc* and unrealistic when dealing with the Apennines.

The interpretation of the seismic crisis of Central Italy is therefore here carried out on some objective “top-down” physical basis, with no reference to any fashionable and unproven “generally agreed” paradigm or *ad hoc* modeling.

A preliminary comment is required about the definition of a reference frame for geodynamic models and investigation. The existence of a hotspot reference frame has been debated. But hotspots are not fixed. The best hypothesis is the aforementioned *NUVEL-1* model. However, in general, owing to several indirect inferences that owing to brevity purpose cannot be here recalled, it appears that Antarctica and Africa are the comparably approximately most firmly “rooted” continents on the mantle.

Therefore, as far as the Italian peninsula is concerned, it is reasonable to guess that Africa is approximately standing, while Eurasia is moved westward by the loading tide originated by the Pacific Ocean water. An obstacle to this motion is represented by Sicily, which is well known to be a northward “promontory” of the African continent. That is, some kind of “hinge” exists across the Messina Straights. This “hinge” obviously is associated to the development of a huge amount of friction heat.[14] A huge amount of heat requires a suitable security valve to release it, and Etna seems to be the most obvious candidate for this crucial role. Etna steadily replenishes its energy reservoir much like a calorimeter, and when its storage is above a suitable threshold, it outpours some magma etc., with a typical timing of one eruption every few years.

In this respect, the isotopic chemism of the Etna’s lavas is similar to the Mid-Atlantic volcanism (Zindler and Hart, 1986). According to Gvirtzman and Nur (1999), “*Mount Etna …. lies close to the subduction-related Aeolian magmatic arc but shows no trace of subducted material in its magmas. Mount Etna is also situated on continental crust yet shows oceanic basalt affinities …. with isotopic ratios of He and C suggesting that it is fed by the same type of mantle source as are* MOR *basalts …*” According to the rationale of the present study, this should imply that the sources of *MOR*s and of Etna are at a comparable depth. *MOR*s basalt is originated at, say, ~ 100 km (Forsyth et al., 1998). Hence, ~ 100 km ought to be the depth where the “hinge”' between the African lithosphere and Eurasia generates the bulk friction-heat that supplies Etna.

As a curiosity (Alberto Incoronato, private communication, 2016), fishermen reported an anomalous fish abundance that they explained by an increased sea bottom fumarolic activity, while a few days afterwards the Etna activity - as it could be observed from the Calabrian coast - appeared anomalously large.

GPS measurements show that the Apennines (**Figure 6**) - altogether with the belt located east of their divide - experience the major stress and displacement. In contrast, their western side – where geothermal areas and volcanism are observed – behaves like a region that is left in the wake of the counterclockwise rotation of the peninsula. Indeed, the development of the Tyrrhenian Sea volcanism - including the seismicity of the so-called Calabria arc - is to be interpreted by this rationale.[15]

[14]The role of friction heat in geodynamic processes ought to require a very long discussion that cannot be here even only mentioned. Refer to the aforementioned 8-volume set.

[15]The dating of volcanic rocks dragged on the Tyrrhenian floor are reviewed by Beccaluva et al. (1981).

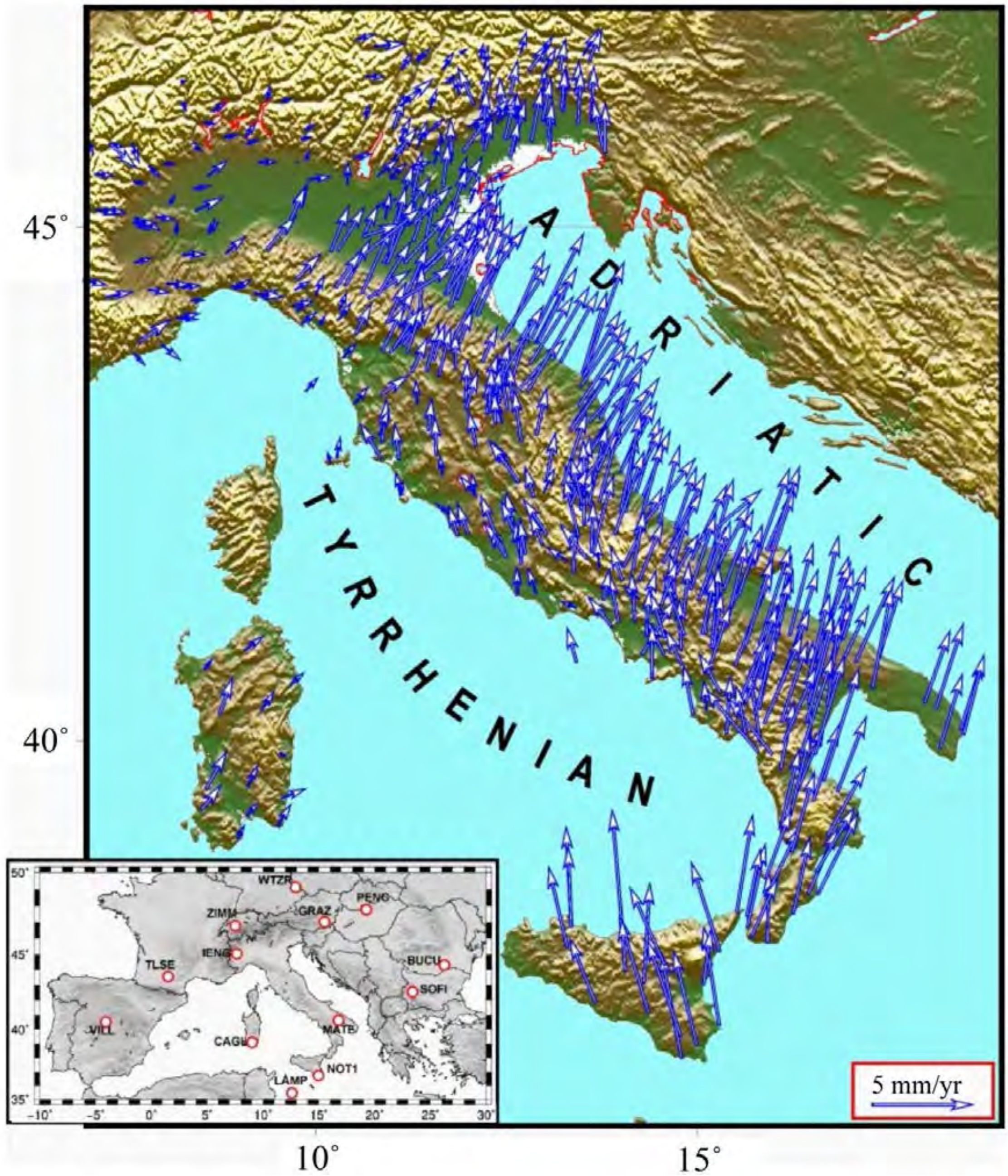

Figure 6 - *"Horizontal velocities (blue vectors) of the* GPS *sites with respect to a fixed Eurasian frame (Euler pole at* 54.23°N, 98.83°W, omega = 0.257°/Ma *(Altamimi et al., 2012). The inset shows the location of the* 13 IGS *stations that have been used to align the daily solutions of the network to the* ITRF 2008 *references frame (Altamimi et al., 2012)."* Figure and captions after Mantovani et al. (2015a).

Note that **Figure 6** is drawn with respect to a reference frame fixed with Europe. But, Sicily ought to result to be approximately standing in the case that this figure is redrawn with respect to a reference frame fixed with Africa. Hence, all other velocity vectors ought to be accordingly changed by adding a downward point arrow. This is also consistent with several other evidences (already mentioned above) that clearly envisage that a large amount of endogenous heat is being released underneath the whole northern polar cap (see e.g. Gregori, 2015b). Therefore, a superswell uplift is presently in progress under the northern polar cap.

Therefore refer to **Figure 7**. Italy is represented by an approximately rectangular slab, with one fixed point close to Etna and a stress applied at its lower right corner in **Figure 7**. The stress starts from this lower right point. It originates a reaction-stress starting from the “hinge”, seemingly located roughly close to Etna. Then the stress propagates northward along the rectangular slab.

This is the explanation of the northward seismic transmigration discussed in “paper III”.

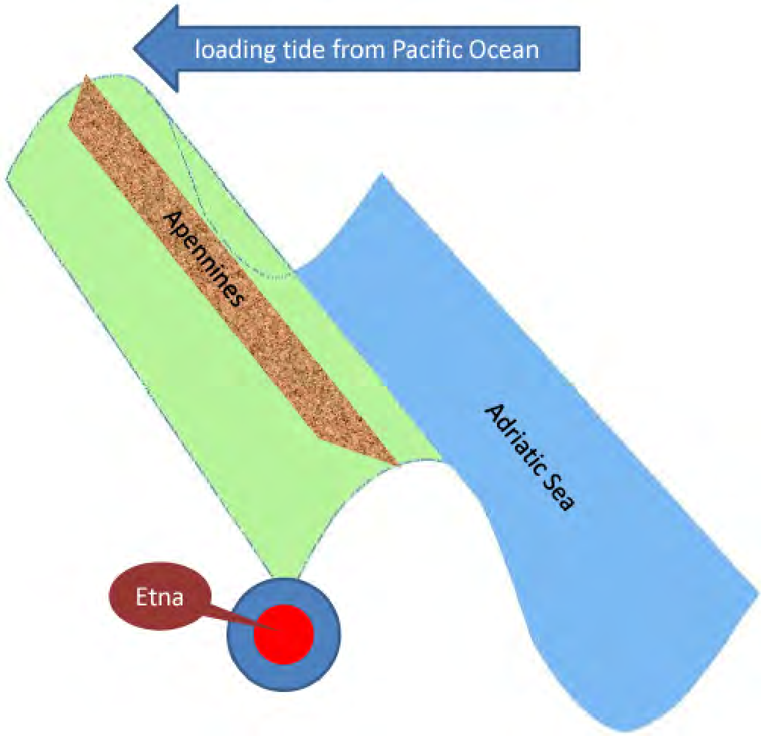

Figure 7 - Origin of seismicity in the Italian peninsula.

The mechanism of the Amatrice-Norcia events can thus be easily explained, as per **Figure 8**. The upper side of the crust breaks, and its two crustal margins are opened. Thus, the loose soil, which is located on top the rigid crustal basement, sinks due to a lack of support.

The central Italian peninsula is characterized by several active faults that appear to be roughly parallel one another. They are carefully mapped and investigated by the geologists and seismologists of *INGV*. A few different faults of this set are responsible for the seismic crisis that is in progress since August 2016 in this area. **Figures 8, 9, 10, 11** and **12** show the effect measured by satellite, by means of differential radar interferometry.

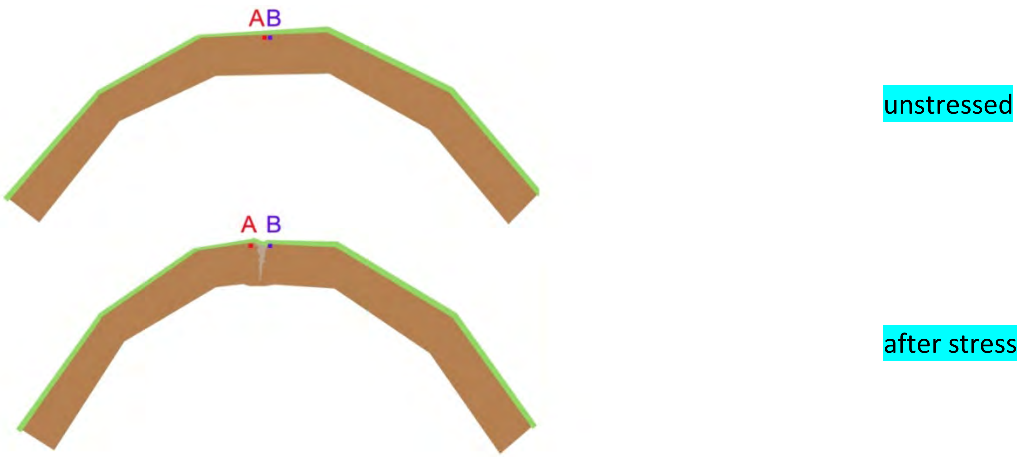

Figure 8 - Cartoon showing a rupture of the crust when it is bent, and its curvature is oriented towards deeper layers. Two points A and B at the Earth's surface that were formerly close each other, after the rupture are laterally displaced, while some empty space is left between them. Thus, the upper loose soil has to subside.

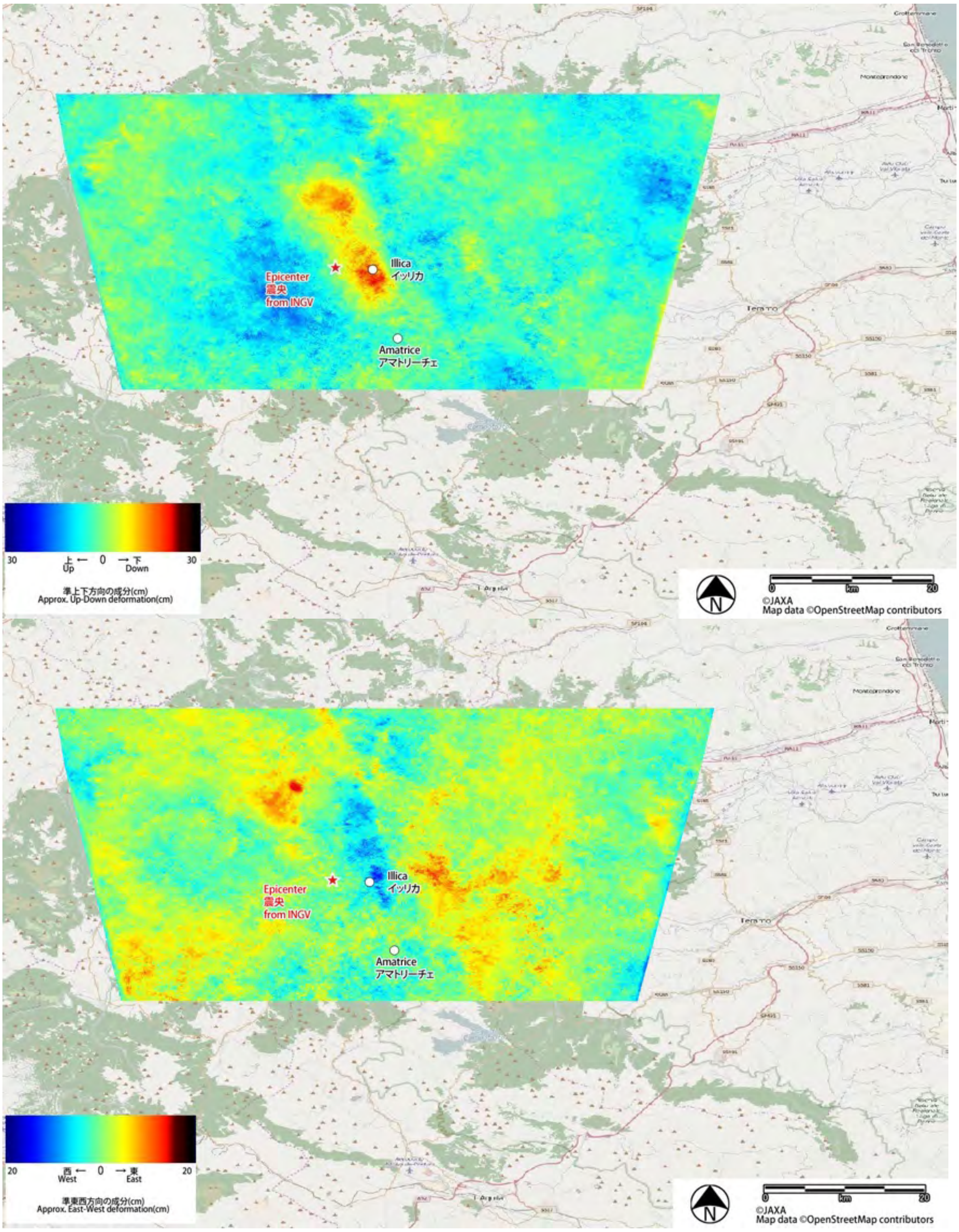

Figure 9 - *"(a) Decomposed east-west displacement. (b) Decomposed up-down displacement"* drawn by means of measurements carried out on August 24th through August 31st. Figure and captions after *Anonymous* (2016n).

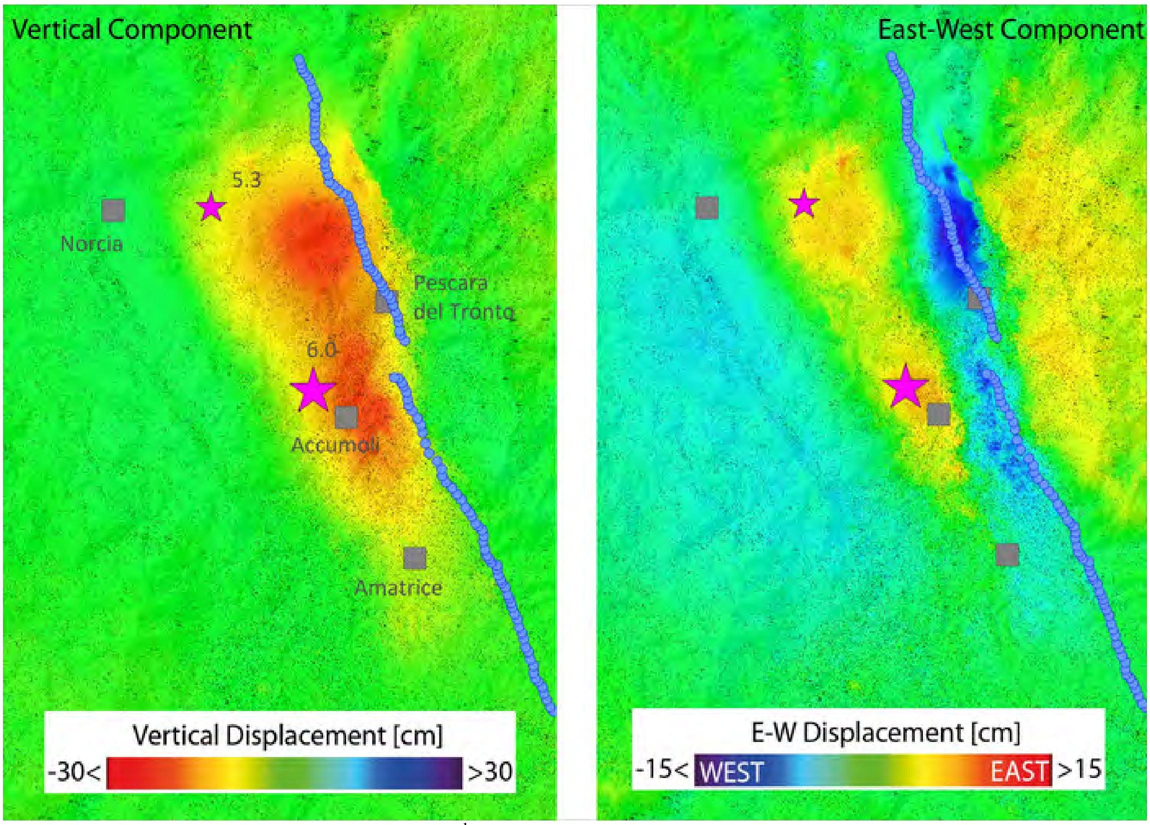

Figure 10 - Ground displacement for the 2nd August 2016 central Italy earthquake. Modified after *Copernicus Sentinel data (2016)/ESA/CNR-IREA*. Figure after *Anonymous* (2016o).

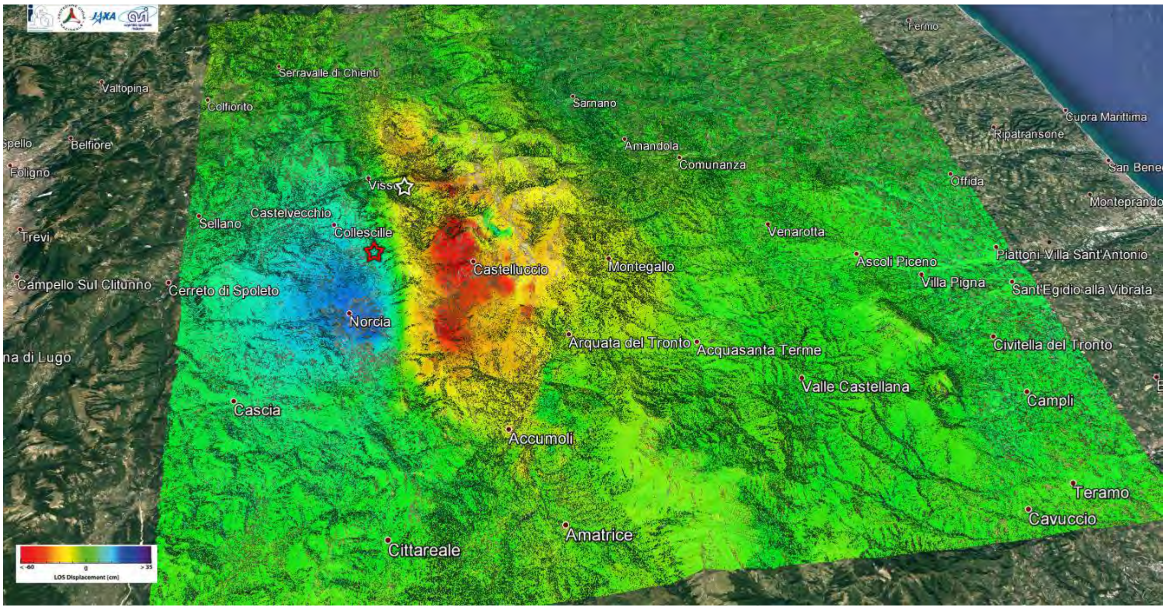

Figure 11 - *"Co-seismic deformation map (along the line of sight of the satellite) obtained by differential radar interferometry relying on* ALOS-2 *records measured on 24th August and on 2nd Nov 2016, respectively , during ascending orbits."* Figure and captions after Lanari et al. (2016).

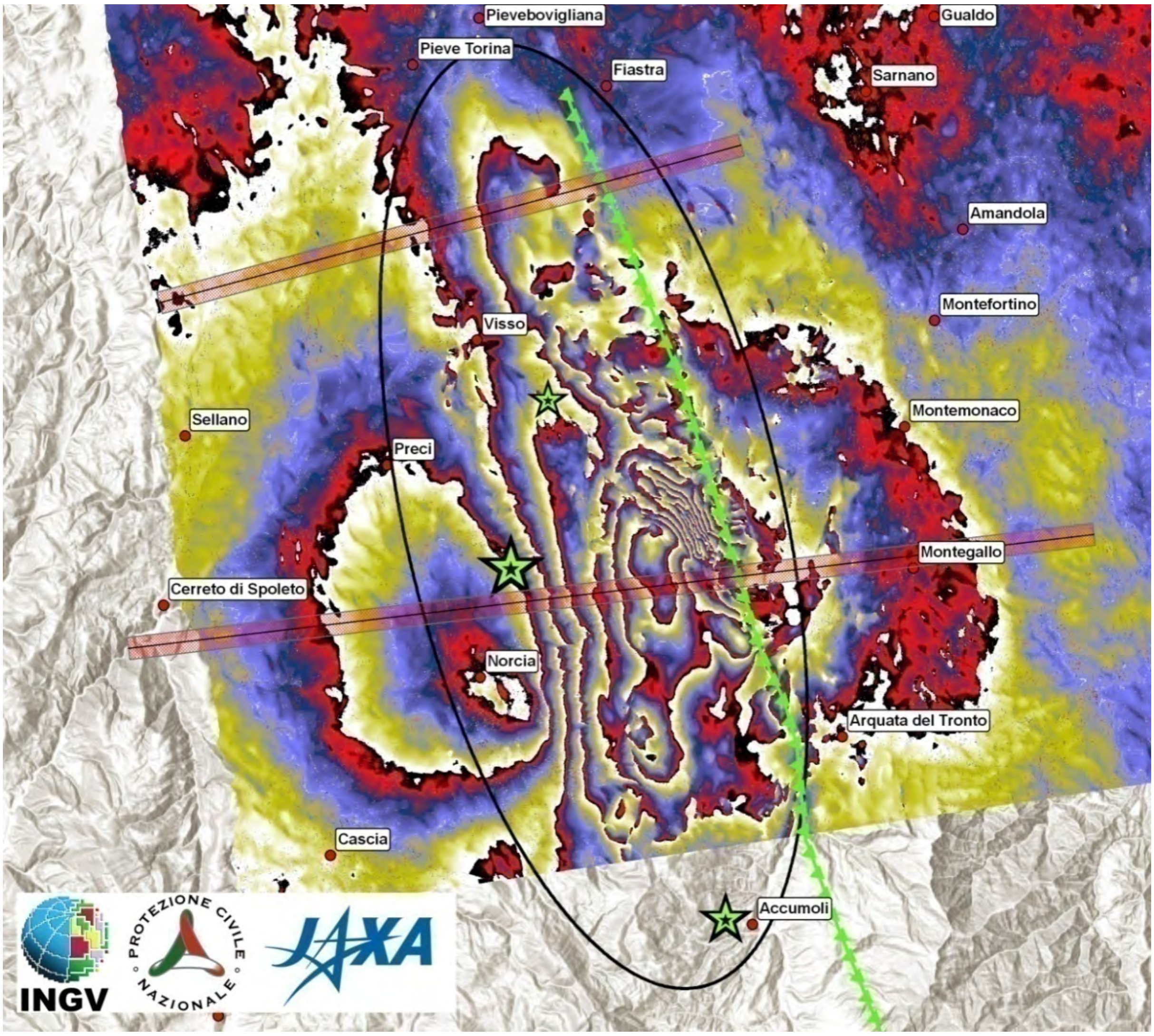

Figure 12 - "ALOS-2 *interferogram. The ellipse shows the area where ground moved away from the satellite along its line of sight. This direction is* 34° *inclined eastward with respect to vertical. The two straight lines denote the profiles shown in Figure 13."* Figure and captions after Lanari et al. (2016).

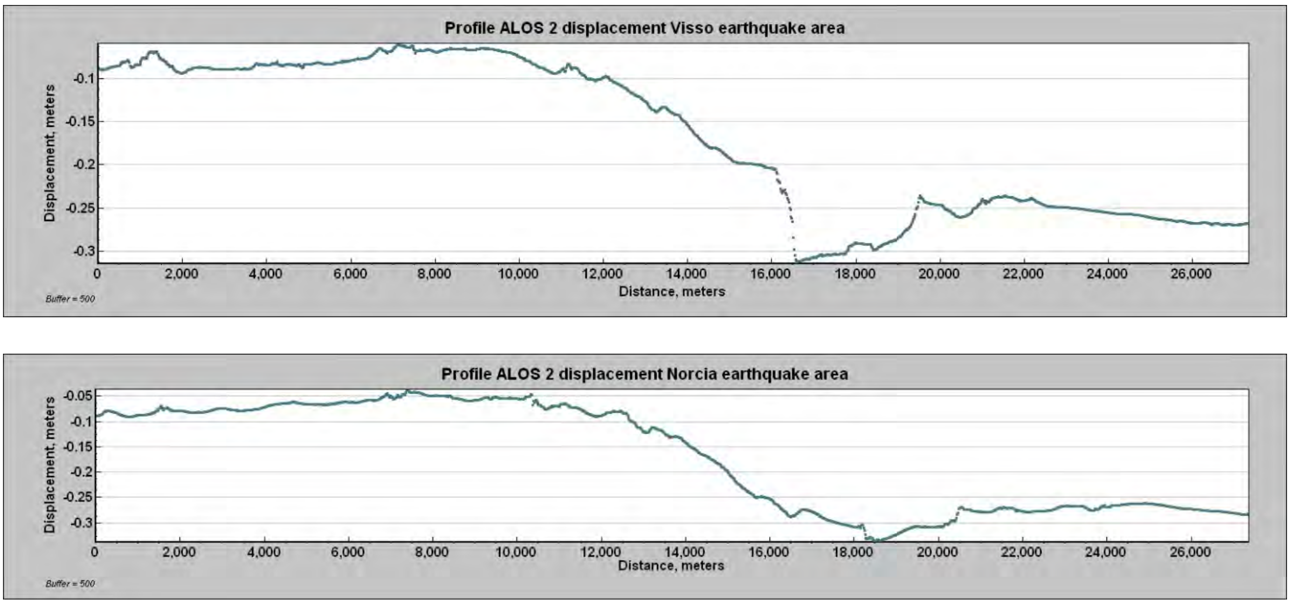

Figure 13 - *"Values of ground motion caused by the Visso and Norcia events, measured along the profiles shown in Figure 12."* Figure and captions after Lanari et al. (2016).

Note that the aforementioned Emilia earthquakes (see Figure 5 of "paper I") of May 20th, 2012 ($M = 6.1$) and of May 29th, 2012 ($M = 5.8$), likewise the November 30th, 2016 earthquake (at 05:52:55, $Mw=3.5$, hypocenter *26 km*), the December 9th, 2016 earthquake (at 07:21:50.17. $ML=4.0$, hypocenter *7.6 km*), the January 13th, 2017 (at 07:15:46, $ML=3.0$, hypocenter *5.3 km*), and the February 9th, 2017 (at 08:14:08, $ML=3.6$, hypocenter *11.3 km*) – upon mentioning only $M \geq 3.0$ events - rely on a completely different mechanism, as the southern fraction of the Italian peninsula, owing to its counterclockwise rotation, is pushed like a cleft against the Po Valley. See all earthquakes in Table S1 and in Figure S1 of the Addendum to "paper III".

Summarizing, an array of a few *AE* stations through the Italian peninsula could substantially improve our understanding of its seismicity and also of its eventual, and often debated, fracturing by some deep-seated faults (refer to "paper I" for better discussion).

3 - **Conclusion**

The 2016-2017 seismic crisis in Central Italy is an effective natural laboratory to test geodynamic models. The final target is to manage and mitigate the seismic risk. As shown in "paper I", the *AE* records seem to be a very effective diagnostic tool suited to provide with some unprecedented and detailed monitoring of the natural system before the occurrence of a catastrophe, i.e. *before* the irreversible evolution of the crust.

In "paper I" it has also been shown that earthquake hazard can be operatively managed in terms of a four-level approach. The present paper critically evaluates the need for a correct geodynamic interpretation of the available observational evidence, by freeing ourselves from the constraints of unproven "generally agreed" paradigms that rely on consensus science forgetting about any critical evaluation either of ideas or of our basic gnoseological concern. The interpretation can be rather carried out on the only basis of straight and concrete physical arguments.

The resulting scenario and interpretation is a realistic operative setting suited to mitigate and manage the seismic hazard in the Italian peninsula.

An accompanying "paper III" is devoted to apparent transmigration phenomena and to the inference of the estimate of the size of the focal volumes that are involved in the seismic phenomena in this peculiar tectonic setting.

Acknowledgements – We feel deeply indebted to Prof. Alfredo Raponi, professional architect and renowned painter, and to his wife Prof. Anna Maria Vigo, as for several years they hosted our *AE* station - and also gave operative facilities - in the basement of their house at Capodacqua di Foligno, at the site named Orchi. We could exploit our investigations only due to their generous and very long-lasting unselfish help. We are very glad to warmly acknowledge their cooperation. We are also deeply indebted to Prof. Alberto Incoronato, Roberto Mortari and Giuliano F. Panza, and to Dr. Franco Bonavia and Bruce Leybourne, for their accurate reading and commenting on a previous preliminary draft from which the present set of three papers was derived. Their feedback resulted very important for us in order to focus on items that required a better specific and more detailed explanation. This improved the clarity of our papers, although we have full responsibility for their scientific content.

References

Altamimi, Z., Métivier, L. and Collilieux, X., 2012. ITRF2008 plate motion model. *J. Geophys. Res*., **117**, B07402; doi: 10.1029/2011JB008930.

Anonymous, 2016n. ALOS-2/PALSAR-2 Observation Results on M 6.2 earthquake in central Italy, website *ALOS-2.ALOS, "DAICHI-2"*, updated Nov 4, 2016.

Anonymous, 2016o. Sentinel-1 provides new insight into Italy's earthquake, *ESA News (Sentinel-1)*, issued 29 Aug 2016.

Beccaluva, L., Gabbianelli, G., Lucchini, F., Rossi, P.L., Savelli,, C. and Zeda, O., 1981. Magmatic character and K/Ar ages of volcanics dredged from the Eolian seamounts (Tyrrhenian Sea). In Wezel (1981), 361-368.

Doglioni, C. and Panza, G., 2015. Polarized plate tectonics. *Adv. Geophys*., **56**, 1-167; doi: 10.1016/bs.agph.2014.12.001.

Drake, P.R., 2010. High-energy-density physics. *Phys. Today*, **63**, (6), 28-33.

Forsyth, D. W., Scheirer, D.S., Webb, S.C., Dorman, L.M., Orcutt, J.A., Harding, A.J., Blackman, D.K., Phipps Morgan, J., Detrick, R.S., Shen, Y., Wolfe, C.J., Canales, J.P., Toomey, D.R., Sheehan, A.F., Solomon, S.C. and Wilcock, W.S., 1998. Imaging the deep seismic structure beneath a mid-ocean ridge: the MELT experiment, *Science*, **280**, 1215-1237.

Gregori, G. P., 2002. Galaxy – Sun – Earth relations. The origin of the magnetic field and of the endogenous energy of the Earth, with implications for volcanism, geodynamics and climate control, and related items of concern for stars, planets, satellites, and other planetary objects. A discussion in a prologue and two parts. *Beiträge zur Geschichte der Geophysik und Kosmischen Physik*, Band **3**, Heft 3, 471 pp. [http://www.sme-ae.it/ → letteratura → Galaxy Sun Earth relations].

Gregori, G.P., 1993. Geo-electromagnetism and geodynamics: "corona discharge" from volcanic and geothermal areas. *Phys. Earth Planet. Interiors*, **77**, 39-63.

Gregori, G.P., 1999. Variational principles and geomagnetism. In *Schröder (1999),* 268-303.

Gregori, G.P., 2000c. Galaxy-Sun-Earth relations. The dynamo of the Earth, and the origin of the magnetic field of stars, planets, satellites, and other planetary objects. In Wilson (2000), 329-332.

Gregori, G.P., 2006e. The Earth's interior-Myth and science. In Schröder (2006b), 108-126.

Gregori, G.P., 2009. The Earth's interior – Myth and science. *New Concepts Global Tect. Newslett*., (53), 57-75. [Revised edition of Gregori (2006e).]

Gregori, G.P., 2013. Crustal storms of continental/planetary scale-Earth's battery and Earth's electrocardiogram, internal state, structure, and time variation, endogenous energy production and release, the role of solar modulation, and the "French Revolution" jerk. *NCGT Journal*, **1**, (2), 40-64.

Gregori, G.P., 2014. Climate and the atmospheric electrical circuit: the electromagnetic coupling between solar wind and Earth. *NCGT Journal*, **2**, (1), 99-112.

Gregori, G.P., 2015b. Anthropic global warming. *NCGT Journal*, **3**, (4), 544-560.

Gregori, G.P., 2016. Some reflections on science and on the management of environmental catastrophes. *NCGT Journal.,* **4**, (3), 456-472.

Gregori, G.P., Paparo, G., Poscolieri, M., Rafanelli, C., Ventrice,G., Garilli, G., Imperatori, L., Lo Castro, F. and Zimatore, G., 2016. The seismic sequence in Central Italy (August-November 2016) - AE monitoring and analysis, *New Conc. Global Tect. J.,* **4**, (4), 637-663.

Gregori, G.P., Paparo, G., Poscolieri, M., Rafanelli, C., Ventrice, G., Garilli, G., Imperatori,L., Lo Castro, F. and Zimatore, G., 2016. The seismic sequence in Central Italy (August-November 2016) - AE monitoring and analysis, *New Conc. Global Tect. J.,* **4**, (4), 637-663.

Gregori, G.P., Poscolieri, M., Paparo, G., De Simone, S., Rafanelli, C. and Ventrice, G., 2010. "Storms of crustal stress" and AE earthquake precursors, *Nat. Hazards Earth Syst. Sci.*, **10**, 319–337.

Gvirtzman, Z. and A. Nur, 1999. The formation of Mount Etna as the consequence of slab rollback, *Nature, Lond*., **401**, 782-785; 10.1038/44555.

Judd, A. G. and Hovland, M., 2007. *Submarine fluid flow, the impact on geology, biology, and the marine environment.* 475 pp., Cambridge University Press.

Lanari, R., Salvi, S., Ferrazzoli, M., Mattoni, S. and Rea, F., 2016. Dal giapponese ALOS 2 nuovi dettagli sugli effetti del terremoto, *CNR Press release*, issued on 4 Nov 2016.

Mantovani, E., Viti, M., Cenni, N., Babbucci, D. and Tamburelli, C., 2015a. Present velocity field in the Italian region by GPS data: geodynamic/tectonic implications. *Int. J. Geosci*., **6**, 1285-1316; http://dx.doi.org/10.4236/ijg.2015.612103.

Planck, M., 1956. *Autobiografia scientifica*. Einaudi.

Poscolieri, M., Gregori, G.P., Paparo, G. and Zanini, A., 2006a. Crustal deformation and *AE* monitoring: annual variation and stress-soliton propagation, *Nat. Hazards Earth Syst. Sci.*, **6**, 961-971.

Schröder, W. (ed.), 1999. Physics and geophysics (A compilation with special historical case studies), 335 pp., History Commission of the German Geophysical Society, *Mitteilungen des Arbeitskreises Geschichte der Geophysik der DGG*, **18**, Jahrgang (1999), Heft 1-3, Science Edition/DGG, Bremen.

Schröder, W. (ed.), 2006b. Case studies in physics and geophysics. *Beiträge zur Geschichte der Geophysik und Kosmischen Physik*, special issue (2006/2), 126p. (Journal for the history of Geophysics and Cosmical Physics), Science Editions, AKGG, Bremen-Roennebeck.

Showstack, R., 2011. Scientists examine challenges and lessons from Japan's earthquake and tsunami. *EOS, Trans. Am. Geophys. Un*., **92**, (12), 97-99.

Tukey, J.W., 1977. *Exploratory data analysis*. 688p., Addison-Wesley Publ. Co., Reading. Massachusetts, etc.

van Bemmelen, R.W., 1972. *Geodynamic models. An evaluation and a synthesis*. 267p., Elsevier Publ. Co., Amsterdam etc.

Viti, M., Mantovani, E., Babbucci, D. and Tamburelli, C., 2011. Plate kinematics and geodynamics in the Central Mediterranean, *J. Geodyn.*, **51**, (2/3), 190–204; doi: 10.1016/j.jog.2010.02.006.

Wezel, F.C., (ed.), 1981. *Sedimentary basins of Mediterranean margins*. Tecnoprint, Bologna.

Wilson, A., (ed.), 2000. The first solar and space weather conference. The solar cycle and terrestrial climate. *ESA SP-463*, 680p., European Space Agency, ESTEC, Noordvijck, The Netherlands.

Zindler, A., and Hart, S.R., 1986, Chemical geodynamics, *Ann. Rev. Earth Planet. Sci.*, **14**, 493–571.

The seismic sequence in Central Italy (2016-2017) III - Heuristic seismic transmigration, and focal volume estimate

Giovanni P. Gregori[(a)(b)(c)(d)], Gabriele Paparo[(a)], Maurizio Poscolieri[(a)], Claudio Rafanelli[(a)], Giuliano Ventrice[(e)], Gianpaolo Garilli[(a)], Luca Imperatori[(a)], Fabio Lo Castro[(a)], and Giovanna Zimatore[(a)(f)]

(a) – *IDASC – Istituto di Acustica e Sensoristica Orso Mario Corbino (CNR)*, Roma (Italy);
(b) – *IEVPC (International Earthquake and Volcano Prediction Center)*, Orlando (Florida)
(c) – *IASCC (Institute for Advanced Studies in Climate Change)*, Aurora (Colorado)
(d) - *ISSO (International Seismic Security Organization)*
(e) – *PME* srl, Roma (Italy)
(f) - *Department of Health Sciences, University of Rome "Foro Italico"*, Roma (Italy)
Corresponding author: giovanni.gregori@idasc.cnr.it

(Received 27 February 2017. Accepted 12 March 2017)

Abstract: The seismic sequence in Central Italy that started in August 2016 - and is still in progress in February 2017- is investigated like a pilot-study in order to focus on a multidisciplinary perspective for a realistic seismic hazard mitigation and management. A clear distinction has to be made with the "bottom-up" approach which is typical of a geologist or of a seismologist, who investigate phenomena *after* the occurrence of an earthquake, and upon consideration either of a subset of known phenomena – or of "all" them - that are available and that preceded every given shock. Statisticians, altogether with seismologists, apply a formally rigorous and careful approach, based on complicated algorithms etc. Their *rigorous* approach is certainly indicative and useful for hazard management, unlike every less rigorous statistical analysis that cannot be comparably reliable. In fact, the boundary is not always clearly stated between an "implicit suitable assumption" and logical rigor.

A first paper ("paper I") in the present series was concerned with a real-time monitoring of crustal stress propagation, aimed to provide with new and physically more precise observational information. It relies on acoustic emission *(AE)* monitoring of the crustal stress propagation and evolution *before* the occurrence of an eventual earthquake. That is, its focus is on the preliminary diagnosis of the state of the crust *before* the eventual occurrence of a seismic shock. The approach is from the viewpoint of the geophysicist ("top-down"), i.e. just apply the known laws of fundamental physics to the physical system and infer its evolution until an eventual catastrophe.

A second paper ("paper II") was focused on a correct "top-down" and rigorous approach to the geodynamic interpretation. Its purpose was to show how the present standard way to approach geodynamics is unsuited for any real physical discussion. In fact, it relies on the "bottom-up" approach of geologists in terms of some more or less intuitive, certainly reasonable although often physically unreliable, argument.

The present paper ("paper III") completes the series. It is focused on the empirical evidence that is generally denoted as seismic (and eventually also volcanic) "transmigration". Two viewpoints are however to be distinguished. One approach deals with an analysis of single case histories. This is physically correct, because compared to all others every occurrence is a different case history. On the other hand, single case histories can allow for no statistical inference, hence with no "confidence limit" or error bar etc., which is the "dream" of every statistician (or of every experimenter). On the other hand, the alternative approach - which is formally applied to the seismic catalogues by means of the formal methods of statistics - has the drawback to manage a supposedly homogenous database that, in reality, is physically heterogeneous. Hence, every formal statistical result has the hazard of being only a mathematical exercise with no physical correspondence to natural reality.

Notwithstanding this warning and all logical constraints, this three-paper set shows how an earthquake appears to be a local response to a planetary paroxysm that somewhere is eventually manifested as a seismic shock, although in general it can even be associated to no earthquake. No "simple" "thumb rule", or no "magic" precursor, will ever be found.

Similarly to every conscience-driven medical doctor who wants to take care of the health of his patient, the seismic hazard can be managed only by applying some suitable objective monitoring of the natural system. In "paper I" it is shown that this effort can be optimized by a 4-level approach: *(i)* level 1 gets advantage mostly from satellite monitoring; *(ii)* levels 2 and 3 rely on *AE* records to be collected either on the planetary scale (for level 2) or by means of temporary arrays located along some already known active fault (for level 3); and *(iii)* level 4 is aimed to focus - and hopefully specify - at every given date and site, two short time intervals when an earthquake can occur. Finally, "paper II" shows how a correct, unbiased and physically reliable, analysis of the geodynamics - including the apparent transmigration phenomena of single case histories which are discussed in the present "paper III" - is fundamental for a correct interpretation of the *AE* records, and therefore for the management of the seismic hazard in every given area. In any case, it is fundamental to get rid of the unfortunate paradigms that at present bias the "generally agreed" - and often *ad hoc* and arbitrary - interpretation.

Keywords*: seismic catastrophes, acoustic emission, seismic transmigration, 4 level approach, geodynamics of Italy and of the Tyrrhenian Sea, physical analysis of single case histories, statistical investigation of seismic catalogues*

Acronyms:

AE – acoustic emission	*LF* – low frequency
ENSO – El Niño Southern Oscillation	*MJO* - Madden Julian Oscillation
gfv – generalized focal volume	*ppa* – pole position algorithm
HF – high frequency	*USGS – United States Geological Survey*
INGV – Istituto Nazionale di Geofisica e Vulcanologia	*WMT* - warm mud tectonics

1 – Introduction. Seismic transmigration - Logical constraints and implication

Starting in August 24th 2016 and still continuing through February 2017,[16] the regions of Central Italy were struck by a series of earthquakes. Even though their magnitude was not very strong, they resulted particularly destructive. The *AE* (acoustic emission) monitoring and interpretation has been discussed by Gregori et al. (2016), to be quoted henceforward as "paper I". Its main focus was on crustal stress phenomena and on envisaging a 4-level approach to the mitigation and management of seismic catastrophes.

A second paper ("paper II"), which accompanies the present "paper III", is focused on the strict need for an unbiased geodynamic interpretation, based on a correct application of the known laws of physics to the Earth system. That is, a rigorous "top-down" approach is considered (i.e. the laws are considered first, and their consequences applied to the natural system, independent of the occurrence or not of an earthquake). However, it is fundamental to avoid to refer to all "generally agreed" models based on paradigms that in reality only rely on some conventionally "well assessed" "believes". Those ''believed'' models were constructed by geologists, according to a "bottom-up" approach by means of some "simple" and intuitive analysis. They started from the seismic events that already occurred, and they attempted to infer what might have preceded every shock. Their rationale is certainly very reasonable for organization purpose of their huge observational database, although their models are not suited for being considered a physical interpretation of geodynamic phenomena.

In contrast, a formal "top-down" approach is strictly required. The methodological "top-down" vs. "bottom-up" distinction is fundamental in order to avoid misunderstandings, and eventual nonsensical debates pros or cons (that often even remind about hooliganism, rather than about a scientific debate).

The present "paper III" deals with a different kind of approach that searches for some apparent transmigration of seismic (or sometimes also volcanic) activity while referring - both in space and time - to some suitable region and scale-size.

Note, however, that this is just a simple empirical inference that might be only a matter of a coincidence, although, maybe, it might also be an important hunch suited to get some better insight in phenomena. That is, every evidence of this kind can be of potential paramount importance, but it has always to be carefully considered with a suitable understating and realistic feeling.

In this respect, a basic preliminary distinction has to be made between two different approaches, i.e. whether the focus is *(i)* on some specific single sequence of events, or rather *(ii)* on some suitable - either

[16]In "paper I" the seismic crisis was referred to as August-November 2016. But, the seismic crisis was substantially reactivated along the same faults by a new series of M>5 earthquakes and it is still in progress in February 2017 with repeated shocks of magnitude >3.

large or restricted - seismic catalogue.

The first approach is *per se* physically more rigorous, because every case history is a different phenomenon, and in principle it is nonsensical to consider a statistical inference based on a dataset composed of non-homogeneous elements. Similarly, a zoologist can formally evaluate a mean between a bird and a fish, but his result is meaningless. That is, every rigorous statistical algorithm always gives a formal result, with confidence limits, error bars, etc. But, a mathematically sound information can also be physically meaningless. Hence, the zoologist must apply a preliminary filter in order to select animals that can be considered to be comparable one another. In contrast, in the case of seismic events we cannot know whether different phenomena can be considered to be physically comparable one another, or not. On the other hand, separate consideration of every case history is correct, but it gives no confidence limits and/or error bars. Hence, one can only rely on some inference that might be a coincidence or not. But, in general, it is always correct to consider that nothing in natural phenomena can occur by chance, and nothing is coincidental.

This transmigration approach is “bottom-up”. The unique way suited to get rid of its intrinsic logical bias is therefore to apply – as far as possible - a “top-down” approach, i.e. by envisaging some tentative physical model that can explain observations. Then, the laws of physics are applied, and one attempts to forecast phenomena. Note that every tentative physical model can be eventually improved in order to get a better agreement with observations. All this is part of the exploratory analysis (Tukey, 1977).

The second approach to transmigration relies on some suitably defined and sufficiently large seismic catalogue. This approach leads to a precise evaluation of confidence limits and errors bars, although with the aforementioned drawback of the assumption of comparable elements.

Upon referring to concrete investigations, up to our knowledge, three main kinds of attempts are to be recalled, respectively, by Blot-Choi, by Tsunoda, and by Vikulin et al.[17] In fact, every investigation deals with “bottom-up” transmigration. But, according to a “top-down” approach, in general every different investigation has to be considered independent of others.

I - It can be shown that the Blot-Choi approach[18] can be interpreted in terms of a physical model that can be intuitively illustrated in **Figure 1**. An extensive discussion of this explanation ought to require a series of papers. This physical model refers to what - according to plate tectonics - is generally called a “subduction zone”. But, as explained in “paper II”, plate tectonics has to be rebutted. Let us say that, somewhere the mechanical support is lacking for the lithosphere that, therefore, must sink and bend downward. The lithospheric slab eventually breaks due to its weight, pulled by its deeper sinking segment that “hangs” inside an environment that provides with an insufficient mechanical support.

As briefly mentioned in “paper II”, the rationale is in terms of warm mud tectonics (*WMT*), i.e. of huge superswells and of the lithosphere that slides down along their slopes. One huge superswell is presently uplifting underneath the northern large polar cap, with mainly climatic implications (see Gregori, 2015b and references therein). Another even larger superswell is roughly located around the Kerguelen Island. It pushed Antarctica to its present location. It is pushing Arabia underneath Iran etc. causing also the counterclockwise rotation of the Anatolian peninsula that penetrates like a cleft into the Aegean Sea etc. It pushed – and it is still pushing - India against Eurasia.

[17]A detailed discussion is given in an 8-volume set in preparation by one of the authors (GPG) while, owing to brevity purpose only a few conclusions can be here anticipated. For a few preliminary highlights of this 8-volume set see Gregori (2014).

[18]See Blot et al. (2003), Blot and Choi (2004, 2006a and 2007), Blot (2004, 2005), Choi (2010, 2010a, 2011b and 2012a), Pesicek et al. (2010) and references therein.

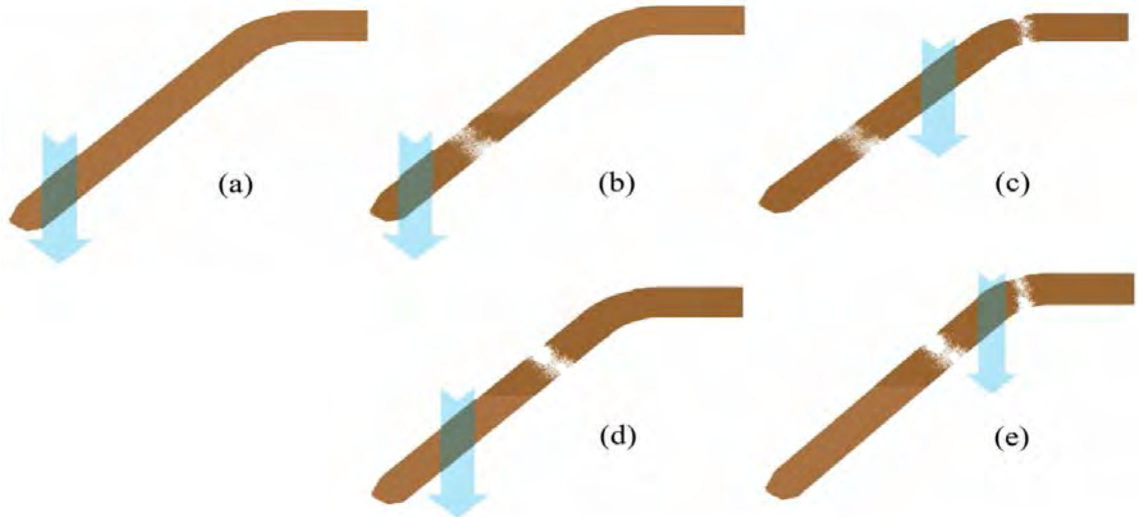

Figure 1 - Qualitative tentative mechanism aimed to explain the Blot-Choi seismic (and volcanic) transmigration including the observed variation of the apparent "propagation speed" between precursor and main shock. The blue arrows denote the gravity pull inside the non-supporting environment of the sinking lithospheric slab. The rationale is the rupture of the sinking lithospheric slab. Owing to brevity purpose, the details of single steps cannot be here discussed upon specifically referring to every single observed case history.

The combined result is a huge megasyncline that ranges from the Pyrenees through Japan, including some well observed specific geomagnetic anomaly signatures.

This kind of transmigration analysis deals with several case histories referred to the most intricate tectonic region of the world. In fact, this region results from the interaction of the northeast push originated from the Kerguelen superswell, combined with the effect of the westward motion of Eurasia, which is pushed by the loading tide of the Pacific Ocean. Thus, a particularly complicated tectonic setting is generated, such as e.g. the Moluccas Sea, the Banda Sea, the Sunda archipelago, etc.

That is, the Blot-Choi approach is physically interpreted in terms of the mechanism of a slab of lithosphere that bends and sinks into a trench. Note that this slab can be either visible or also hidden underground. That is, this is a typical process that occurs inside the standard tectonism of an island arc and of its trench, i.e. inside a so-called “subduction zone”. But, it also occurs in regions where - according to the reported geophysical evidence as stressed in the Blot-Choi papers - no clearly detectable trench is eventually observed.

II - Instead, the Tsunoda approach[19] refers to transmigration along the “ring of fire” of the Pacific Ocean. Its explanation can be envisaged in terms of an uplift to the whole Pacific Ocean floor that looks almost like a unique large superswell,[20] with effects that - according to a pattern in space and time - appear to propagate along the borders of this huge pattern. Or it is concerned with a continental-, or planetary-, scale perspective and its findings are consistent with the rationale of *WMT*, i.e. of superswells, of the lithosphere that slides on their slope, and of the resulting correlation of the seismic and volcanic activity along the outer boundaries of every superswell when it is eventually experiencing an ongoing uplift.

III - The Vikulin et al. approach[21] is rather a formal statistical analysis of the world seismic catalogue, with all formal estimates of errors bars and confidence limits etc. But, it has the aforementioned logical bias deriving from consideration of a set of supposedly homogeneous case histories.

It is very difficult to envisage any kind of physical model suited to explain the more or less clear apparent regularities that result from this kind of statistical analysis. In fact, a formal statistical approach always

[19]See Tsunoda (2009a, 2010 and 2010a), Tsunoda et al. (2015), Choi (2014f and 2014g), Choi et al. (2014 and 2014a) and references therein.

[20]This reminds about the related classical debate on the so-called Darwin rise. But, owing to brevity purpose no reference can be here given.

[21]See Vikulin et al. (2012) and references therein.

gives a mathematical result. In addition, every evidence is certainly an observational matter of fact. But, it in general it is the consequence of the overlapping of several different physical drivers that determine specific effects on some physical subsystem. Different subsystems interact one another etc. The final result is that the physics is there, and the analysis is rigorous and correct. But, it is almost impossible to derive any "simple" and expected regularity or rule that ought to control the whole system according to some specific cause-and-effect chain.

That is, the Vikulin et al. approach is a mere formal statistical analysis with some inferences that represent some mean trend and correlation inside the observational database. But, unlike it can be made for the Blot-Choi's and the Tsunoda's approaches, no ''simple'' - tentative and straightforward - physical explanation can be inferred, as the Earth is a complex system and the planetary distribution of the seismic and/or volcanic activity responds to a sum of different drivers. The final statistical inference is the result of a weighted mean of different unknown effects with a weight that in general can vary both in space and time.

Another approach that shares the same planetary perspective was exploited by Krishnamurti et al. (2009). It is worthwhile to report here their whole abstract.

"*Taking the* USGS *global daily data sets for 31 years we have tabulated the earthquake intensities on a global latitude longitude grid and represented them as a finite sum of spherical harmonics. An interesting aspect of this global view of the earthquakes is that we see a low frequency modulation in the amplitudes of the spherical harmonic waves. There are periods when these waves carry larger amplitudes compared to other periods. A power spectral analysis of these amplitudes clearly shows the presence of a low frequency oscillation in time with a largest mode around 40 days. That period also coincides with a well know period in the atmosphere and in the ocean called the Madden Julian Oscillation (*MJO*).*

This paper also illustrates the existence of a spatial oscillation in strong earthquake occurrences on the western rim of the Pacific plate. These are like pendulum oscillation in the earthquake frequencies that swing north or south along the western rim at these periods. The spatial amplitude of the oscillation is nearly 10,000 km and occurs on an intraseasonal time scale of 20-60 days. A 34 year-long USGS *earthquake database was examined in this context; this roughly exhibited 69 swings of these oscillations. Spectral analysis supports the intraseasonal timescale, and also reveals higher frequencies on a 7-10 day time scale. These space-time oscillations of these pendulums like oscillation are similar to those of the* MJO. *Fluctuations in the length of day on this time scale are also connected to the* MJO. *Inasmuch as the atmospheric component of the* MJO *will torque the solid Earth through mountain stresses, we speculate the* MJO *and our proposed earthquake cycle may be connected. The closeness of these periods calls for future study.*"[22]

The *MJO* is the best evident phenomenon occurring with an intraseasonal (*~30-90 days*) variability in the tropical atmosphere. It is not a standing pattern (like the better-known *ENSO*). It is a traveling pattern that propagates eastwards at ~*4-10 m/sec*, moving above the warm parts of the Indian and Pacific Oceans. It is manifested as a sequence of regions of either enhanced or suppressed tropical rainfall. The wet phase of enhanced precipitation is followed by a dry phase with no thunderstorm activity, and every cycle lasts ~30-60 days. The *MJO* is therefore sometimes called the ~30-60-day oscillation, ~30-60-day wave, or intraseasonal oscillation.

MJO modulates *(i)* monsoon variability in the Asian-Australian sector, and also *(ii)* hurricane activity over the Atlantic sector, and *(iii)* weather over the Northern Hemisphere extratropics, *(iv)* ocean chlorophyll, and *(v)* total ozone concentration. It has connections with tropical cyclogenesis, and with *ENSO*.

That is, the Krishnamurti et al. (2009) study is not specifically concerned with seismic transmigration, rather it is focused on the search for a possible modulation of seismic activity by the atmospheric baric field. This effect is presently the object of investigation (see e.g. Panza et al., 2010). But additional studies

[22]This item reminds about the investigation carried out since several decades by Bruce Leybourne and co-workers, who attempt to infer the planetary correlation between tectonic and atmospheric phenomena.

and harder thinking is required.[23]

In any case, and independent of the comparative heuristic relevance of either one aforementioned logical perspective, one cannot compare on another *(i)* a rigorous "top-down" approach based on physical laws applied to a given model of the Earth, with *(ii)* the inferences got by means of some empirical hunch interpreted by a tentative physical model, with *(iii)* the evidence provided by a formal statistical analysis based on a mathematical rigorous handling of a database that ought to include all kinds of multidisciplinary precursor information (refer to the rigorous and intricate Keĭlis-Borok, Panza, Peresan et al. approach in terms of pattern recognition extensively mentioned in "paper I").

It must be stressed that every approach has its advantages and drawback, its pros and cons, and every conscience-driven Earth scientist must consider all evidences with the suitable warning about their possible physical significance and/or logical limits. In any case, one should refrain from considering either one approach "better" than any other. Every evidence must rather be critically taken into account, and everybody must refrain from presenting his approach as a paradigm. All inferences are to be considered, because different possible hunches – if correctly considered - can contribute to some better understanding of phenomena.

IV - Note that, in principle, also other transmigration investigations are likely to exist in the literature, although their reports are sporadic. In general, every paper has no direct concern about quoting other papers. Therefore, the list here given has no presumption for being exhaustive. It is only aimed to introduce the discussion dealing with the Italian peninsula which is carried out in section 3.

In this respect, a pertinent mention is to be given - always from a "top-down" perspective - about the serpentinization process, which is mentioned in "paper II". That is, water penetration through deep crustal fractures triggers a chemical reaction that implies a large volume expansion. The final result is just like an explosion that causes additional fracturing in the nearby crust. This fracturing favors additional water penetration through rocks, and additional serpentinization etc. The final effect is the propagation of phenomena like a domino play - that occurs preferentially along the comparably more fractured regions of the crust, i.e. along the areas that, according to plate tectonics, are identified with the so-called plate boundaries.

Note that, according to the more traditional geological schools, serpentinization is considered as an almost secondary curiosity, with no leading role such as envisaged above.

In reality the objective intensity of this effect can be measured, and also its actual role and relevance suitably checked. This investigation, however, was never carried out, as – according to the plate tectonic paradigm – this has always been unduly considered an unrealistic hypothesis.

A formal algorithm can be easily defined that provides with an objective result that can either give the expected evidence or disprove this hypothesis. Hence, this is a way to test the real physical implications of serpentinization, and also a way to estimate its propagation speed, which is presently unknown.

That is, this is much more than a simple and tentative empirically inferred transmigration phenomenon that ought to be observed and seemingly applied to some specific case histories. It is rather a way to infer some regular directional patterns of the teleconnection of seismic activity through different regions from the local- through the planetary-scale.

The algorithm can be briefly described as follows. Start from one given area suitably defined. That is, this area is not point-like. Rather, it has some physical extension. It ought to refer to some reasonably homogenous tectonic setting through a given area. Call this area the "pole position area". The algorithm will be briefly denoted as "pole-position algorithm", or "*ppa*".

[23]The control of atmospheric pressure on volcanic phenomena is a very old hypothesis, and it is even difficult to track back its first proposal. But, no final and systematic assessment seems to exist. Some evidence appears to be definitely in favor of this effect (see e.g. Gregori and Paparo, 2006).

Consider one given earthquake that strikes the pole-position area. Consider a global seismic catalogue, containing all earthquakes of magnitude larger than some pre-chosen threshold. Consider the time difference Δt between the given earthquake striking the pole-position area and every given earthquake of the catalogue that occur at any given location. Plot on a map, e.g., a circle with center at the epicenter of this location, and radius proportional to this Δt. Use a different color, depending on whether Δt is positive or negative.

Repeat this for every earthquake of the catalogue.

The final map shows whether there are tracks of teleconnection that propagate earthquakes on the planetary scale. The different color denoting either positive or negative Δt ought to show whether the earthquake that strikes at the pole-position area either preceded or followed earthquakes occurred in other parts of the Earth and along what teleconnection track. The evolution of the radii of the plotted circles denotes the propagation speed of the crustal stress along the track of seismic transmigration.

Unfortunately, as already mentioned, this conceptually simple and objective "*ppa*" analysis was never carried out, basically because its rationale cannot be consistent with the paradigm of plate tectonics.

Note that the serpentinization process plays a fundamental role in the global climate cycle, as the endogenous heat causes a de-hydration of the hydrated rocks that are the result of serpentinization. Thus the heated and newly de-hydrated rocks are again ready for serpentinization, etc. These details are outside the leading focus of the present paper.

The information inferred by this "*ppa*" can be reasonably expected to open some relevant unprecedented understanding of geodynamic phenomena.

Let us mention the planning of the present paper. The following sections can be summarized as follow: section 2 deals with some inference about some possible transmigration observed in the Italian peninsula, and section 3 deals with the evaluation of the size of the focal volumes of the associated seismic activity. Finally, Section 4 highlights some general conclusion.

It is shown how the three different perspectives of research – illustrated respectively in "paper I", in "paper II" and in the present "paper III" – are to be considered closely complementary one another. They deal, respectively, *(i)* with an *AE* monitoring and suitable interpretation of crustal stress propagation and diagnosis ("paper I"), *(ii)* with a correct "top-down" geodynamic interpretation ("paper II"), and *(iii)* with the hunches that can be inferred by the tentative empirical observation of seismic transmigration.

Summarizing the case history of this seismic crisis in Central Italy is treated like a pilot-experiment aimed to show how the seismic hazard can be managed while dealing with one given region.

In this respect, note, however, that in general every different region requires its specific approach and methodology, depending on its peculiar tectonic setting. This is much like every patient of a medical doctor who requires his personalized diagnosis and therapy.

Differently stated, every attempt appears unrealistic - and even ridiculous - to manage the seismic hazard by means of any pre-chosen one-sided "simple" or "synthetic" "magic" approach, based on one method alone, presented like a "miracle" way to deal with earthquakes.

Indeed, science is not made of certainties. Science is mostly made of unexplained phenomena, and of doubts about what is believed to be understood. It is profoundly incorrect to believe that science must give the "perfect" interpretation by which, e.g., the decision makers can operate at their best capability. In this respect, *it is often disquieting and disappointing to realize the profound ignorance among mass media, decision makers and legislators about the same significance of "science".*

2 - Seismic transmigration in the Italian region

According to the careful and detailed investigations and seismic monitoring systematically carried out by the geologists and seismologists of *INGV*, the Apennines are associated with a large set of distinct active faults that run approximately parallel one another. At different times they are activated in some seemingly erratic way. Hence, in general one can easily envisage what earthquakes occur along every given fault, while they are to be distinguished from others that involve a different active fault.

The northward trend in figure 4 and Table 1 of "paper I" (from the event with code A through the event with code O in Table 1) implies a span of *~25 km* run during *~71 day*, i.e. at a mean speed of the order of *~25/71=0.35 km/day* to be compared with the speed of the "domino effect", i.e. *10 cm/sec = 8.64 km/day* (see "paper I" and Gregori, 2013a).

In this same respect, the new series of earthquakes started on January 18th, 2017 is along the same fault system, though slightly south of it. That is, it is a rejuvenation of the seismic crisis, rather than an evolution of the August-October 2016 events. Hence, it is incorrect to consider this as a southward transmigration.

In this same respect, Mantovani et al. (2015) focused on a different empirical phenomenon. He noted "*the time pattern of major earthquakes that occurred at the main periAdriatic zones since AD 1400 (**Figure 2**)*". They tentatively stress that "*one could recognize a progressive northward migration of seismic crises, through the eastern (Northern Hellenides and Dinarides) and western (Apennines) boundaries of Adria, up to reach the northernmost boundary zones (Eastern Southern Alps and Northern Dinarides). The presumed migrating seismic sequences are tentatively evidenced by different colors (grey, orange, green, yellow and blue in **Figure 2**).*" In this figure, all events are grouped in segments ordered according to the time sequence. The segments are denoted by A, B, . . . , H in the inset of **Figure 2.**

But, a basic warning must be specified. Remind about the distinction between a "bottom-up" and a "top-down" approach, and between a "working hypothesis" and a "model", and also remind about a correct use of the term "proof". That is, if some observations are in agreement with a working hypothesis, it *cannot* be claimed that this is a "proof" of any "working hypothesis", because a proved working hypothesis is considered to be a "model". This basic methodological misunderstanding is very frequent, although it is completely misleading, and false, hence irresponsible.

Differently stated, this tentative empirical analysis of transmigration can be compared with no "top-down" hopefully rigorous geophysical approach ("paper II"), and/or with no rigorous statistical analysis carried out by a "pattern recognition", applied to the multidisciplinary information of any kind dealing with possible precursory phenomena (this is the aforementioned pattern recognition analysis mentioned in "paper I"). That is, every approach has its logical pros and cons and it must always be considered according to an understanding and realistic viewpoint.

Therefore, **Figure 2** is the tentative observational support for a guessed, possible, northward trend through the areas A, B, C… H indicated in the inset of **Figure 2**. Obviously, no evaluation is possible at all of the statistical significance of this tentative inference. You may believe that it is reliable or not, and nothing else. That is, this is just a simple vague hunch, although it is eventually physically important. The observational evidence is just expressed only by **Figure 2** and by its color code, including the classification of phenomena according to the scheme A, B, C, … This hunch can be either true or false. But, every conscience-driven scientist must consider it as a possibly reliable feature, and thus he has to investigate whether it can be related to the northward trend observed in figure 4 of "paper I".

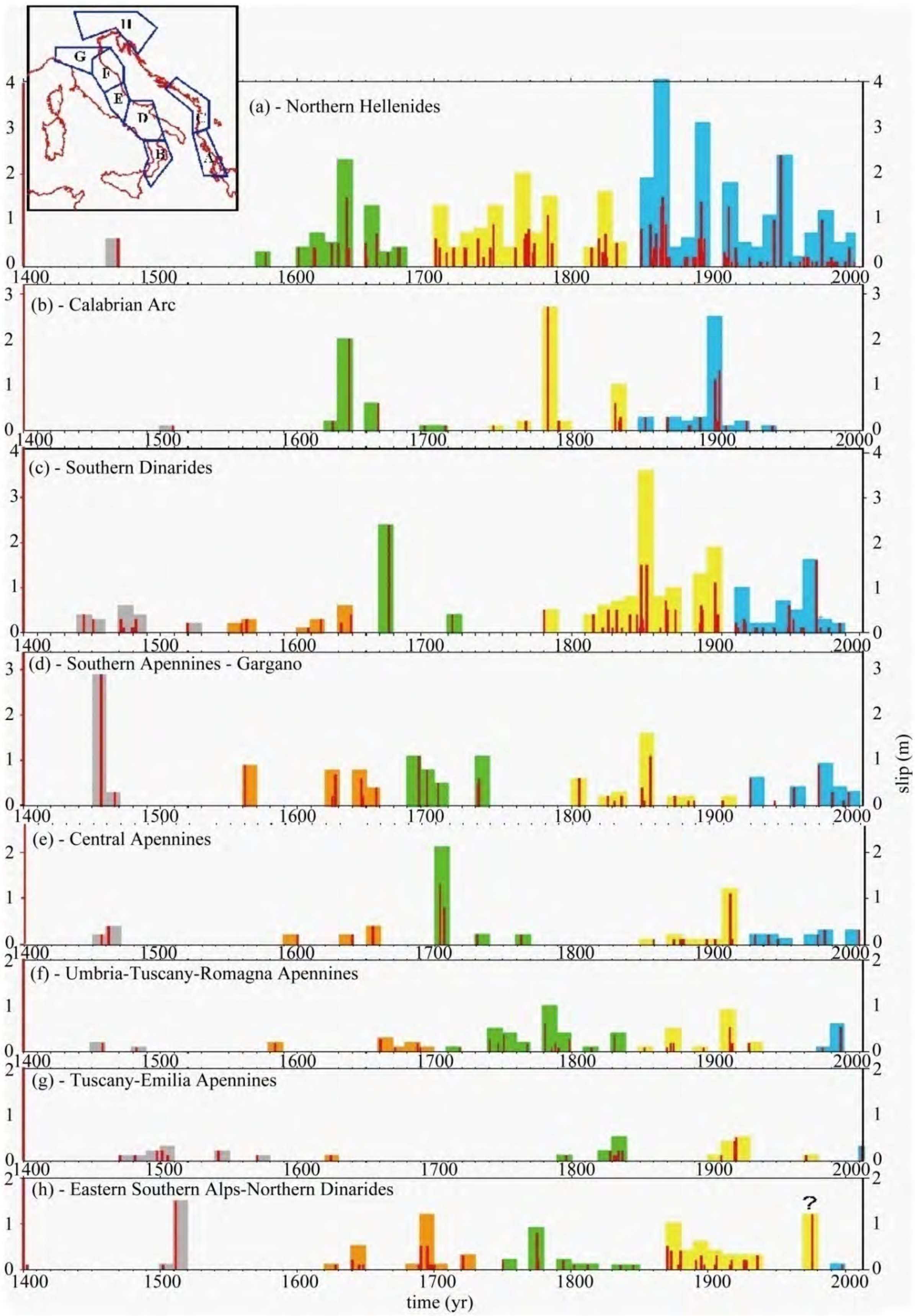

Figure 2 – "*Time patterns of seismic slip associated with major shallow (*h ≤ 30 km*) seismicity (*M ≥ 5.5*) in the main periAdriatic seismic zones since AD 1400. The geometries of the zones considered are shown in the inset. Red bars in the diagrams indicate the total seismic slip (meters) occurred during the related year, computed by the relation* $log_{10}\, u = -4.8 + 6.9\, M$, *where* u *is the average seismic slip on the fault (in meters) and* M *is the earthquake magnitude . . .Vertical boxes indicate the sum of seismic slips over decades. Colors tentatively evidence the seismic sequences during which major decoupling earthquakes have undergone a progressive migration from the southern to the northern periAdriatic zones . . .* " Figure and captions after Mantovani et al. (2015).

Note, the zigzag pattern A, B, . . . , H in the inset in **Figure 2**. It is along a path that displays a total length that is roughly of the order of, say, *~2000 km* and that - according to the green and yellow sequences in **Figure 2** - ought to be run during, say, *~160 years*, i.e. at a mean speed of, say, *~2000/160 = 12.5 km/year*, to be compared with the speed of the "domino effect" (Gregori, 2013a), i.e. *10 cm/sec = 3156 km/year*.

That is, these are totally different phenomena. In fact, the "domino effect" is a spontaneous self-triggered sequence of microcracks, where every event triggers a new event at its next boundary. In contrast, this Mantovani et al. seismic transmigration responds to some stress applied at the tectonic boundaries of the peninsula. Concerning this crucial point, see the geodynamic interpretation given in "paper II" (specifically figure 7).

Similarly, compared either to the ''domino effect'' or to the Mantovani et al. transmigration, also consider the different phenomenon with a speed *~0.35 km/day* that is the aforementioned northward propagation of earthquakes envisaged in figure 4 and Table 1 of "paper I" .

Note that Mantovani et al. (2015) strictly apply an exploratory analysis. Hence, they arbitrarily envisage and distinguish a few observational sequences. This is certainly a correct way to proceed in every phenomenological investigation. Their approach is "bottom-up" and, as already stressed - owing to the arbitrariness in recognizing these sequences - one can be concerned with their real physical significance. In any case, nothing happens by chance. Neither it is correct to consider a statistic between events that compose a set of physically non- uniform elements. The reliability of every inference has therefore to be evaluated *a posteriori* depending on the reasonability of its eventual subsequent confirmation. That is, this is a prerequisite before attempting to implement a given phenomenological inference into some tentative "top-down" interpretation. See section 3 on this crucial item.

Mantovani et al. (2015) state: "*thus, assuming that seismic activity in the periAdriatic zones is characterized by a systematic tendency to migrate from south to north, the evidence shown in **Figure 2** … would suggest that at present the probability of major earthquakes in the northern zones (Northern Apennines, Northern Dinarides and Eastern Southern Alps) is significantly higher than the one in the southern zones (Calabrian Arc and Southern Apennines). An intermediate probability may tentatively be assigned to the Central Apennines, where the seismic energy so far released during the ongoing sequence phase (i.e., Maiella 1933,* M = 6.0, 5.1*; Laga 1943* M = 5.8*; Gran Sasso 1950* M = 5.1, 5.7 *and L'Aquila 2009* M = 6.3*) is lower than the one released in previous sequences …*"

That is, since the apparent tendency is a northward migration of the seismic activity – and upon taking into account the time series of the past historical earthquakes in the Italian peninsula – they conclude that the future events ought to involve the Central Apennines rather than their southern range. In fact, the Amatrice/Norcia earthquake sequence in central Italy of August 2016-February 2017…. can be considered in the framework of this tentative inference. Note that this feature applies indistinctly to the aforementioned whole set of roughly parallel active faults that longitudinally cross through the Italian peninsula.

The Mantovani et al. (2015) interpretation, however, relies on the standard plate tectonics paradigm. A substantially different physical explanation is given in "paper II" in terms of a "top-down" viewpoint. But, in any case, the phenomenological observed northward trend of seismic activity seems to be a permanent feature through the peninsula.

For the sake of completeness, concerning transmigration phenomena, a latitudinal - although southward - trend is also reported dealing with geochemistry, i.e. with the K enrichment of basalt (Beccaluva et al., 1981). From north to south, the interested volcanic complexes[24] are: Vulcano Vulsino (close to Viterbo; dating since ~ *0.85 Ma* ago), Vulcano Vicano (close to the Lake of Vico; dating since ~ *0.8 Ma* ago), Vulcano Sabatino (slightly North of Rome; dating since ~ *0.7 Ma* ago), Vulcano Laziale (or Colli Albani, or in English Alban Hills, ~ *30 km* South of Rome; dating since ~ *0.7 Ma* ago), Vulcano Ernico (close to

[24]The dating values, which are here listed, are simply borrowed after Beccaluva et al. (1981), while no critical evaluation can be here given of every specific estimate, as we have no specific competence in mineralogy. For instance, concerning the Vulcano Rocca Monfina some previous authors report *~1.1 Ma* rather than ~ *0.65 Ma* which is quoted by Beccaluva et al. (1981). We are indebted to Roberto Mortari for this remark.

Frosinone; dating since $\sim 0.7\ Ma$ ago), and also the Vulcano Rocca Monfina (just behind the border of Latium with Campania, in the Province of Caserta; dating since $\sim 0.65\ Ma$ ago). That is, the total time span is $\sim 0.2\ Ma$, or - compared to all previously mentioned speeds - the mean southward speed of the K enrichment is extremely slow.

In this same respect, according to Wright (1971; reported also by Ollier and Clayton, 1981, p. 110), the K content of andesites across an island arc shows that the magma, which is originated from a comparatively deeper source underground, has a greater K_2O concentration.

Therefore, in the case of the aforementioned Beccaluva et al. (1981) Central Italy volcanic line, the different K enrichment ought (perhaps, see “paper II” for some geodynamic details referring to its figure 7) to be explained by the dynamics of the Italian peninsula while it moves (counterclockwise rotation) and it removes step-by-step the lithospheric loading - or “tap” - represented by its weight: thus, it progressively permits magma outpouring originated from a different depth. However, this explanation is speculative, and harder thinking is in any case required for its eventual confirmation or denial.

In any case, it appears at least reasonable to guess that the magma chemism could be determined, perhaps, by the local intensity of the endogenous energy that is likely to experience a violent gradient while moving from the Tyrrhenian Sea through the Apennines. In addition, note that this whole inference seems to be supported by the analogy with the isotopic chemism of ocean basalt. A hierarchy of *5* classes has been recognized for ocean basalt, depending on the primary energy supply. This hierarchy is also shown to be consistent with the variation of the bathymetry of the Indian Ocean ridge.[25]

Also note that - as already mentioned in “paper II” - Beccaluva et al. (1981) investigated the magmatic character and K/Ar ages of volcanics dredged from the southern Tyrrhenian Sea and from the Aeolian archipelago and its surrounding seamounts.

All these different items and observational features have to be explained.

3 - Seismic transmigration and an estimate of the seismic “focal volume”

Table 1 is a list of different transmigration phenomena that have been empirically observed by different authors who applied different approaches and viewpoints. The speeds mentioned in section 2 are included in **Table 1**, according to their respective discussion. But, for completeness sake, a mention is also given of a few additional investigations.

It should be emphasized that all these investigations share the common feature of being “bottom-up”, i.e. they are a “blind eye” phenomenological search for regularity inside every respective observational dataset. That is, they have no presumption to propose any physical process. Nobody ever gave any physical explanation of their findings other than, at most, some tentative guess.[26]

The three kinds of studies (by Blot-Choi, by Tsunoda, and by Vikulin et al., respectively) are here mentioned only in order to emphasize that several kinds of “bottom-up” - or “blind eye” - investigations can be attempted. These studies are a correct application of the exploratory analysis that sometimes provides with intriguing evidences, although they become heuristically useful only when they can be included into a framework of some tentative “top-down” model. This is an early step of the confirmatory analysis (Tukey, 1977).

[25]It is impossible to quote here all the needed literature dealing with the comparatively recently-born discipline of “chemical geodynamics”. An extensive account of this item is given in the aforementioned 8-volume set. Only some mentions are given in Gregori and Crisci (1995).

[26]The full physical discussion of the transmigration processes mentioned in section 2 is given in the aforementioned 8-volume set.

Table 1 – Seismic transmigrations

Speed	*Identification name*	*Ref.*	*Comment*
8.64 km/day	"Domino effect"	Gregori (2013a)	Several experiments from continental size, through a bar of a few tens centimeters
1 km/day	Crustal substorms in Central Italy	"paper I"	*HF AE* crustal substorm precedes *LF AE* crustal substorm
0.35 km/day northward	Central Italy 2016 seismic sequence	"paper I"	See Tables 1 and 2 of "paper I"
12.5 km/year northward	Italian peninsula and Balkans	Mantovani et al. (2015)	See **Figure 2**
extremely slow, and southward	Volcanism in Central Italy	Beccaluva et al. (1981)	K enrichment
? (never measured)	Serpentinization, every scale, including continental and/or planetary effects	Judd and Hovland (2007) and references therein	See section 2 concerning the discussion of the "*ppa*" algorithm
varying with depth [*2.6 km/day* at *600 km, 0.9 km/day* at *200 km, 0.5 km/day* at *100 km,* and *0.15 km/day* at *33 km*]	Blot-Choi "*Blot's migration law*" typical of island arc environment	Blot et al. (2003), Blot and Choi (2004, 2006a, 2007), Blot (2004, 2005), Choi (2010, 2010a, 2011b, 2012a), Pesicek et al. (2010) and references therein	Explained by considering the timing of the rupture process of the lithospheric slab while it sinks into a trench. See text
different values depending on phenomenon (seismic or volcanic) and on the region	Tsunoda planetary scale and continental scale analysis	Tsunoda (2009a, 2010, 2010a), Tsunoda et al. (2015), Choi (2014f, 2014g), Choi et al. (2014, 2014a) and references therein	Explained by the *WMT* rationale, in terms of superswells, and lithospheric sliding on their slope. See text
See text	Vikulin et al. Planetary seismic and volcanic catalogues	Vikulin et al. (2012) and references therein	Formal statistical analysis

Therefore, the next target here is to show how these different apparent transmigration-speeds ought to be explained.

In this respect, consider that the literature concerning transmigration phenomena either deals with the mere phenomenological observation, or at most it contains some tentative and *ad hoc* intuitive interpretation that very often, as a standard, relies on the plate tectonics paradigm.

But, as explained in "paper II", the plate tectonics model seems to be *ad hoc*, oversimplifying, not proven, or better disproved by observations. A model rather holds when it can be proven, while it should be critically re-considered - and eventually also rejected whenever it relies on some *ad hoc* assumption.

Let us consider the case history of crustal substorms in Central Italy - as it is extensively discussed in "paper I" - and let us consider these phenomena according to the "domino effect" viewpoint. On the occasion of every given earthquake, one given active fault has to be considered that caused it, altogether with its associated generalized focal volume (*gfv*). These items are discussed in detail in "paper I". The *gvf* can be approximately represented by an elongated prism of some cross-section and length, lying along the fault.

Suppose that an applied stress causes a starting micro crack at a terminal of this *gfv*. Note that, according to the argument of figure 7 of "paper II", the southern terminal ought to be this starting point. The micro crack propagates through the *gfv* at the typical speed of the "domino effect", i.e. *~8.64 km/day*. Its propagation is detected by means of *HF AE* records.

However, a rupture of the *gfv* can occur only whenever the micro cracks start to coalesce and generate wider microcracks: only at this stage the system releases *LF AE*.

But, as long as the *gfv* has a sufficient cross-section, its mechanical resistance is strengthened by its large cross-section. In fact, new small micro cracks are eventually formed across it whole cross-section, while the solid object opposes its reaction to the applied external force. As long as the mechanical resistance is effective, no relevant amount of coalescence occurs.

For clarity purpose, imagine e.g. to attempt to bend and stress separately two steel bars of identical length but of different cross-section: the bar with greater cross-section can be bent only by a much larger stress applied during some suitable time interval.

Therefore, the micro crack formerly propagates through the *gfv*. This is the initial stage of the response of the system to the external applied force that, thus, weakens its mechanical performance through its whole volume, while mainly *HF AE* are released.

But, when the whole volume has been almost uniformly filled-up with "flaw domains" associated to a given observed *HF AE*, its "flaw domains" start to coalesce into larger "flaw domains". Only at this stage the system begins to release a relevant amount of *LF AE* and an important ageing process occurs. This is just the same rationale outlined in figure 10 of "paper I".

Consider the ratio of the two measured speeds that are listed in **Table 1**, i.e. ~[*8.64 (km/day) / 1 (km/day)*] ~ *8.64*. During one day the crustal substorm, at its typical speed of *~1 km/day*, progresses by *~1 km* along the linear extension of the *gfv*. But, during the same time interval, i.e. during *1 day*, owing to the "domino effect" the micro crack propagates through a slice - of thickness *1 km* and volume ~$8.64\ km^2$ - of the cross-section perpendicular to the linear extension of the *gfv*.

Hence, it can be stated that the order of magnitude of the linear dimension of the cross-section of the *gfv* can be indicatively expressed as $\sqrt{8.64}$ *km*, which seems to be physically reasonable. Differently stated the cross-section of the *gfv* is ~$9\ km^2$. That is, according to the lexicon of seismologists, this is the size of the cross-section of the crustal volume located along the active fault that originated the earthquake, or this is the size of the cross-section of the "focal volume" of the earthquake. Not that these are mean values along the fault, while locally these values can be different.

As a next step, consider the whole list of earthquakes that occurred in the area shown in figure 4 of "paper I", including both the events that are indicated in figure 4 of "paper I" and also all other less strong earthquakes that occurred during the same time interval and that are not shown in figure 4 of "paper I".

Define a *gfv* of the *whole* natural system - which is involved by *all* these events – by means of the sum of all the aforementioned *gfv*, everyone associated *(i)* to one of the faults that caused a really observed earthquake or *(ii)* to one of the faults that could potentially be activated and thus cause an earthquake, even in the case that they did not originate a measured earthquake.

That is, this definition of *gfv* is some kind of "thermodynamic" or "calorimetric" concept, as it refers to the ensemble of *all* possible active faults inside a given area of a linear size of, say, a few to several ten kilometers.

The same argument can thus be considered that was applied to one active fault alone. It is thus concluded that the observed seismic crisis, which was distributed along *71 days* while it ran along *~25 km*, is represented by a volume of linear size *~25 km* with a cross-section of ~[*8.64 km/day / 0.35 km/day*]~$24.7\ km^2$. Or the linear size of this cross-section of this *gfv* is of the order of *~5 km*, which seems physically reasonable.

Then, consider the seismic events that led Mantovani et al. (2015) to the inference related to **Figure 2**, and consider the inset of **Figure 2** with the sequence from event A through event H, thus spanning an apparent track of *~2000 km* length run during *~160 years*. Define the *gfv* of the physical system composed of *all* active faults that - along this track from event A through event H - could be potentially activated and originate an eventual earthquake. Note that this physical system includes the whole Italian peninsula plus a fraction of the Balkans peninsula.

Apply the same aforementioned argument and state that the observed Mantovani et al. sequence can be illustrated by some kind of equivalent *gfv* of *~2000 km* linear extension and cross section of ~[*8.64 km/day / 12.5 km/year*] ~[*8.64 km/day / 0.0342 km/day*]~*252.6* km^2. Or the linear size of this cross-section is of the order of *~16 km*. **Table 2** is a summary of the three estimates.

Table 2 – Comparing three "generalized focal volumes"

Kind of transmigration	*Apparent speed*	*Length of the* gfv	*Cross-section of the* gfv	*Linear size of the cross-section*
Crustal substorms in Central Italy (figures 8 and 9 of "paper I")	*1 km/day*	*~130 km*	*~8.64* km^2	*~3 km*
Central Italy 2016 sequence (figure 4 of "paper I")	*0.35 km/day* northward	*~25 km*	*~24.7* km^2	*~5 km*
Italian peninsula and Balkans (**Figure 2**)	*12.5 km/year* northward	*~2000 km*	*~252.6* km^2	*~16 km*

Note that this inference is derived as a byproduct of the general rationale concerned with the general interpretation of *AE* released by a solid material, consistently with several other applications, and similarly to the empirical inference of the "domino effect" (Gregori, 2013a).

That is, a physical result is tentatively guessed, and its reliability is finally checked by its final result. If the inferred physical quantities sound reasonable, it is concluded that the guess is an approximately reliable tool suited to evaluate order-of-magnitude estimates. If the results appear unbelievable, the guess is not suited to describe phenomena, or even their rough order-of-magnitude. Hence, it has to be rebutted.

In the present case, the *gfv* cross sections listed in **Table 2** appear of the expected order of magnitude. Hence, this is an additional confirmation of the reliability of the whole *AE* rationale that was already confirmed by several other different and independent evidences.

However, one can always be reasonably concerned with the amount of speculation and intuitive modeling that is required in order to get these inferences. Indeed, even though they appear reasonable, one should always be understating and prudential.

On the other hand, every time that one tries to put a "top-down" framework into a "bottom-up" evidence, it is unavoidable to supplement the insufficient available observational information by appealing to some speculation. As it is well known, several famous physicists claimed that a real physicist knows the solution of his equations before solving them. In any case, as a standard this is the best-known way to proceed in science, as every speculated interpretation is suggestive of some unprecedented measurements aimed either to confirm or to deny it.

In the present case history, we should need for an array of *AE* stations spanning the whole Italian peninsula and also part of the Balkans peninsula, in order to monitor the time sequence of the different events related to crustal stress propagation.

That is, the model which is here envisaged is certainly speculative, although it appears reasonable. But, in science speculation can never be overcome by other speculation: there is need for new unprecedented physical observation. Indeed, the speculation which is here envisaged can be formally checked whenever new measurements, i.e. *AE* records, will be eventually available. This will be the final confirmatory analysis.

Differently stated - and likewise when dealing with several other issues - a permanent monitoring by means of a suitable *AE* array is fundamental in order to get rid of speculation and thus to infer a final assessment.

Consider that an earthquake is a holistic and planetary phenomenon. An endless number of different phenomena exists, such that every phenomenon is a precursor that we can - or we cannot - detect only depending on the availability of a suitable monitoring array. In addition, no physical reason requires that the identical precursor is observed in different case histories, neither that - when it is eventually observed - its time advance is always the same. Much in the same way, a medical doctor knows very well that every patient has a given response-time and reaction that is very different compared to all other patients.

In this respect, consider the basic difference between *AE* monitoring and all other kinds of precursors.

AE monitoring is directly focused on the *local* stress of the crust, on its evolution, on the ageing and loss of performance of a fault. That is, its information is *not* directly concerned with the occurrence - or not - of an earthquake. Rather, it deals with a *diagnosis* of the state and evolution of the mechanical response of the crust when an external perturbation is applied.

In contrast, a precursor is a phenomenon that, owing to its same definition, must be correlated with a forthcoming seismic event, while *AE* monitoring is directly concerned with the "health" of the local crust independent of the forthcoming earthquake. In this way, *AE* provides with information much before the degradation of the mechanical performance that finally can eventually lead to a catastrophe.

In addition, a permanent monitoring by an *AE* array can monitor in real time the crustal stress propagation. By this, it can foresee when a crustal stress perturbation is going to cross through a given area, where it is known that the mechanical performance is eventually already weak of the crust and of its faults.

Note the difference between issuing a certain "prediction" - which in principle will never be possible - and diagnosing the "health" of the local crustal features, which is a sound physically reliable information.

That is, the perspective is not to search for a "prediction" of a seismic catastrophe, rather to assess when and where the crust is eventually ready of yield and to originate a possible destructive catastrophe.

4 - **Conclusion**

The seismic crisis in Central Italy was started in August 2016 and it is still in progress. Central Italy is an effective natural laboratory suited to carry out a test of geodynamic models. The final target is to manage and mitigate the seismic risk. *AE* records seem to be a very effective diagnostic tool suited to provide with some unprecedented and detailed monitoring of the natural system and of its state *before* the occurrence of a catastrophe, i.e. *before* its irreversible evolution.

Remind about the 4-level approach mentioned in "paper I".

"Paper I" is focused on levels 2 and 3, and it shows its twofold perspective. On the one hand, the timing can be monitored of phenomena, from the propagation of crustal stress, from the planetary scale through local phenomena, including an interpretation of different seismic transmigration phenomena. On the other, the ageing and loss of performance of the local crustal features and faults can be diagnosed in real time.

"Paper II" shows that a correct geodynamic "top-down" approach is strictly needed in order to get a sound interpretation of natural phenomena, and also in order to get rid of unproven arbitrary "generally agreed" paradigms.

The present "paper III" shows how transmigration phenomena can provide with some empirical phenomenological evidence that can be tentatively integrated into a physical "top-down" physical interpretation.

In any case, it appears that the availability of a suitable array of *AE* stations is a strictly crucial prerequisite in order to get objective physical inferences, and to get rid of the need for speculation while attempting to construct a "top-down" interpretation.

Differently stated, if we want to manage on a sound objective basis the seismic hazard, we do need for unprecedented observational information. In this respect, *AE* records seem to be a feasible candidate for this substantial improvement of our concrete operative capabilities.

Note that every other rigorous attempt to manage observational data - such as e.g. the Keĭlis-Borok, Panza, Peresan et al. analysis by means of pattern recognition (see "paper I") - is a potential source of reliable physical information. In this respect, note that it is very important to afford to recognize what is objectively contained inside observations, and what is rather a consequence of our arbitrary, implicit, even though often reasonable and/or unconscious, assumptions.

In any case, a synergy of the different truly reliable inferences and rigorous methods can help to get rid of the seismic hazard mitigation and management.

The present three-paper set deals with a whole approach that seems to be the realistic way to manage this dramatic and disquieting concern.

In contrast, all searches for some "magic" phenomena that should be "certain" and "highly reliable" "red alert" precursors, etc. - likewise every "blind eye" attempt to search for some "simple" "magic" and reliable "universal" precursor or method - appears naïve and basically physically hopeless.

Acknowledgements – We feel deeply indebted to Prof. Alfredo Raponi, professional architect and renown painter, and to his wife Prof. Anna Maria Vigo, as for several years they hosted our *AE* station - and also gave operative facilities - in the basement of their house at Capodacqua di Foligno, at the site named Orchi. We could exploit our investigations only due to their generous and very long-lasting unselfish help. We are very glad to warmly acknowledge their cooperation. We are also deeply indebted to Prof. Alberto Incoronato, Roberto Mortari and Giuliano F. Panza, and to Dr. Franco Bonavia and Bruce Leybourne, for their accurate reading and commenting on a previous preliminary draft from which the present set of three papers was derived. Their feedback resulted very important for us in order to focus on items that required a better specific and more detailed explanation. This improved the clarity of our papers, although we have full responsibility for their scientific content.

References

Beccaluva, L., Gabbianelli, G., Lucchini, F., Rossi, P.L., Savelli, C. and Zeda, O., 981. Magmatic character and K/Ar ages of volcanics dredged from the Eolian seamounts (Tyrrhenian Sea). In Wezel (1981), 361-368.

Blot, C. and Choi, D.R., 2004. Recent devastating earthquakes in Japan and Indonesia viewed from the seismic energy transmigration concept. *New Conc. Global Tect., Newlett*., (33), 3-12.

Blot, C. and Choi, D.R., 2006a. The great southern Java earthquake on July 17, 2006 and its tectonic perspective, *New Conc. Global Tect., Newlett*., (40), 19-26.

Blot, C. and D. R. Choi, 2007. The great September 12, 2007 southern Sumatra earthquake, as predicted by the seismic energy transmigration concept – Part I. *New Conc. Global Tect., Newlett*., (44), 38-42.

Blot, C., 2004. Volcanic eruptions predicted by the energy transmigration phenomenon - A case of Mt. Stromboli Volcano, Italy, *New Conc. Global Tect., Newlett*., (31), 10-14.

Blot, C., 2005. On the recent Sumatrian earthquakes and their forerunners, *New Conc. Global Tect., Newlett*., (35), 3-7.

Blot, C., Choi, D.R. and Grover, J.C., 2003. Energy transmigration from deep to shallow earthquakes: a phenomenon applied to Japan - Toward scientific earthquake prediction. *New Conc. Global Tect., Newlett*., (29), 3-16.

Choi, D. R., John Casey, Lev A. Maslov, and Fumio Tsunoda, 2014a. Global increase in seismic and magmatic activities since 1990 and their relation to solar cycles, *New Conc. Global Tect., J*., **2**, (2), 82-83. *The Global Climate Status Report (GCSR)*, June 2014, p. 7-19. www.spaceandscience.net/id73.html.

Choi, D.R., 2010. Global seismic synchronicity, *New Conc. Global Tect., Newslett*., (55), 66-73.

Choi, D.R., 2010a. The January 2010 Haiti seismic disaster viewed from the perspective of the energy transmigration concept and block tectonics. *New Conc. Global Tect., Newlett*., (54), 36-44.

Choi, D.R., 2011b. Geological analysis of the great East Japan earthquake in March 2011, *New Conc. Global Tect., Newlett*., (59), 55-68.

Choi, D.R., 2012a. Geological structure which controlled the gigantic 11 April 2012 northeastern Indian Ocean earthquakes. *New Conc. Global Tect., Newlett*., (63), 72-75.

Choi, D.R., 2014f. Seismo-volcanic energy propagation trends in Central America and their relationship to solar cycles. *New Conc. Global Tect., J*., **2**, (3), 19-28.

Choi, D.R., 2014g. Seismo-volcanic energy flow observed in the 16 March 2014 M6.7 earthquake off Tarapaca, Chile. *New Conc. Global Tect., J*., **2**, (1), 61-65.

Choi, D.R., Fumio Tsunoda, and Leo Maslov, 2014. Seismo-volcanic energy propagation trends in the Aleutian Islands and North America. *New Conc. Global Tect., J*., **2**, (2), 13-22.

Gass, I.G., Smith, P.J. and Wilson, J.B. (eds.), 1971. *Understanding the Earth*. Artemis Press, Sussex.

Gregori, G.P. and Paparo, G., 2006. The Stromboli crisis of 28÷30 December 2002. *Acta Geod. Geophys. Hung*., **41**, (2), 273-287.

Gregori, G.P., 2013a. Space-time constraints on earthquake predictability - A 10 cm/sec "domino effect" typical of every fracture phenomenon. *New Conc. Global Tect., J.*, **1**, (2), 23-39.
Gregori, G.P., 2014. Climate and the atmospheric electrical circuit: the electromagnetic coupling between solar wind and Earth. *New Concepts Global Tect. Journal*, **2**, (1), 99-112.
Gregori, G.P., 2015b. Anthropic global warming, *New Conc. Global Tect., J.*, **3**, (4), 544-560.
Gregori, G.P., and G.M. Crisci, 1995. The isotopic chemistry of basalts vs. melting depth. Geomagnetic correlations and a proposal for an explanation, (abstract 01875498), *1995 IUGG General Assembly*, Boulder, Co.
Gregori, G.P., Paparo, G., Poscolieri, M., Rafanelli, C., Ventrice, G., Garilli, G., Imperatori,L., Lo Castro, F. and Zimatore, G., 2016. The seismic sequence in Central Italy (August-November 2016) - AE monitoring and analysis, *New Conc. Global Tect. J.,* **4**, (4), 637-663.
Judd, A.G. and Hovland, M. 2007. *Submarine fluid flow, the impact on geology, biology, and the marine environment.* 475p., Cambridge University Press.
Krishnamurti, T.N., Krishnamurti, R., Sagadevan, A.D., Chakraborty, A., Dewar, W.K., Clayson, C.A. and Tull, J.F., 2009, Space-time structures of earthquakes, *Meteor. Atmos. Phys*., **105**, (1/2), 69-83; doi: 10.1007/s00703-009-0034-7.
Mantovani, E., Viti, M., Babbucci, D., Tamburelli, C., Cenni, N., Baglione, M. and D'Intinosante, V., 2015. Present tectonic setting and spatio-temporal distribution of seismicity in the Apennine belt. *Int. J. Geosci*., **6**, 429-454; http://dx.doi.org/10.4236/ijg.2015.64034.
Ollier, C.D., and Calyton, K.M., 1981. *Tectonics and landforms*, 324p., Longman Publishing Group.
Panza, G.F., Peresan, A. and Zuccolo, E., 2010. Climatic modulation of seismicity in the Alpine–Himalayan mountain ranges. *Terra Nova*, **23**, (1), 19–25; doi: 10.1111/j.1365-3121.2010.00976.x.
Pesicek, J.D., Thurber, C.H., Zhang, H., DeShon, H.R., Engdahl, E.R. and Widiyantoro, S., 2010. Teleseismic double-difference relocation of earthquakes along the Sumatra-Andaman subduction zone using a 3-D model. *J. Geophys. Res., Solid Earth*, **115**, (B10); doi: 10.1029/2010JB007443.
Tsunoda, F., 2009a. Habits of earthquakes – Part 1: Mechanisms of earthquakes and lateral thermal seismic energy transmigration. *New Conc. Global Tect., Newlett*., (53), 38-46.
Tsunoda, F., 2010. Habits of earthquakes – Part 2: Earthquakes corridors in East Asia, *New Conc. Global Tect., Newlett*., (54), 45-56.
Tsunoda, F., 2010a. Habits of earthquakes – Part 3: Earthquakes in the Japanese Islands. *New Conc. Global Tect., Newlett*., (55), 35-65.
Tsunoda, F., Kawabe, T., Kubota, Y., Hayakawa, M. and Choi, D.R., 2015. Tendency of volcano-seismic activity developed in the central part of the Honshu arc. *New Conc. Global Tect*., **3**, (1), 34-42.
Tukey, J.W., 1977. *Exploratory data analysis*. 688p., Addison-Wesley Publ. Co., Reading. Massachusetts, etc.
Vikulin, A.V., Akmanova, D.R., Vikulina, S.A. and Dolgaya, A.A., 2012. Migration of seismic and volcanic activity as display of wave geodynamic process, *New Conc. Global Tect., Newlett*., (64), 94-110. [with minor modifications after *Geodyn. Tectonophys*., **3**, 1-18, 2012].
Wezel, F.C. (ed.), 1981. *Sedimentary basins of Mediterranean margins*. Tecnoprint, Bologna.
Wright, J.B., 1971. Volcanism and the Earth's crust. In *Gass* et al. (1971), 301-313.

Authors:
Giovanni P. Gregori[(a)(b)(c)], giovanni.gregori@idasc.cnr.it,
Gabriele Paparo[(a)], gabrielepaparo.ing@gmail.com,
Maurizio Poscolieri[(a)], maurizio.poscolieri@idasc.cnr.it,
Claudio Rafanelli[(a)], Claudio.Rafanelli@idasc.cnr.it,
Giuliano Ventrice[(d)], info@pmesrl.eu,
Gianpaolo Garilli[(a)], gianpaolo.garilli@idasc.cnr.it,
Luca Imperatori[(a)], luca.imperatori@idasc.cnr.it,
Fabio Lo Castro[(a)], fabio.locastro@idasc.cnr.it, and
Giovanna Zimatore[(a)], giovanna.zimatore@uniroma1.it

Addendum:

After the submission of this "paper III", a new series of earthquakes was reported hitting a wider region.

Table S1 (data credit *INGV*) is a list of 12 events with magnitude M≥3 - which are here denoted by our code Ea, Eb, Ec, …, El, respectively - that hit a larger region, north of the Central Italy area that was involved in the seismic crisis.

Other 5 events are included in **Table S1** - denoted by our code G1, G2, … G5, respectively - that hit Central Italy with magnitude M≥5 during this whole long-lasting seismic crisis.

The 12 events Ea, Eb, Ec, …, El with M≥3 are shown in the map of **Figure S1**. The 5 events with M≥5 are south of this map.

Even though these 12 events had limited magnitude and were not destructive, they permit to recognize two impulses of northward seismic transmigration.

The determination of their propagation speed can be, however, only approximate, due to the indicative character of the information provided both by epicenter location, and by their timing, because every single "event" ought rather to be considered as one element of a cloud of different earthquakes.

Three events with M≥3 are shown as red circles in **Figure S1**. They are denoted in **Table S1** by the codes Ea, Eb, Ec, respectively. They display a regular northward transmigration that is likely to have been started in Central Italy, on October 30, 2016.

Apply the same argument of **Table 2** of "paper III" (the present paper). The distance between Central Italy and the code Ec event is, say, *~500 km*, and the time elapsed is, say, *~44 days*. This seemingly implies a speed of *~ 11.4 km/day*. Hence, this can be interpreted in terms of some equivalent *gfv* of *~500 km* linear extension and cross section ~[*8.64 km/day / 11.4 km/day*] *~0.8 km^2*. Or the linear size of its cross-section is of the order of *~1 km*.

The remaining events of **Table S1** - denoted by codes Ed, Ee, … El and represented by blue circles in **Figure S1** - envisage another northward seismic transmigration, as shown by **Figure S2**. The distance between event Ed and event El is, say, *~400 km*, and the time elapsed is, say, *~127 days*. This seemingly implies a speed of *~ 3.15 km/day*. Hence, this can be interpreted by an equivalent *gfv* of *~400 km* linear extension and cross section of ~[*8.64 km/day / 3.15 km/day*] *~2.7 km^2*. Or the linear size of its cross-section is of the order of *~1.7 km*.

Note that, if it is speculated that this second transmigration episode was started by the event denoted by code G3 or G4 in **Table S1**, the distance between Central Italy (event of August 24, 2016) and event El is, say, *~550 km*, and the time elapsed is, say, *~131 days*. This seemingly implies a speed of *~ 4.2 km/day*. Hence, this can be interpreted in terms of an equivalent *gfv* of *~550 km* linear extension and cross section of ~[*8.64 km/day / 4.2 km/day*] *~2.1 km^2*. Or the linear size of this cross-section is of the order of *~1.4 km*.

These estimates are to be compared with the analogous values listed in **Table 2** of "paper III" (the present paper).

Note that the larger (smaller) is the mean cross-section of the *gfv*, the stronger (weaker) are the earthquakes that are involved.

The seismic crisis in this larger region is evidently in progress.

If the interpretation which is here proposed is correct, the resulting scenario envisages a discontinuous series of successive impulses of crustal stress - seemingly originated by the westward rift of Eurasia according to the mechanism envisaged in figure 7 of "paper II". These impulses are then propagated northward. Only an array of *AE* stations can prove or disprove this model.

Table S1 – Five earthquakes (M≥5) in the Central Italy seismic-crisis area, and twelve earthquakes (M≥3) north of it

Code	#Event ID	Date	Time	Julian time (+ 2457000.)	Lat.°N	Lon.°E	Depth (km)	Author (INGV)	Mag. type	Mag.	Location name (Prov.)
G1	7073641	**2016-08-24**	01:36:32.00	624.57	42.6983	13.2335	8.1	BULL.	Mw	6.0	Rieti
G2	7076161	08-24	02:33:28.89	624.61	42.7922	13.1507	8.0	BULL.	Mw	5.4	Perugia
G3	8663031	10-26	17:10:36.34	688.22	42.8802	13.1275	8.7	BULL.	Mw	5.4	Macerata
Ea	7588601	09-02	17:01:47.05	634.21	44.4975	9.6002	7.3	SURVEY	ML	3.1	Parma
Eb	7880681	09-10	15:13:52.87	642.13	45.4968	9.6577	31.1	SURVEY	ML	3.3	Bergamo
Ec	8400771	10-07	07:27:07.13	668.81	46.5365	9.5392	10.3	SURVEY	ML	3.5	Swiss border
G4	8669321	10-26	19:18:05.85	688.30	42.9087	13.1288	7.5	BULL.	Mw	5.9	Macerata
G5	8863681	10-30	06:40:17.36	691.78	42.8322	13.1107	9.2	BULL.	Mw	6.5	Perugia
Ed	8877961	10-30	10:49:43.34	691.95	44.1418	12.2677	20.7	BULL.	ML	3.6	Forlì-Cesena
Ee	10298211	11-21	03:05:11.77	713.63	44.4343	9.7933	7.9	SURVEY	ML	3.2	Parma
Ef	10299341	11-21	03:33:52.73	713.65	44.4382	9.7967	7.5	SURVEY	ML	3.1	Parma
Eg	10320361	11-21	12:16:01.08	714.01	44.2770	10.6868	9.6	SURVEY	ML	3.0	Modena
Eh	10793661	11-30	05:52:55.56	722.75	44.7732	10.6738	25.6	SURVEY	ML	3.5	Reggio Emilia
Ei	11272441	12-09	07:21:50.17	731.81	44.3298	10.5002	7.6	SURVEY	ML	4.0	Reggio Emilia
Ej	11845521	12-22	01:34:42.83	744.57	45.0652	11.2013	5.0	SURVEY	ML	3.0	Rovigo
Ek	13435551	**2017-**02-09	08:14:08.31	793.84	45.7815	11.1588	11.3	SURVEY	ML	3.6	Trento
El	14014761	03-06	20:12:06.79	819.34	46.9157	8.9308	3.2	SURVEY	Mw	4.0	Switzerland

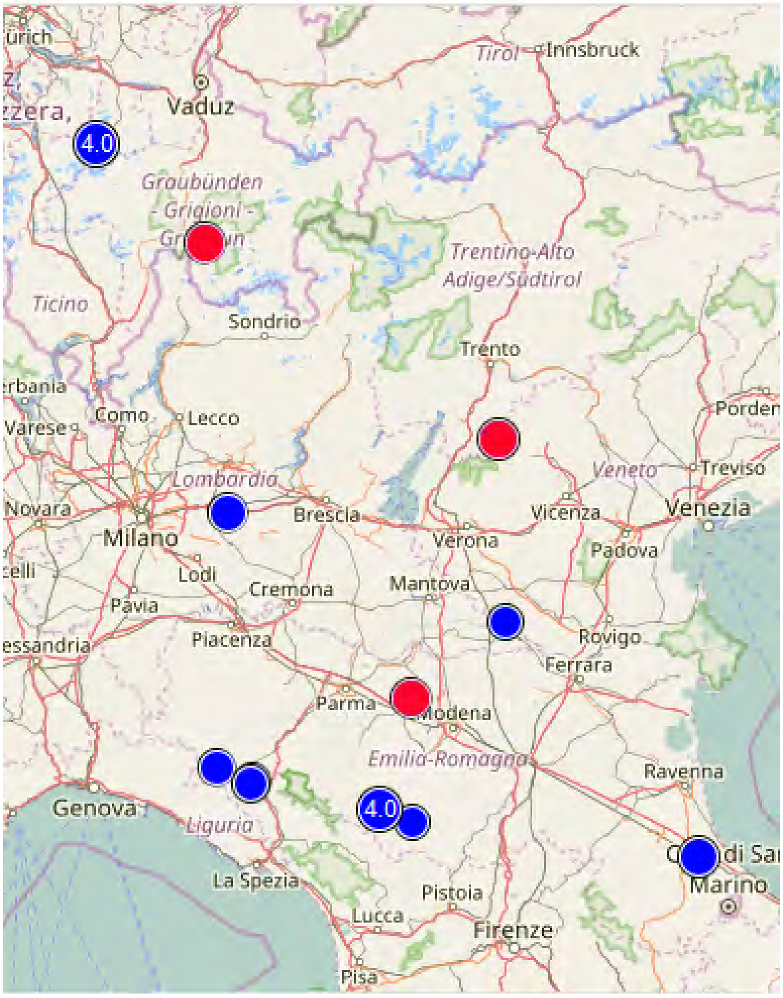

Figure S1 – Two episodes of seismic transmigration, started from Central Italy, are shown by different colors. The trigger of one episode occurred on October 26, or 30, 2016, followed by the northward migrating sequence that is here shown by red dots. The other episode, triggered on August 24, 2016, propagated northward (blue dots) as shown in detail by **Figure S2**. See text.

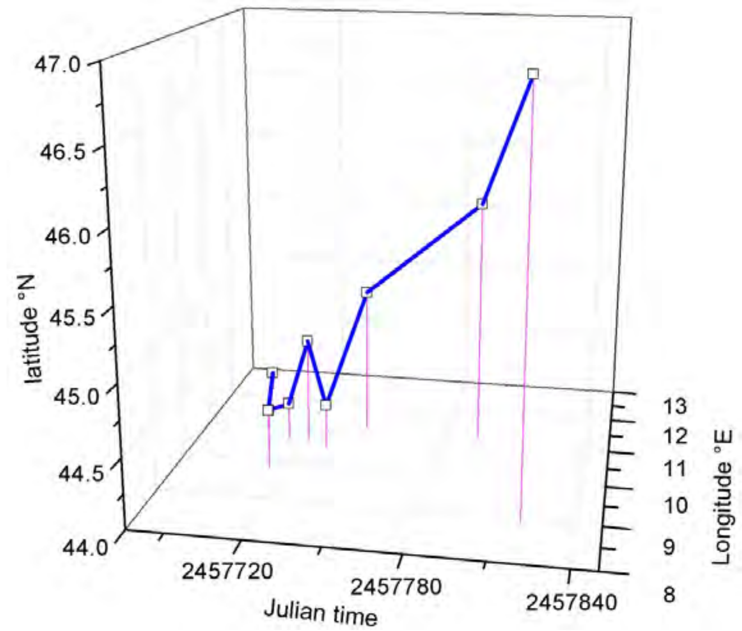

Figure S2 – This transmigration episode is clearly shown by the events, denoted by code Ed, Ee, …, El in **Table S1**, that are shown by blue circles in **Figure S1** and that are represented in this 3D plot. See text.

New planetology and geology: tectonic identity and principal difference of terrestrial oceans and lunar basins

Gennady G. Kochemasov
Institute of ore deposits, petrography, mineralogy and geochemistry of the Russian Academy of Sciences
35 Staromonetny, 119017 Moscow. kochem.36@mail.ru

Abstract: "Orbits make structures" – a main point of the new wave planetology based on one important property of the Keplerian elliptical planetary orbits. The ellipticity implies periodical changes of accelerations and, thus, orbital forces structuring cosmic bodies. The Earth and the Moon sharing the same circumsolar orbit have similar main structural features. Among them there are terrestrial Oceans and lunar Basins. The most obvious are two tectonic triads: Pacific Ocean – Malay Archipelago – Indian Ocean on Earth and Procellarum Basin – Mare Orientale – SPA Basin on the Moon (Figs. 1-3). The planetary depressions of both bodies are covered with basalts, but basaltic effusions are drastically different in age: the AR on Moon and Mz-Cz on Earth. These ages well correlate with the body masses. The more massive and inert Earth has heated and melted mantle much later (The Newton's law of inertia). Energy of movement transfers to the heat energy.

Keywords: *new planetology, new geology, terrestrial Oceans, lunar Basins, planetary waves, basalt compositions.*

(Received 13 February 2017. Accepted 12 March 2017)

Observations

Easily visible wide dark areas on the Moon surface are covered by basalts Basins and Marea. Other cosmic bodies of terrestrial group (Earth, Venus, Mars, Mercury) also have large depressions covered with basalt effusions (Kochemasov, 2013-2016; **Figs. 1-5**).Not regarding other basaltic formations in these bodies of various ages we compare here only the planetary wide basaltic covers filling lowlands and partially surrounding highlands and presenting most profuse massive formations (Campbell, 2005; Ernst, .2007; Ernst et al., 2005; Hergt et al., 1991). This "uniform" characteristic for all terrestrial body's processes of delivering dense substances to surface is explained by necessity to "heal" lost angular momentum of the bodies due to slowing their rotation.

Depressions filling basalt complexes are not only present on surfaces of all terrestrial planets and the Moon but they have widely different ages (from the AR to Cz-Present) and chemical compositions (Mg, Fe, Mg/Fe) (Campbell, 2005; Kochemasov, 2013). Belonging to bodies of various masses these "basaltic episodes-outbursts" show certain correlation with masses. Smaller bodies start "outbursts" earlier, larger ones later. Here acts the first Newton's law – the law of inertia. Larger masses are sluggisher (more inert) than smaller ones. Massive melting basalts in mantles is caused by temperature rise due to change of movement energy of bodies to the heat energy (classic physics).A sufficient level of heating for basalts melting is achieved earlier in small bodies (Moon – the AR) than in large bodies (Earth – Mz-Cz). Other planets with intermediate masses produce "basalt outbursts" during intermediate times.

The first theorem of Newton and the Le Chatelier principle in the Earth-Moon system evolution are clear. Analytical methods have shown significant time lapse of massive basalt effusions in the Earth's Oceans and the Moon's Basins and Marea (Hiesinger and Head, 2016).

The both cosmic bodies, as well as other bodies, are tectonically dichotomous. Many planetologists have noted that some difference between hemispheres of cosmic bodies "strangely" exists. Attempts to explain this was not adequate. Applying methods of the wave planetology, this phenomenon was explained by a warping action of the fundamental wave 1 long the great planetary circle ($2\pi R$). This wave, caused by moving a body in an elliptical Keplerian orbit with periodically changing acceleration, uplifts one hemisphere and sinks the opposite one. The Earth, as an example, shows the risen continental eastern hemisphere deeply cracked – giant rifts, and the opposed subsided western Pacific hemisphere faulted, squeezed, wrinkled. Subsidence – diminishing of the planetary radius causes expulsion of an extra mantle material observed on the ocean bottom as the ocean ridge and giant volcanoes (Hawaii and others). Very manifesting of the dichotomous structure are small cosmic bodies (asteroids, comet cores) often having bent forms.

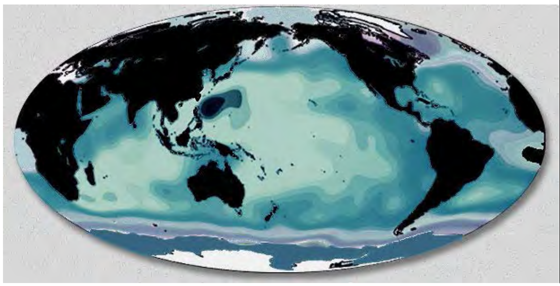

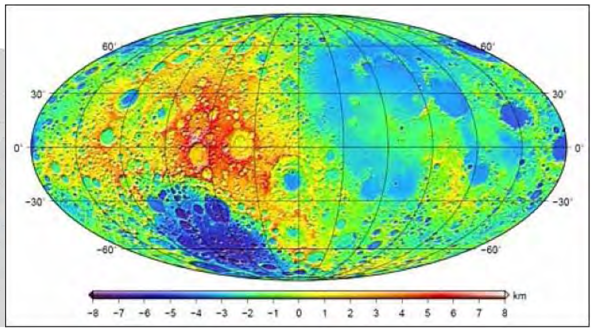

Fig. 1 (left). Earth. Tectonic triad: Pacific Ocean (2πR structure) – Malay Archipelago (πR/4-structure) – India Ocean (πR-structure).
Fig. 2 (right). Moon. Tectonic triad: Procellarum Basin (2πR) - Mare Orientale (πR/4) – SPA (South Pole-Aitken) Basin (πR).

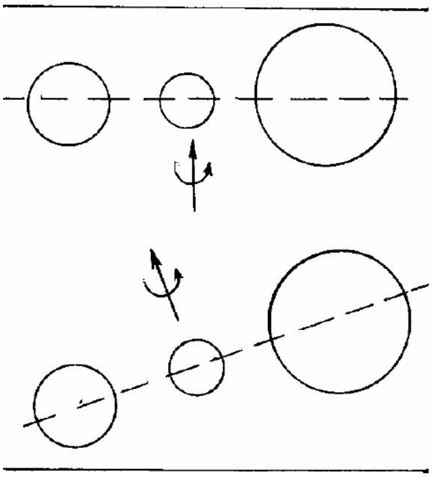

Fig. 3. Schematic presentation of both (terrestrial, Fig. 1 and lunar, Fig. 2) triads.

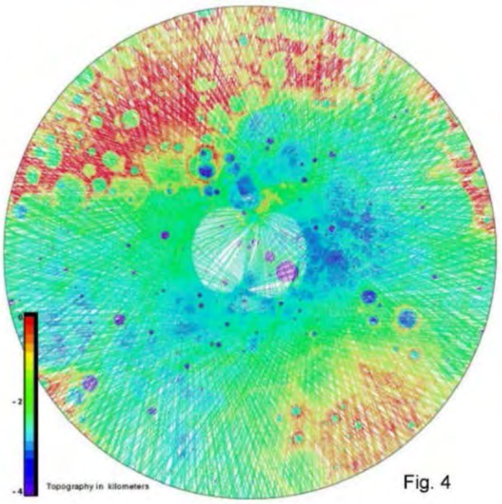

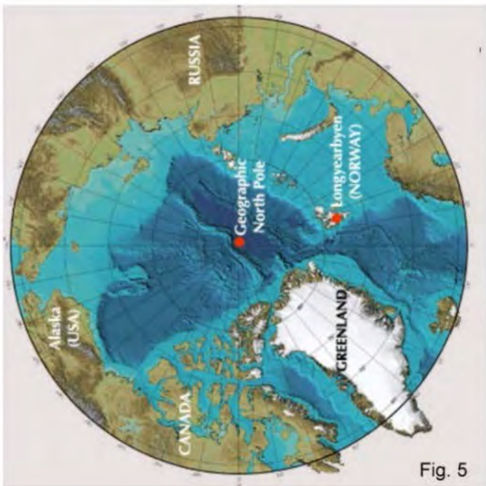

Fig. 4 (left). Northern topography of Mercury, PIA 16951 Polar stereographic projection, extending southwards to 65 N, with 0 longitude at the bottom. The diameter of this projection is 2130 km.
Fig. 5 (right). Arctic Ocean of Earth. Compare with Fig. 4.

The Earth and Moon's subsided hemispheres, for keeping angular momenta of hemispheres equal, are filled with dense basaltic material. But times of the fillings are significantly different. The Earth-Moon system expands with time. This means increasing its angular momentum. A natural response to it is in slowing down rotation of both bodies diminishing their angular momentum (action - opposite action). Diminishing momenta are compensated by melting and uplifting to surfaces dense basaltic material [Kochemasov, 2016]. But on the Moon it happened much earlier (4.5-3 billion years ago) (Hiesinger et al., 2000; Hiesinger and Head, 2016) because of diminished inertia of the small mass satellite. At Earth - much larger and massive body than Moon – 81 times – it happened much later. (3-4.5 billions): 81 = 37-55 million years. According to this calculation, a "peak" of the basaltic reaction of Earth, filling in by basalts of oceanic depressions is in the boundary of Mesozoic and Cenozoic.

Two groups of terrestrial rocky planets are distinguished: slowly rotating inner Mercury and Venus; fastly rotating outer Earth and Mars. Strongly braked inner planets with significant loss of angular momentum require profuse deposits of basalts on the surfaces to restore the loss (the Le Chatelier principle). This means very deep melting mantle material seizing more difficultly melted (refractory) magnesium rich parts. Opposite is true for the outer planets. Moderately braked Earth and Mars require less abundant mantle melting producing relatively iron rich products. Thus, the inner planets have magnesium rich basaltic covers, the outer ones have iron rich covers (Kochemasov, 2013). The lunar basalts along with high iron contents have significant magnesium contents. The Moon, in sense of rotation, is between slow inner planets and fast outer planets. This explains dual (Mg-Fe) composition of its basalts. Extra iron not hidden in pyroxenes finds its place in ilmenite forming rather enigmatic lunar Ti-basalts.

Conclusion

General trend in evolution of terrestrial planets and the Moon is slowing their rotation rates with time. Losing thus angular momentum bodies, according to the Le Chatelier rule, bring to the outer geospheres dense basaltic material to restore angular momentum. Melted in the mantle depths basalts fill geomorphologic depressions on surfaces. The mantle melting requires an energy source. A main source is a transition of the orbital mechanic energy to thermal energy. Some additional source is in radioactive decay of K, U, Th (Earth, Moon). The small mass of the Moon is heated much earlier (the AR), 81 times more massive and inert Earth is heated to a necessary level much later (Mz-Cz). Other planets with intermediate masses have intermediate ages of the planetary basalts "outbursts". Two inner planets – Mercury and Venus – with very slow rotation and very important angular momentum loss require very significant basaltic effusion intervention. The massive melting means magnesium reach products. This is proved by existing analyses. The outer fastly rotating bodies do not require comparatively massive "healing momentum" basalt interventions. Thus, basalts of Mars and the Moon are comparatively Fe-rich meaning not deep mantle melting. Extra iron in the lunar basalts is tied in ilmenite –famous ilmenite basalts.

Acknowledgements: I acknowledge a very fruitful discussion with Dr. N. I. Pavlenkova leading to necessary corrections to the text.

References

Campbell, I.H., 2005. Large igneous provinces and the mantle plume hypothesis. *Elements*, v. 1, p. 265-269.

Ernst, R.E., 2007. Mafic-ultramafic large igneous provinces (LIPs): importance of the Pre- Mesozoic record. *Episodes,* v. 30, # 2, p. 108-114.

Ernst R.E., Kenneth L.B. and Campbell I.H., 2005. Frontiers in Large Igneous Province research. *Lithos*, v. 79, # 3-4, p. 271-297.

Hergt, J.M., Peate, D.W. and Hawkesworth, C.J., 1991. The petrogenesis of Mesozoi Gondwana low-Ti flood basalts. *Earth and Planetary Science Letters,* v. 105, # 1/3, p. 134-148.

Hiesinger, H., Jaumann, R., Neukum, G. and Head, III, J.W., 2000. Ages of mare basalts on the lunar nearside. *Jour. Geoph. Res*., v. 185, #E12, p. 29239-275.

Hiesinger H. and Head, III, J.W., 2016. Ages of Oceanus Procellarum basalts and other nearside mare Basalts. Workshop on New Views of the Moon II, 2016, abs. 8030.

Kochemasov, G.G., 2013. Analogy between lowlands of Earth and Mars, Earth and Mercury and a glance at tectonic granulations: a severe blow to the plate tectonics from the comparative wave planetology. *NCGT Journal,* v. 1, # 4, p. 23-28.

Kochemasov, G.G., 2014. Earth and Moon: similar structures – common origin. *NCGT Journal*, 2014, v. 2, # 2, p. 28-38.

Kochemasov G.G., 2015. A lunar "mould" of the Earth's tectonics: four terrestrial Oceans and four lunar Basins are derivative of one wave tectonic process. *NCGT Journal*, v. 3, # 1, p. 29-33.

Kochemasov, G.G., 2016. The Moon and Phobos: specific responses of two satellites moving off and nearer their respective planets. DPS 48/EPSC 11, Pasadena, Oct. 16-21, 2016. *Bulletin of the American Astronomical Society*, v. 48, # 7, p. 175, Abstract 318.08, Session 318: Formation and Evolution of Planets and Satellites Posters.

SELF-ELF Electromagnetic signals correlated to M5+ Italian Earthquakes occurred on August 24, 2016 and January 18, 2017

Gabriele Cataldi[1], Daniele Cataldi[2], Riccardo Rossi[3] and Valentino Straser[4]

[1]Radio Emissions Project, Rome (I). ltpaobserverproject@gmail.com
[2]Radio Emissions Project, Rome (I). daniele77c@gmail.com
[3]Friuli Experimental Seismic Network (FESN), Udine (I). posta.fesn@gmail.com
[4]Department of Science and Environment UPKL Brussels (B). valentino.straser@gmail.com

Abstract: The authors of this study want to verify the existence of a possible relationship between the natural radio emission observed between the SELF (Super Extremely Low Frequency band; 3Hz>f>0Hz) and the ELF (Extremely Low Frequency; 3Hz≤f≤30Hz) and earthquakes of medium-high intensity registered in Central Italy on August 24, 2016 and on January 18, 2017: 1) M6.2 occurred on August 24, 2016 at 01:36:32 UTC near Norcia (PG); 2) M5.6 occurred on August 24, 2016 at 02:33:29 UTC near Norcia (PG); 3) M5.3 occurred on January 18, 2017 at 09:25:41 UTC near Amatrice (RI); 4) M5.7 occurred on January 18, 2017 at 10:14:11 UTC near Amatrice (RI); 5) M5.6 occurred on January 18, 2017 at 10:25:25 UTC near Amatrice (RI); 6)M5.2 occurred on January 18, 2017 at 13:33:37 UTC near Montereale (AQ). The study results revealed that the six earthquakes occurred in Central Italy on August 24, 2016 and on January 18, 2017 were preceded by a few days by the appearance of SELF-ELF radio emissions not related to the variation of the geomagnetic field and solar activity in general, much less to human activity. Instead, it is considered that the detected signals may be considered potential candidates pre-seismic.

Keywords: *Central Italy earthquakes, SELF-ELF Radio anomalies, VLF radio anomalies, seismic electromagnetic precursors (SEPs), seismic precursors.*

(Received 19 February 2017. Accepted 13 March 2017)

Introduction

Between August 24, 2016 and January 18, 2016 the Central Italy was hit by nine M5+ earthquakes of variable intensity between M5.2 and M6.6 (**Fig. 1**) caused by the movement of fault segments with high structural complexity. The seismic sequence caused damage in 131 Italian cities located in territory of Lazio, Umbria, Marche and Abruzzo. The earthquakes killed more than 300 people. Italy is currently classified as one of the countries with the highest seismic risk present in the European continent and it is necessary that the scientific community make every effort so that research on earthquake prediction comes close, from a methodological and conceptual point of view, to United States and Japan and it is on new consideration that is grafted the electromagnetic monitoring.

On the Italian territory, there are two electromagnetic monitoring networks created for studying the pre-seismic radio emissions: the first, located in Central Italy in the province of Rome, at the foot of the famous Latium Volcano is managed by Dr. Gabriele Cataldi and Dr. Daniele Cataldi as part of project called "Radio Emissions Project"; the second, located in the North-East of Italy, in the province of Udine is managed by Friuli Experimental Seismic Network (FESN) Group. The two networks are an integral part of a major project of electromagnetic monitoring called "*Project SDT - Signals from the Earth*", promoted in 2007 by the Italian Radio Amateurs Association (ARI) and realized by FESN, through which the authors of this work and other Italian collaborators constantly monitor the natural electromagnetic background of the SELF (Super Extremely Low Frequency) band and VLF (Very Low Frequency) band (0<f<30kHz) in search of electromagnetic signals with seismic predictive characteristics, ie pre-seismic radio signals: the so-called "Seismic Electromagnetic precursors". The electromagnetic monitoring stations of FESN and

Radio Emissions Project are active 24h7 and allow to automatically store data obtained from the monitoring activity on informatic support. Following are shown the technical characteristics of the stations:

1) SELF-ELF (0-15Hz) monitoring station, Trasaghis (UD), FESN.
    - Induction magnetometer (18-bit), coil antenna, vertical polarization (Bz).
2) SELF-ELF (0-15Hz) monitoring station, Pasian Di Prato (UD), FESN.
    - Induction magnetometer (18-bit), coil antenna, vertical polarization (Bz).
3) VLF (300-30000Hz) monitoring station, Albano Laziale (RM), Radio Emissions Project.
    - VLF receiver (24-bit), loop antenna, horizontal polarization (41°N-E).
4) SELF-ELF (0-5Hz) monitoring station, Lariano (RM), Radio Emissions Project.
    - Induction magnetometer (24-bit), coil antenna, vertical polarization (Bz).

Fig. 1 – Central Italy earthquakes: The picture shows (red arrow) the seismic epicentres (orange circles) of M5+ earthquakes occurred in Central Italy between 24 August 2016 and 18 January 2017. At the top, the two yellow round icons indicate the two SELF-ELF electromagnetic monitoring stations realized by "Friuli Experimental Seismic Network" (FESN) located in Trasaghis, Udine (the top one) and at Pasian Di Prato, Udine (the lower). The two colored icons visible on the bottom of the image indicate the electromagnetic monitoring stations of Radio Emissions Project located at Albano Laziale, Roma (the green icon) and in Lariano, Rome (the red icon).

Methods and Data

To verify whether the Italian seismic sequence occurred between August 2016 and January 2017 was preceded by pre-seismic radio emissions, the authors analyzed the data on electromagnetic monitoring products through the SDT Project, between August 2016 and January 2017, and in particular the data produced by the stations of Pasian Di Prato (UD), Trasaghis (UD), Albano Laziale (RM) and Lariano (RM). These data were compared with data on M5+ seismic activity recorded in Central Italy between 24 August 2016 and 18 January 2017 by United States Geological Survey (USGS).

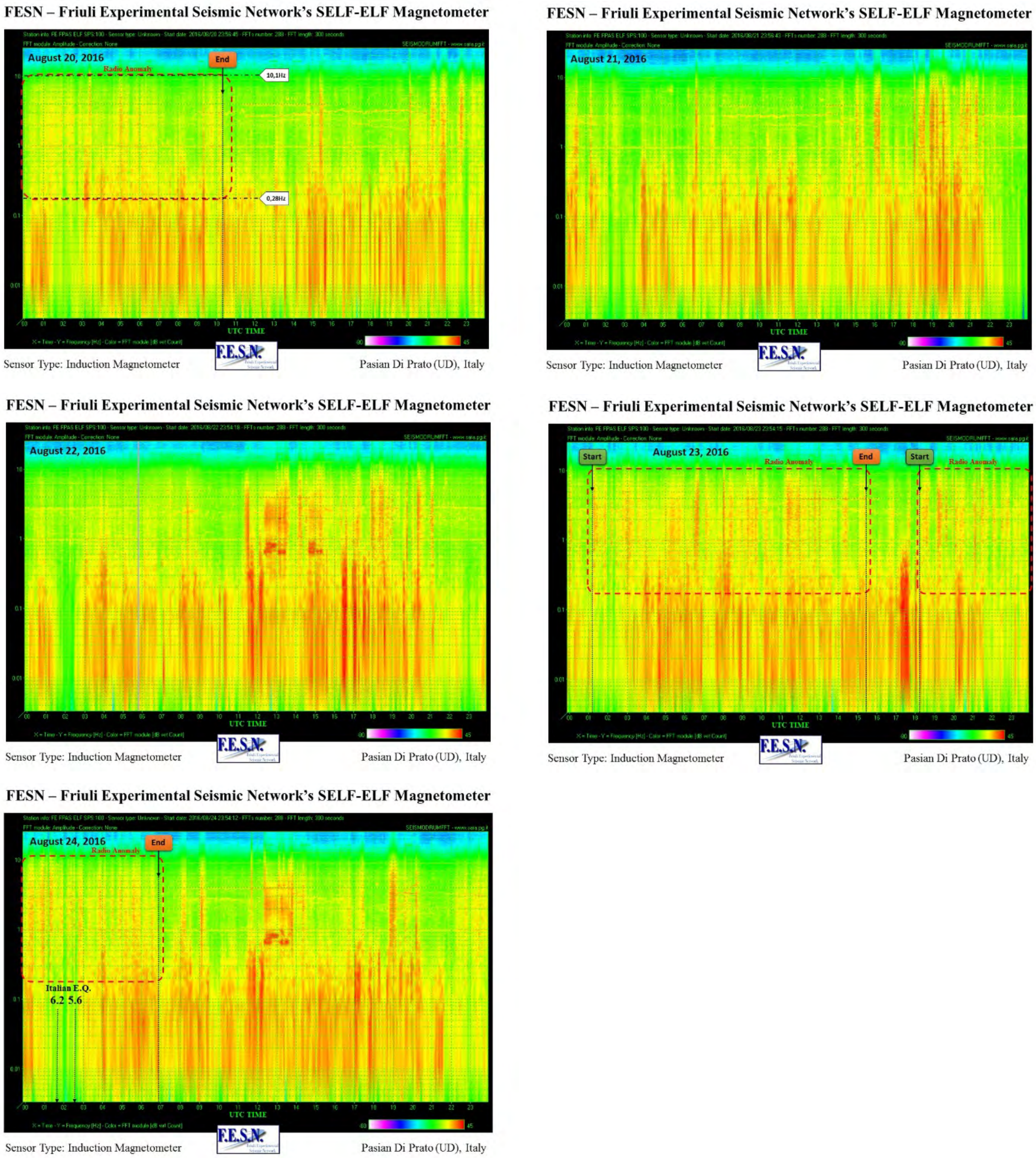

Fig. 2 – Seismic Electromagnetic Precursor of seismic sequence recorded in Central Italy on August 24, 2016. The picture shows five dynamic spectrograms related to electromagnetic environmental monitoring realized by the Friuli Experimental Seismic Network (FESN) between 20 and 24 August 2016 through the monitoring station located in Pasian Di Prato (UD). The areas of the circumscribed spectrogram with the red dotted line represents pre-seismic electromagnetic emissions that preceded the M5+ seismic sequence of August 24, 2016. "Start" and "End" labels indicate respectively the start and end of the Electromagnetic earthquake precursor registered precede earthquakes.

Results

The study results confirmed that, with the exception of earthquakes occurred in Central Italy between 26 and 30 October 2016, the earthquakes that occurred on August 24, 2016 and on January 18, 2017 were preceded by radio emissions that could not be associated to anthropogenic broadcasters or emissions of geomagnetic nature:

- M6.2 and M5.6 Central Italy earthquakes occurred on August 24, 2016: the electromagnetic monitoring station of Pasian Di Prato (UD) has detected an electromagnetic emission equivalent to an increase of natural electromagnetic background between 0.28 to 10,1Hz at a maximum intensity centered around 3Hz. This radio signal appeared on August 20, 2016 just after 00:00 UTC and ended at 10:20 UTC of the same day. Then it was re-recorded on August 23, 2016 between 01:15 UTC and 15:25 UTC; and then between 18:14 UTC on August 23, 2016 for terminate at 06:54 UTC on August 24, 2016 (**Fig. 2**).

- M6.2 and M5.6 Central Italy earthquakes occurred on August 24, 2016: the electromagnetic monitoring station of Albano Laziale (RM) has detected an electromagnetic emission with wide bandwidth (13,37kHz). This electromagnetic anomaly that has been recorded on August 18, 2016 between 02:47 UTC and 06:21 UTC, thus remained visible for about 3 hours and 34 minutes between 9.63 kHz and 23kHz, with greater intensity between 9.63 kHz and 20,5kHz and preceded the Italian M6.2 earthquake of the August 24, 2016 of 142 hours and 49 minutes (almost 6 days) (**Fig. 3**).
- M6.2 and M5.6 Central Italy earthquakes occurred on August 24, 2016: the electromagnetic monitoring station located in Lariano (RM) has detected a number of electromagnetic emissions within the SELF (Super Extremely Low Frequency) band, some of which preceded the major seismic events (M6.2 e M5.6) and others are taking place close to other earthquakes with small magnitude (**Fig. 4**). The M6.2 earthquake was preceded about 70 minutes by an increase of the electromagnetic background with a bandwidth comprised between 0 and 0,6Hz. The most intense pre-seismic electromagnetic emission, however, was recorded 17 hours before the M6.2 earthquake and had a duration of 40 minutes.
- M5.3, M5.7, M5.7 and M5.2 Central Italy earthquakes occurred on January 18, 2017: the electromagnetic monitoring station of Pasian Di Prato (UD) has detected an electromagnetic emission with very tight bandwidth, centered at 4,8Hz. This emission was registered for the first time on January 13, 2017 at 11:30 UTC and disappeared on January 18, 2017 at 09:10 UTC, about 15 minutes before the M5.3 earthquake occurred at 09:25 hours: 41 UTC (**Fig. 5**).

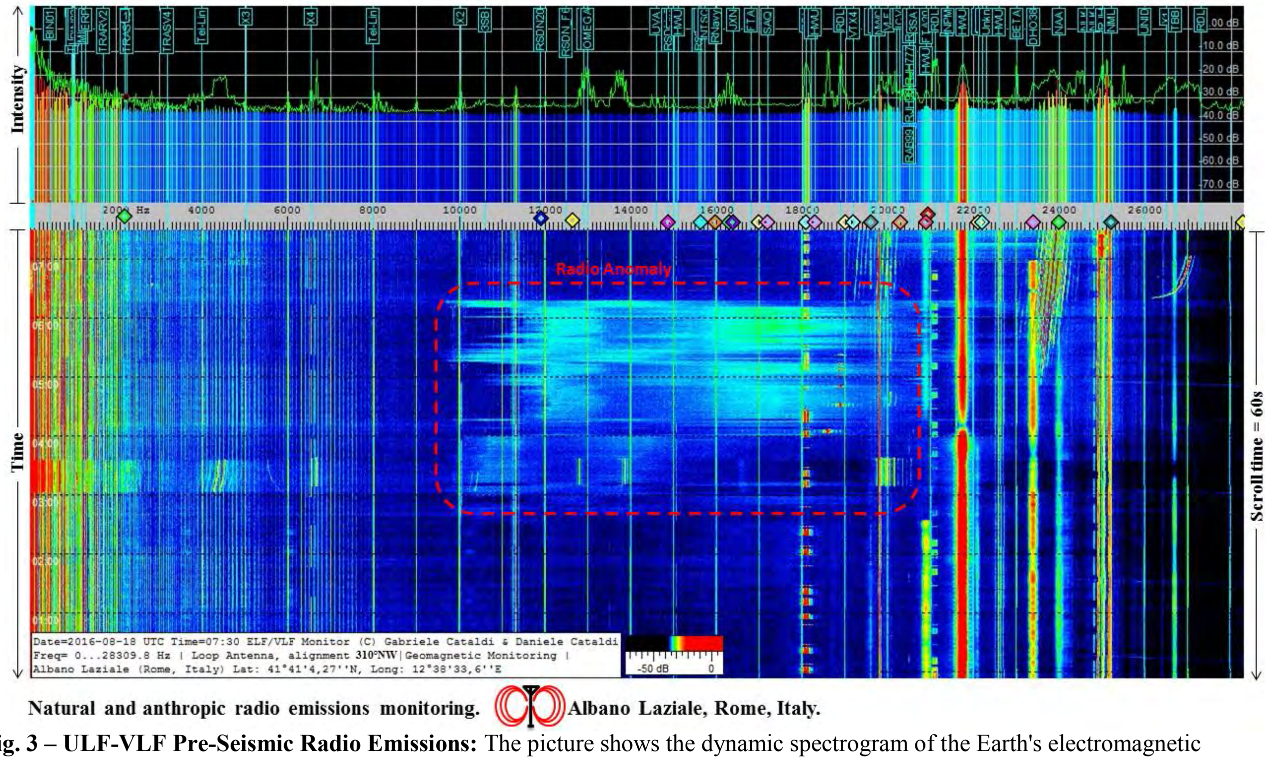

Fig. 3 – ULF-VLF Pre-Seismic Radio Emissions: The picture shows the dynamic spectrogram of the Earth's electromagnetic field recorded on August 18, 2016 between 00:00 and 07:30 UTC from the ULF-VLF electromagnetic environment monitoring station of Radio Emissions Project, located at Albano Laziale (RM), Italy. At the center of the spectrogram, inside the red dotted line, is present the radio anomaly that has been recorded precede the M6.2 Italian earthquake occurred on August 24, 2016 at 01:36 UTC. The emission appeared at 02:47 UTC and disappeared at 06:21 UTC. The labels at the top of the spectrogram (in light blue) indicate known radio stations, prevalently of anthropic type. On the Y axis of the spectrogram indicates the UTC time of the registration: this proceeds from top to bottom at 1 horizontal line to minutes. On the X axis is instead reported the emission

frequency of the radio signals (the frequency increases going to the right): these are represented in different colors according to their intensity.

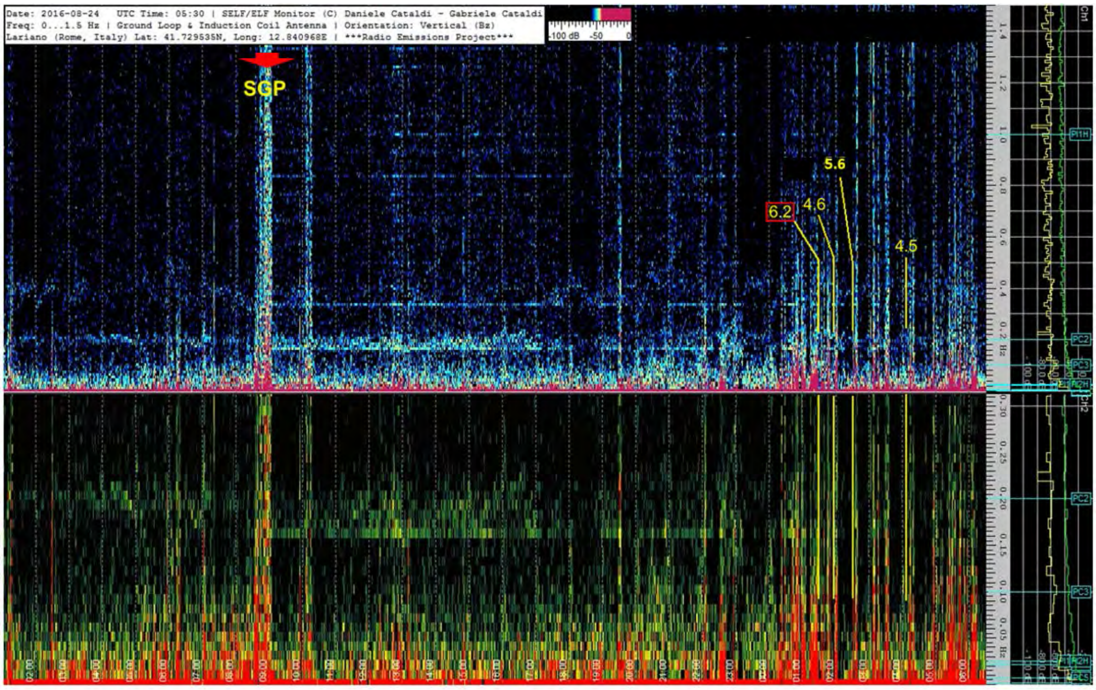

Fig. 4 – SELF-ELF Monitor: The image represents the dynamic spectrogram of the Earth's electromagnetic field registered between 02:00 UTC on August 23, 2016 and 06:30 UTC on August 24, 2016 by environmental electromagnetic monitoring station of Radio Emissions Project, located in Lariano (RM), Italy; it monitors the band SELF and ELF with a resolution of 10.1 mHz. The upper portion of the spectrogram is centered in the SELF band between 0 and 1.5Hz, while the lower portion is centered in the SELF band between 0 and 0.31Hz. The spectrogram is acquired through a radio receiver prototype developed by Gabriele Cataldi designed to work efficiently between the SELF band (0<f<3 Hz) and the ELF band (3-30Hz). The used antenna is a coil antenna aligned vertically (Bz geomagnetic component). The word "SGP", indicated by the vertical red arrow, is an acronym coined by the authors that identifies the radio emission of geomagnetic nature that was observed to precede large earthquakes (Seismic Geomagnetic Precursor): this electromagnetic emission preceded the M6.2 Italian earthquake of approximately 17 hours and had a duration of about 40 minutes.

The monitoring stations located in Trasaghis (UD) was not set properly to get comparable readings (data) with those of Pasian Di Prato (UD).

Fulmination

To confirm the objectivity of the electromagnetic monitoring related data, the authors have verified if in the vicinity of the Radio Emissions Project's ULF-VLF and SELF-ELF monitoring stations had occurred storms on August 18, 2016. The radio signals produced by lightning, in fact, can be detected by radio receivers tuned to a wide range of frequencies, for this reason it is essential to reject the hypothesis that electromagnetic anomalies detected near the (VLF and SELF-ELF) electromagnetic monitoring station of Radio Emissions Project are in reality the marks left by a storm. To run this check, were utilized weather data provided by the Italian Air Force (AMI) and found that on August 18, 2016 there were no thunderstorms near the ULF-VLF and SELF-ELF monitoring stations located in Central Italy, but light rain were recorded in Northern Italy. Also the Regional Agency for Environmental Protection of Friuli Venezia Giulia (ARPA-FVG) has confirmed that in the days when the Pasian Di Prato (UD) monitoring station has detected anomalies there were no storms on the site station. Identical results were obtained by verifying the weather conditions for the period from 13 to 18 January 2017. Moreover, from a spectrographic point of view, on ULF-VLF spectrogram and are not found typical signals related to lightning discharges, ie the so-called "Spherics" (abbreviation of "atmospherics", also known as "statics").

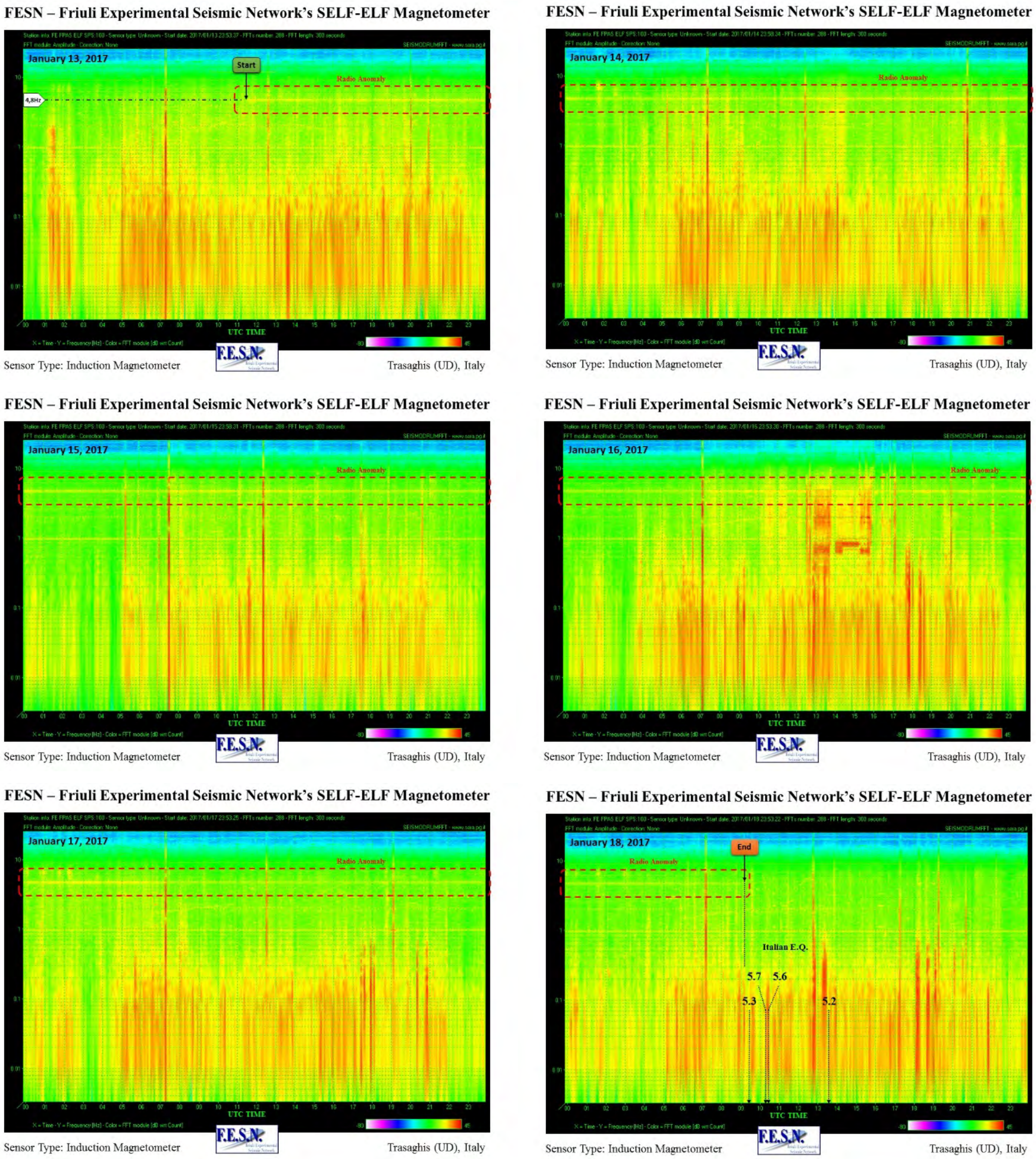

Fig. 5 – Seismic Electromagnetic Precursor of seismic sequence recorded in Central Italy on January 18, 2017: The picture shows five dynamic spectrograms related to electromagnetic environmental monitoring realized by the Friuli Experimental Seismic Network (FESN) between 20 and 24 August 2016 through the monitoring station located in Pasian Di Prato (UD). The areas of the circumscribed spectrogram with the red dotted line represents pre-seismic electromagnetic emissions that preceded the M5+ seismic sequence of August 24, 2016. The vertical black arrows represent the temporal markers of M5+ earthquakes occurred in Central Italy on January 18, 2017. The label says "Start" and "End" respectively indicate the start and end of the electromagnetic earthquake precursor registered precede the earthquakes.

Discussion

Radio emissions with seismic predictive characteristics were observed for the first time in 1880 (Milne, 1890). Today we know that there are two main families of pre-seismic radio emissions: 1) those of "local" type produced as a result of the creation of micro-fractures in the focal zone of the earthquake (piezoelectricity); 2) those of "non-local" type detectable from anywhere on the Earth's surface because they are assimilated to the terrestrial geomagnetic field disturbances (Cataldi et al., 2016).

In the specific case the radio emissions detected by SDT stations of Pasian Di Prato (UD), Albano Laziale (RM) and Lariano (RM) with exception for the electromagnetic emission identified by the acronym "SGP" (Seismic Geomagnetic Precursors) recorded on August 23, 2016 at 09:00 UTC, do not have any spectrographic and spectrometric characteristics that allows us to establish that it is related to electromagnetic phenomena correlated to Earth's geomagnetic activity, so it is very likely that this is electromagnetic emissions produced locally, i.e. in the focal zone of earthquake sequence. This is because the radio emissions associated to geomagnetic activity (and therefore to solar activity), are observed with greater intensity within the SELF (Super Extremely Low Frequency) band becoming less intense as the frequency increases.

The anomalies recorded precede earthquakes of August 24, 2016 and January 18, 2017 have features that are incompatible with those of a geomagnetic disturbance:

1) the radio emission related to Italian seismic sequence of January 18, 2017 (recording made through the electromagnetic monitoring station of Pasian Di Prato, Udine), was recorded during a state of solar quiet, in fact, the ion density of the interplanetary medium was at its lowest. In addition, the signal bandwidth is too tight (only 0.4 Hz) to hypothesize that it may be a emission of a geomagnetic nature, also considering that this signal has remained visible uninterruptedly for almost five days.

2) the SELF-ELF anomaly registered by Pasian Di Prato station precede the seismic sequence of August 24, 2016 has, on the contrary, a wide bandwidth (9.82 Hz) This signal may be produced by the earthquake preparation processes (piezoelectric effect) but we have no large series about, especially for Pasian Di Prato's Monitoring Station with the maximum centered around 3Hz. This anomaly has been detected three times from 20 to 24 August 2016 and ended four hours and 30 minutes after the last M5+ earthquake recorded on August 24, 2016, also its intensity has increased from August 23, 2016. From a spectrographic point of view, this radio signal has not undergone morphological variations and this fact allows us to exclude that it may be an emission of geomagnetic nature.

3) The station of Lariano (RM), although it was the only electromagnetic monitoring station to record emission comparable to a geomagnetic disturbance (in fact between 18 and 23 August 2016 was found an increase of "gradual" type of interplanetary medium ion density near Earth). It is possible but the Lariano's station has detected disturbances in the SELF-ELF band even for the earthquakes to tens of thousands of kilometers away; We consider them non-local seismic precursors that preceded the M6.2 earthquake of August 24, 2016 (01:36:32 UTC), approximately 17 hours, has also allowed us to record a series of impulsive emissions of the natural electromagnetic background that preceded the M6.2 earthquake about 70 minutes remaining visible at least up to 06:30 UTC of 24 August 2016.

These impulsive emissions have had a shorter duration and a narrower bandwidth in respect to tie electromagnetic emissions that the authors associated with a variation of the geomagnetic field that was recorded at 09:00 UTC of 23 August 2016, therefore, the signal must be of local origin, is generated in the focal zone of seismic sequence recorded on August 24, 2016. Observing spectrograms can be calculated the time lag that elapsing between the pre-seismic radio emissions have appeared and the time at which it started the seismic sequence in Central Italy (**Fig. 6**):

- Respect to the monitoring data provided by the station of Pasian Di Prato (UD), the pre-seismic electromagnetic anomaly has appeared 120 hours and 30 minutes before the M5+ earthquake sequence recorded on January 18, 2017.
- Respect to the monitoring data provided by the station of Pasian Di Prato (UD), the pre-seismic electromagnetic anomaly appeared about 97 hours before the M6.2 earthquake recorded on August 24, 2016.
- Respect to the monitoring data provided by stations of Lariano (RM), the pre-seismic electromagnetic anomaly appeared about 17 hours before the M6.2 earthquake recorded on August 24, 2016.

- Respect to the monitoring data provided by the station of Albano Laziale (RM), the pre-seismic electromagnetic anomaly appeared about 143 hours before the M6.2 earthquake recorded on August 24, 2016.

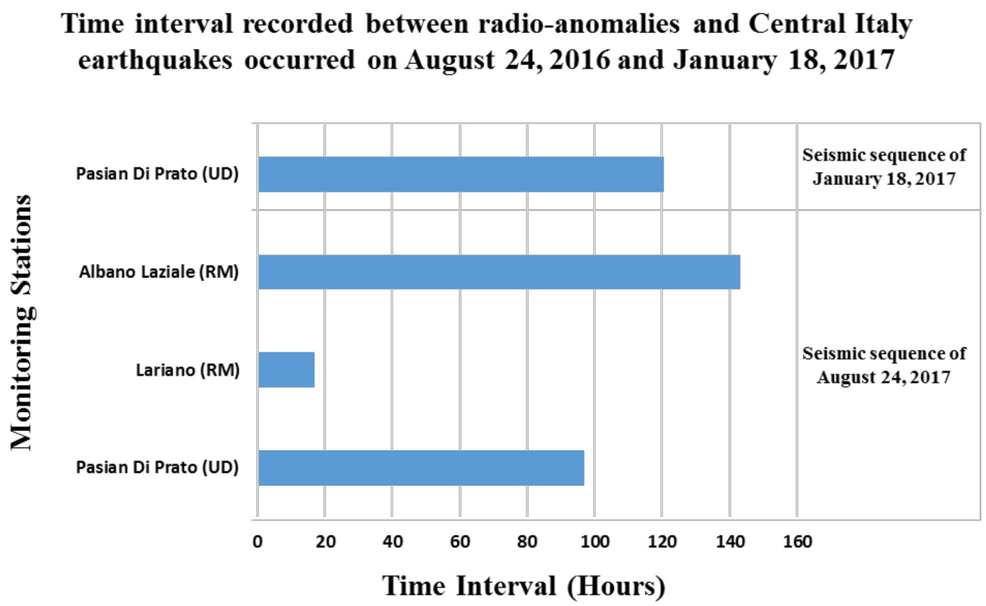

Fig. 6 – Time interval between radio-anomalies and Central Italy seismic activity: The graph shows the time intervals recorded between radio anomalies (pre-seismic radio emissions) and the Central Italy seismic sequences recorded on August 24, 2016 and on January 18, 2017. The data were provided through the "SDT Project". The monitoring station of Pasian Di Prato (UD) was the only one to detect pre-seismic electromagnetic anomalies that preceded the seismic sequences of January 18, 2017

Conclusions

In recent decades, many nations of the world are making substantial efforts to try to develop an innovative seismic forecasting methodology that separates definitively from seismometric data. To achieve this goal, however, it is essential realize an interdisciplinary and multidisciplinary research project shared globally in which research on pre-seismic radio emissions, the monitoring of space weather and the heliophysics study must be integrated in the same context and interpreted by a team of researchers with undisputed expertise. The authors of this study have proposed many times at national and international level, the creation of a research project on seismic precursors that is shared globally.

In Italy this scientific approach is not widely shared among researchers and this made it impossible to create a center for the study of pre-seismic radio emissions recognized in academic or governmental level. Currently in Italy the research on pre-seismic radio emission is performed by amateurs, technicians of various kinds, amateur radio operators and researchers who fully self-financed their work producing important scientific studies. The Radio Emissions Project and the Friuli Experimental Seismic network (FESN) are two Italian teams of researchers who dedicate a part of their lives to the study of pre-seismic radio emissions. Together with other researchers and enthusiasts are an integral part of an electromagnetic monitoring network designed to monitor the environmental electromagnetic background between 0 and 22 kHz; this network (born in 2007) has been called "SDT Project - Signals From The Earth" and all monitoring stations that are part of it must have specific technical requirements to ensure that the network is able to perform an electromagnetic monitoring more objective possible. This new approach aimed at pre-seismic radio emissions has allowed in recent years to produce some very interesting and important scientific papers on electromagnetic seismic precursors (SEP) and on seismic geomagnetic precursor (SGP), (Straser et al., 2016; Cataldi et al, 2016-2017).

The analysis of the electromagnetic spectrum between 0 and 22 kHz, especially between the SELF band and the ELF band (Ohta et al., 2013) allows to monitor the pre-seismic electromagnetic emissions associated with large earthquakes (M6+), to understand their characteristics and develop best electronic devices, in the perspective to realize a seismic prediction method based on monitoring and on understanding of these radio signals; in fact it is impossible to think that the future of research on seismic prediction has yet to be essentially linked to the historical data of seismometric measurements and to the geodynamics and geological characteristics of the faults..

The SDT Project has shown that it is possible to detect pre-seismic radio signals that occur on Italian territory and it is hoped that this monitoring network undergoes a rapid expansion in the coming years: this will allow us to get a lot more electromagnetic data associated by seismic activity that occurs in our country enabling us to better understand the characteristics of these radio emissions. A technology that must be integrated in this system is the Radio Direction Finding (RDF), because it is currently possible to realize radio receivers that allow to understand from which direction spreads an electromagnetic emission; this technology allowed to identify the seismic epicenter of the famous M9.0 Japanese earthquake that occurred on March 11, 2011 at 14:46:24 UTC+9 (Ohta et al, 2013). Italy, along with Greece, is the European area of high seismic risk, and this has to be translated into opportunities for Italian researchers: a seismic district with these characteristics allows us to make an imposing study on electromagnetic seismic precursors that can certainly produce significant results. Those produced under the "SDT" Project in August 2016 and January 2017 are an example of the great results that can be achieved by exploiting technological potential and the right ideas in a country, Italy, which has the potential to become among one of the first countries in the world where it can be conducted innovative research on seismic prevision.

Acknowldegements: The authors wish to thank Dr. Bruce Leybourne for the suggestions that have improved our paper and we also will improve our studies in the future. Thanks also to Dr. Choi Dong for the support he gave in recent years to our research.

References

Cataldi, G. and Cataldi, D., 2013. Reception of Natural Radio Emissions in the ELF Band. *The INSPIRE Journal*, v. 20, Spring/Summer 2013.

Cataldi, G., Cataldi, D. and Straser, V., 2013. Variations Of Terrestrial Geomagnetic Activity Correlated To M6+ Global Seismic Activity. EGU (European Geosciences Union) 2013, General Assembly, Geophysical Research Abstracts, v. 15. Vienna, Austria. Harvard-Smithsonian Center for Astrophysics, High Energy Astrophysics Division, SAO/NASA Astrophysics Data System.

Cataldi, G., Cataldi, D. and Straser, V., 2014. Earth's magnetic field anomalies that precede the M6+ global seismic activity. European Geosciences Union (EGU) General Assembly 2014, Geophysical Research Abstract, Vol. 16, Natural Hazard Section (NH4.3), Electro-magnetic phenomena and connections with seismo-tectonic activity, Vienna, Austria. Harvard-Smithsonian Center for Astrophysics, High Energy Astrophysics Division, SAO/NASA Astrophysics Data System.

Cataldi, G., Cataldi, D. and Straser, V., 2016. VLF electromagnetic signals unrelated to the Central Italy earthquakes occurred between 26 and 30 October 2016. *New Concepts in Global Tectonics Journal*, v. 4, no. 4, p. 543–552.

Cataldi, G., Cataldi, D. and Straser, V., 2017. SELF-VLF electromagnetic signals and solar wind proton density variations that preceded the M6.2 Central Italy earthquake on August 24, 2016. *International Journal of Modern Research in Electrical and Electronic Engineering*, v. 1, no. 1, p. 1-15. DOI: 10.20448/journal.526/2017.1.1/526.1.1.15.

Cataldi, G., Cataldi, D. and Straser, V., 2017. SELF and VLF electromagnetic emissions that preceded the M6.2 Central Italy earthquake occurred on August 24, 2016. European Geosciences Union (EGU), General Assembly 2017. Seismology (SM1.2)/Natural Hazards (NH4.7)/Tectonics & Structural Geology (TS5.5) The 2016 Central Italy Seismic sequence: overview of data analyses and source models. Geophysical Research Abstracts, v. 19, EGU2017-3675, 2017.

Cataldi, G., Cataldi, D. and Straser, V., 2017. Solar and Geomagnetic Activity Variations Correlated to Italian M6+ Earthquakes Occurred in 2016. European Geosciences Union (EGU), General Assembly 2017. Seismology (SM1.2)/Natural Hazards (NH4.7)/Tectonics & Structural Geology (TS5.5) The 2016 Central Italy Seismic sequence: overview of data analyses and source models. Geophysical Research Abstracts, v. 19, EGU2017-3681, 2017.

Cataldi, G., Cataldi, D. and Straser, V., 2017. Solar wind proton density increase that preceded Central Italy earthquakes occurred between 26 and 30 October 2016. European Geosciences Union (EGU), General Assembly 2017. Seismology (SM1.2)/Natural Hazards (NH4.7)/Tectonics & Structural Geology (TS5.5) The 2016 Central Italy Seismic sequence: overview of data analyses and source models. Geophysical Research Abstracts, v. 19, EGU2017-3774, 2017.

Ohta, K., Izutsu, J., Schekotov, A. and Hayakawa, M., 2013. The ULF/ELF electromagnetic radiation before the 11 March 2011 Japanese earthquake, *Radio Sci*., v. 48, p. 589–596, doi:10.1002/rds.20064

Straser, V., G. Cataldi, G. and Cataldi, D., 2015. Radio-anomalies: tool for earthquakes and tsunami forecasts. European Geosciences Union (EGU) General Assembly 2015, Natural Hazard Section (NH5.1), Sea & Ocean Hazard – Tsunami. Geophysical Research Abstracts, v. 17, Vienna, Austria. Harvard-Smithsonian Center for Astrophysics, High Energy Astrophysics Division, SAO/NASA Astrophysics Data System.

Straser, V., Cataldi, G. and Cataldi, D., 2016. SELF and VLF electromagnetic signal variations that preceded the Central Italy earthquake on August 24, 2016. N*ew Concepts in Global Tectonics Journal*, v. 4, no. 3, p. 473-477.

Evolution of Earth as a stellar transformer

The Institute for Advanced Studies in Climate Change (IASCC)
Bruce Leybourne[1], James "Mick" Davis[2], Giovanni P. Gregori[3], John M. Quinn[4] and N. Christian Smoot[5]

[1] Principal Investigator, IASCC, [2] Director, IASCC, [3, 4 and 5] Senior Fellows, IASCC
Corresponding author: Bruce Leybourne, leybourneb@iascc.org

See Youtube video: http://www.iascc.org/the-science
"Earth as a Stellar Transformer: Climate Change Revealed"

Abstract: Presented in 2015, the "Stellar Transformer" breakthrough was recognized when John Quinn's magnetic modeling of Earth's polar magnetic z-pinch anomalies aligned with polar Delta-Y electrical circuit configurations. Polar circuit geometries align with Earth's North-South tectonic ridge systems, exhibiting global mantle gravity signatures with global temperature anomalies.

Electrical "heater" circuit relationships correlate a theoretical double layer, ring-to-ring step down energy transformer circuit. Energy is transferred from ionospheric polar plasma rings, steps down through induction to the mid-ocean ridge system encircling Antarctica, then connects with deeper induction into concentric spherical configurations of Earth's inner and outer core.

This energy can be stored in the magnetic field as it strengthens from charging during lighting storms, or energy can be dissipated as magnetic field weakens from discharges driving earthquakes and volcanism. The interplay between these charging and discharging phases is a large factor in modulating Earth's climate. Data relationships and theoretical evolution of this tectonic "Stellar Transformer" concept is examined.

Keywords: *Stellar Transformer, induction, magnetic modeling, Delta-Y electrical circuits, plasma ring, space weather, tesla climate*

(Submitted 18 March 2017. Accepted 23 March 2017)

INTRODUCTION:

This paper will present novel concepts that show links between global weather mechanisms and large-scale natural hazards such as earthquakes. Research papers encountered on El Niño's and seismicity reported by Daniel Walker (1988, 1995 and 1999) provided the initial impetus for Institute for Advanced Studies in Climate Change (IASCC) to research and uncover unknown climate links. Originally a concept understood as gravitational teleconnections (Leybourne, 1996 and 1997) was proposed as an active mechanism or link between tectonics and atmospheric pressure oscillations driving El Niño Southern Oscillation (ENSO). Finally after many years of study, in 2014 the Institute for Advanced Studies in Climate Change began embracing and promoting the "Earth as a Stellar Transformer" (EAST) concept (Leybourne and Davis, 2014)

In conventional 20th century theoretical scientific terms, earthquakes are driven by a collision of slow moving tectonic plates. So what could connect a relationship between earthquakes and climate change? The IASCC's concluding hypothesis is that solar electromagnetic activity driving energy and related space weather appears to dominate the relationships between earthquakes and naturally occurring climate drivers (Leybourne and Smoot, 2005). Birkeland currents (**Fig. 1**) sometimes "overcharge" the earth's core like a leaky capacitor (Gregori, 2002 and 2006) stimulating earthquakes when the earth's core discharges. This may be associated with inner core jerks (Dziewonski, 1984, Quinn and Leybourne, 2010) coupled with electromagnetic fluid dynamics linked to orbital physics, and magnetic decay cycles (Quinn, 2010; Davis, 2014).

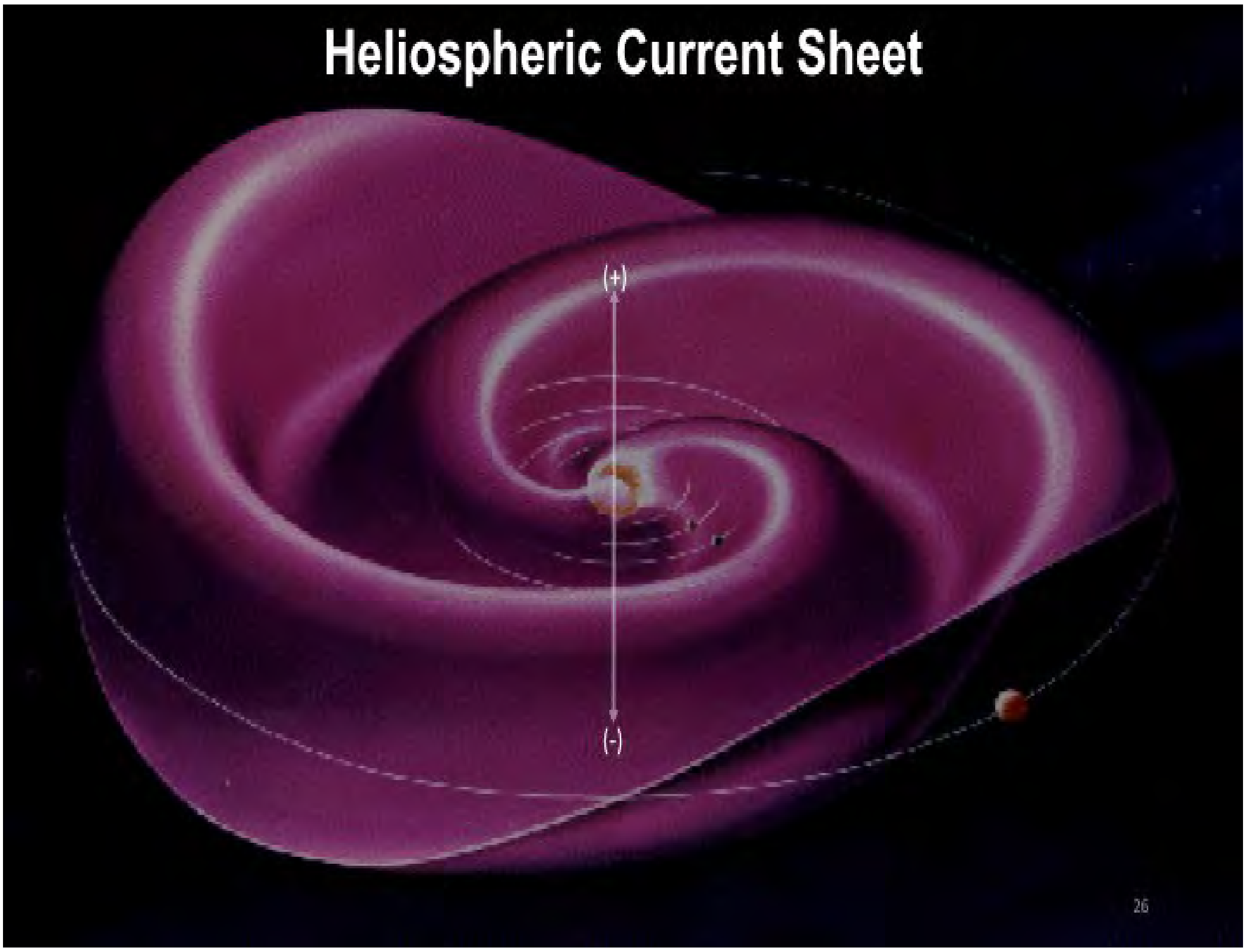

Fig. 1. The warped Heliospheric or Birkeland current sheet in the inner solar system (inside of 6 AU). The surface divides the heliospheric magnetic field into two regions with oppositely directed field lines. The surface is here shown for a 4-sector structure at a time intermediate between solar minimum and solar maximum.

It appears from historical geology, archeology, astronomy, and mythology, the ancients may have previously uncovered this knowledge beforehand or perhaps were informed by more highly evolved or intelligent life forms. Perhaps these mysteries will eventually be resolved, but how has this science evolved in more modern times? How did we recently take steps toward the "Earth as a Stellar Transformer" as more than an intellectual concept?

SCIENTIFIC BREAKTHROUGH:

In 2015, the Stellar Transformer breakthrough was recognized when John Quinn's magnetic modeling (Quinn, 1997 and 2010) of Earth's polar magnetic anomalies (considered as a z-pinch, Peratt, 1992) aligned with polar Delta – Y electrical circuit configurations (**Figs. 2a and 2b**).

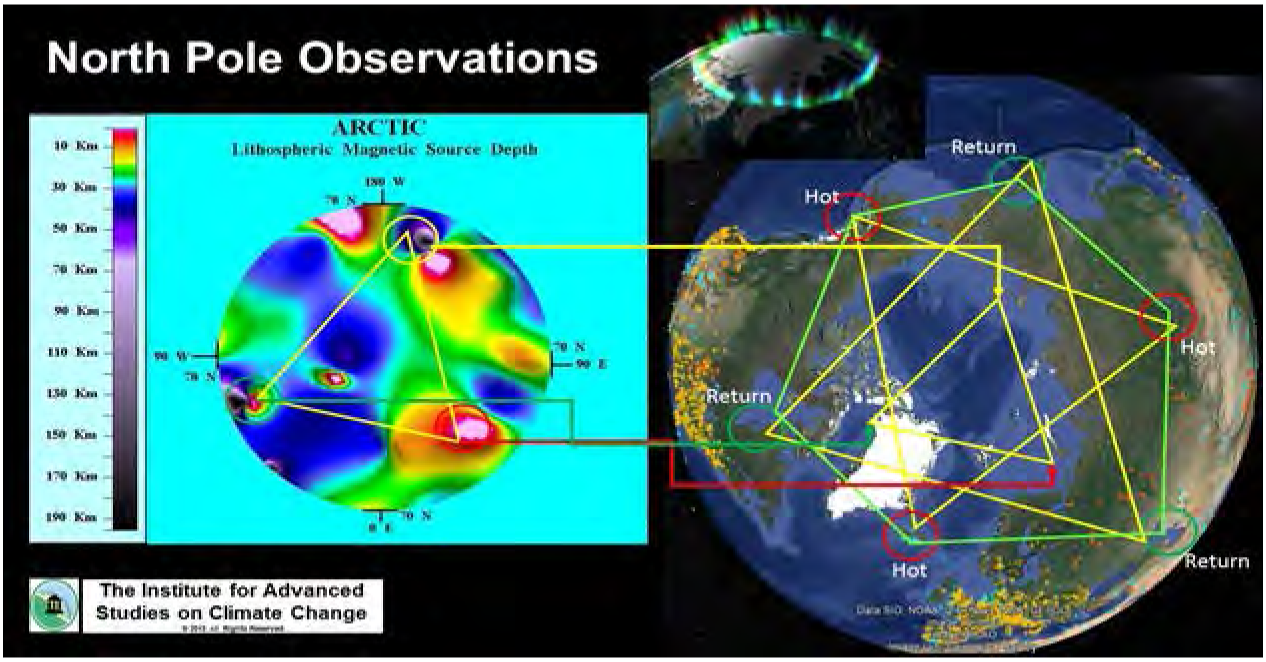

Fig. 2a. North Pole Observations of Delta Circuit Patterns with Co-Rotating Double Layers resembles hex star pattern. Inner Delta circuit connects magnetic anomalies and creates Artic depression along the Gakkel Ridge. Delta Hot Circuit (Red circles) connects 3 tectonic features electrically modulating Pacific Decadal Oscillation (PDO) a 30-35 year oscillation controlling global temperature trends and Icelandic Low part of the North Atlantic Oscillation (NAO) between Iceland and the Azores controlling European weather patterns. Delta Return Circuit (Green Circles) seems connected to Hudson Bay, Caspian Sea and the Northern tip of Kamchatka, where the Hawaiian Island elbow also connects, providing pathways to the core.

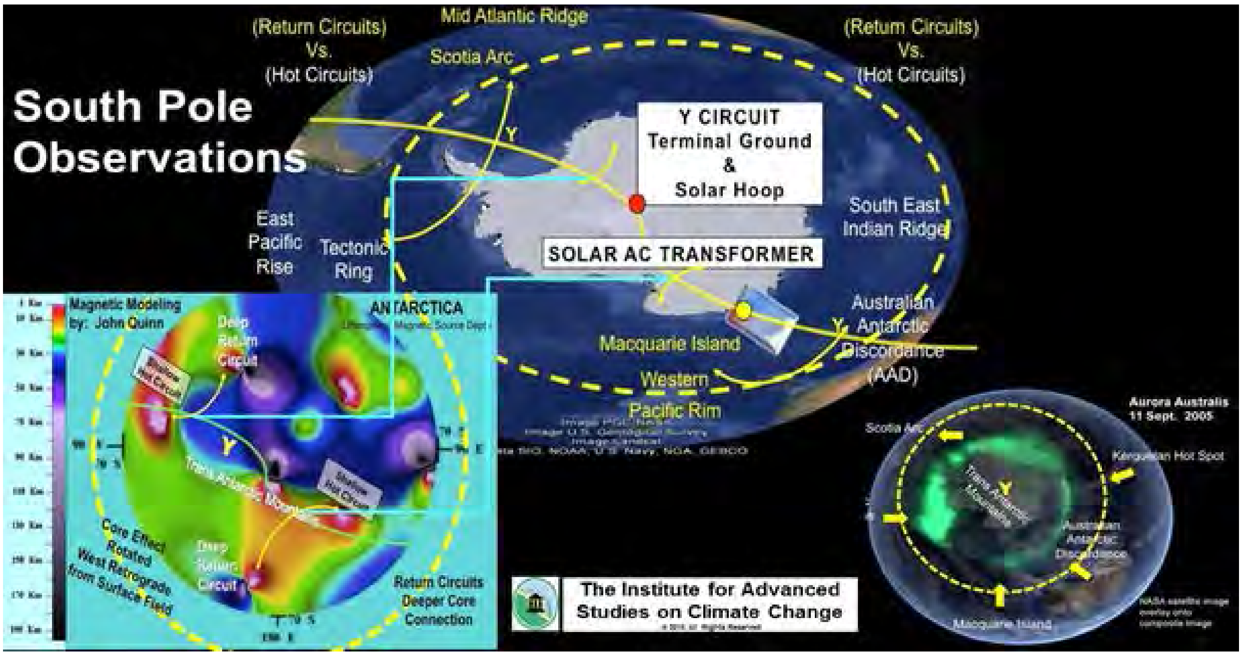

Fig. 2b. South Pole Observations of Y circuits of the Southern Aurora Australis Listed features on the ridge ring are indicated in yellow and are considered as surface expression of Gregori's theoretical Joule Antennae. Aurora Australis occurs within the ionosphere around 350 km altitude, and is shifted toward Australia likely because of proximity of the south magnetic pole to the Australian Antarctic Discordance. Bright spots around the tip of South America are the most likely tesla stream induction centers (Leybourne, Davis) at time this image was taken, indicating the Interplanetary Magnetic Field (IMF) as likely charging point. Magnetic modeling by John Quinn shows the structure in lithospheric magnetic source depths along "Joule Antennae" locations characterized by Davis and Gregori. These indicate magnetic "circuits" connected to inner core. The "hot circuits" have a different configuration than the return circuits. The return circuits have a large depth differential, while the "hot" circuit has a smooth and gradual depth differential.

These circuit geometries align with Earth's tectonic mantle gravity signatures (**Fig. 3**) exhibiting global temperature anomalies (**Fig. 4**).

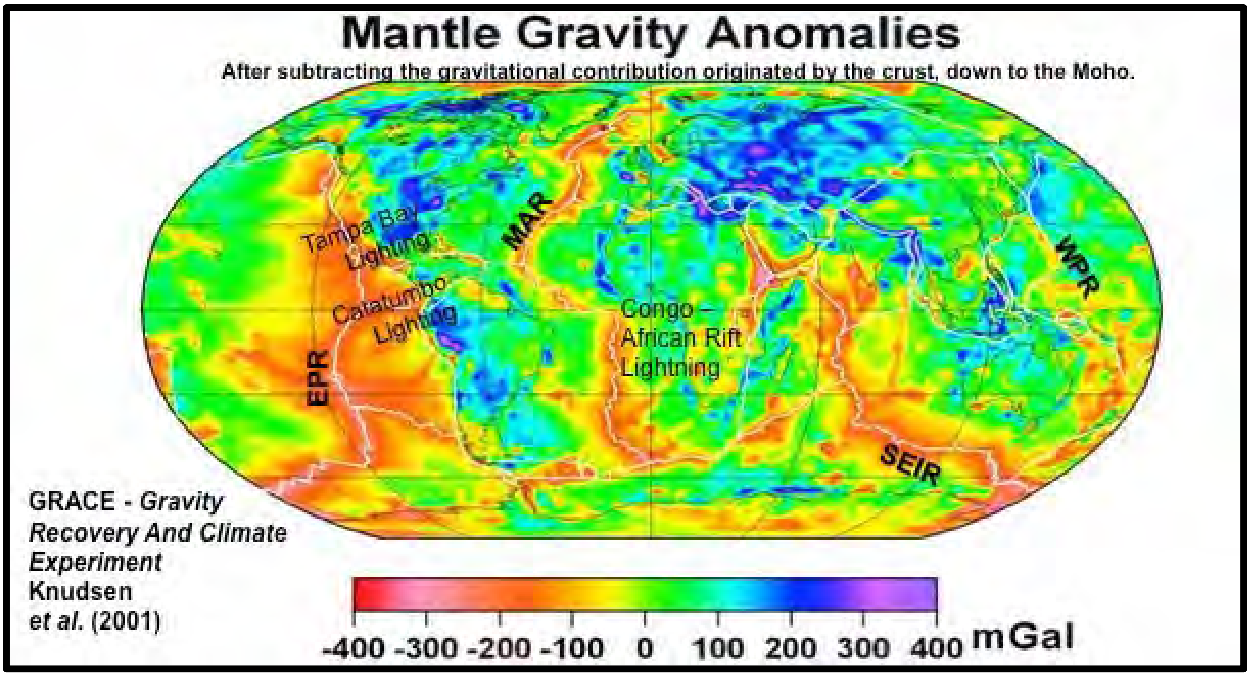

Fig. 3. Mantle Gravity from GRACE satellite mission data indicates mantle circuit continental connections to Catatumbo, Tampa Bay and African Rift/Congo global lighting anomalies. The EPR inline and SEIR global gravity signatures exhibit a classic collapsed the vortex structure discussed by IASCC's YouTube Electric Universe 2016 video "Geometry of Earth's Endogenous Energy: Geophysical Evidence". Also see: Fig. 5: Mantle gravity anomalies [mGal] calculated by subtracting from observed gravity (EIGEN-GRACE01S) the crustal gravity effect including topography (bathymetry) and crustal density variations down to the Moho boundary

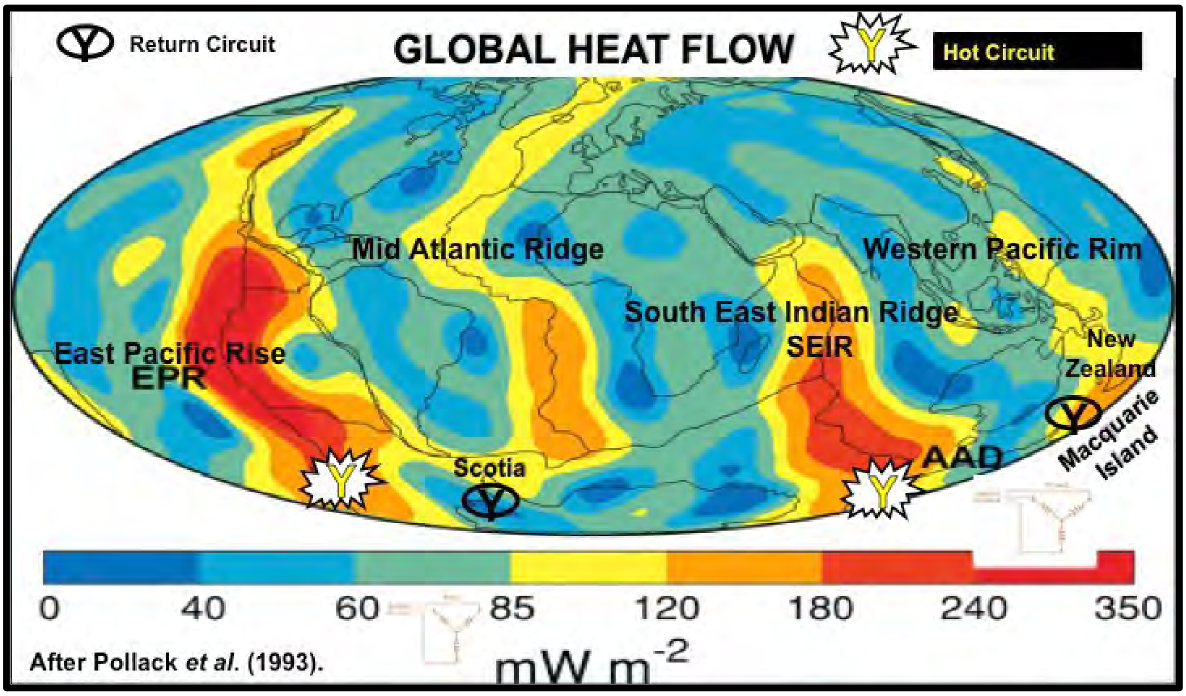

Fig. 4. Global Heat flow from Induction heating along the ridges occurs with 3-phase 40 day AC power from solar rotation. This effect alternatively heats the Southeast Indian Ridge (SEIR) when the Interplanetary Magnetic Field (IMF) is positive, and then shifts to the East Pacific Rise when IMF turning negative. The return circuitry for the Australian Antarctic Discordance (AAD) is along the Western Pacific Rim via New Zealand while return circuitry for the East Pacific Rise is along the Mid-Atlantic Ridge. The secondary DC conversion occurs in the upper Y circuit charges the core. This induction charging, effects ionosphere attraction stimulating lightning and storms or alternatively during discharging supplies a steady flow of energy like a battery to certain volcanoes as a tidally driven process. Modified after Pollack et al. (1993).

These electric circuit relationships seem to confirm a theoretical transformer ring-to-ring step down energy circuit observed from polar plasma rings (**Fig. 5**). The mid-ocean ridge encircling Antarctica (**Fig. 6**) connects with the deeper concentric spherical configurations of Earth's inner and outer core. Polar auroras seem to reflect relative positions of the inner/outer core relationship, while intense aurora bright spots (yellow & orange in **Fig. 5**) within the auroras signal energy transfers between Earth's circuitry. While these relationships or this particular scientific hypothesis has yet to be confirmed by "scientific authorities", the interrelationships between these geophysical datasets has a certain self-evident quality that a knowledgeable or reasonable person may base their own conclusions.

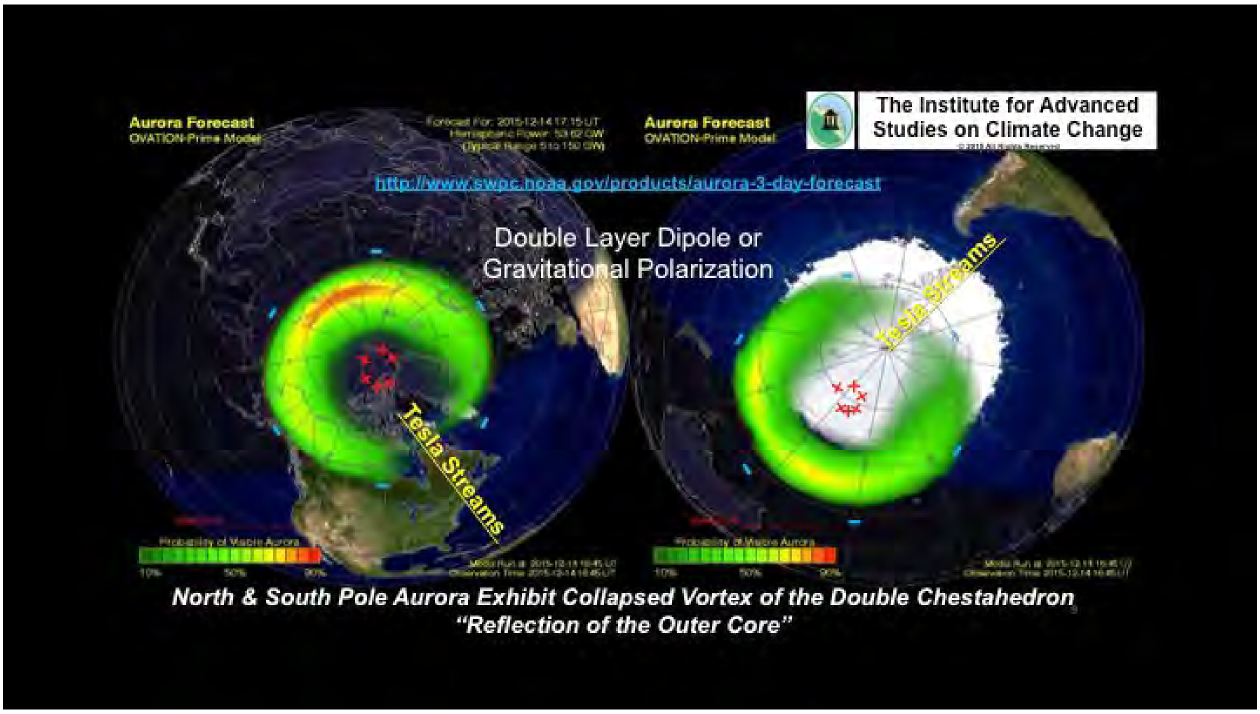

Fig. 5. Polar Aurora seems to have a Relation to Earth's Core. Polar Aurora exhibit collapsed vortex signature in plasma ring currents. Aurora appear to be a reflection of the inner and outer core, notice inner core signature (lack of aurora) stays attracted toward the daytime Sunny side, while collapsed vortex signature (active aurora) points toward midnight away from the Sun on both poles. Is this simply an influence of the solar wind, or is there a deeper core affect linked to this signature? Likely both influences are active. As the Earth spins, the inner stays attracted toward Sun, while induction currents within Tesla streams in the Aurora and Earth's core interacts with circuits in the mantle.

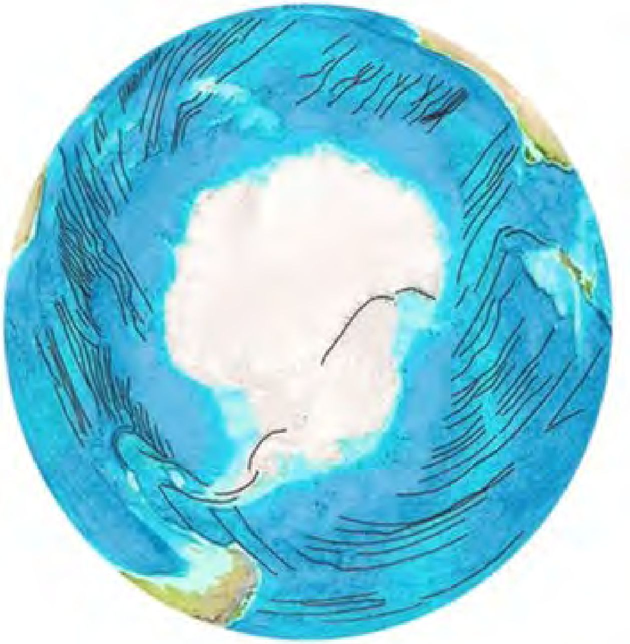

Fig. 6. Polar stereographic projection of the Southern Ocean region with structural features, such as fracture zones and mountain ranges portrays the ridge encircling Antarctica outlined in black (Smoot, 2015).

THEORETICAL CONSTRUCTS:

To better understand these insights, we need to review Quinn's magnetic modeling (Fig. 7, Quinn, 1997) as understood in terms of Giovanni Gregori's "Sea Urchin" model (Fig. 8) wonderfully described in his book "Galaxy-Sun-Earth Relations. The origin of the magnetic field and of the endogenous energy of the Earth, with implications for volcanism, geodynamics and climate control, and related items of concern for stars, planets, satellites, and other planetary objects." (Gregori, 2002). In **Fig. 7**, Quinn's inverse harmonic magnetic modeling techniques showcase anomalies aligned with geologic hotspots, tectonic triple junctions and climate oscillation centers. While Gregori's endogenous electrical "Sea Urchin" energy model in **Fig. 8** provides a framework to understand and support Quinn's magnetic modeling data. Gregori also includes a host of observational evidence outlined in his volume of works related to earthquakes, volcanoes, environmental and astronomical observations (Gregori, 2002 and 2006). In order to explore these relationships, an earlier synthesis transpired before tectonic electromagnetic relationships were explored. Without this earlier stage, no breakthrough discoveries of this kind would be forthcoming.

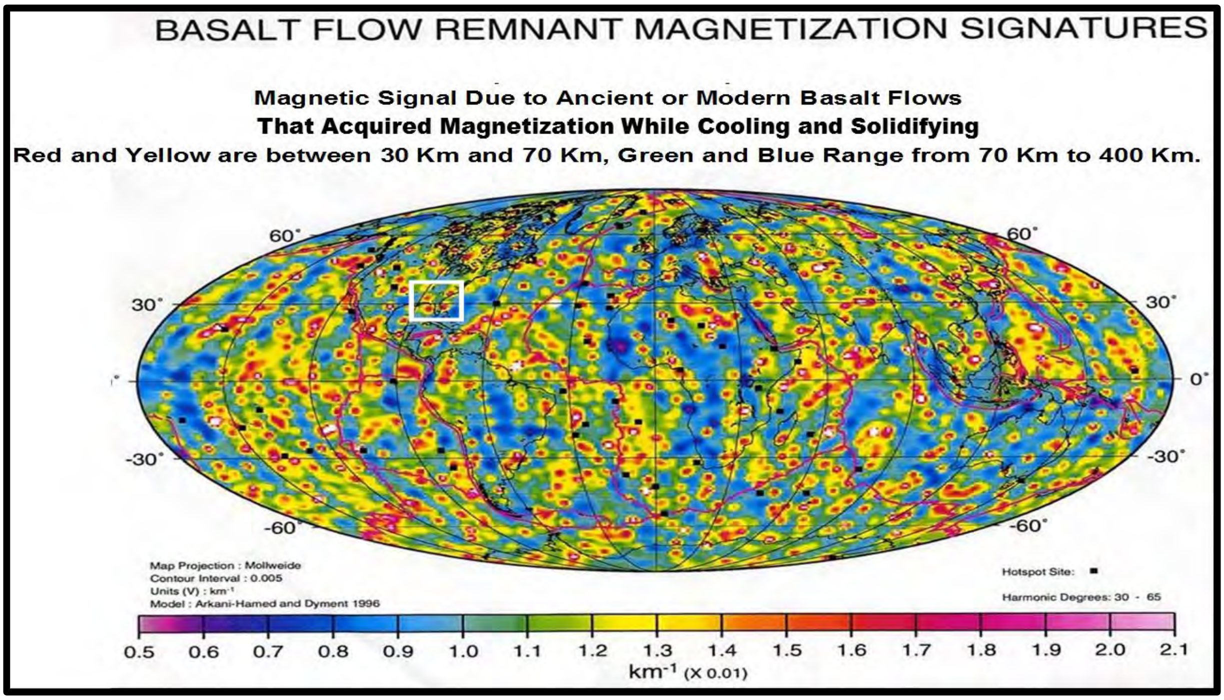

Fig. 7. Quinn's Remnant Magnetization Signatures are considered the tips of Gregori's "Sea-urchin Spikes" within the Endogenous Earth Energy theoretical framework. Some may also be meteorite impacts. White square indicates ancient features in Southeast U.S. likely associated with Triassic Rifting. (Courtesy - John M. Quinn, Solar- Terrestrial Environmental Research Institute (STERI)).

Quinn's Remnant Magnetization Signatures are computed as the ratio of the total geomagnetic- tensor-intensity to that of the total geomagnetic vector-intensity. This image (**Fig. 7**) was generated from by John Quinn and distributed around the geomagnetism community in 1997. **Figure 7** was computed from the MAGSAT satellite model of Hamed and Dyment using spherical-harmonic degrees-and-orders between nm=30 and nm=60. This geomagnetic ratio parameter is described in more detail by Quinn and Shiel, (1993a). An application using their prism technique in combination with regional rectangular-harmonic modeling is given by Quinn and Shiel (1993b), while an example of the combined use of magnetic source-depth inversion using prisms with global spherical harmonic modeling is given by Quinn (2017).

The geomagnetic field model referred to in the legend on the bottom left-hand side of **Figure 7** was generated from MAGSAT satellite data by Arkani-Hamed and Richard Dyment (1996). It was a degree-and order-90 geomagnetic-field model. During the first decade of the 20th century a much higher resolution spherical-harmonic geomagnetic-field model was generated from CHAMP satellite data to degree-and-order 720 (Maus et. al., 2008). The most recent global, geomagnetic, spherical-harmonic-field model has been derived from the SWARM set of satellites (Olsen et. al., 2015).

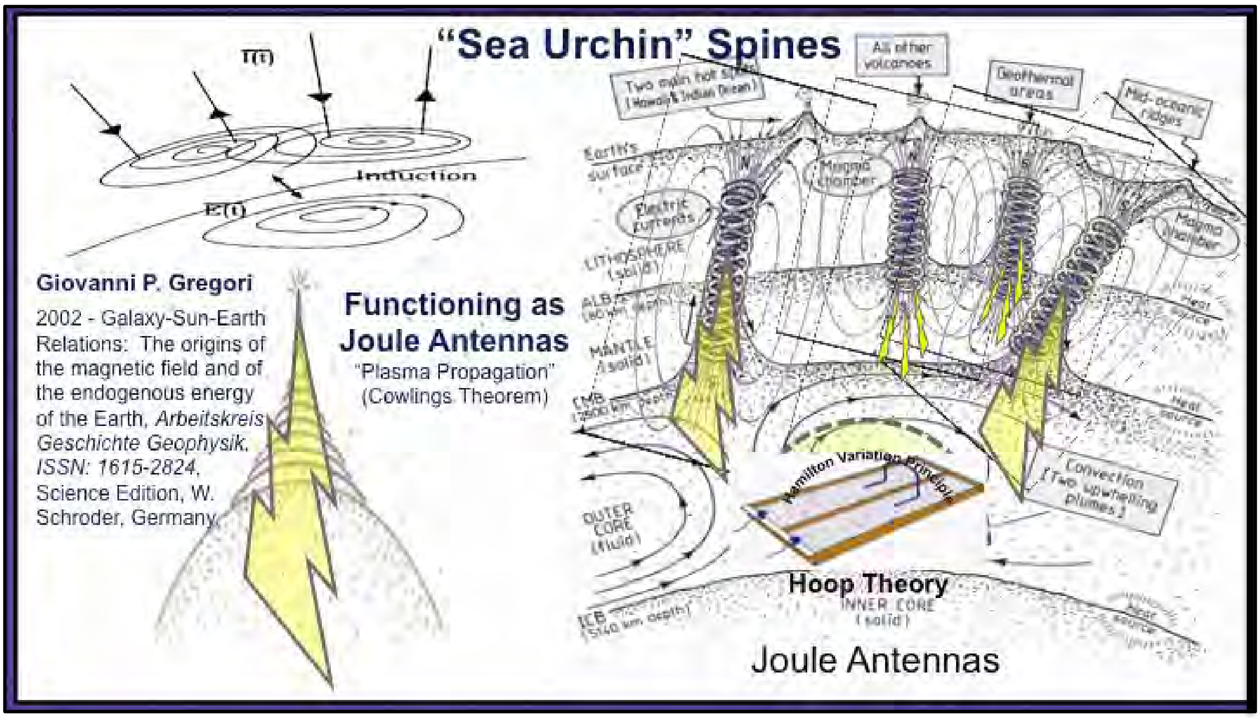

Fig. 8. Earth "Internal" Sea Urchin Spine… Antenna model by Giovanni Gregori proposed in his 2002 book, "Galaxy-Sun-Earth Relations: The origins of the magnetic field and of the endogenous energy of the Earth". Introduces the concept of electrical potential joule spikes emanating from the core proposing induction processes along antennae or spines connecting the core to the surface electrically. Using a model similar in nature to a "sea- urchin", Gregori explains the propagation of electrical "Joule" energy along these "sea urchin" spines to Earth's core and geologic hotspots around the globe. Joule energy in this sense means "electrical energy" at termination this results in heat, like a toaster or oven element, i.e. a "shorted circuit". Induction mechanism is the key to internal forcing. Davis characterizes this process as an electrical weather pattern or "Tesla Climate", meaning the electrical induction and discharge circuitry has a substantial and transformative energy affect on the Earth's atmospheric and tectonic processes.

EARLIER THEORETICAL CONSTRUCTS:

Evolution of "Earth as a Stellar Transformer" originated by considering the scientific dilemma behind plate tectonic theory's failure to explain a link uncovered between El Niño's with the occurrence of six-month precursor earthquakes in the Pacific Basin by Daniel Walker. To address this mystery, a useful framework for investigating this scientific dilemma was considered. The concept of "Surge Tectonics" (Meyerhoff, 1992 and 1996) reveals an interesting relationship between tectonic energy releases and climate dynamics (Leybourne, 1998a, 1999, 2001 and 2002).

Observations were made that atmospheric pressure centers of the primary climate oscillation indexes, such as El Nino Southern Oscillation (ENSO – Leybourne and Adams, 1999 and 2001) align directly over huge physical planetary tectonic vortex structures with significant magnetic and gravity signatures. "Surge Tectonics" (Meyerhoff, 1992, 1996) explain plate tectonic triple junctions in terms of intersecting flows of "tectonic mantle structures" that twist into vortex like columns. Traversing along and underneath the plate boundaries, "surge channels" flow into downward and upwelling spinning spirals (Smoot and Leybourne, 1997 and 2001) similar to jet streams exerting control of high and low pressure cells in the atmosphere. These "Tectonic Vortexes", Gregori's "Sea Urchin Spikes", Quinn's "Magnetic Anomalies" contain induction field energies linked to Solar and Earth Stellar Transformers. These contribute to the electromagnetic attraction or repulsion driving ionospheric disturbances and related atmospheric pressure oscillations, originally introduced as gravitational teleconnections (Leybourne in 1996 and 1997).

The original concept of gravitational teleconnection suggested that released thermal energy from increased earthquakes created density changes concentrated within tectonic vortex structures as the driver of atmospheric oscillations driving climate change (Leybourne, 1998). There were early objections to this influence on thermal convection concept. Conventional scientific corners insisted that "geologic processes" took place over a very long time spans and did not possess the capacity to affect short-term climate drivers or weather patterns. At the time, this was a reasonable objection using simplified plate tectonic theory, which purported that the mantle plumes and Hadley Cell like circulation convection actions underneath tectonic ridges, took eons to rise through the mantle driving plate motions.

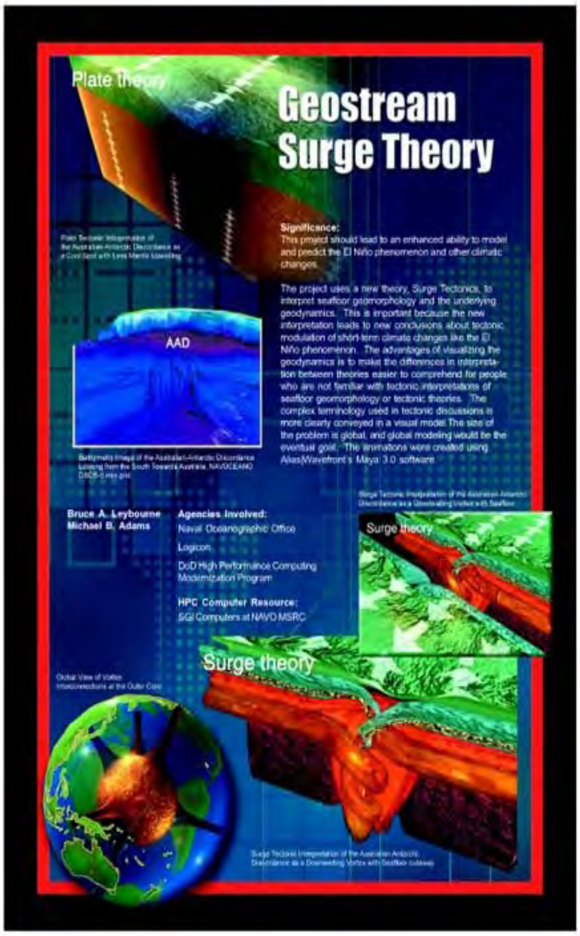

Fig. 9. NAVOCEANO –MSRC Viz Lab) Surge Theory Visualized by Bruce Leybourne

Using an airflow analogy, comparing an atmospheric Jetstream to a "Geostream" can be made to help visualize this phenomenon (**Fig. 9**). Given that this analogy holds true, it is a fairly simple step to appreciate how electrical charge, or joule energy associated with gravity density changes within tectonic vortex structures may transform climate through geo-electric processes of the Stellar Transformer. This dramatically influences density changes in the atmosphere directly above them like a spring altering pressures in the atmosphere.

Once you consider electrical transfer of induction energy from the earth's core ingested from solar energy through the magnetic poles, the slow "geologic processes" objection easily disappears as the geo-electro-mechanical driver becomes more evident during large solar storm impacts on our planet. The concept of Stellar Transformer electrical driver connecting solar activity, space weather and earth electrical capacitance is more probable once this consideration is incorporated into solar energy impact models as they affect large-scale natural hazards such as hurricanes and earthquakes.

CLIMATE CHANGE CONNECTION:

Solar induced electro-magnetic forces influencing the earths own internal magneto-dynamo and tectonics is likely a governing agent on earth's climate change. This is supported by early stellar dynamo pioneers such as Joseph Larmor, Thomas Cowling and Subrahmanyan Chandrasekhar and Eugene Parker bringing space energy concepts such as "cosmical magnetohydrodynamics" ushering in the study of "space weather" starting with the solar wind.

In recent years, the characterization of magnetic reconnection from the Sun to the earth as undergone rapid transformations from the steady state Sweet–Parker model to seemingly unpredictable stochastic plasmoid chains offered by plasma physicist N.F. Loureiro and D.A. Uzdensky.

Leybourne and Davis believe that episodic electrical discharges from the core (along with attendant magnetic earth field changes) linked to solar winds and changes in the solar gravitational/magnetic fields substantially influences earth's climate. These episodic electrical discharges result in joule heating (Giovanni, 2001) and other phenomenon in the upper mantle at hotspot/rift, certain ridge, trench and other locations. This in turn yields episodic seismicity, and hydrothermal venting of such significance to influence short-term climate patterns. More specifically these events generate change in ocean and atmospheric circulation patterns, temperatures, and atmospheric pressure oscillations.

The earth magnetic moment decay curve (**Fig 10**, Quinn) demonstrates a correlation between velocity changes in the magnetic moment decay to changes in ocean warming, specifically El Nino and the Pacific Decadal Oscillation (PDO). These correlations appear to capture every major El Nino of the past century. The slope of the magnetic dipole moment % decay trend (**Fig. 10**, Quinn) related to solar magnetism provides global switching components related to climate power and momentum linked to decadal El Nino/La Nina, Southern Oscillation (ENSO) cycles, and longer centennial 20-30 year global warming/cooling trends such as the Pacific Decadal Oscillation (PDO, **Fig. 10**).

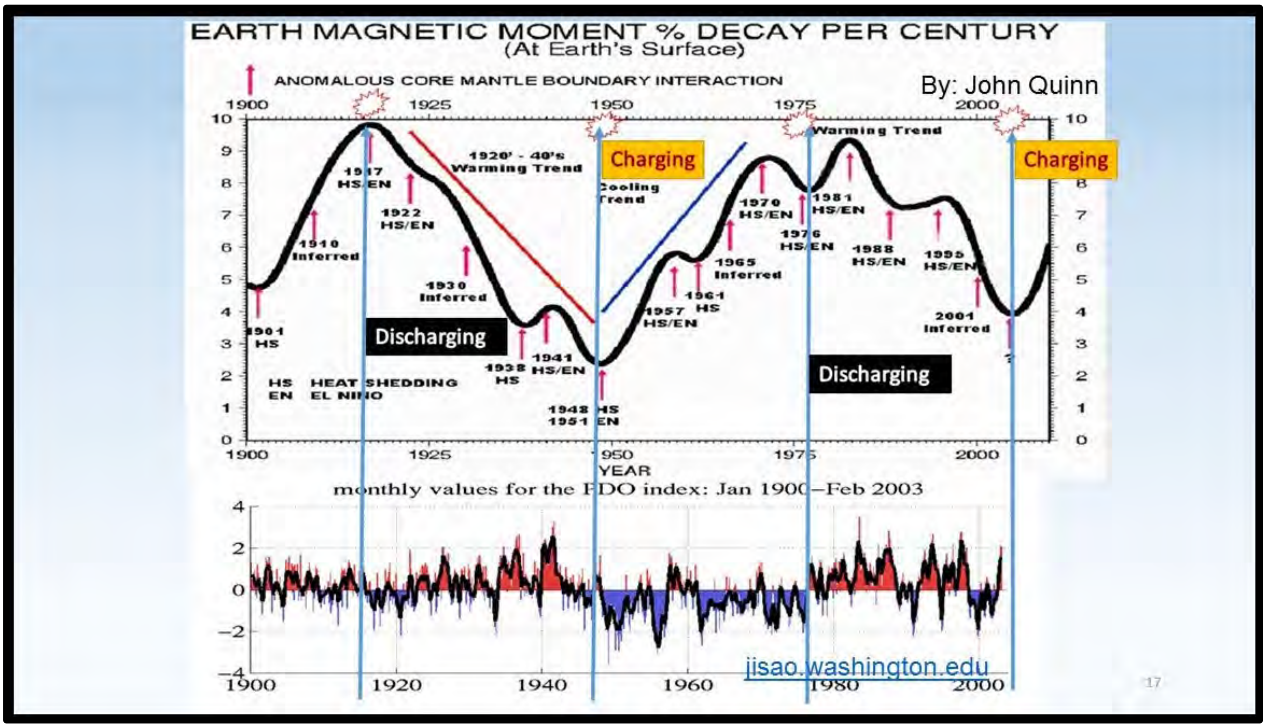

Fig. 10. Scientific Basis for Solar Magnetism Direct Climate Modulation. Major Trends in the Decay Rate of the Earth's Magnetic Moment (IAGA, 2000 - Models Compiled by Quinn, Climatologic Inputs by Leybourne and Orr) Correlate to Long Term Warming/Cooling Trends. Warming 1920-1940 Cooling in the 1950-1960's until a Second Warming Trend in the 1970's reflect the trends of the Pacific Decal Oscillation (PDO). Inflection Points Correlate as Precursors to Strong El Nino Events, Surface Magnetic Pulses and Inner Core Jerks, as evidenced in the 1971 Great Pacific Warming Event.

POPULAR CLIMATE CHANGE:

There is no mention CO_2, as a driving factor or even a lagging indicator, but climate scientist cannot escape the topic. It is a well-documented fact that carbon dioxide and methane out gassing is common with fossil fuel mining, energy exploration, water drilling, hydrothermal venting, and volcanic eruptions. These outgasses are associated with the Earth's physical and chemical transformation during joule heating energy release mechanics. Traditionally CO_2 and CH_4 levels are considered lagging evolutionary indicators of global warming in accordance with ice core data and modern records (Quinn, 2010). Milankovitch cycles (Serbian geophysicist and astronomer Mutin Milankovic, 1920's) consider orbital physics of eccentricity, axial tilt and precession as the main drivers of long-term climate cycles as seen in the ice and sediment core data (Leybourne, 1998c). It is difficult to understand how CO_2 and CH_4 drive climate change if they are laggards to global warming episodes in documented climate data. Regardless, we are not attempting to support or debunk carbon dioxide as a driver or indicator of human impacts on climate change.

IASCC MISSION:

Our mission at the institute of advanced studies on climate change IASCC is to improve the deeper understanding of climate change by collaboration among the greater scientific research communities. We want to encourage multi-disciplinary research studies to expand the climate change knowledge base, and implement an improved understanding into global short and long range space weather, communications, earth weather, earthquake and climate modeling, mapping, and forecasting systems.

We believe that the concept of Earth as a Stellar Transformer (EAST) is one of many possibilities of the electrical affect that impacts the earth's large-scale natural drivers and has an effect of risk forecasting and high-energy disaster prediction.

AFFILIATED RESEARCH:

One of the associated groups IASCC collaborates with is the Suspicious Observers (SO). They have a daily YouTube webcast along with other information and historical observations exhibiting examples of these phenomena. Another independent research group we enjoy working with is the Electric Universe (EU) - Thunderbolts Project (Thornhill and Talbott, 2007) who explains some of these relationships in broader scales as interacting plasma fields (Peratt, 1991). They discuss many relationships between solar activity and the larger environment.

The International Earthquake and Volcano Prediction Center (IEVPC) conducts ongoing research successfully forecasting some of these natural hazard events based on solar activity and other methods. New Concepts in Global Tectonics (NCGT) has supported this area of research for over two decades, and publishes related articles many which would stand no chance of passing a conventional scientific "peer review" due to the controversial nature of the subject matter. Many other sites, including the National Philosophy Alliance (NPA), individual researchers, other research institutes, international and governmental agencies, too many to list here, contain and have exposed useful knowledge related to this area of science.

INDEPENDENT COLLABORATION:

The IASCC is always interested in entertaining and enabling collaboration, as part of our mission at the Institute of Advanced Studies in Climate Change. If you would like to join the conversation and contribute your specific thoughts or body of research for consideration and inclusion, please review "about us" on our website. www.iascc.org

References:

Dziewonski, A.M., 1984. Mapping the lower mantle: Determination of lateral heterogeneity in P-velocity up to degree and order 6. *Jour. Geophys. Res.,* v. 89, p. 5929-5952.

Gregori, G.P., 2002. Galaxy – Sun – Earth relations. The origin of the magnetic field and of the endogenous energy of the Earth, with implications for volcanism, geodynamics and climate control, and related items of concern for stars, planets, satellites, and other planetary objects. A discussion in a prologue and two parts. *Beiträge zur Geschichte der Geophysik und Kosmischen Physik*, Band **3**, Heft 3, 471p.

Gregori, G.P., 2006. Galaxy-Sun-Earth relations: the origin of the magnetic field and of the endogenous energy of the Earth, with implications for volcanism, geodynamics and climate control and related items of concern for stars, planets, satellites, and other planetary objects. *NCGT Newsletter*, no. 38, p. 34-36.

Jafar Arkani-Hamed, 1996. Magnetic Anomalies Modeling. *Springe*r, p. 485-490.

Knudsen, P., Andersen, O., Abbas Khan, S. and Høyer, J., 2001. Ocean tide effects on *GRACE* gravimetry, 8p. Sideris, M.G. (ed.), 2001. Gravity, geoid, and geodynamics 2000, *IAG Symposia,* **123**, 398p., Springer-Verlag, New York. http://op.gfz-potsdam.de/grace/results/

Leybourne, B.A., 1996. A tectonic forcing function for climate modeling, *EOS, Transactions, American Geophysical Union, Western Pacific Geophysics Meeting*, 1996, May 28th supplement, #A42A-10.

Leybourne, B.A., 1997. Earth-ocean-atmosphere coupled model based on gravitational teleconnection. Proc. Ann. Meet. *NOAA Climate Monitoring Diag. Lab*. Boulder Co. March 5-6, 1997, p. 23. Also: *Proc. Joint Assemb. IAMAS-IAPSO*. Melbourne, Australia. July 1-9, 1997. JPM9-1.

Leybourne, B.A., 1998a. Mechanism of vortex gravity/density oscillation. *New Concepts in Global Tectonics Newsletter*, 1998, Mar., no. 6, p. 6-8.

Leybourne, B.A., 1998b. "Can El Nino be controlled by tectonic vortex structures and explained with surge tectonics?". *New Concepts in Global Tectonics Newsletter*, no. 6, p. 5-6.

Leybourne, B.A., 1998c. Gravitational Teleconnection, and Milankovitch Series Correlations Implications of Surge Tectonics. *New Concepts in Global Tectonics Newsletter*, no. 7, p. 8.

Leybourne, B.A., 1999. Surge theory vs. plate theory: El Nino has the last word - A theoretical discussion of the driving forces behind El Nino. *New Concepts in Global Tectonics conference proceedings* at Tuskba Research Center, Japan, Nov 1998. And *New Concepts in Global Tectonics Newsletter*, 1999, Mar., no. 10, p. 19-32

Leybourne, B.A., 2001. Surge hypothesis implies gravitational teleconnection of tectonics to climate. New Concepts in Global Tectonics, *Wadia Institute of Himalayan Geology*, Dehradun, India, v. 22, no.1, 2001, p. 139.

Leybourne, B.A., 2002. Surge theory weighs in on the balance of evidence in the debate on global warming. *Global Warming XII Abstracts*, Cambridge, UK. *World Resource Review*, p 167-188, June 2002.

Leybourne, B.A. and Adams, M.B., 1999. Modeling mantle dynamics in the Banda Sea triple junction: Exploring a possible link to El Nino Southern Oscillation. *Marine Technology Society Oceans '99 Conference Proceedings, Seattle*, Washington. p. 955-966, Sept., 1999.

Leybourne, B.A. and Adams, M.B., 2001. El Nino tectonic modulation in the Pacific Basin. *Marine Technology Society Oceans '01 Conference Proceedings,* Honolulu, Hawaii, Nov. 2001.

Leybourne, B. A. and Smoot, N.C., 2005. Tectonic Links to the Global Oscillation System: A Unification Concept of Climate Modulation by Internal Joule Heating Teleconnections. *AGU Chapman Conf. on Tropical-Extratropical Climate Teleconnections*, Hawaii.

Maus, S., Yin, F., Manoj, C., Rother, M., Raugerg, J., Michaelis, J., Stolle, C. and Mueller, R.D., 1991. Resolution of Direction of Oceanic Magnetic Lineations by the Sixth Generation Lithosphere Magnetic-Field-Model from CHAMP Satellite Magnetic Measurements. *Geochemistry, Geophysics, and Geosystems*, v. 9, no. 7.

Milankovitch (Milankovic), M., 1941. Kanon der Erdbestrahlungen und seine Anwendung auf das Eiszeitenproblem Belgrade. (English Translation - Canon of Insolation and the Ice Age Problem. Belgrade), Zavod za Udžbenike i Nastavna Sredstva. ISBN 8617066199.

Olsen, N., Hulot, G., Lesur, V., Finlay, C.C., Beggan, C., Chulliat, A., Sabaka, T.J., Floberghagen, R., Ffrisd-Christensen, E., Haagmans, R., Kotsiaros, S., Lühr, H., Toffner-Clausen, L. and Vignern, P., 2015. The Swarm Initial Field Model For the 2014 geomagnetic field; *AGU Fall Meeting* (2014) and *Geophysical Research Letters*, p. 1092-1098, v. 42, no. 4.

Peratt, A., 1992. *Physics of the Plasma Universe*. Springer-Verlag, 372p.

Pollack, H.N., Hurter, S.J. and Johnson, J.R., 1993. Heat flow from the earth's interior: analysis of the global data set. *Reviews of Geophysics*, v. 31, no. 3, p. 267-280.

Quinn, J. and Shiel, D., 1993a. A unified approach to geopotential field modeling. U. S. Naval Oceanographic Office, Technical Report No. TR-308.

Quinn, J. and Shiel, D., 1993b. Magnetic Field Modeling of the Northern Juan De Fuca and Explorer Plates, U. S. Naval Oceanographic Office, Technical Report No. TR-309.

Quinn, J.M., 1997, Use of satellite geomagnetic data to remotely sense the lithosphere, to detect shock-remnant-magnetization (SRM) due to meteorite impacts and to detect magnetic induction related to hotspot upwelling. *International Association of Geomagnetism and Aeronomy*, Uppsala, Sweden. Aug. 1997.

Quinn, J.M., 2010. *Global Warming: Geophysical counterpoints to the enhanced greenhouse theory*. Dorrance Pub., 118p.

Quinn, J.M., 2017. Global remote sensing of Earth's magnetized lithosphere, *Solar-Terrestrial Environmental Research Institute (STERI)*.

Quinn, J.M. and Leybourne, B.A., 2010. Jerks as guiding influences on the global environment: Effects on the solid Earth, its angular momentum and lithospheric plate motions, the atmosphere, weather, and climate. *American Geophysical Union San Francisco Annual Fall Meeting*, 13-17 Dec. 2010 (A33A-0152).

Smoot, N.C., 2015. *Marine Geomorphology 3rd Edition* (Mindstar, Portsmouth), 265p.

Smoot, N.C. and Leybourne, B.A., 1997. Vortex structures on the world-encircling vortex street: Case study of the South Adriatic basin. *Marine Technology Society Journal,* v. 31, no. 2, p. 21-35.

Smoot, N.C. and Leybourne, B.A., 2001. The Central Pacific Megatrend. *International Geological Review*, v. 43, no. 4, April 2001.

Thornhill, W. and Talbott, D., 2007. *The Electric Universe*, Mikamar Publishing (May 24, 2007), 132p.

Walker, D.A., 1988. Seismicity of the East Pacific: correlations with the Southern Oscillation Index? *EOS Trans. AGU*. V. 69, p. 857.

Walker, D.A., 1995. More evidence indicates link between El Ninos and seismicity. *EOS Trans. AGU.,* v. 76, no. 33.

Walker, D.A., 1999. Seismic Predictors of El Nino Revisited. *EOS Trans. AGU*, v. 80, no. 25.

GLOBAL CLIMATE CORNER

Sea level narratives conflict with tide gauge measurements

Albert Parker
School of Engineering and Physical Science, James Cook University, Townsville QLD 4811, Australia.
albert.parker.2014@gmail.com

ABSTRACT: While the sea level at the tide gauges are rising and falling, without any positive acceleration component, and rising on average at an everything but dramatic rate, the contributing National Academy of Science (NAS) member, the authors of the Proceedings of the National Academy of Science (PNAS) paper "*Coastal sea level rise with warming above 2 °C*" and the editorial board of PNAS wanted us to believe approaching the United States (US) Presidential elections that the sea levels may rise along the East Coast of the US of 40 cm by 2040 and even more than 2 metres by 2100. I show that the sea level by 2040 will more likely rise along the East Coast of 8.36 cm on average (minimum 4.40 cm and maximum 14.83 cm), while along the West Coast it will fall of -3.08 cm on average (maximum rise 11.50 cm, maximum fall -43.98 cm), and by 2100, the differences in between sea levels forecasted based on measurements and predicted following a narrative will further expand.

Keywords: *climate change, sea levels, sea level rise, sea level acceleration, cherry-picking*

(Received 2 December 2016. Accepted 17 February 2017)

EXPERIMENTAL SEA LEVEL EVIDENCE VS. "THE NARRATIVE"

Jevrejevaa, Jackson, Riva, Grinstede and Moore (2016) claim that the 2 °C of global warming above the preindustrial level is an appropriate threshold beyond which climate change risks become unacceptably high and this threshold is likely to be reached between 2040 and 2050 for both Representative Concentration Pathway (RCP) 8.5 and 4.5. They claim the resulting sea level rises will not be globally uniform, even if they neglect the role of subsidence or isostasy, due to ocean dynamical processes and changes in gravity associated with water mass redistribution. They predict that with a 2 °C warming by 2040, more than 90% of coastal areas will experience sea level rise exceeding the global estimate of 0.2 m, with up to 0.4 m along the Atlantic coast of North America. They also predict that with a 5 °C rise by 2100, the sea level will rise 0.9 m median, but 80% of the coastline will exceed the global sea level rise at the 95th percentile upper limit of 1.8 m. Under RCP8.5, by 2100, they predict for New York sea level rises of 1.09 m, with the 95th percentile upper limit of 2.24 m, 1.93 m, and 1.92 m, respectively. The analysis of the paper is purely speculative, as the sea levels at the tide gauges are rising and falling, mostly driven by the localised subsidence or the uplift of the instrument, with on average a small rising trend without any detectable acceleration component over the last decades (Parker, 2013a & b; Parker and Ollier, 2016; Parker, 2016). The tidal gauge evidence makes unrealistic the projections.

Table 1 presents the rates of rise measured (NOAA, 2016) along the Atlantic and Pacific coasts of the United States. Previous similar surveys return about same relative sea level rises since more than a decade. Along the East (Atlantic) Coast of the United States, the most likely sea level rise by 2040 (25 years from now) is on average 83.5 mm, minimum 44.0 mm and maximum 148.25 mm. Along the West (Pacific) Coast of the United States, the most likely sea level rise by 2040 is on average -30.79 mm, minimum -439.75 mm and maximum 115.0 mm.

Figure 1 proposes the monthly average mean sea levels measured in Sewells Point, VA (largest East Coast sea level trend >60 years, minimum time window to infer realistic trends cleared of the multi-decadal oscillations, Parker, 2013a & b; Parker and Ollier, 2016; Parker, 2016) and Juneau, AK (smallest West Coast sea level trend >60 years) vs. respectively the +400 mm and +200 mm hypothesis of sea level rise by 2040. In Sewells Point, VA the sea level rises mostly because of land subsidence (Boon, Brubaker and Forrest, 2010), as in Juneau, AK it is falling mostly because of isostasy (Larsen, Motyka, Freymueller, Echelmeyer and Ivins, 2005). In the location of the largest >60 years measured sea level rise, the likely sea level rise over 40 years of this century is expected to be 18 cm. In the location of smallest >60 years measured sea level rise, the likely sea level rise over 40 years of this century is expected to be -53 cm.

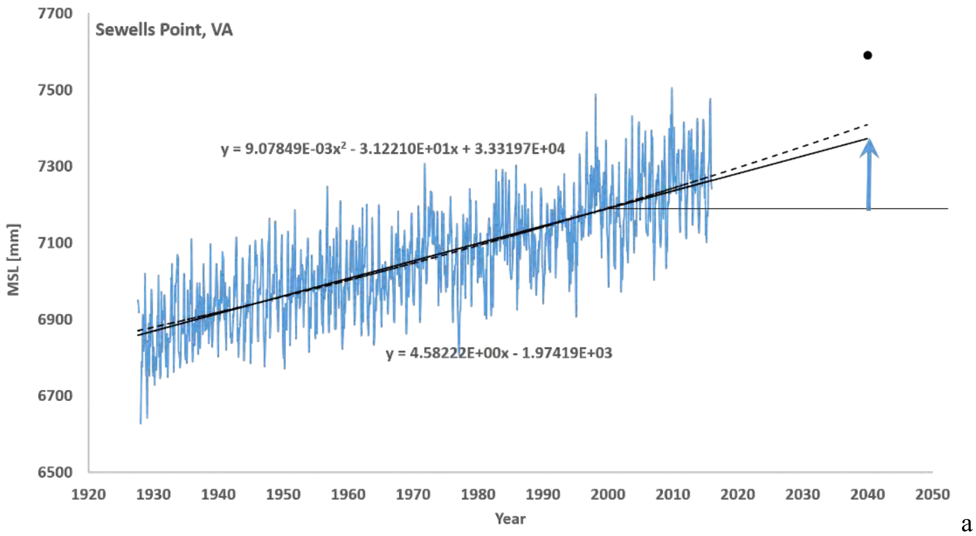

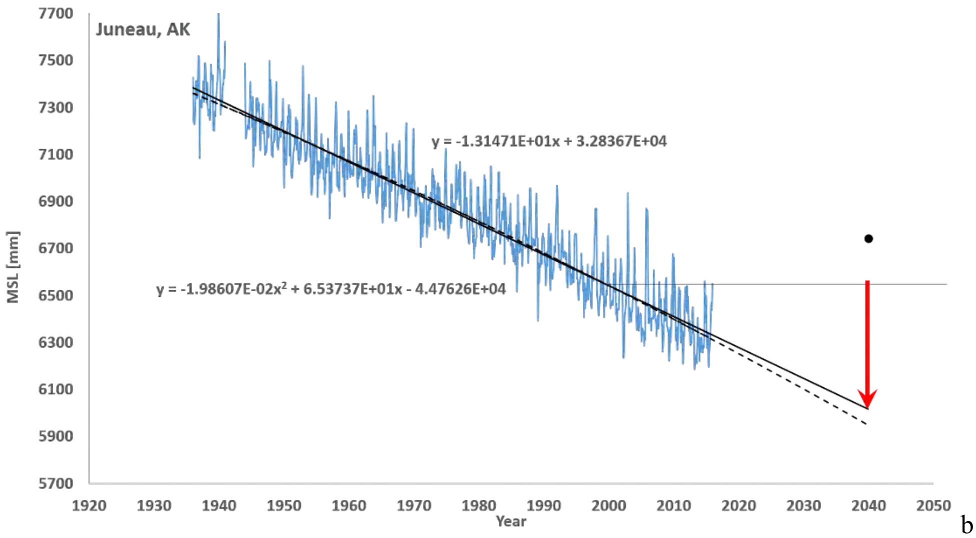

Figure 1 - Monthly average mean sea levels measured in (a) Sewells Point, VA (largest East Coast sea level trend >60 years) and (b) Juneau, AK (smallest West Coast sea level trend >60 years) vs. respectively the +400 mm and +200 mm hypotheses of sea level rise by 2040. Data from NOAA (2016).

Table 1 – Sea level rates of rise at the tide gauges of the continental US. Data from NOAA (2016).

Station ID	Station Name	First Year	Last Year	Year Range	% Comple-teness	Years to compute trend	MSL Trends (mm/yr)	likely sea level rise by 2040 (mm)
Atlantic Coast of the US								
8410140	Eastport, ME	1929	2015	86	95	81.70	2.11	53
8411250	Cutler, ME	1979	2010	31	94	29.14	2.34	59
8413320	Bar Harbor, ME	1947	2015	68	91	61.88	2.18	55
8418150	Portland, ME	1912	2015	103	99	101.97	1.87	47
8419870	Seavey Island, ME	1926	2001	75	74	55.50	1.76	44
8443970	Boston, MA	1921	2015	94	99	93.06	2.79	70
8447930	Woods Hole, MA	1932	2015	83	95	78.85	2.81	70
8449130	Nantucket Island, MA	1965	2015	50	96	48.00	3.52	88
8452660	Newport, RI	1930	2015	85	87	73.95	2.72	68
8454000	Providence, RI	1938	2015	77	87	66.99	2.22	56
8461490	New London, CT	1938	2015	77	97	74.69	2.55	64
8467150	Bridgeport, CT	1964	2015	51	97	49.47	2.81	70
8510560	Montauk, NY	1947	2015	68	93	63.24	3.21	80
8514560	Port Jefferson, NY	1957	1992	35	98	34.30	2.44	61
8516945	Kings Point, NY	1931	2015	84	20	16.80	2.50	63
8518750	The Battery, NY	1856	2015	159	90	143.10	2.84	71
8519483	Bergen Point, NY	1981	2015	34	94	31.96	4.35	109
8531680	Sandy Hook, NJ	1932	2015	83	99	82.17	4.05	101
8534720	Atlantic City, NJ	1911	2015	104	91	94.64	4.07	102
8536110	Cape May, NJ	1965	2015	50	91	45.50	4.54	114

8545240	Philadelphia, PA	1900	2015	115	22	25.30	2.93	73
8551910	Reedy Point, DE	1956	2015	59	60	35.40	3.54	89
8557380	Lewes, DE	1919	2015	96	62	59.52	3.40	85
8570283	Ocean City Inlet, MD	1975	2015	40	35	14.00	5.60	140
8571892	Cambridge, MD	1943	2015	72	60	43.20	3.69	92
8573364	Tolchester Beach, MD	1986	2014	28	75	21.00	4.25	106
8573927	Chesapeake City, MD	1972	2015	43	53	22.79	3.81	95
8574680	Baltimore, MD	1902	2015	113	100	113.00	3.14	79
8575512	Annapolis, MD	1928	2015	87	97	84.39	3.53	88
8577330	Solomons Island, MD	1937	2015	78	66	51.48	3.74	94
8594900	Washington, DC	1924	2015	91	90	81.90	3.22	81
8631044	Wachapreague, VA	1978	2015	37	73	27.01	5.37	134
8632200	Kiptopeke, VA	1951	2015	64	99	63.36	3.58	90
8635150	Colonial Beach, VA	1972	2010	38	88	33.44	4.89	122
8635750	Lewisetta, VA	1974	2015	41	99	40.59	5.42	136
8637624	Gloucester Point, VA	1950	2003	53	97	51.41	3.81	95
8638610	Sewells Point, VA	1927	2015	88	99	87.12	4.59	115
8638660	Portsmouth, VA	1935	1987	52	100	52.00	3.76	94
8638863	Chesapeake Bay Bridge	1975	2015	40	99	39.60	5.93	148
8651370	Duck, NC	1978	2015	37	98	36.26	4.48	112
8652587	Oregon Inlet Marina, NC	1977	2015	38	59	22.42	3.84	96
8656483	Beaufort, NC	1953	2015	62	71	44.02	2.89	72
8658120	Wilmington, NC	1935	2015	80	97	77.60	2.19	55
8659084	Southport, NC	1933	2008	75	16	12.00	2.00	50
8661070	Springmaid Pier, SC	1957	2015	58	64	37.12	3.90	98
8665530	Charleston, SC	1921	2015	94	99	93.06	3.21	80
8670870	Fort Pulaski, GA	1935	2015	80	97	77.60	3.17	79
8720030	Fernandina Beach, FL	1897	2015	118	78	92.04	2.08	52
8720218	Mayport, FL	1928	2015	87	17	14.79	2.55	64
8721120	Daytona Beach Shores, FL	1925	1983	58	11	6.38	2.32	58
8722670	Lake Worth Pier, FL	1970	2015	45	41	18.45	3.56	89
8723170	Miami Beach, FL	1931	1981	50	93	46.50	2.39	60
8723970	Vaca Key, FL	1971	2015	44	91	40.04	3.53	88
8724580	Key West, FL	1913	2015	102	93	94.86	2.37	59
Pacific Coast of the US								
9410170	San Diego, CA	1906	2015	109	98	106.82	2.13	53
9410230	La Jolla, CA	1924	2015	91	95	86.45	2.19	55
9410580	Newport Beach, CA	1955	1993	38	100	38.00	2.22	56
9410660	Los Angeles, CA	1923	2015	92	99	91.08	0.95	24
9410840	Santa Monica, CA	1933	2015	82	86	70.52	1.52	38
9411270	Rincon Island, CA	1962	1990	28	92	25.76	3.22	81
9411340	Santa Barbara, CA	1973	2015	42	58	24.36	1.11	28
9412110	Port San Luis, CA	1945	2015	70	94	65.80	0.84	21
9413450	Monterey, CA	1973	2015	42	99	41.58	1.40	35
9414290	San Francisco, CA	1897	2015	118	99	116.82	1.94	49
9414523	Redwood City, CA	1974	2015	41	45	18.45	1.96	49
9414750	Alameda, CA	1939	2015	76	99	75.24	0.72	18
9415020	Point Reyes, CA	1975	2015	40	98	39.20	1.97	49
9415144	Port Chicago, CA	1976	2015	39	98	38.22	1.55	39
9416841	Arena Cove, CA	1978	2015	37	79	29.23	0.42	11
9418767	North Spit, CA	1977	2015	38	98	37.24	4.60	115
9419750	Crescent City, CA	1933	2015	82	93	76.26	-0.81	-20
9431647	Port Orford, OR	1977	2015	38	82	31.16	-0.08	-2
9432780	Charleston, OR	1970	2015	45	98	44.10	0.98	25
9435380	South Beach, OR	1967	2015	48	100	48.00	1.55	39
9437540	Garibaldi, OR	1970	2015	45	45	20.25	2.46	62
9439011	Hammond, OR	1983	2014	31	28	8.68	-1.22	-31
9439040	Astoria, OR	1925	2015	90	96	86.40	-0.23	-6
9440910	Toke Point, WA	1973	2015	42	92	38.64	0.40	10
9443090	Neah Bay, WA	1934	2015	81	97	78.57	-1.73	-43
9444090	Port Angeles, WA	1975	2015	40	99	39.60	0.14	4
9444900	Port Townsend, WA	1972	2015	43	97	41.71	1.82	46
9447130	Seattle, WA	1899	2015	116	99	114.84	2.01	50
9449424	Cherry Point, WA	1973	2015	42	97	40.74	0.25	6
9449880	Friday Harbor, WA	1934	2015	81	82	66.42	1.12	28
9450460	Ketchikan, AK	1919	2015	96	92	88.32	-0.31	-8
9451600	Sitka, AK	1924	2015	91	81	73.71	-2.28	-57

9452210	Juneau, AK	1936	2015	79	92	72.68	-13.14	-329
9452400	Skagway, AK	1944	2015	71	80	56.80	-17.59	-440
9453220	Yakutat, AK	1988	2015	27	95	25.65	-14.10	-353
9454050	Cordova, AK	1988	2015	27	94	25.38	-0.04	-1
9454240	Valdez, AK	1988	2015	27	95	25.65	-8.60	-215
9455090	Seward, AK	1964	2015	51	86	43.86	-2.62	-66
9455500	Seldovia, AK	1964	2015	51	96	48.96	-10.08	-252
9455760	Nikiski, AK	1973	2015	42	52	21.84	-10.42	-261
9455920	Anchorage, AK	1972	2015	43	86	36.98	-0.54	-14
9457292	Kodiak Island, AK	1975	2015	40	53	21.20	-10.41	-260
9459450	Sand Point, AK	1972	2015	43	96	41.28	0.92	23
9461380	Adak Island, AK	1957	2015	58	89	51.62	-2.83	-71
9462620	Unalaska, AK	1957	2015	58	64	37.12	-5.08	-127
9463502	Port Moller, AK	1984	2015	31	41	12.71	2.64	66
9497645	Prudhoe Bay, AK	1990	2014	24	92	22.08	1.20	30

CONCLUSIONS

The sea level projections of Jevrejevaa, Jackson, Riva, Grinstede and Moore (2016) are plainly conflicting with the tide gauge measurements. The differences in between the sea levels forecasted based on actual measurements and predicted by wrongly assuming the sea levels follow the temperatures that follow the anthropogenic carbon dioxide emission are huge in 2040, and the differences further expand in the year 2100. As confirmed by Morner (2016), the expected global average sea level rise in the 21st century based on observational facts, physical laws and long-term scientific experience is +5 cm ± 15 cm by the year 2100, not certainly 1 or 2 metres.

Acknowledgements: The author thanks the anonymous reviewer of a US climate institute that provided his/her feed back.

REFERENCES

Boon, J.D., Brubaker, J.M. and Forrest, D.R., 2010. Chesapeake Bay land subsidence and sea level change. *App. Mar. Sci. and Ocean Eng.*, Report, 425, p. 1-73.

Jevrejevaa, S., Jackson, L.P., Riva, R.E.M., Grinstede, A. and Moore, J.C., 2016. Coastal sea level rise with warming above 2 °C, PNAS, 2016, doi: 10.1073/pnas.1605312113

Larsen, C.F., Motyka, R.J., Freymueller, J.T., Echelmeyer, K.A. and Ivins, E.R., 2005. Rapid viscoelastic uplift in southeast Alaska caused by post-Little Ice Age glacial retreat. *Earth and Planetary Science Letters,* 237(3), p. 548-560.

NOAA, 2016. MSL US TRENDS TABLE. http://tidesandcurrents.noaa.gov/sltrends/mslUSTrendsTable.htm, visited November 10, 2016.

Mörner, N.-A., 2016. Rates of Sea Level Changes—A Clarifying Note. *International Journal of Geosciences*, v. 7, p. 1318-1322.

Parker, A., 2013a. SEA LEVEL TRENDS AT LOCATIONS OF THE UNITED STATES WITH MORE THAN 100 YEARS OF RECORDING, Natural Hazards, 2013, Vol. 65, Issue 1, p. 1011-1021.

Parker, A., 2013b. Apparent hot and cold spots of acceleration along the Atlantic and Pacific coasts of the United States, Nonlinear Engineering, v. 3, Issue 1, p. 51–56.

Parker, A. and Ollier, C.D., 2016. Coastal planning should be based on proven sea level data. Ocean and Coastal Management, v. 124, p. 1–9.

Parker, A., 2016. The Sea Levels are Now Reducing in the "Hotspots of Acceleration" of Washington and New York. *Journal of Earth and Atmospheric Sciences,* v. 1, no. 1, p. 1-9.

Without cherry picking, the sea level acceleration is zero in Newlyn

Albert Parker
School of Engineering and Physical Science, James Cook University, Townsville QLD 4811, Australia.
albert.parker.2014@gmail.com

Abstract: It is very well known that the linear fitting of the monthly average mean sea levels (MSL) with short time windows returns apparent rates of rise of the sea levels very far from reasonable because of the multi-decadal oscillations. Nevertheless, Bradshaw, Woodworth, Hibbert, Bradley, Pugh, Fane & Bingley (2016) propose a misleading picture with linear fittings over time windows 1915 to 2014 and 1993 to 2014 of the MSL measured in Newlyn to say "The record of monthly MSL at Newlyn during the past century. The average rates of change of MSL for the complete record and for the recent period 1993–2014 are 1.8 and 3.8 mm/year respectively and are shown by the black lines". Once more, the natural oscillations about a nearly constant trend are wrongly used as an indication of increased rates of rise of the sea level that is not rising in Newlyn at an increased rate over the last 40 years.

Keywords: *climate change, sea levels, sea level rise, sea level acceleration, cherry-picking*

(Received 19 October, 2017. Accepted 17 February 2017)

SHORT TIME WINDOWS ARE MISLEADING

Bradshaw, Woodworth, Hibbert, Bradley, Pugh, Fane & Bingley (2016) propose a misleading picture, **Figure 1.a** below, with linear fittings with time window 1915 to 2014 and 1993 to 2014 of the MSL measured in Newlyn to say "*The record of monthly MSL at Newlyn during the past century. The average rates of change of MSL for the complete record and for the recent period 1993–2014 are 1.8 and 3.8 mm/year respectively and are shown by the black lines*". With only 22 years of data, there is no opportunity to compute meaningful relative rates of rise of sea levels, and the comparison makes no sense.

To mitigate the above wrong statement, it is then written: "*Figure 8 shows that high rates were observed in previous 22-year periods, including those centered on approximately 1926, 1950, and 1980 (with rates of approximately 3 mm/year), with the lowest rates centered on 1934 and 1968 (approximately 0 mm/year), with such accelerations and decelerations in the record similar to those seen in other parts of the world.*" However, Figure 8 does not show any rate of rise of the sea level computed with 22 years' time windows, only the two MSL fittings 1993-2014 and 1915-2014. Therefore, the authors know to be wrong to use short time windows to compute the rate of rise of the sea levels, but they can't refrain from the visual impact of a much sloped fitting line to supporting scaring messages about sea level rises.

As explained in Parker (2016a), by computing the sea level rate of rise (SLR) as the slope of the linear fitting of the MSL measured up to a certain time, we may then investigate the pattern of SLR (velocity), **Figure 1.b and 1.c,** and properly compute the acceleration (SLA) as the time rate of change of this velocity, **Figure 1.d and 1.e**. If x is the time and y the MSL, for a distribution $\{x_i, y_i\}$ i=j,…., k, the equation for the slope of the regression line is:

$$b_{j,k} = \frac{\sum_{i=j}^{k}(x_i - \bar{x})(y_i - \bar{y})}{(x_i - \bar{x})^2}$$

where $\bar{x}$ and $\bar{y}$ are the sample averages of the distribution. As the MSL distribution is characterized by oscillations with well–known inter-annual, decadal and multi-decadal periodicities detected up to quasi-60 years, a time window $\delta x_{j,k} = (x_k - x_j)$ exceeding 60 years is needed to compute a realistic relative rate of rise of sea levels (SLR) as the slope of the linear fitting. The relative sea level acceleration is then simply the time rate of change of this sea level velocity.

We consider here the data of Newlyn and North Shield. The sea level velocities are not higher now than 50-

60 years ago. In terms of accelerations, in North Shields and Newlyn, there have been only oscillations in positive and negative.

Similar conclusions to ours may be inferred from the graphs proposed by NOAA for the variation of the 50-Year Mean Sea Level Trends, i.e. the SLR computed by using 50 years' time windows, **Figure 1.f and 1.g** (images from NOAA 2016a & b). There is no sign these SLR are increasing, as they are actually only oscillating.

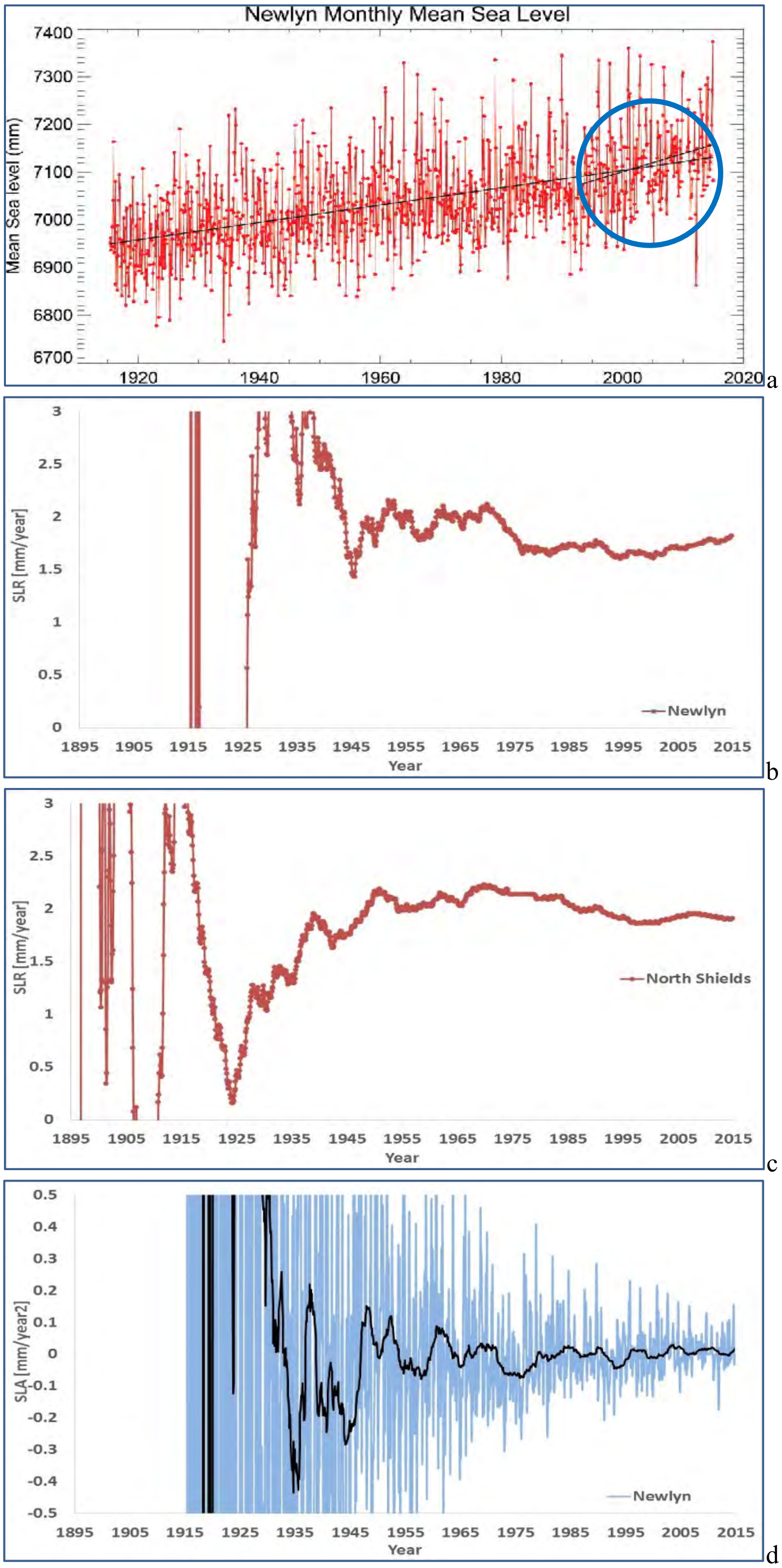

Fig. 1. Continued to the next page.

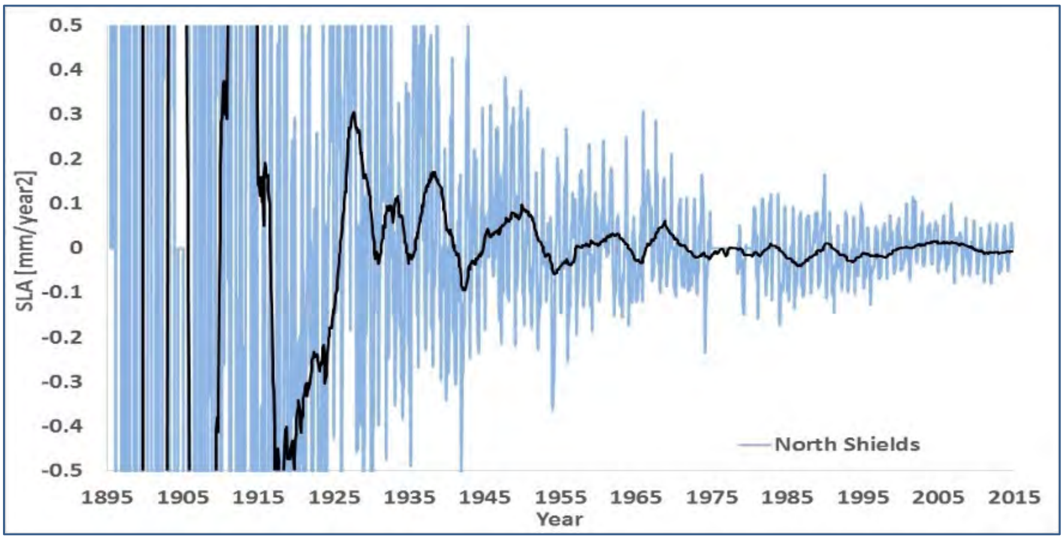

e

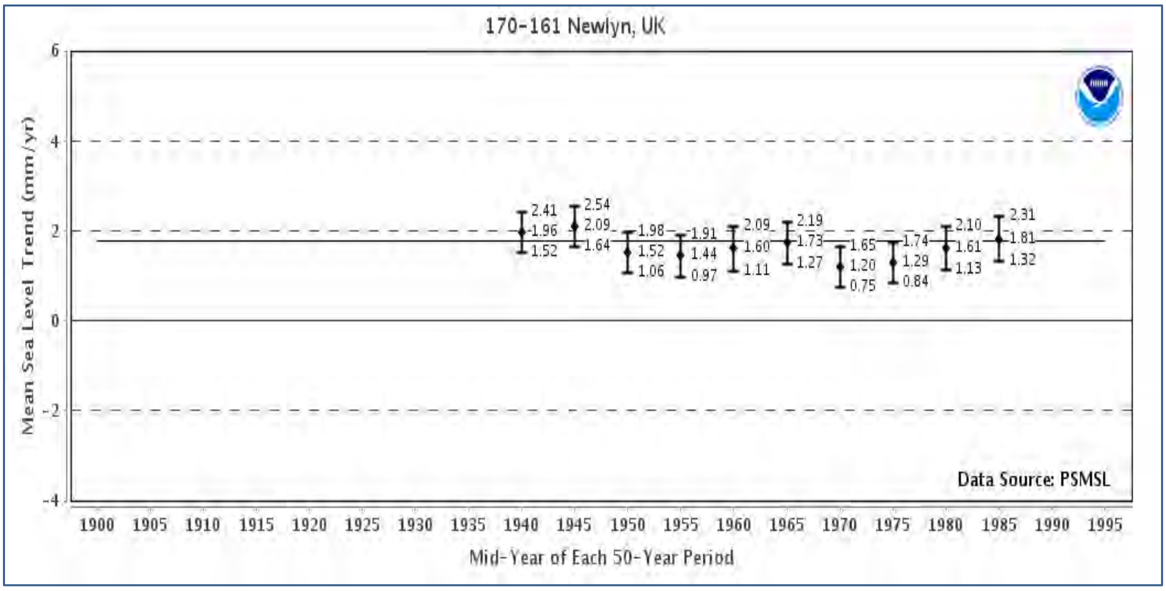

f

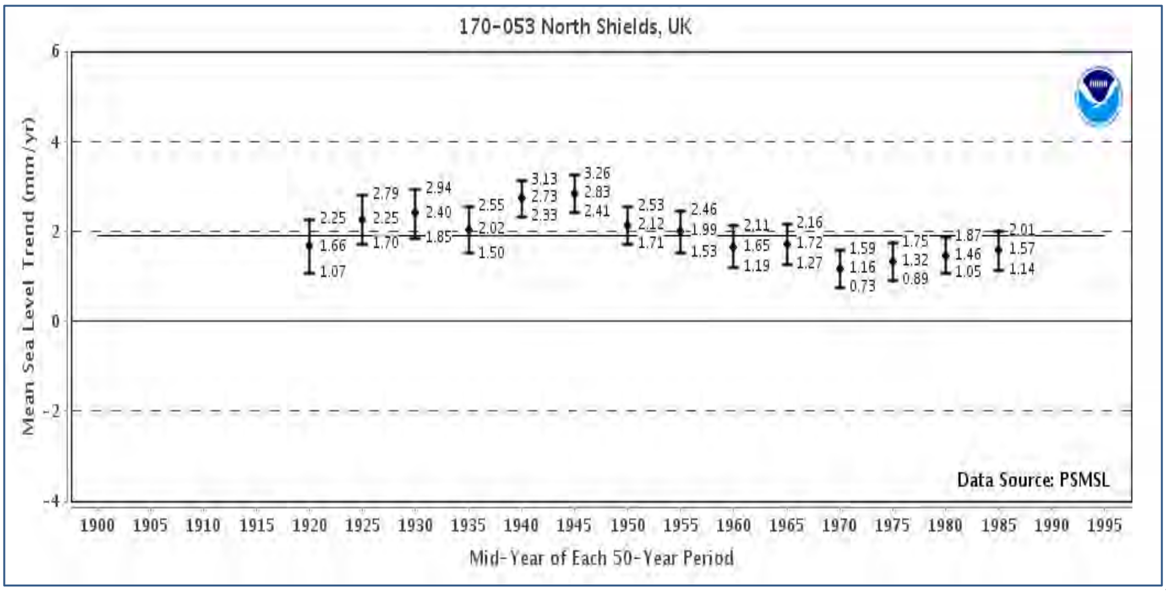

g

Figure 1 – a) MSL and SLR in Newlyn (Figure 8 of [1]). Only the black line indicating the average rate of change of MSL for the complete record is meaningful. b) and c) relative rates of rise of sea levels in Newlyn and North Shields computed by using at any time all the available data (from [2]). d) and e) relative sea level accelerations in Newlyn and North Shields (from [2]). f) and g) SLR computed by using 50 years' time windows (images from NOAA 2016a,b). The relative rates of rise of sea levels have been only oscillating over the last 60 years.

DICUSSION AND CONCLUSION

As shown in **Figure 1.b to g**, the sea level accelerations 1960 to present in Newlyn and North Shields, UK are very close to zero, and not always positive, opposite to what may be wrongly guessed by comparing relative rate of rise of sea levels computed with time windows of 100 or 22 years in Newlyn as proposed in Bradshaw et. al. (2016).

Bradshaw et al. (2016) in fact concede that "*However, the observed rate of sea level change at Newlyn over 1993–2014 has been much larger at 3.8 mm/year (we use 1993 somewhat arbitrarily for the start of the modern era in sea level monitoring as that was when precise altimeter information from space became available). This highest rate in the record may represent the start of a long-term acceleration in sea level due to climate change (Church et al., 2014), or simply be a feature of the decadal variability in MSL that has been evident throughout the Newlyn record (and indeed in all tide gauge records)*." Therefore, Bradshaw et al. (2016) acknowledge the existence of transient accelerations in the tide gauge record, but even if the authors know to be wrong to use short time windows to compute the rate of rise of the sea levels, they can't refrain from the visual impact of a much sloped fitting line and the statement "*The average rates of change of MSL for the complete record and for the recent period 1993–2014 are 1.8 and 3.8 mm/year respectively"* to support scaring messages about sea level rises.

The analysis contained in the manuscript is still state-of-the-art for detecting acceleration in mean sea level from long tide gauge records, even if many may certainly argue the nanometer per year squared computed with more complicated, but not certainly more accurate algorithms, to defocus from the missing nearly full meter of the purely speculative 1 meter sea level rise in 2,100. On average, the sea levels have risen at the world's tide gauges of 4 mm over the first 16 years of this century (Parker, 2016b).

Acknowledgements: The author thanks an anonymous reviewer of a US climate institute that provided his/her feedback.

REFERENCES

Bradshaw, E., Woodworth, P.L., Hibbert, A., Bradley, L.J., Pugh, D.T., Fane, C. and Bingley, R.M., 2016. A Century of Sea Level Measurements at Newlyn, Southwest England. *Marine Geodesy*, v. 39, Issue 2, p. 115-140.

NOAA, 2016a. 50 yr trend in Newlyn, https://tidesandcurrents.noaa.gov/sltrends/global_50yr.htm?stnid=170-161

NOAA, 2016b. 50 yr trend in North Shields, https://tidesandcurrents.noaa.gov/sltrends/global_50yr.htm?stnid=170-053

Parker, A., 2016a. THERE IS NO PRESENT SEA LEVEL ACCELERATION IN UK AND WESTERN EUROPEAN COASTS. *New Concepts in Global Tectonics Journal*, v. 4, no. 2, p. 314-321. www.ncgt.org.

Parker, A., 2016b. Sea level rises: arguing the nanometre to defocus from the missed meter. *Environmental Science, An Indian Journal,* v. 12, Issue 1, p. 22-29.

The temperature record of Berlin-Dahlem shows a warming only by arbitrary correction

Albert Parker
School of Engineering and Physical Science, James Cook University, Townsville QLD 4811, Australia.
albert.parker.2014@gmail.com

Abstract: I analyse the temperature time series for Berlin-Dahlem included in the Global Historical Climatology Network-Monthly (GHCN-M) temperature datasets v2 and v3 to compute the most likely 20th century warming trend. It shows that without arbitrary corrections the warming rate in this station subjected to minimal urban heat island effects is negligible. It also shows that the corrections of the past temperatures of the most part of the worldwide locations including Berlin-Dahlem introduced with GHCN v3 have no truly scientific basis.

Keywords: *climate change, temperature profiles, Berlin-Dahlem*

(Received 29 December 2016. Accepted 17 February 2017)

GLOBAL HISTORICAL CLIMATOLOGY NETWORK (GHCN)

The continuous revision of the temperatures of the past to magnify the warming trend, is one of the building blocks of the science of climate change. The Global Historical Climatology Network-Monthly (GHCN-M) temperature dataset exemplifies this issue. The GHCN data set was first developed in the early 1990s. The first version (v1) was already a subjective interpretation of the actual measurements of air temperatures by thermometers to be considered for assessing the extent of global warming depurated of Urban Heat Island (UHI) effects. A second version (v2) of this data set was released in 1997. The third version (v3) of the data set was released in May of 2011. This is the latest version being updated continuously to reflect new measurements. The GHCN data base is described in (NOAA NCDC, 2016). The global data for all the stations is available for download from (NOAA NCDC, 2016). The National Aeronautics and Space Administration (NASA) Goddard Institute for Space Studies (GISS) presents the individual station data v2 as well as v3 (see for example in (NASA GISS, 2016a) and (NASA GISS, 2016b) the data for Berlin Dhalem) for only the monthly average temperatures. The new data v3 is further adjusted and homogenised vs. the v2 raw GHCN data plus United States Historical Climatology Network (USHCN) correction.

The aim of this paper is to show the arbitrary correction introduced in 2011, and to determine the most likely temperature time series 1890 to 2016 for Berlin-Dahlem to properly compute the warming rate for the 20th century.

BERLIN-DAHLEM GHCN-M TEMPERATURES V2 VS. V3

In the following sections, for sake of simplicity, I indicate as “GHCN v2” the NASA GISS v2 raw GHCN data plus USHCN correction, and as “GHCN v3 adj.hom.” the NASA GISS v3 GHCN data v3 adjusted and homogenised.

The Berlin-Dahlem meteorological station is operated by the Free University of Berlin (Senate Department for Urban Development and the Environment, 2015). It has been in operation since April 1, 1908 in various sites. The annual mean of the air temperature 1981 to 2010 was 9.5 °C, the highest temperature ever measured up to the end of 2013 was 37.8 °C on July 11, 1959 and the lowest temperature ever measured also up to the end of 2013 was -26.0 °C on February 11, 1929. The measuring sites were Königin-Luise-Str. 22 from April 1, 1908 to an unspecified date of 1962, Kiebitzweg 20 from December 1, 1949 to October 3, 1951, Podbielskiallee 62 from October 3, 1951 to July 11, 1997, and finally Botanical Garden from July 12, 1997 (ongoing).

Figure 1 presents the yearly average temperatures in Berlin-Dahlem in the GHCN v2 (a) and v3 (b) data sets. The images are from (NASA GISS, 2016a) and (NASA GISS, 2016b). In 2011, the temperatures measured during the first part of the 1900s were cooled significantly down in many worldwide locations and Berlin-Dahlem was no exception.

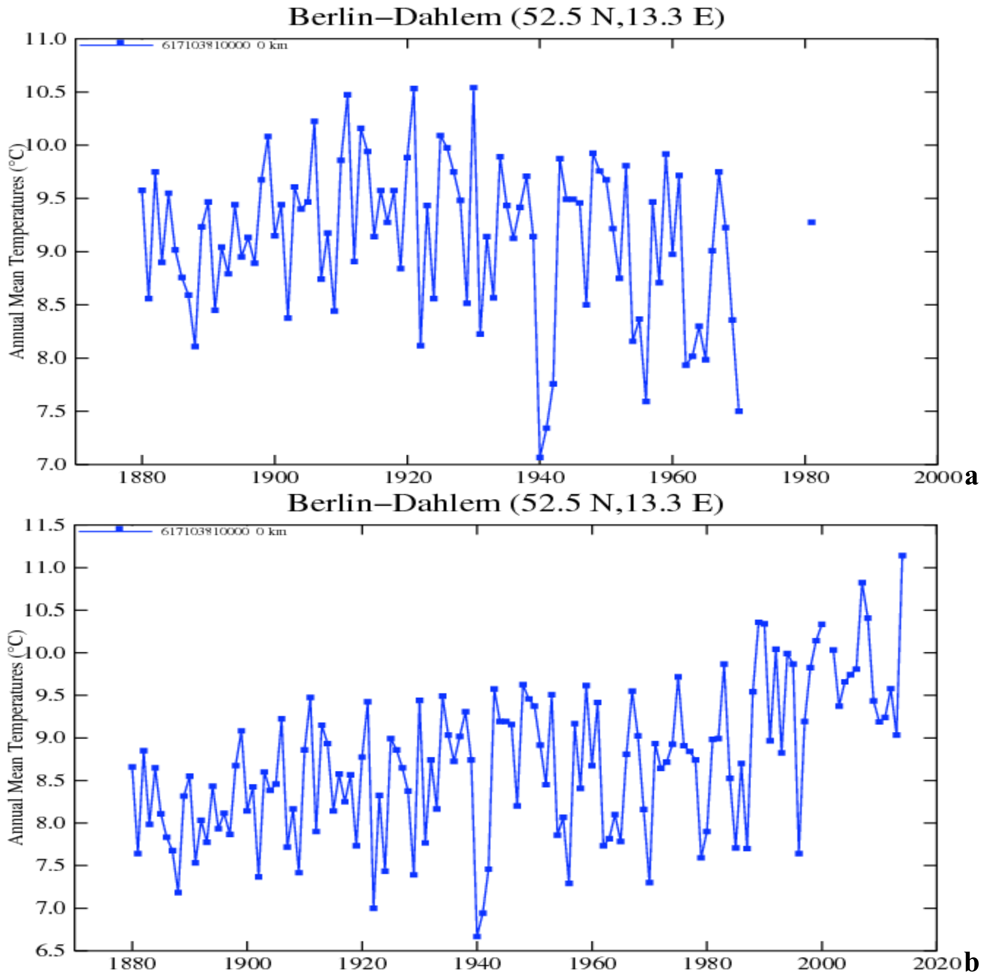

Figure 1 – Yearly average temperatures in Berlin-Dahlem in the GHCN v2 (a) and GHCN v3 adg. hom. (b) data sets. Images from (NASA GISS, 2016a) and (NASA GISS, 2016b).

To understand the nature of the correction, **Figure 2** presents in *a* and *b* the monthly average temperatures in Berlin-Dahlem GHCN v3 adj. hom. (NASA GISS, 2016a) and GHCN v2 (NASA GISS, 2016b), while in c is their difference. The correction is quite crude, and certainly not derived from complicated simulations or the discovery of other measured data. The correction is quickly built to deliver the desired warming by adding a step-wise distribution. The correction does not seem to follow any specific logic, but arbitrarily lowers the temperatures of the past to add more than 1 ºC of warming to the original trend.

Over the period 1880 to 1930, the arbitrary cooling is -1 ºC. Over the period 1930 to 1950, the arbitrary cooling is -0.4 ºC. Over the period 1950 to 1970, the arbitrary cooling is 0.3 ºC. 1970 to 1990, no correction is introduced, and after 1990 there are only the measurements of v3 to consider.

As the corrections are applied 1880 to 1970, if we remove from the latest GHCN v3 adg. hom, updated to 2016 the arbitrary corrections, then it is possible to estimate the temperature trend 1880 to 2016. Not surprisingly, without the corrections, the warming trend in Berlin-Dahlem practically disappears, as shown in d.

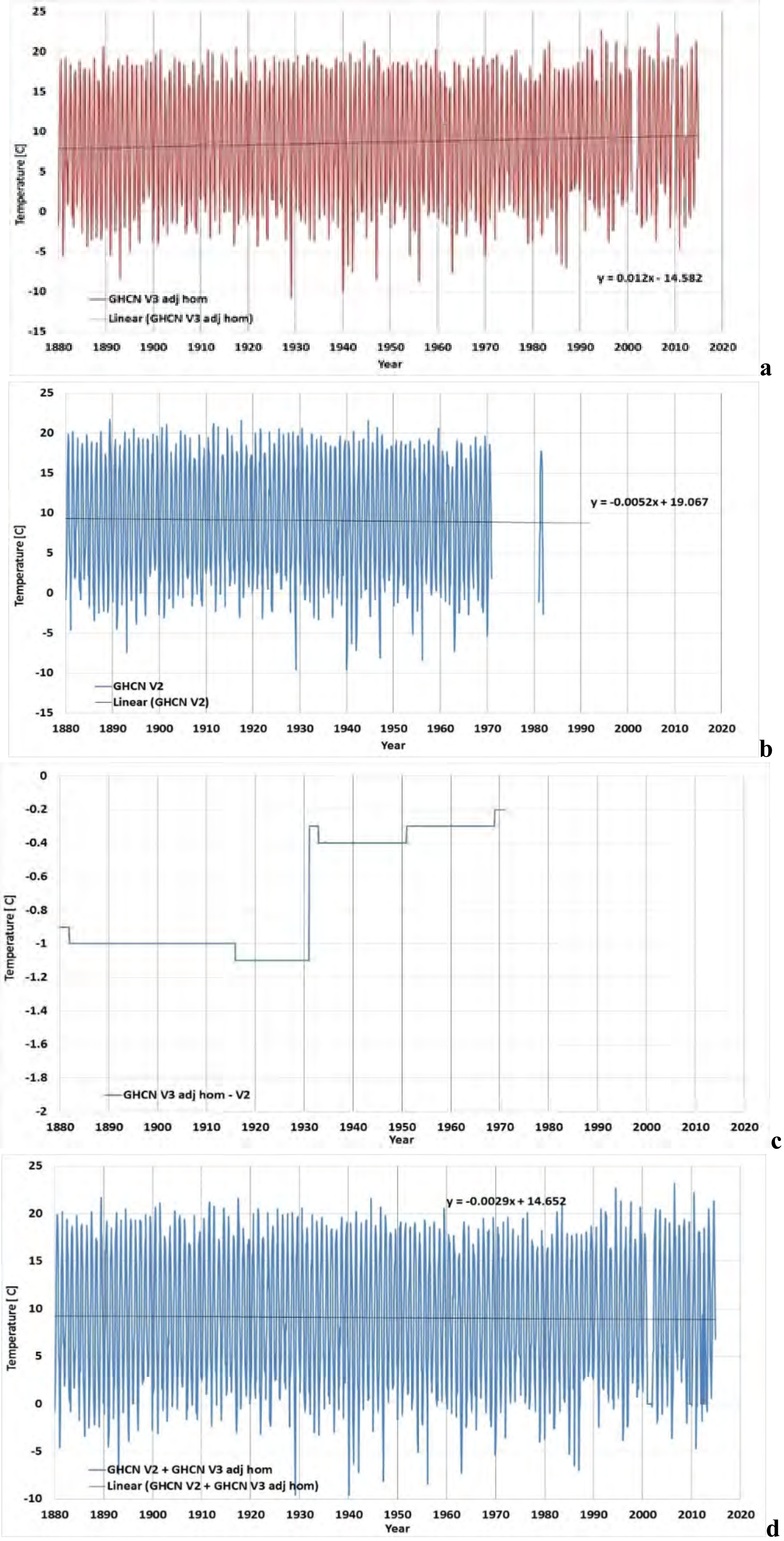

Figure 2 - Monthly average temperatures in Berlin-Dahlem GHCN v3 adg. hom. (NASA GISS, 2016a) (a) and GHCN v2 (NASA GISS, 2016b) (b). Monthly differences v3 adg. hom. – v2 (c). GHCN v3 adg. hom. with arbitrary corrections removed (d).

DISCUSSION

I note that the mean temperature is not the best parameter to detect a warming process, as the urban heat island (UHI) effect is very well known to increase drastically the average temperature. As Berlin Dhalem is a location where the heat island effect is considered negligible, the lack of a significant warming for the average temperature is particularly evident.

This lack of warming for Berlin-Dahlem was already shown in Ewert (2009), where other data recorded since the 1700s were also used to prove an oscillatory pattern of temperatures about a minimal warming trend. **Figure 3** (from (Ewert, 2009) shows the yearly average temperature time series for Berlin. Several short term temperature variations are identified with trend lines. The temperatures were higher between 1750 and 1780, as well as around 1830 than around the year 2000. Similar warming periods occurred in the 18th and 19th century. The rate of warming is minimal, consistently with the trends for other locations listed in (Ewert, 2009).

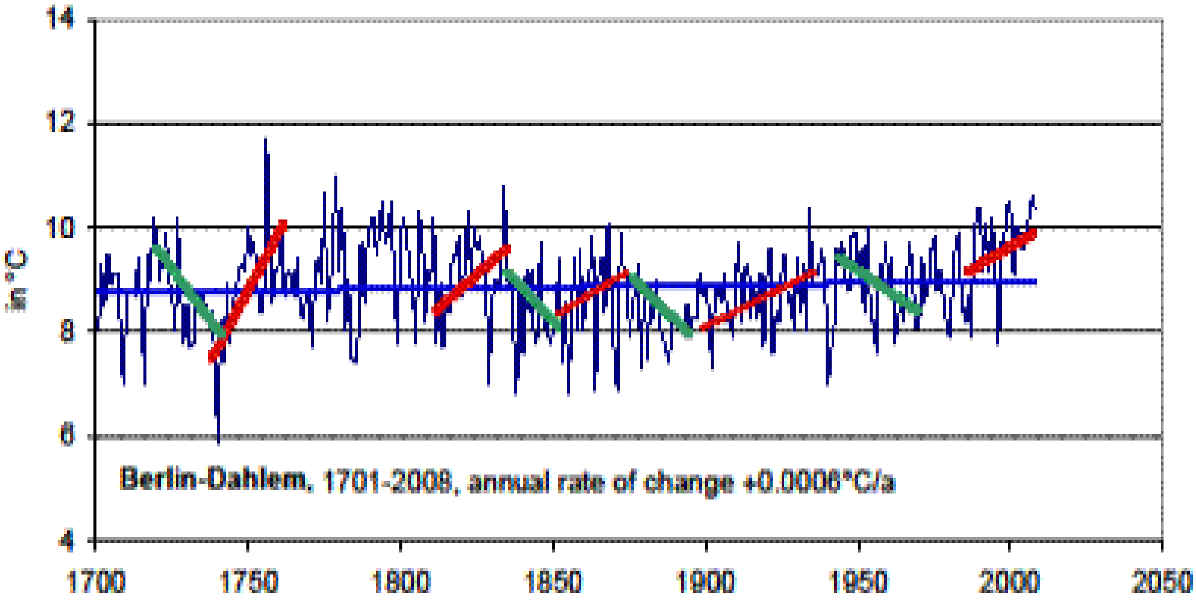

Figure 3 – Yearly temperatures in Berlin-Dahlem (from Ewert, 2009).

As previously noted, Berlin-Dahlem is not the only station that has been subjected to the arbitrary cooling of the past. Many other stations had their data revised. In other stations, as for example Alice Springs, the correction was even larger. **Figure 4** present the yearly average temperatures in Alice Springs in the GHCN v2 (a) and GHCN v3 adg. hom. (b) data sets. The images are from (NASA GISS, 2016c) and (NASA GISS, 2016d).

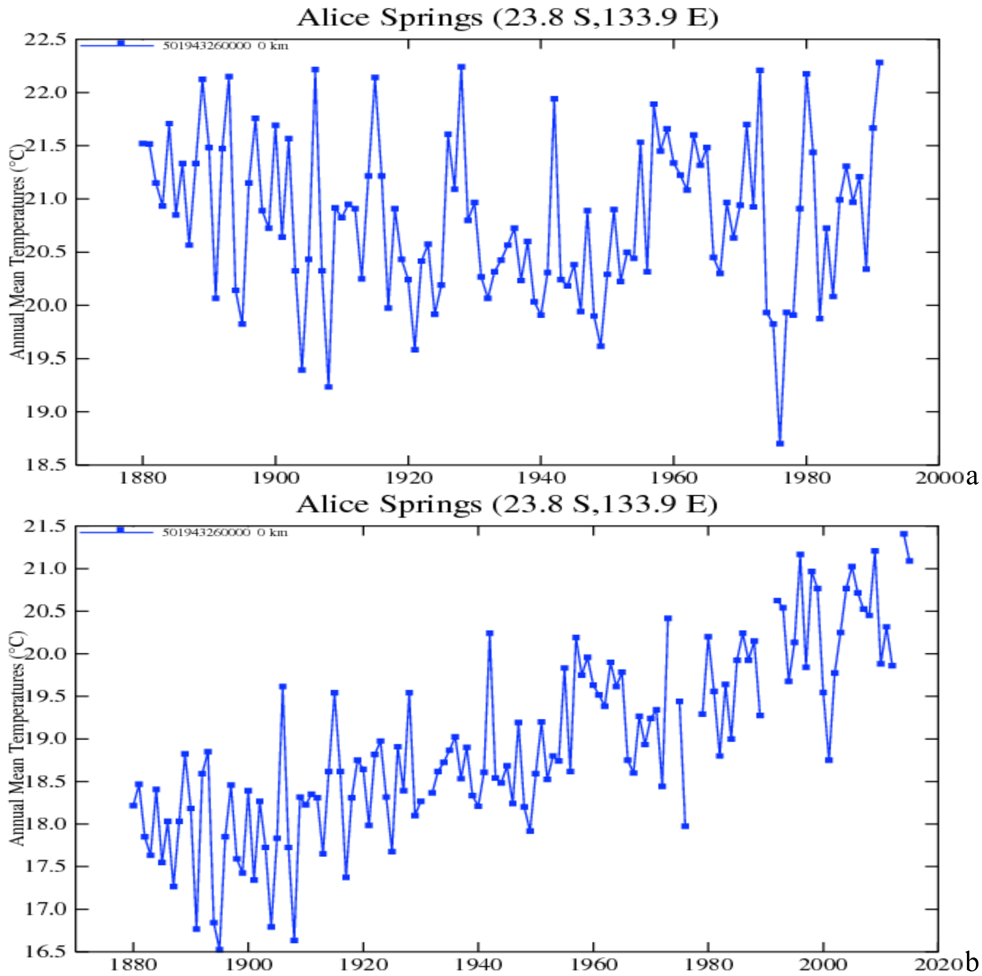

Figure 4 – Yearly average temperatures in Alice Spring in the GHCN v2 (a) and GHCN v3 adg. hom. (b) data sets.. Images from (NASA GISS, 2016c) and (NASA GISS, 2016d).

To understand the nature of the corrections, **Figure 5** presents the monthly average temperatures in Alice Springs GHCN v3 adg. hom. (NASA GISS, 2016c) (a) and GHCN v2 (NASA GISS, 2016d) (b), while (c) is their difference. The correction is little bit more elaborated than in Berlin-Dahlem, but still quite crude. It is similarly not originating from complicated simulations, or the disclosure of new data never considered before, but simply built to deliver the desired warming.

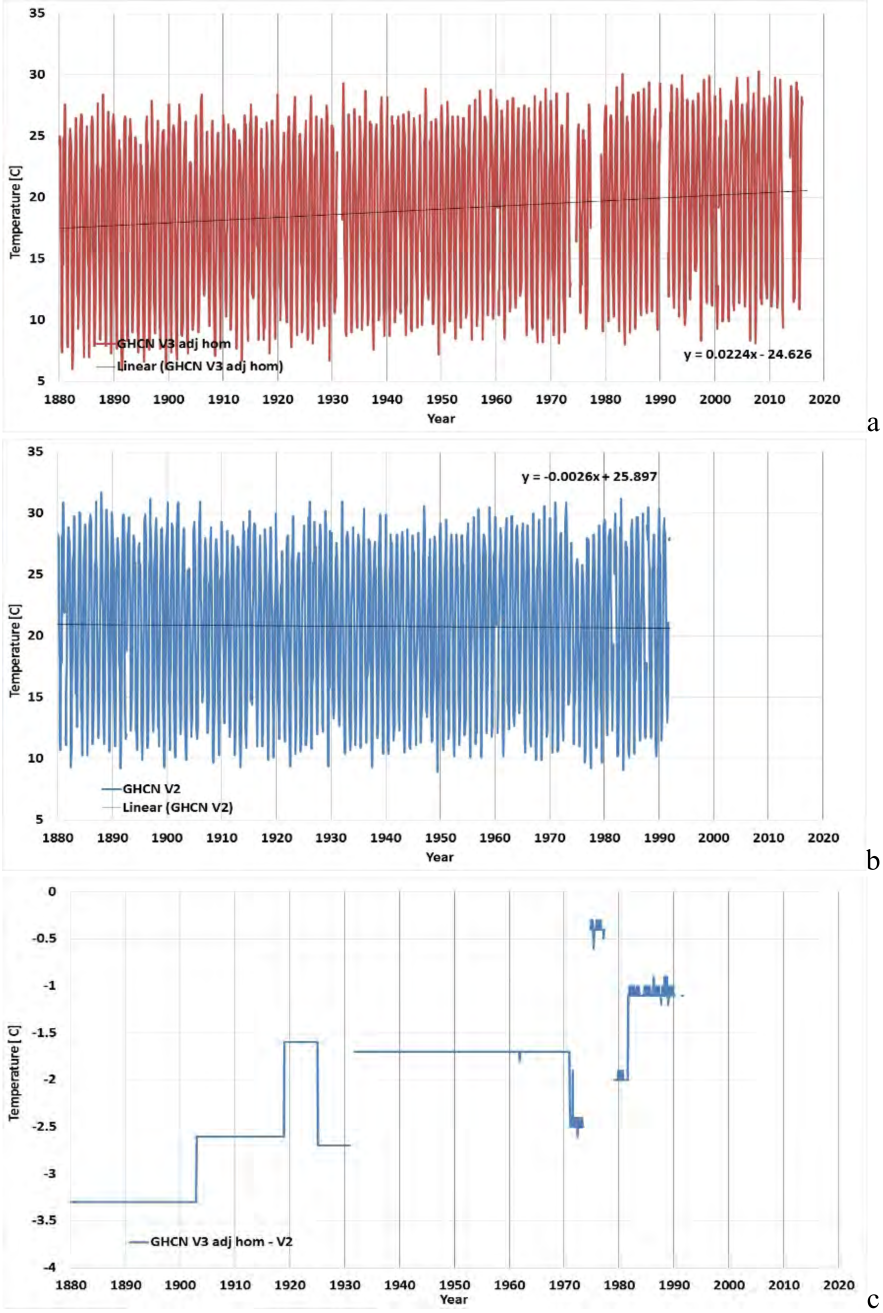

Figure 5 - Monthly average temperatures in Alice Spring GHCN v3 adg. hom. (NASA GISS, 2016a) (a) and GHCN v2 (NASA GISS, 2016b) (b). Monthly differences v3 adg. hom. – v2 (c).

CONCLUSIONS

The temperature record of Berlin-Dahlem shows a warming only by arbitrary correction. There is no legitimate reason why the historical record of temperatures should be rewritten. It is done to make the temperatures of the past cooler with the clear intent of making a warming trend. Quoting Oppenheimer (1951), “We do not believe any group of men adequate enough or wise enough to operate without scrutiny or without criticism. We know that the only way to avoid error is to detect it, that the only way to detect it is to be free to enquire.” Claim of warming trends of +1.2 ºC/century in Berlin Dhalem (or +2.4 ºC/century in Alice Spring) are plainly in error.

Acknowledgements: The author thanks the anonymous reviewer that provided his/her helpful comment.

REFERENCES

Ewert, F.K., 2009. Key issues disproving global warming. http://www.eike-klima-energie.eu/uploads/media/Key_issues_Climate_change_August_09.pdf

National Oceanic and Atmospheric Administration (NOAA) National Climatic Data Centre (NCDC), 2016. Global Historical Climatology Network-Monthly (GHCN-M) temperature dataset. https://www.ncdc.noaa.gov/ghcnm/

National Aeronautics and Space Administration (NASA) Goddard Institute for Space Studies (GISS), 2016a. GISS Surface Temperature Analysis Station Data: Station Data: Berlin-Dahlem (52.5N,13.3E). GHCN v2. http://data.giss.nasa.gov/cgi-bin/gistemp/show_station.cgi?id=617103810000&dt=1&ds=0

National Aeronautics and Space Administration (NASA) Goddard Institute for Space Studies (GISS), 2016b. GISS Surface Temperature Analysis Station Data: Station Data: Berlin-Dahlem. http://data.giss.nasa.gov/cgi-bin/gistemp/show_station.cgi?id=617103810000&dt=1&ds=14

Senate Department for Urban Development and the Environment (2015), 04.13 Long-term Development of Selected Climate Parameters. http://stadtentwicklung.berlin.de/umwelt/umweltatlas/ed413_06.htm

National Aeronautics and Space Administration (NASA) Goddard Institute for Space Studies (GISS), 2016c. GISS Surface Temperature Analysis Station Data: Station Data: Alice Spring. GHCN v2. http://data.giss.nasa.gov/cgi-bin/gistemp/show_station.cgi?id=501943260000&dt=1&ds=0

National Aeronautics and Space Administration (NASA) Goddard Institute for Space Studies (GISS), 2016d. GISS Surface Temperature Analysis Station Data: Station Data: Alice Spring. http://data.giss.nasa.gov/cgi-bin/gistemp/show_station.cgi?id=501943260000&dt=1&ds=14

Oppenheimer, J.R., 1951. Encouragement of Science (Address at Science Talent Institute, 6 Mar 1950). *Bulletin of the Atomic Scientists*, v. 7, no. 1 (Jan 1951), p. 6-8.

PUBLICATIONS

The correlation of seismic activity and recent global warming

Arthur Viterito. *Journal of Earth Science & Climatic Change*, volume 7, issue 4, 2016.
http://dx.doi.org/10.4172/2157-7617.1000345. Arthurv@csmd.edu.

Abstract
The latest report from the Intergovernmental Panel on Climate Change states with high confidence that the warming of global temperatures since 1901 has been driven by increased radiative forcing. The gases responsible for this enhanced forcing are greenhouse gases of anthropogenic origin, and include carbon dioxide, methane, and halocarbons. The Nongovernmental International Panel on Climate Change has challenged these findings and concludes that the enhanced forcing from these gases is minimal and diminishing. They add that modelling attempts of past and future climate states are inaccurate and do not incorporate important solar inputs, such as magnetic strength and total irradiance. One geophysical variable that has been overlooked by both groups is geothermal flux.

This study will show that increasing seismic activity for the globe's high geothermal flux areas (HGFA), an indicator of increasing geothermal forcing, is highly correlated with average global temperatures from 1979 to 2015 ($r = 0.785$). By comparison, the correlation between carbon dioxide loading and global temperatures for the same period is lower ($r = 0.739$). Multiple regression indicates that HGFA seismicity is a significant predictor of global temperatures ($P < 0.05$), but carbon dioxide concentrations do not significantly improve the explained variance ($P > 0.1$). A compelling case for geothermal forcing lies in the fact that 1) geothermal heat can trigger thermobaric convection and strengthen oceanic overturning, important mechanisms for transferring ocean heat to the overlying atmosphere, and 2) seismic activity is the leading indicator, while global temperature is the laggard.

****

Some interesting blogs and youtubes

Electric Earth – Michael Csuzdi
http://breakthroughinenergy.com/index.php?&pageid=1
http://www.mantleplumes.org/Cartoons.html

Global climate
http://clexit.net/
https://www.iceagenow.info/
https://www.youtube.com/watch?v=dzat16LMtQk Bureau of Meteorology, Australian Government.
https://www.youtube.com/watch?v=DJBDI7jVMqM Global warming hoax, best document ever.

Lost continent in the Southwest Pacific – Zealandia
http://www.msn.com/en-us/news/technology/scientists-claim-theyve-found-a-massive-lost-continent/ar-AAn5qpf?li=BBnb7Kz&ocid=UE09DHP

NEWS

Ancient continental crust in the Indian Ocean!!

Lewis D. Ashwal, Michael Wiedenbeck, and Trond H. Torsvik, 2017. Archaean zircons in Miocene oceanic hotspot rocks establish ancient continental crust beneath Mauritius. *Nature Communications*. DOI: 10.1038/ncomms14086. Email: lewis.ashwal@wits.ac.za.

ABOUT THE NCGT JOURNAL

The New Concepts in Global Tectonics Newsletter, the predecessor of the current NCGT Journal, was initiated on the basis of discussion at the symposium "Alternative Theories to Plate Tectonics" held at the 30th International Geological Congress in Beijing in August 1996. The name is taken from an earlier symposium held at Smithsonian Institution, Washington, in association with the 28th International Geological Congress in Washington, D. C. in 1989. The NCGT Newsletter changed its name to NCGT Journal in 2013. Now in March of 2017 the NCGT Journal initiates its commercialized phase.

Aims include:

1. Providing an international forum for the open exchange of new ideas and approaches in the fields of geology, geophysics, solar and planetary physics, cosmology, climatology, oceanography and other fields that affect or are closely related to physical processes occurring on the Earth from its core to the top of its atmosphere.
2. Forming an organizational focus for creative ideas not fitting readily within the scope of dominant tectonic models.
3. Forming the basis for the reproduction and publication of such work, especially where there has been censorships or discrimination.
4. Create a publication that can serve as an exchange of methods and concepts devoted to the prediction, well in advance, of catastrophic earthquakes. Forum for discussion of such ideas and work which has been inhibited in existing channels.